NUREG/CR-4900
UCID-21002
Vol. 1

Component Fragility Research Program
Phase I Demonstration Tests

Volume 1: Summary Report

G. S. Holman, C. K. Chou, G. D. Shipway, V. Glozman

Prepared for
U.S. Nuclear Regulatory Commission

Lawrence Livermore National Laboratory

DISCLAIMER

NUREG/CR--4900-Vol.1

TI87 013697

Component Fragility Research Program
Phase I Demonstration Tests

Volume 1: Summary Report

Manuscript Completed: December 1986
Date Published: August 1987

Prepared by
G. S Holman,* C. K. Chou,* G. D. Shipway,† V. Glozman†

Lawrence Livermore National Laboratory
7000 East Avenue
Livermore, CA 94550

Prepared for
Division of Engineering
Office of Nuclear Regulatory Research
U.S. Nuclear Regulatory Commission
Washington, D.C. 20555
NRC FIN No. A0400

* Nuclear Systems Safety Program, Lawrence Livermore National Laboratory
† Scientific Services & Systems Group, Wyle Laboratories

ABSTRACT

This report describes tests performed in Phase I of the NRC Component Fragility Research Program. The purpose of these tests was to demonstrate procedures for characterizing the seismic fragility of a selected component, investigating how various parameters affect fragility, and finally using test data to develop practical fragility descriptions suitable for application in probabilistic risk assessments. A three-column motor control center housing motor controllers of various types and sizes as well as relays of different types and manufacturers was subjected to seismic input motions up to 2.5g zero period acceleration. To investigate the effect of base flexibility on the structural behavior of the MCC and on the functional behavior of the electrical devices, multiple tests were performed on each of four mounting configurations: four bolts per column with top bracing, four bolts per column with no top brace, four bolts per column with internal diagonal bracing, and two bolts per column with no top or internal bracing. Device fragility was characterized by contact chatter correlated to local in-cabinet response at the device location. Seismic capacities were developed for each device on the basis of local input motion required to cause chatter; these results were then applied to develop probabilistic fragility curves for each type of device, including estimates of the "high-confidence low probability of failure" capacity of each.

CONTENTS

FIGURES

TABLES

ACKNOWLEDGEMENTS

This work was funded by the U.S. Nuclear Regulatory Commission, Office of Nuclear Regulatory Research, through its Structural Engineering Branch. Dr. John O'Brien was the technical monitor for this project.

The Component Fragility Research Program is a multi-disciplinary effort drawing on the talents of many individuals. The authors would like to particularly acknowledge the contributions of Craig Smith (ANCO Engineers), who chaired our Component Testing Working Group, of Robert Campbell (NTS Engineering) and Richard Mensing (LLNL), who developed the probabilistic fragility descriptions based on the test data, of the Wyle Laboratories technicians who performed the actual tests, and of the following organizations which sent representatives to our fragility workshop:

Babcock & Wilcox Owners Group

Bechtel Corporation

Combustion Engineering

Commissariat a l'Energie Atomique

Commonwealth Edison

Duke Power

Duquesne Light

Electric Power Research Institute

Northeast Utilities

Northern States Power

Pacific Gas & Electric

Philadelphia Electric

Sargent & Lundy

Stone & Webster

Westinghouse

Yankee Atomic

The authors would like to offer special thanks to Julius Herbst of the Pacific Gas and Electric Company for his participation in this effort. One of the principal electrical designers of the Diablo Canyon nuclear power plant and a key figure in the seismic qualification of its electrical equipment, Mr. Herbst not only provided significant technical support in the design of our experiments, but through his expertise offered insights which allowed us to better focus our efforts on the practical issues surrounding seismic performance of electrical equipment. In acknowledging Mr. Herbst's contributions, we would also like to thank PG&E for funding his participation and for their continued interest in our research programs.

EXECUTIVE SUMMARY

Over the past decade methods have been developed to probabilistically assess how large earthquakes would affect nuclear power plants, particularly the associated risk to public health and safety. These probabilistic risk assessment (PRA) techniques combine "event trees", which describe the postulated accident scenarios (or "initiating events") capable of causing core melt, with "fault trees" describing the likelihood of equipment failures leading to a reduction in or loss of the ability of certain plant systems to perform their designated safety functions given that an initiating event occurs. A key element in the fault tree analysis is the "fragility" -- or likelihood of failure -- of various components under postulated accident conditions. "Seismic fragility" is a term commonly used to describe the severity of earthquake motion under which a component would be expected to fail. Failure can be characterized as either functional (e.g., erratic behavior, failure to perform intended function) or structural, or as the exceedance of some predetermined performance criteria (such as a limit given in a design code).

One interpretation of fragility, the "fragility level", evolves from qualification testing. In qualification testing, a component is subjected to input motion characterized by a specified waveform describing input level (seismic acceleration) as a function of frequency. The component is "qualified" if it continues to perform its intended function when its response to this input motion (the "test response spectrum") meets or exceeds predetermined acceptance limits (the "required response spectrum"). Although it may establish the adequacy of a component for a particular seismic environment, a successful qualification test does not directly provide data on what input motion levels actually result in component failure. This can be done by retaining the original input spectrum and then increasing the input level until "failure" (however it is defined) occurs. The test response spectrum at failure represents the "fragility level" of the component; the difference between the fragility level and the qualification level thus represents the seismic margin of the component.

Fragility is described differently when used for PRA purposes or for other types of probabilistic analysis. In this case, the fragility of a component represents the probability of its failure conditioned upon the occurrence of some level of forcing or response function. It may be expressed in terms of a local response parameter (for example, input motion at the component mounting location), or can be tied to a more global forcing function such as free field peak ground acceleration as is generally done in PRA applications.

The probability of failure is typically described by "fragility curves" plotted at various levels of statistical confidence. These curves include a "median" function representing the best estimate of the "true" fragility of the component, bounded by other curves ("confidence limits") which describe the uncertainty in this estimate due to variation in the parameters affecting fragility. Such uncertainty may result, for example, from differences in real earthquake ground motion compared to the input motion that a component is subjected to in qualification or fragilities testing, or from lack of knowledge about such parameters as component damping values.

Resource and time constraints make it impractical to directly develop probabilistic fragility descriptions solely by empirical means (e.g., by subjecting a large population of identical components to successively higher levels of acceleration and recording the distribution of failures as a function of acceleration level). Even for functionally identical components, variations among models and manufacturers, and in mounting and loading conditions imply that any fragility estimate will be based in large part on engineering judgement. Meaningful fragilities testing can, however, be conducted within practical constraints if it focuses on understanding how various factors influence component behavior rather than on developing fragilities explicitly. Such testing would be conducted according to the following steps:

1. Identify a representative component or sample of components for testing. Such a sample might not necessarily be "generic" in the purest statistical sense, but should attempt to include significant variations

within a given component type (armature- vs reed-type relays, for example).

2. Identify failure modes and the relevant forcing or response functions. Characterize "failure" (either functional or structural) in terms of a suitable parameter that can be measured experimentally.

3. Identify factors or "technical issues" affecting component failure; such factors might include, but not necessarily be limited to, variations in mounting, input motion, and component damping. Design experimental program to parametrically vary those factors judged to be important.

4. Perform tests to identify when failure occurs, i.e., component median capacity. Such tests might, for example, follow qualification procedures (e.g., use of same input spectra) but at elevated input motion levels. Alternatively (particularly for "high capacity" components), test to a pre-determined level to establish a "lower bound" failure threshold.

5. Use test results to empirically estimate median capacity; note that this result is equivalent to the deterministic "fragility level" generated as a part of some qualification tests. Based on component behavior over all conditions considered, develop estimates of random variability and modeling uncertainty in the empirically derived median capacity.

Although this approach does not remove subjectivity from the process of describing component fragility, it does improve the basis on which these judgements are made. Furthermore, it can provide an improved basis for interpreting data from other sources or for defining test conditions if more rigorous testing of a specific component is deemed necessary.

To demonstrate our approach to fragilities testing, we performed fragility tests on a three-column Westinghouse Five-Star motor control center containing 8 Westinghouse motor controllers of various types and sizes as well as 14 relays of different types and manufacturers. The Five-Star is the

current basic model marketed by Westinghouse for industrial and power system applications; it is essentially identical to the Type W motor control center manufactured by Westinghouse from 1965 to 1975, various configurations of which are found in many nuclear power plants of this vintage. The particular electrical devices selected represented a sample of standard MCC devices typical in function of those found in actual plants, but are not necessarily generic for all similar devices. To investigate the effect of base flexibility on the structural behavior of the MCC and on the functional behavior of the electrical devices, we conducted multiple tests on each of the following four mounting configurations:

- Four bolts per column with top bracing.
- Four bolts per column with no top bracing.
- Four bolts per column with internal diagonal bracing.
- Two bolts per column with no top or internal bracing. This was the "standard" mounting configuration recommended by the MCC supplier.

We performed a total of 56 test runs, including 43 biaxial random motion tests (vertical plus one horizontal axis). Table input motions in the random motion tests ranged up to 2.5 g zero period acceleration (ZPA), which yielded in-cabinet spectral accelerations up to 20 g and higher at the device locations. The desired response spectrum applied in each test was characteristic of qualification spectra (i.e., 250% of ZPA between 4 Hz and 15 Hz); each test run was about 45 sec in duration of which approximately 30 sec was strong motion.

In these tests we investigated both the functional behavior of the individual electrical devices -- relays and starters -- and the structural response of the MCC cabinet for various levels of table input motion and for four different cabinet mounting configurations. Device "fragility" was characterized by contact chatter correlated to local in-cabinet response

measured at the device location, with functional "failure" being defined as the first sign of chatter. Among the topics investigated were (1) the relative susceptibility of normally-open and normally-closed contacts, (2) the chatter susceptibility of energized vs deenergized contacts, and (3) the ability of the devices to respond to commanded changes of state during strong seismic excitation.

In these tests we also observed the structural behavior of the MCC cabinet for various levels of table input motion and for the different mounting configurations. Although substantial damage (cracked and broken welds) was observed in later tests, the cabinet nevertheless withstood some 20 strong motion tests at ZPA levels up to 1.9g before any significant damage was observed. In general, the results of our demonstration tests suggested the following:

- In general, two distinct response modes can be identified for the MCC cabinet. The first of these, which we refer to as the "frame" response, reflects global motion of the MCC structure. Results of low-level (0.2g sine-sweep) transmissibility tests indicated that the cabinet frame resonance lies between about 3.5 Hz and 12 Hz, depending on cabinet mounting configuration. The second mode, typically lying between about 14 Hz and 26 Hz, reflects the local response of the individual draw-out units (or "buckets") which house the relays and starters. We refer to this as the the "bucket" response; the resonant frequency measured for each draw-out unit is referred to as its "bucket" resonance.

- Contact "chatter" appears to be influenced more by spectral acceleration than by ZPA, although the likelihood of chatter will, on the whole, increase with ZPA. Device fragilities based on spectral accelerations should in principle be "more appropriate" but at the same time would be more difficult to apply in a PRA.

- Chatter appears to be influenced more by low-frequency input motion (i.e., less than about 10 Hz) than by high-frequency motion.

Consequently, the lower-frequency "frame" resonances will affect device performance more than higher-frequency local "rattling" of the cabinet structure. This observation was further supported by the results of supplementary single-axis sinusoidal tests on one armature-type relay and one motor starter which showed these devices to be most sensitive to input motions in the 2.5 Hz to 8 Hz range.

- Normally-closed contacts were more prone to chatter than normally-open contacts. At no time, however, was chatter observed in energized contacts regardless of their normal (i.e., deenergized) state; consequently, deenergized normally-closed contacts were found to be most susceptible to seismically-induced chatter. Furthermore, at no time did device chatter affect the ability of the devices to respond normally to commanded changes of state; in other words, the devices performed as intended even during strong motion.

- Reed-type relays, which we did not observe to chatter at any time during our tests, appear to be more resistant to seismic motion than the more conventional armature-type relays.

- Top bracing of the motor control center can increase the seismic capacity of both the MCC structure (by limiting cabinet motion) and the internal electrical devices (by increasing the resonant frequency of the cabinet frame).

We later applied these experimental results to develop probabilistic fragility descriptions for each type of electrical device in the MCC, referencing fragility to local ZPA at the device location. In addition to "best estimate" descriptions of device fragility, we estimated a "high confidence, low probability of failure" (HCLPF) capacity for each type of device; this parameter provides a convenient "lower bound" representation of device capacity useful for regulatory decision-making purposes. In general, the median capacity for the armature-type relays considered ranged from 5.2 to

6.1g local ZPA (i.e., local in-cabinet response, not motion at the cabinet base) with HCLPF ("lower bound") capacities ranging from 3.2g to 4.3g local ZPA. Taken as a group, these relays have a median estimated capacity of 5.6g and a HCLPF capacity of 3.6g local ZPA. Corresponding capacities for the starters tested were similar or higher depending on starter size. Note also that these results assume that input motion is oriented with the direction of contact motion; the results of our tests indicated that virtually no chatter occurs when the direction of input motion is perpendicular to that of contact motion.

As noted earlier, resource and time constraints make it impractical to explicitly develop probabilistic fragility descriptions by empirical means alone. Meaningful yet cost-effective fragilities testing can, however, be conducted within these constraints if it seeks not to explicitly develop "generic fragilities" broadly applicable to wide ranges of components, but rather to enhance understanding of how certain components fail ("failure modes"), what the important factors are that affect component performance, and what the relative influence of these factors is.

Testing in the form of "sensitivity studies" provides one method of gaining this understanding. In our Phase I demonstration tests, for example, we investigated MCC behavior (primarily functionability of electrical devices) through a carefully structured series of parametric sensitivity tests. The test results provided actual seismic capacities of the specific components tested, as well as a basis for estimating "single-parameter" fragility descriptions (i.e., referenced to local ZPA) including confidence limits and practical "lower bound" (i.e., HCLPF) seismic capacities. The tests also suggested possible hardware modifications to increase seismic capacity, such as top bracing of the cabinet or use of reed- rather than armature-type relays. More importantly perhaps, the test results suggest that other descriptions of fragility -- incorporating frequency effects, for example -- might be "more appropriate" for characterizing component behavior.

The "sensitivity study" concept applies to the interpretation of existing (e.g., qualification) data as well. For example, as part of our Phase I

component prioritization activities, we developed fragility descriptions for five components based on "high-level" seismic qualification data. Although not true "fragility" data, these test results provided useful information on component behavior under conditions exceeding any anticipated change in peak ground acceleration for plant sites in the eastern United States. It is important to recognize, however, that "sensitivity studies" in qualification testing often arise out of necessity as equipment is modified to meet requirements. The fragility analyst must therefore pay careful attention to the specific modifications made, particularly when seeking to apply data to similar components.

Clearly, even for functionally identical components, variations among manufacturers and models, in size and type, and in mounting and loading conditions imply that any fragility estimate -- or, for that matter, other methods of assessing component performance -- will be based to a certain extent on engineering judgement. It is important that this judgement be supported by as firm a technical basis as possible within practical constraints. Testing for "understanding" rather than for explicit fragilities would provide the following:

- Guidance to the fragility analyst as to what should be considered in developing a specific fragility description for a specific component.

- An improved basis for interpreting and applying test data obtained from other sources. This is particularly valuable, for example, using qualification data to assess actual component capacity.

- An improved basis for defining test conditions if more rigorous testing of a specific component is required.

- Guidance for developing screening techniques for reviewing actual plant equipment ("walkdown" techniques) and suggesting modifications for enhancing the seismic capacity of critical components.

We demonstrated through our Phase I tests how these objectives can be achieved for a motor control center and its internal devices. Testing following this basic approach could be similarly applied to develop failure probabilities and improve the seismic performance of other types of components.

1. INTRODUCTION

1.1 Background

Over the past decade methods have been developed to assess probabilistically how large earthquakes would affect nuclear power plants, particularly the associated risk to public health and safety. These probabilistic risk assessment (PRA) techniques combine "event trees", which describe the postulated accident scenarios (or "initiating events") capable of causing core melt, with "fault trees" describing the likelihood of equipment failures leading to a reduction in or loss of the ability of certain plant systems to perform their designated safety functions given that an initiating event occurs. A key element in the fault tree analysis is the "fragility" -- or likelihood of failure -- of various components under postulated accident conditions.

Application of these analysis techniques, both in NRC-sponsored research such as the Seismic Safety Margins Research Program and in commercial PRA studies, has indicated that potential accidents initiated by large earthquakes are one of the major contributors to public risk. However, component fragilities used in these analyses are for the most part based on limited data -- primarily design information and results of component "qualification" tests -- and engineering judgement. The seismic design of components, in turn, is based on code limits and NRC requirements that do not reflect the actual capacity of a component to resist failure; therefore, the real "seismic margin" between design conditions and conditions actually causing failure may be quite large. These elements combine to produce fragilities that are not only highly uncertain but also, in the view of many experts, are overly pessimistic descriptions of the likelihood of failure for many components. The observed performance of mechanical and electrical equipment in non-nuclear industrial facilities that have experienced strong-motion earthquakes tends to support this view. However, this same experience has also indicated that although a component may itself perform well in an earthquake, poor or inadequate support conditions may increase the likelihood of its "failure" in a safety sense. This also holds true in certain cases for aging or

environmental effects, which may require attention if an "adequate" description of fragility is to be achieved.

In order to improve the present fragility data base and develop realistic input for probabilistic risk assessments and seismic margin studies, the NRC commissioned a Component Fragility Research Program (CFRP). The CFRP is being conducted in two phases. Phase I comprised parallel efforts to (1) develop and demonstrate procedures for testing components to obtain new fragilities data, (2) identify by systematic ranking those components that most influence plant safety and are therefore candidates for NRC testing, and (3) compile and evaluate existing fragilities data obtained from various sources. The results of these three activities form the basis for a comprehensive evaluation of component behavior, based both on available data and on new testing, to be performed in Phase II of the program.

The CFRP supports the need for realistic inputs for probabilistic risk assessments and margin studies. This research seeks to test the hypothesis that electrical and mechanical components have greater seismic capacity that is presently assumed in seismic risk assessments, and, as a consequence, that the significance of the earthquake threat might be diminished in licensing decision making. In particular, the CFRP will result in the following:

- more realistic inputs for PRA applications. Improved descriptions of component fragility, based on actual failure data, will reduce the uncertainty inherent in subjective fragilities drawn from design information and results of equipment qualification testing.

- better understanding of component failure modes, of how various individual factors affect failure, and of the real "margin" between design or qualification requirements and conditions that might actually cause failure.

- guidance for development of seismic review procedures for existing plants, for interpretation of existing qualification or fragility data, and for specification of test procedures of equipment for which in-depth testing to "failure" is warranted.

These results will combine to improve our ability to more realistically assess seismic risk while at the same time contributing to elimination of unnecessary licensing delays to respond to seismic issues.

During Phase I, the Lawrence Livermore National Laboratory (LLNL) has performed component testing and prioritization, while the existing fragilities data base has been compiled by the Brookhaven National Laboratory (BNL). The specific objectives of the Phase I LLNL effort have been as follows:

Component Prioritization

- systematically identify and categorize electrical and mechanical components influencing plant safety, taking into account system and subsystem functional descriptions, operating and maintenance experience, expert opinion, past PRA results, regulatory concerns and existing test data.

- collect and utilize existing test data and operating experience to judge the relative seismic capacity of each component identified.

- identify "very important, low seismic capacity" components which then become priority candidates for future comprehensive testing.

Demonstration Testing

- develop procedures for component fragilities and seismic margins testing and demonstrate the effectiveness of these procedures through actual component tests.

- obtain useful fragilities and seismic margins data for the components tested.

- enhance understanding of failure mechanisms of the components tested.

This report describes our Phase I component prioritization activities. The Phase I demonstration testing program is documented in a companion report [1].

1.2 The Charleston Issue

One immediate issue facing the NRC in particular and the nuclear industry as a whole is that of potential revisions in the seismic design bases for older plants. Most older plants located in the eastern U.S. were either not subjected to the in-depth seismic design typical of more modern plants, or were designed for relatively low levels of safe shutdown earthquake (SSE). This practice reflected the long-held view that the eastern United States (i.e., east of the Rocky Mountains) was historically an area of generally low seismicity with only a few isolated records of large earthquakes. However, recent studies have suggested that the seismology of the region is such that the effects of large earthquakes -- such as those near Charleston, South Carolina in 1889 and New Madrid, Missouri in 1811-12 -- could affect much wider geographic areas than originally believed. The results of these studies therefore present NRC with the problem of resolving what constitute "more appropriate" design basis earthquakes for plants in this region.

Resolution of the "Charleston issue" brings with it the prospect of SSE levels significantly higher than the original design bases for plants. Reevaluation of certain plants for these higher SSE levels could result in certain design allowables being exceeded, potentially jeopardizing the continued operation of these plants. However, exceedance of design allowables does not necessarily compromise plant safety, if it can be shown that sufficient "reserve" capacity is available to absorb increases in postulated seismic loads. At least three potential options exist for this purpose:

- Demonstrate equipment "ruggedness." Mechanical and electrical equipment related to plant safety is typically "qualified" to demonstrate its ability to function as intended during a site-specific SSE. The "seismic margin" between design level and actual failure is not typically measured as a part of qualification testing; most experts believe, however, that many equipment items have sufficiently high seismic capacity -- or "inherent ruggedness" -- that they would continue to function normally

even when subjected to input motions well in excess of qualification requirements.

Demonstrating that this ruggedness exists, either through actual failure tests or by alternate means, therefore represents one potential response to a revision in SSE levels. Many organizations are actively pursuing this option. The Electric Power Research Institute (EPRI), for example, is currently applying existing qualification data to develop "Generic Equipment Ruggedness Spectra" (or "GERS") for certain items of plant equipment. Together with EPRI, the Seismic Qualification Utility Group (SQUG), comprising plant owners potentially affected by the Charleston issue, is compiling information on the performance of heavy industrial facilities (which contain many equipment items typically found in nuclear power plants) during actual strong earthquakes.

- Perform "less conservative" response analyses. Equipment in many older plants may have high seismic margins owing to relatively conservative response analyses being used in plant design (e.g., to predict equipment input motions). Many factors can affect the degree of conservatism, including (1) the specific analytic methods used to predict component response (e.g., two- vs three-dimensional finite-element analysis, time-history vs response spectrum analysis, coupled vs uncoupled analysis), either singly or in combination, (2) input data such as damping values, and (3) application of safety factors to calculated results to "insure" conservatism. Just what constitutes a "conservative" analysis is subject to interpretation, but in general the less sophisticated an analysis is, the more conservative it tends to be.

  If design is done by analysis, the apparent margin is influenced by the particular analytic method used. A "conservative" method of analysis may result in an artificially low margin. Taking advantage of more refined -- "less conservative" -- analysis techniques to evaluate an older plant thus represents a possible means of more realistically predicting (i.e., reducing) responses to increased seismic loads in order to meet revised design criteria.

- Apply revised NRC requirements. Recent or pending changes in NRC regulations affecting postulated design loads allow or would allow relaxations such as decoupling SSE and certain loss-of-coolant accident (LOCA) loads, elimination of dynamic effects (pipe whip, jet impingement, hydrodynamic loads) associated with certain pipe breaks, and use of alternative descriptions of damping. Plants originally designed for loads or load combinations affected by the regulatory actions might benefit in that these loads or load combinations would no longer need to be considered in a reevaluation for increased seismic loads, or would be reduced through use of alternative (i.e., more realistic) input criteria for calculating loads.

The testing discussed in this report concerns itself with the first of these items, namely equipment ruggedness. It is important to keep in mind, however, that future responses to more stringent seismic design criteria may be able to take credit of all three to one extent or another. Consequently, any assessment of seismic capacity must take the other two factors into account in order to assure it is conducted on a reasonable basis.

1.3 Definition of Component Fragility

"Fragility" is a term commonly used to describe the conditions under which a component (or, in general, a structure, a piping system, or piece of equipment) would be expected to fail. In this report we are concerned with seismic fragility, in other words, what levels of earthquake-induced input motion would be required to cause component failure; it is important to keep in mind, however, that fragility can in principle be defined for any input condition affecting component performance. Failure can be characterized as either functional (e.g., erratic behavior, failure to perform intended function) or physical, or as the exceedance of some predetermined performance criteria (such as a limit given in a design code).*

---

* In this discussion "physical failure" is used instead of the more common term "structural failure" to make clear that we are concerned only with mechanical and electrical equipment, and not with plant structures.

One interpretation of component fragility -- which we will refer to as the "fragility level" -- evolves from qualification testing. In seismic qualification testing, a component is subjected to input motion characterized by a specified waveform describing input level (seismic acceleration) as a function of frequency. The component is "qualified" if it continues to perform its intended function when its response to this input motion -- the "test response spectrum," or TRS -- meets or exceeds pre-determined acceptance limits (the "required response spectrum," or RRS). In qualification testing, the TRS is usually measured at the component support points.

Although it may establish the adequacy of a component for a particular seismic environment, a successful qualification test does not directly provide data on what input motion levels actually result in component failure. This can be (and sometimes is) done by retaining the original input spectrum and then increasing the input level until "failure" (however it is defined) occurs. The TRS at failure represents the "fragility level" or "ruggedness" of the component; the difference between the fragility level and the qualification level thus represents the seismic margin of the component.

Fragility is described differently when used for PRA purposes or for other types of probabilistic analysis. In this case, the fragility of a component represents the probability of its failure -- or more rigorously speaking, the probability of attaining a defined "limit state" -- conditioned upon the occurrence of some level of forcing or response function. It may be expressed in terms of a local response parameter (for example, input motion at the component mounting location) or can be tied to a more global forcing function such as free field peak ground acceleration (PGA). Note however that when fragility is anchored to a forcing function, the further removed the component is from that forcing function, the more factors there are (such as structural response and soil-structure interaction) that must be considered in the fragility description.

The probability of failure is typically described by a family of "fragility curves" plotted at various levels of statistical confidence (see Fig. 1-1). The central, or "median" function represents the fragility analyst's best estimate of the "true" fragility of the component taking into account all significant factors which, in the analyst's judgement, might contribute to failure. The central point (50% probability of failure) on this curve represents the "median capacity" of the component; ideally, this probabilistic value would correspond with the deterministic "fragility level" of the component. The fragility function is a cumulative distribution usually characterized by a log-normal function with this median value and a logarithmic standard deviation β_R which describes the "random" variation in the parameters affecting fragility. In a description of seismic fragility, for example, this parameter might represent the differences in real earthquake ground motion compared to the input motion that a component is subjected to in qualification or fragilities testing. Note that the random uncertainty controls the slope of the fragility function; the less random uncertainty, the steeper the fragility function becomes. As random uncertainty is reduced towards zero, the fragility "curve" approaches a step function with its break point at the fragility level of the component.

The 5% function and 95% function in Fig. 1-1 represent the "modeling uncertainty" in the median fragility function. These bounds, which may also be referred to as 5% and 95% confidence limits, are based on the assumption that there is uncertainty in the median capacity; this uncertainty is characterized by a logarithmic standard deviation β_U. Simply stated, the 95% confidence limit implies the following:

- there is only a 5% subjective probability ("confidence") that the actual fragility level is less than the median capacity indicated for the 95% fragility function.

- we are 95% confident that the "true" fragility function for the component would be equal to or greater than the 95% function.

Modeling uncertainty, often described as "lack of knowledge" about the component in question, reflects the adequacy (or inadequacy) of information -- component damping values, for example -- used by the fragility analyst to form his judgements about component capacity. Thus, modeling uncertainty in fragility descriptions has a subjective rather than a "random" basis as is true in the statistical sense.

For any given component, empirically developing a statistically meaningful seismic fragility would require that a large population of identical components (e.g., several hundred or several thousand) be subjected to successively higher levels of acceleration and the distribution of failures (however "failure" is defined) be recorded as a function of acceleration level. Practical constraints on time and resources clearly make this infeasible for a single component under well-defined load conditions, let alone for the effectively infinite combinations and permutations of component type, manufacturer, mounting, and loading conditions that could be identified for actual nuclear power plants. Therefore, an alternative approach is necessary to experimentally gain an insight into fragility.

Our approach to assessing fragility takes advantage of the fact that for practical PRA applications, a limited or "lower bound" fragility description may be adequate. In a probabilistic analysis, failure occurs only when the probability distributions of response and fragility overlap; therefore, only the lower tail end of the fragility curve may be of interest from a PRA standpoint. For components having a high seismic capacity (high "ruggedness"), the overlap of the response and fragility distributions could conceivably be so small under all credible loading conditions as to imply that the probability of failure is negligibly low.

One method of developing a "lower bound" fragility is to estimate the so-called "HCLPF" (High Confidence, Low Probability of Failure) capacity for the component. The HCLPF capacity considers both the random and modeling uncertainty in the median capacity. The definition of HCLPF used in the CFRP is that adopted by the LLNL Seismic Design Margin Program, namely that value of the forcing or response function (such as seismic acceleration) for which

we have "95% confidence" that the probability of "failure" is less than 5 percent.[2] According to this definition, if the median capacity of a component is defined by a peak acceleration with value A, the corresponding HCLPF capacity (i.e., HCLPF acceleration) is obtained from the following numerical relationship:

$$A_{HCLPF} = A \exp [-1.65 (\beta_R + \beta_U)] \quad (1\text{-}1)$$

where β_R and β_U represent the random and modeling uncertainties, respectively. The median capacity A can be determined by component tests, either to actual failure or to some threshold or "cut-off" limit. The cut-off might be applied, for example, in testing certain components whose actual median capacities were significantly above any response levels of regulatory interest.

The HCLPF capacity provides a practical means of addressing variations that inevitably arise between actual plant conditions and test conditions, variations that might otherwise be difficult to parametrically quantify by testing alone. For example, the random uncertainty β_R allows for variations in real earthquake motion compared to test input motion, variations in building floor response, or (e.g., for cabinet-mounted electrical devices) random variations in cabinet response. The modeling uncertainty β_U can account for variations in real damping values, or in component mounting conditions, or in the response of functionally similar components of different size or supplied by different manufacturers. These uncertainties can be quantified by systematically structuring test conditions in the form of "sensitivity studies" to investigating the effect of various parameters on the measured median capacity of the device tested. This was the basic approach taken in our Phase I demonstration tests.

The HCLPF approach has the added advantage that, in the absence of complete fragility data, a "lower bound" fragility can still be defined for a seismically qualified component by assuming its qualification level also represents its HCLPF capacity. Engineering judgement can then be applied to estimate the uncertainty parameters and thus make inferences about the median capacity

Note that because the HCLPF capacity by definition presumes a five percent probability of failure, while "qualification" implies no failure, this approach tends to be conservative. It may in fact be overly conservative if qualification levels are low, as would be the case for many plants in the eastern United States. However, HCLPF capacities based on "high level" qualification data -- from plants in the western United States, for example -- can provide useful lower bound fragilities for plants having relatively low design basis earthquakes. Section 3 of this report describes how we used this approach to infer the actual capacity of selected electrical equipment.

In itself, the HCLPF capacity is a useful parameter on which to base regulatory decisions concerning seismic performance. However, extreme care must be exercised in selecting "reasonable" values of β_R and β_U when using a HCLPF capacity derived from qualification data to infer the actual capacity or "fragility level" of a component. The reasons for this are two-fold:

- as shown in Fig. 1-2, the slope of the fragility curve becomes more shallow as random uncertainty (β_R) increases. Therefore, the resultant median capacity on the 95% curve (and, for constant β_U, the inferred fragility level) also increases with increasing random uncertainty.

  As shown in Fig. 1-3, however, if the fragility level of the component is known (e.g., from actual failure tests), then the HCLPF capacity derived from the median capacity decreases with increasing random uncertainty.

- similarly, as modeling uncertainty (β_U) increases, the offset between the 95% fragility function and the 50% function also increases, implying an increase in the inferred fragility level. If, on the other hand, the fragility level is known, an increase in modeling uncertainty drives the HCLPF capacity towards lower (i.e., more conservative) values.

The above exercise illustrates how a "bottom-up" approach towards estimating median capacity (i.e., inferred from HCLPF capacity) can imply that fragility

level increases with uncertainty, which is clearly non-conservative. This observation suggests that the reverse approach -- basing HCLPF capacities on measured fragility levels -- is preferable for assessing seismic performance. For a given fragility level, such a "top-down" approach yields lower (i.e., more conservative) HCLPF capacities as uncertainty increases.

1.4 General Approach to Fragilities Testing

As discussed earlier, resource and time constraints make it impractical to develop meaningful fragility descriptions by empirical means alone. Even for nominally identical components, variations among models and manufacturers, and in mounting and loading conditions imply that any fragility estimate will be based in large part on engineering judgement. Meaningful fragilities testing can, however, be conducted within practical constraints if it focuses on understanding how various factors influence component behavior rather than on developing fragilities explicitly. Such testing would be conducted according to the following steps:

(1) identify a representative component or sample of components for testing. Such a sample might not necessarily be "generic" in the purest statistical sense, but should attempt to include significant variations within a given component type (spring-contact vs reed-type relays, for example).

(2) identify failure modes and the relevant forcing or response functions. Characterize "failure" (either functional or physical) in terms of a suitable parameter that can be measured experimentally.

(3) identify factors or "technical issues" affecting component failure; such factors might include, but not necessarily be limited to, variations in mounting, input motion, and component damping. Design experimental program to parametrically vary those factors judged to be important.

(4) perform tests to identify when failure occurs, i.e., component median capacity. Such tests might, for example, follow qualification procedures (e.g., use of same input spectra) but at elevated input motion levels. Alternatively (particularly for "high capacity" components), test to a pre-determined level to establish a "lower bound" failure threshold.

(5) use test results to empirically estimate median capacity; note that this result is equivalent to the deterministic "fragility level" generated as a part of some qualification tests. Based on component behavior over all conditions considered, develop estimates of random variability and modeling uncertainty in the empirically derived median capacity.

Although this approach does not remove subjectivity from the process of describing component fragility, it does improve the basis on which these judgements are made. Furthermore, it can provide an improved basis for interpreting data from other sources or for defining test conditions if more rigorous testing of a specific component is necessary.

1.5 Phase I Test Objectives

Following this general approach, the specific objectives of our Phase I demonstration tests were as follows:

- demonstrate, for a typical item of nuclear power plant hardware, that we could characterize its fragility.

- investigate the dependence of fragility on a specific "technical issue" affecting equipment behavior.

- generate useful information regarding the actual seismic capacity of the equipment tested.

- develop practical fragility descriptions based on the experimental data, suitable for application in probabilistic risk assessments.

- provide guidance for interpretation of test data available from other sources.

We selected as our test specimen a 480-volt motor control center housing relays and motor controllers of various types and sizes. The functional fragility of the electrical devices was evaluated using device chatter as the relevant "failure" mode. The cabinet itself was viewed mainly as a "typical" load transmission device between the floor and the devices.

It is important to note that the selection of an MCC as our test specimen was made with no intent to "target" motor control centers out of any special concern. Instead, we viewed the MCC as having certain characteristics which would allow us to best demonstrate our general approach to fragilities testing. While our prioritization activities have generally identified MCCs (and their internal devices) as important components, our selection of an MCC for demonstration testing did not depend on its importance relative to other components.

As our "technical issue" of interest, we investigated the effect of base flexibility on electrical device behavior by systematically varying the mounting configuration of the MCC. Besides addressing the specific question of how base mounting might affect device behavior, testing with different mounting configurations offers the following useful insights:

- if device (e.g., relay) behavior as a function of <u>local</u> in-cabinet response varies insignificantly with changes in the mounting of the MCC, this result would imply that fragility data from tests on individual devices would also apply for the same devices mounted in cabinets.

- by correlating device fragility <u>only</u> to local in-cabinet response (in particular, ZPA) independent of MCC mounting configuration and device location, the scatter in the experimental results (and thus the uncertainty in fragility descriptions developed from the data) should encompass such issues as variations in cabinet transmissibility and in-cabinet device location.

At the outset of this program we recognized that other factors, such as aging and environmental effects, may also influence device behavior. In Phase I the purpose of our testing was to demonstrate a capability; consequently, we found it most convenient to neglect these effects. A more definitive assessment of MCC behavior, however, would require that these issues be addressed.

1.6 General Assumptions

In the Component Fragility Research Program, we have made certain basic assumptions that have influenced both component prioritization and our Phase I demonstration tests. These include the following:

- Characterization of seismic capacity. We characterize earthquakes by their peak ground acceleration (PGA), taken to be the average value of the two horizontal components and assumed to occur on the soil free surface and at the top of the finished grade. To relate the seismic capacity of a component, however, we have chosen as our basis the local excitation at its support points, in other words, the floor response that it would see as a result of amplification by the structure. We defined as "high capacity" components those that would remain functional when subjected to local response spectra characterized by relatively broad-band frequency content and a 2g (or greater) zero period acceleration (ZPA). Using realistic definitions of earthquake ground motion and structural response prediction, this level of local response is expected to bound structural responses resulting from earthquakes of up to 1g PGA. This level provides a useful threshold for test purposes, because practical lower bounds on fragility can be obtained without necessarily testing a component to destruction.

  Similarly, we defined as "intermediate capacity" components those that would be expected to "fail" (either functionally or physically) when subjected to local ZPA levels between 1g and 2g. "Low capacity" components would fail at local response levels less than 1g ZPA.

Following these general guidelines, we limited our Phase I input motion levels to a maximum 2g horizontal ZPA at the base of the motor control center, although actual ZPA levels as high as 2.5g were recorded during some tests. This table motion resulted in local in-cabinet ZPA levels (i.e., at device locations) as high as 10g depending on location.

- High frequency excitations. Although recent earthquake records confirm that high frequency components of ground motion can be present in the free field, the focus of the CFRP is on earthquake ground motions dominated by low-frequency ground motion, i.e., less than 9 Hz. In our demonstration tests, we concentrated on low-frequency behavior, although some high-frequency response data were also recorded.

- Degraded components or behavior. At least three potential sources of physical component degradation or degraded behavior can be identified: design and construction errors, aging, and partial failure.

  For demonstration testing, we used new components which we assumed had been properly constructed as designed. Although we did not explicitly address the design and construction error issue in our demonstration tests, systematic variation of MCC base flexibility does provide insight into how improper cabinet mounting can affect the behavior of internal electrical devices.

  The behavior of aged components may be addressed in Phase II, either directly (such as testing components removed from actual plant service) or through the results of aging test programs conducted by others.

  We have not identified modes of partial failure for any of the components in our Phase I tests. The definition of "failure" as it relates to the components in our demonstration tests is given as part of the test procedures.

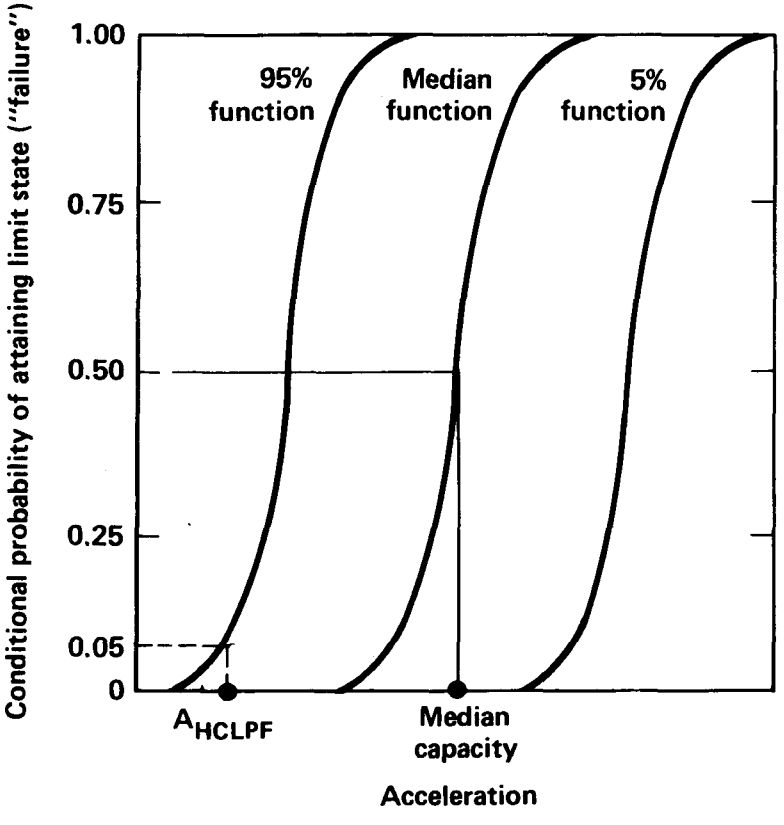

Figure 1-1. Typical curve set representing component fragility.

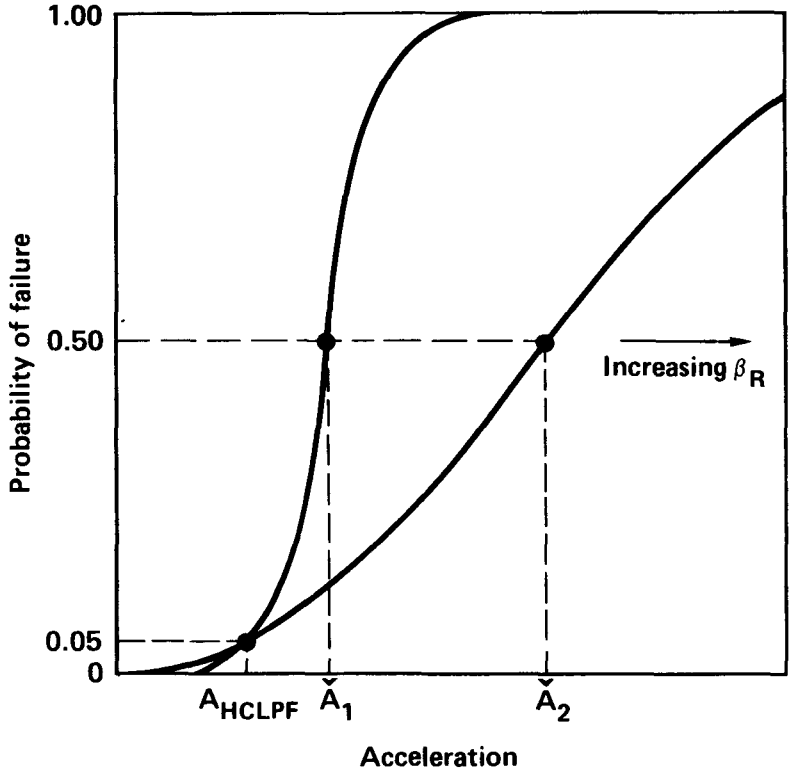

Figure 1-2. Typical 95% fragility function showing how increasing random uncertainty affects median capacity derived from a HCLPF value. For constant β_U, the inferred fragility level of the component (i.e., median capacity of the 50% function) would be similarly affected.

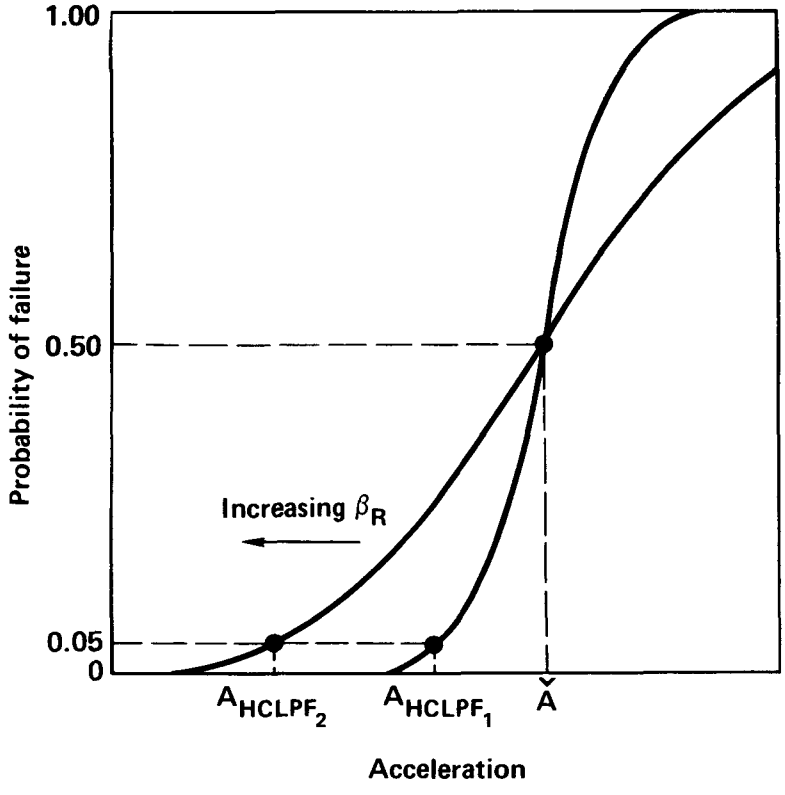

Figure 1-3. Typical 95% fragility function showing how increasing random uncertainty affects the HCLPF value derived from a constant median capacity. For constant β_U, the effect would be the same for HCLPF values derived from a constant component fragility level.

2. TEST SPECIMEN

2.1 General Description

Our Phase I demonstration tests were based on a motor control center as test specimen. We based our selection on the following considerations:

- the behavior of contact-type electrical devices, such as relays, has generally been regarded as important to plant safety. An MCC offers a convenient test bed for simultaneously investigating the behavior of various types and sizes of electrical devices in an environment characteristic of that in actual plants. Note that our demonstration tests focused on the functional fragility of the individual electrical devices in the MCC; the cabinet itself was viewed primarily as a load transmission device.

- variations in the rigidity of the cabinet-to-floor connection in a plant would affect the degree to which building floor responses would be amplified at device locations. We chose to investigate the effect that "base flexibility" has on the behavior of cabinet-mounted electrical devices.

- although not a governing criterion for our selection, we expected that our prioritization activities would generally identify MCCs as an important component. This indeed proved to be the case.

Most U.S. nuclear power plants -- about 80 percent -- use motor control centers manufactured either by Westinghouse or by General Electric. The remaining 20 percent use MCCs supplied by other vendors, mainly Cutler-Hammer. After considering all three vendors, we selected as our test specimen a new 480-volt Westinghouse "Five-Star" MCC. Introduced in 1975, the Five-Star is the current basic model marketed by Westinghouse for industrial and power system applications. Our selection of the Five-Star reflected the following considerations:

- it is essentially identical to the Type W motor control center manufactured by Westinghouse from 1965 to 1975, various configurations of which are found in many nuclear power plants of this vintage. The differences between the Five-Star and the Type W are mainly dimensional (about one inch in column width and depth) and cosmetic. Both use nominally the same electrical devices.

- by selecting new equipment (as opposed to an older MCC removed from actual plant service), we had more control over the initial condition of the specimen. Therefore, prior aging was not a factor in our demonstration tests.

Our selection of the Westinghouse unit over the General Electric and Cutler-Hammer units was based mainly on logistical procurement considerations, and is not to infer that we have any special concern about its seismic capacity relative to MCCs supplied by other vendors.

Structure

The standard vertical structure (or "column") of the Five-Star MCC is 90 inches high by 20 inches wide. Complete motor control centers are typically built up from two to eight column units; Fig. 2-1 shows a three-column MCC with front-mounted electrical devices. Front-mounted MCCs, often located next to building walls, are accessible from one side only and are either 16 inches or 21 inches deep. Back-to-back mounted structures, accessible from either side, are 21 inches deep. The MCC selected for demonstration testing, shown in Fig. 2-2, is a front-mounted assembly composed of three 20"x21"x90" columns. Weighing approximately 1080 pounds, this assembly was the largest that could be tested to the input motions that we required.

The structure framework is made of 12 gauge formed-steel channels. The sub-frames for the front and rear of each structure are welded. These sub-frames are then bolted to longitudinal members to form the complete frame which is rigid and self-supporting. Side, back, and roof sheets are 14 gauge steel, and are mounted with screw fasteners for quick removal when desired.

Each 90-inch high column has 9-inch horizontal wireways at the top and bottom which are connected by a vertical wireway running along one side. The top wireway contains a horizontal bus interconnecting the three columns while the vertical wireways in each column are used for point-to-point wiring. The remaining height is available for up to 12 6-inch high spaces ("X" spaces) which make up, either singly or in combination, the compartments which house the various electrical devices. Doors mounted on removable pin hinges are provided on all MCC compartments, vertical wireways, top horizontal wireways, and bottom horizontal wireways. All doors are 14 gauge steel with a 1/2-inch flange and are each fitted with two quarter-turn screw fasteners [3].

The MCC tested is a three-wire, NEMA* Class 1 unit with gasketed doors and a 600-ampere horizontal main bus consisting of aluminum with tin plate. Electrical devices are mounted in draw-out units (also called "unit wrappers" or "buckets") which fit into the various MCC compartments. Each unit has four mounting points, two on each side, which support the unit in the MCC structure. These engage guide rails located near the top of each compartment; this mounting system allows the units to be inserted and withdrawn easily. The units are secured at the top center by a quarter-turn bolt; additional support is provided by three "stabs" on the back which connect the electrical devices with the MCC vertical bus. A typical draw-out unit is shown in Fig. 2-3, in this case housing a motor controller.

The units in our test specimen are 12 to 18 inches high, but in other applications a single unit may fill the entire available space in a single column. All spare spaces in our test specimen (i.e., those not containing any motor controllers) were fitted with blank draw-out units, most of which we later used for installation of the relays tested; note that these units did not include the stabs found on the back of the controller units.

Certain motor control centers may include sheet metal divider panels between the columns. Although installed to provide <u>electrical</u> separation between columns, these dividers can also act as "shear panels" providing

---

* National Electrical Manufacturers Association

additional rigidity for the MCC cabinet in the front-to-back direction, thereby potentially improving its structural performance. These panels are found in older motor control centers, and may therefore be present in some older nuclear power plants; later vintage motor control centers (including the Type W and the Five-Star) do not include these panels as a standard item.

Cabinet Mounting

During testing the MCC was secured to a 1-inch thick steel plate with 3/8-16x2" mounting bolts; the steel plate was then welded to the shake table. This arrangement allowed us to periodically remove the MCC from the table without disturbing the bolted connection. The cabinet rested on two parallel 3"x5 lb C-channels ("sill channels") through which the bolts passed (see Fig. 2-4). The bolts were torqued to 25 ft-lb; torque values were periodically checked during testing to detect any inadvertent loosening of the bolted connection. As shown in Fig. 2-6, two bolting patterns were investigated: two bolts per column (the pattern recommended by the MCC vendor) and four bolts per column.

To investigate the effect of base flexibility on the structural behavior of the MCC and on the functional behavior of the electrical devices, we conducted multiple tests on each of the following four mounting configurations:

(1) four mounting bolts in the base of each column and a simulated wall support at the top rear of the cabinet (see Fig. 2-5). Top bracing is a common action taken to enhance the stability of cabinet structures during seismic events.

(2) four mounting bolts in the base of each column and no top support.

(3) two mounting bolts in the base of each column and no top support. This configuration represents that most common in actual plants, being a "standard" mounting configuration recommended by the manufacturer.

(4) four mounting bolts in the base of each column with diagonal braces in the lower portion of each column (see Fig. 2-6).

We had originally considered as one mounting configuration a direct welded connection between the cabinet and the steel plate. We did not include this configuration in our final test plan because our main interest was in the effect of more flexible -- and not more rigid -- cabinet mounting. However, the four-bolt mounting pattern does provide insight into the effects of the added stiffness that would be imparted by a welded connection.

2.2 Electrical Devices

For demonstration purposes we chose to investigate the functional behavior of two general types of electrical devices: motor starters and relays. Tables 2-1 and 2-2, respectively, list the specific motor starters and relays tested. The particular models selected represent a sample of standard MCC devices typical in function of those found in actual plants. Nevertheless, we do not represent that any test results obtained for these devices are generically applicable to all similar devices, nor is our selection intended to imply that we necessarily regard these as most important to plant safety. Identification of specific starters and relays "most important" to plant safety was outside the scope of our Phase I test program.

Motor Controllers

Motor controllers stop, start, and (where applicable) reverse motors attached to plant equipment. As shown in Fig. 2-3, a typical controller comprises many components in addition to the actual starter. Our tests included the following front-mounted circuit breaker combination controllers:

- full-voltage non-reversing (FVNR), two each in NEMA sizes 2, 3, and 4. In actual plant applications, non-reversing controllers are used with motors driving single direction of rotation equipment such as pumps and fans. Size 1 starters were excluded from our test program because of their similarity to the Size 2 starters.

- two full-voltage reversing (FVR) in NEMA size 2. In plant applications, reversing controllers are used with bi-directional equipment such as motor-driven valve operators, and may account for up to 80 percent of all controllers in a typical nuclear power plant. In one plant reviewed as part of this study, Size 1 and Size 2 FVR controllers open and close virtually all safety class valves.

All controllers were manufactured by Westinghouse and came equipped with a control transformer, a secondary fuse, and red and green indicating lights. Units containing circuit breakers alone were not included because our emphasis was on the functional behavior of the controller starters. However, testing the combination controllers provides data that is also applicable to breaker-only units.

Table 2-1 lists the specific starters selected for our tests. Starters typically include main contacts, one for each phase of the main power supply to the controlled motor, and auxiliary contacts which are used for various control and instrumentation purposes. In some circuits, one pair of auxiliary contacts is reserved as an electrical "latch" to "seal-in" (i.e., provide a steady current flow to) the solenoid coils that in turn actuate the main contacts. Controller circuits also typically include additional auxiliary relays to, for example, activate lights indicating whether or not the controlled motor is running and, where applicable, in what direction. In actual plant applications, these auxiliary relays may be mounted in the MCC or nearer the indicator light location (e.g., in the plant control room). Figures 2-7 and 2-8, respectively, show diagrams of typical controller circuits for non-reversing and reversing starters. Note that the FVR starter has two identical sets of main contacts; the direction of motor rotation is reversed by switching two phases of the main power supply. Note also for reversing controllers that if, during a seismic event, chatter were to close both sets of main contacts simultaneously, a short circuit -- and possible motor damage -- would result. To prevent this from occurring, reversing controllers in many plants (and in our tests) are equipped with mechanical interlocks which prevent simultaneous closure of the forward and reverse

contacts; note however that these interlocks do not prevent chatter per se from occurring.

Controllers were mounted in a manner consistent with standard commercial practice; Fig. 2-9 shows a typical controller installation in the MCC tested. For all controllers, the starters were oriented such that the direction of contact motion was aligned with front-to-back cabinet motion.

Relays

Fourteen general purpose relays were mounted in the spare draw-out units of the MCC. These relays, listed in Table 2-2, are typical in function to relays used in actual plant motor control centers. The particular relays selected included the following:

- standard industrial relays supplied by three different vendors (Westinghouse, General Electric, and Square-D).

- relays having either wired or plug-in electrical connections. Note that all wired connections utilized either ring lugs attached to screw terminals or bare wire ends held by screwed compression terminals.

- relays having either armature-type or reed-type contacts.

Figure 2-10 shows a sample relay arrangement in one MCC draw-out unit. All relays except for two were mounted such that their direction of contact motion was aligned with front-to-back cabinet motion. The sole exceptions were the two Square-D Type KP relays, whose direction of contact motion was oriented vertically.

Figure 2-11 diagrams all controller and relay locations in the MCC tested. The photographs in Appendix A show "open-door" details of controller and relay installation for each MCC compartment.

2.3 Characterization of Failure

To describe the fragility of any component, one must select (1) a suitable definition of component "failure" (the failure "mode"), and (2) a parameter against which the probability of failure can be referenced. Our demonstration tests focused mainly on the functional behavior ("failure") of the electrical devices housed in the MCC. We also considered structural failure of the MCC cabinet itself, although this was of less concern based on past qualification experience.

In PRA applications, fragility may be referenced to peak ground acceleration (if soil and structural response are known) or to either spectral or zero period acceleration at the component base. In our demonstration tests, we sought to correlate device behavior against local in-cabinet ZPA, i.e., at the device location. This allowed us to describe device fragility on a basis that, in principle, is independent of both device location in the cabinet and the particular mounting configuration of the cabinet itself. The selection of ZPA as our reference parameter, rather than spectral acceleration, reflected the PRA practice of using a "single-parameter" description of fragility.

The structural behavior of the MCC cabinet was correlated against the ZPA of the input table motion; note, however, we did not develop structural "fragility curves" for the cabinet. The following discussion describes how "failure" was characterized in each case.

Functional Failure

We used contact "chatter" -- contact motion causing one or more momentary uncommanded changes of state -- to characterize the functional behavior of each electrical device tested. For qualification purposes, chatter is usually defined as any uncommanded state change longer than a specified duration; the occurrence of chatter therefore indicates "failure" of the device. In our investigation, we did not test to pre-determined acceptance criteria, but instead recorded for each device the following parameters related to its functional behavior:

- the number of chatter events. Single events, such as momentary "bouncing" of contacts, often occur as a normal part of commanded state changes and therefore do not represent "functional failures" according to our definition.

- the duration of individual chatter events. In our demonstration tests, we categorized chatter events according to duration, ranging from 2 ms (the threshold typically applied in qualification tests) to over 80 ms.

- the effect of device state on occurrence of chatter. Past tests on similar devices have indicated that spurious contact motion is highly dependent on whether or not the contact coil is energized at the time strong motion occurs.

As discussed in Section 5 of this report, these parameters were used as the basis for describing the functional fragilities of the various relays and starters housed in the motor control center.

Structural Failure

Vendor tests have shown that electrical devices such as those included in our tests typically show high resistance to structural failure; in other words, seismic excitation would be expected to affect functional behavior before any physical damage to the device occurred. Consequently, the only likely structural failures in our demonstration tests were limited to the MCC cabinet. Types of possible damage anticipated included the following:

- non-destructive effects of cabinet shaking, such as cracking of paint.

- permanent but non-destructive damage such as deformation of cabinet structures, ovalization of bolt holes, or "dishing" of mounting bolt washers.

- cracking or breaking of welds, destruction of cabinet structures, pull-out or breaking of mounting bolts. Although outside the scope of our demonstration testing, pull-out of concrete anchors might also be expected to occur in actual plant applications.

We visually inspected the cabinet for signs of damage after each test. In later tests, as the likelihood of permanent cabinet damage increased, we also measured strain levels at selected locations on the cabinet frame.

2.4 Safety Implications of Contact Chatter

The number and duration of chatter events combine to perturb the output signal from any contact-operated electrical device. Whether or not such perturbations would actually constitute a "failure" affecting plant safety would depend on the mechanical component or the type of electrical circuit that the device was connected to. Consider, for example, a starter connected to a safety injection system pump motor. Chatter in the main contacts of the starter would almost certainly affect the power supply to the motor. If, however, the characteristics of the motor were such that it started and ran normally despite these perturbations, the starter would have performed its intended function; in a safety sense, "failure" would not have occurred.

Similarly, it is conceivable that auxiliary contact chatter may be sufficiently severe (in terms of number and duration of chatter events) that the main contacts would inadvertently change state even if they did not themselves chatter due to seismic acceleration. Whether or not this would actually occur, however, depends on the characteristics of the particular starter, particularly those of the coil actuating the main contacts.

The safety implications of contact chatter can depend on a number of factors, many related to circuit design. Some of these include the following:

- seal-in circuits. As discussed earlier, many motor control circuits use starter auxiliary contacts to provide a "seal-in" function. Seal-in

circuits are particularly sensitive to chatter because once energized, even if by only a momentary "kissing" of contacts, the controlled motor continues to run until stopped by separate operator action. In certain cases, such as for containment cooler fans or for motor-operated isolation valves, inadvertent starting and "sealing in" of a motor may be tolerable. In other cases -- control valves in safety injection systems, for example -- this may not be so.

When inadvertant starting cannot be tolerated, several options are available to the circuit designer. One, of course, is to design or redesign circuits so that auxiliary contacts are not used for sealing purposes. If a sealing function must be retained, other options are to prevent chatter by using starters that have been qualified for suitable required response spectra or, if chatter is anticipated, introduce short delay timers (e.g., pneumatic timers) between the auxiliary contacts and the main contact coil to counteract any chatter effects.

- short circuits in FVR starters. As noted earlier, a reversing starter uses two sets of main power contacts, one for each direction of motor rotation. Although chatter in either contact set might not in itself affect motor operation, simultaneous closure of forward and reverse contacts could cause a short circuit and with it possible motor damage. This potential problem can be avoided by a mechanical interlock between the two contact sets which, while not preventing chatter per se, does prevent simultaneous contact closure.

- auxiliary circuits. Many relays and auxiliary contacts are used, for example, to actuate control panel lights. Contact chatter in such devices might cause momentary flickering of indicator lights but would have no adverse safety implication.

In any case, it is important to keep in mind that contact chatter alone does not necessarily imply "failure" in a safety sense. Any final evaluation of

safety significance must be made on the basis of circuit design; such evaluations were not in the scope of our demonstration test program.

Table 2-1. Motor starters included in Phase I MCC tests.

Vendor	Size	Type	Model No.	Max Hp	Quantity	Code
Westinghouse	2	FVNR	A206	20	2	S-2
Westinghouse	2	FVR	A216	20	2	S-2R
Westinghouse	3	FVNR	A206	40	2	S-3
Westinghouse	4	FVNR	A206	75	2	S-4

Note: Power ratings given are for 480 VAC constant horsepower motors

Table 2-2. General purpose relays included in Phase I MCC tests.

Vendor	Model	Type	Catalog No.	Poles	Quantity	Code
General Electric	CR	Armature	CR120B03322	6	4	GE
Westinghouse	AR	Armature	AR 660A	6	3	W
Square-D	X	Armature	8501 XO-60	6	3	X
Square-D	KP	Armature	8501 KP-12	2	2	KP
Cutler Hammer	Powereed	Reed	D40RR22A	4	2	CH

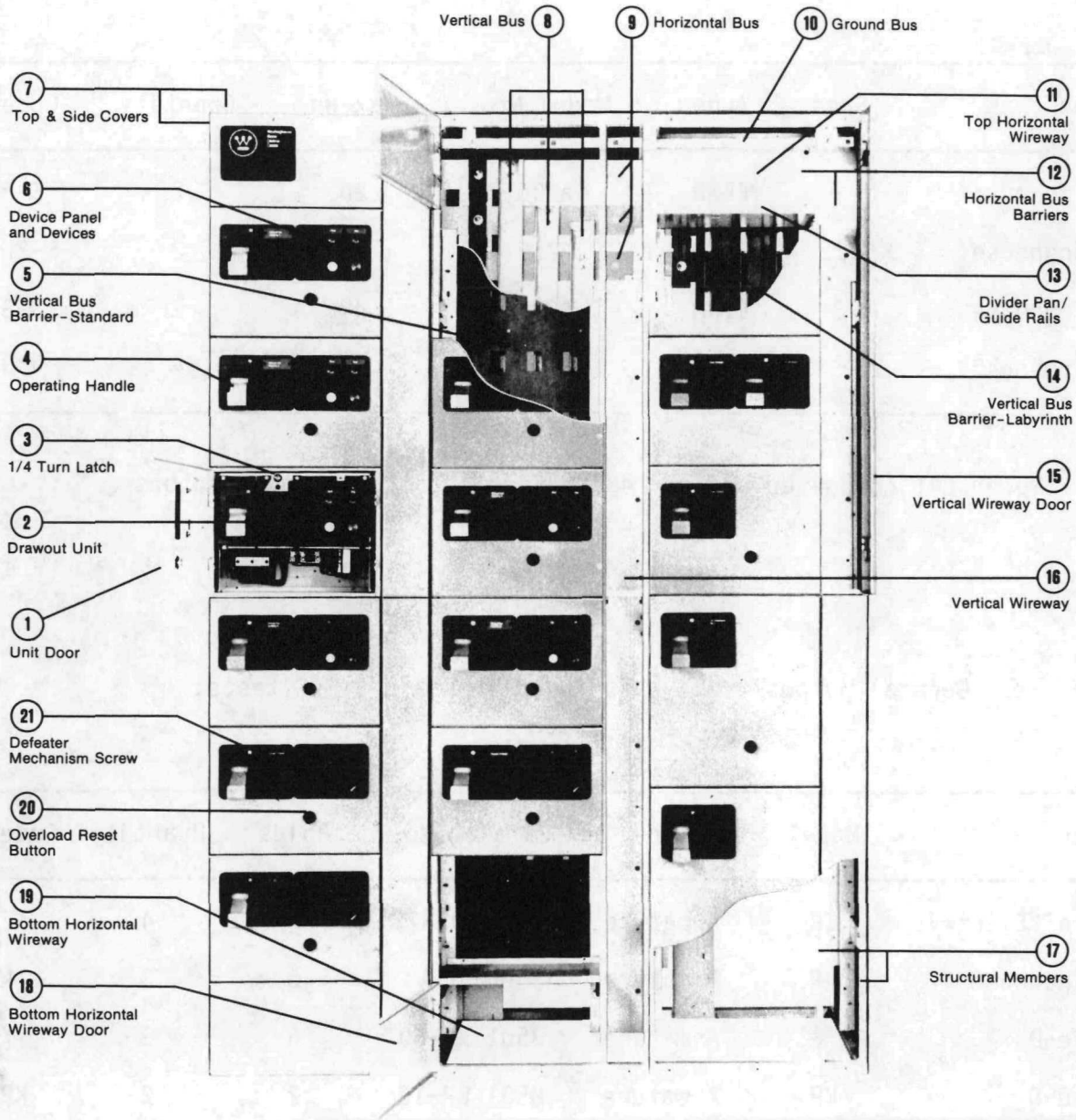

Fig. 2-1. Typical three-column Westinghouse Five-Star motor control center (from Ref. 3).

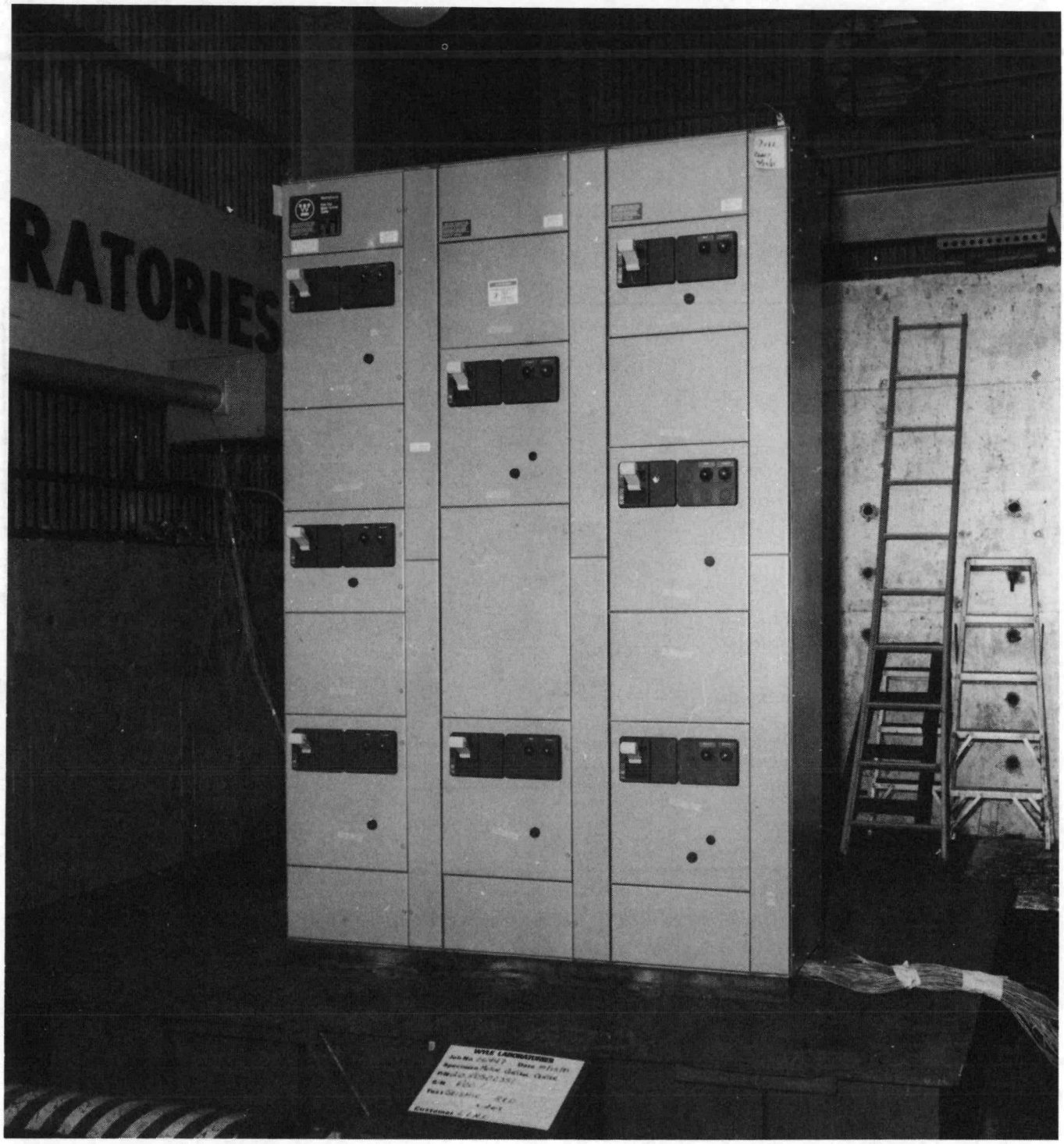

Fig. 2-2. Motor control center used in Phase I demonstration tests, shown mounted on the Wyle shaker table.

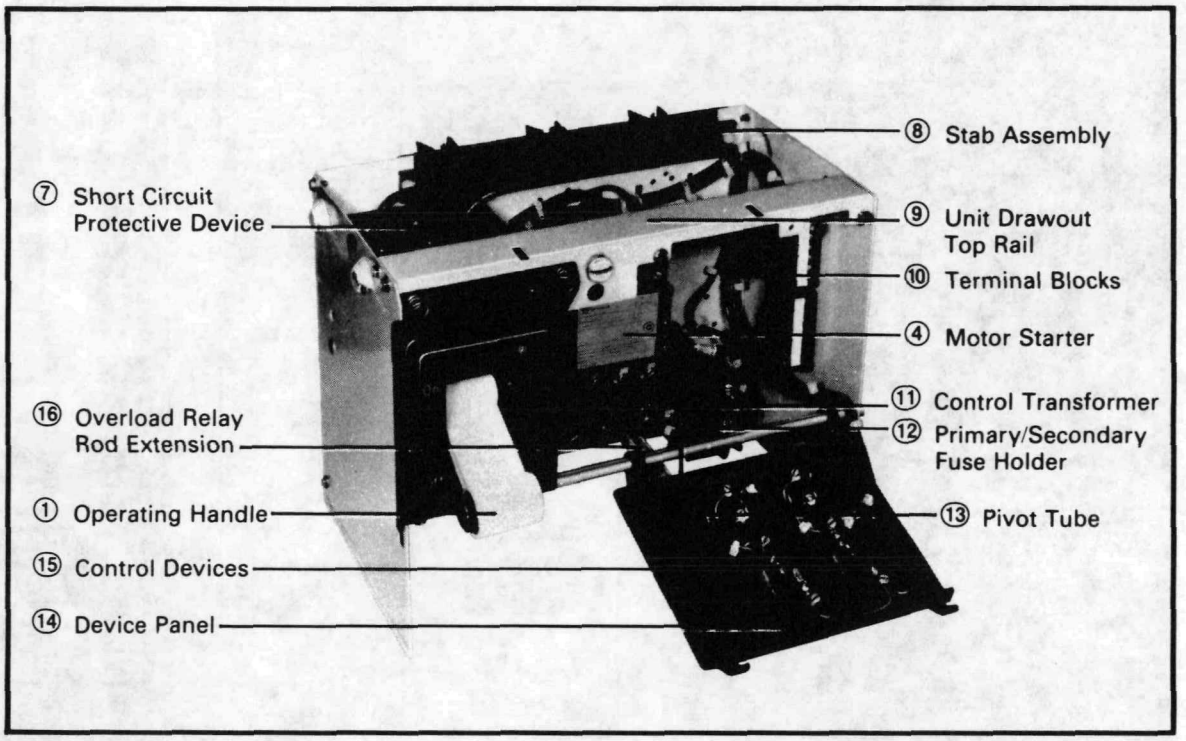

Fig. 2-3. Typical Five-Star draw-out unit ("bucket") housing a motor controller (from Ref. 3).

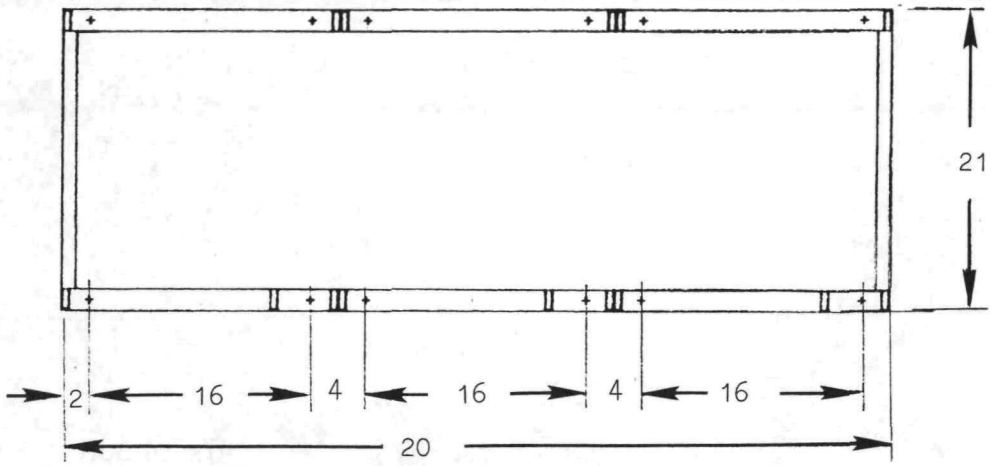

Four bolts per cabinet

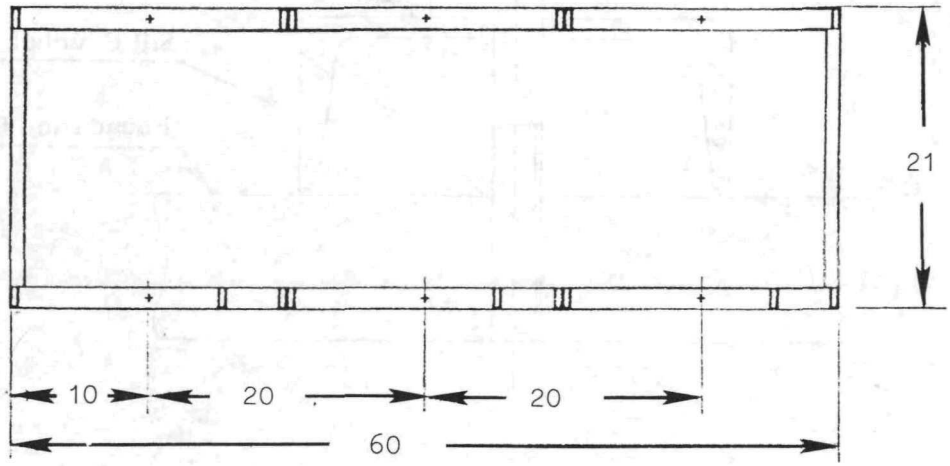

Two bolts per cabinet

Fig. 2-4. Details of bolted connections at the MCC cabinet base.

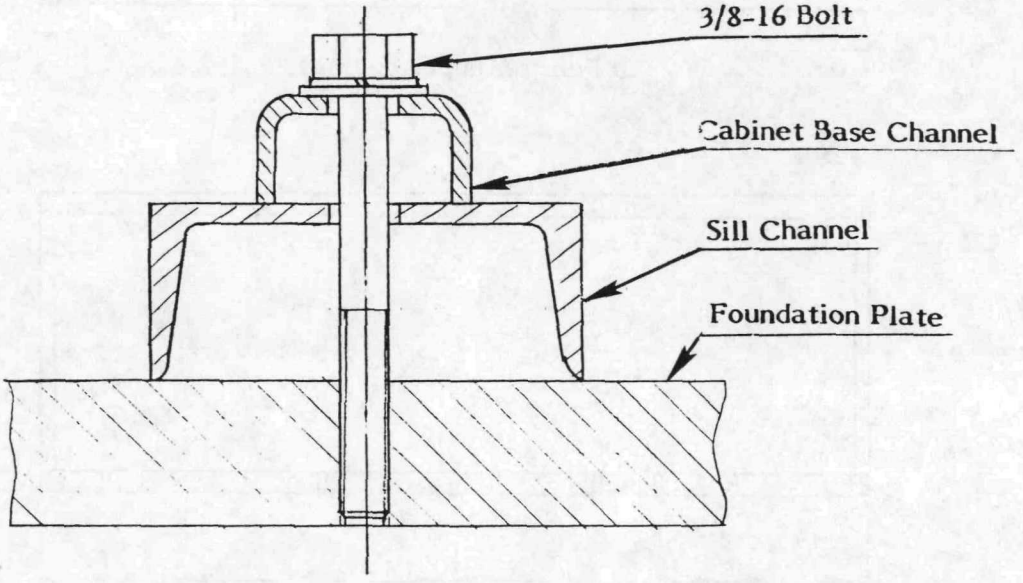

Fig. 2-4 (cont.) Details of bolted connections at the MCC cabinet base.

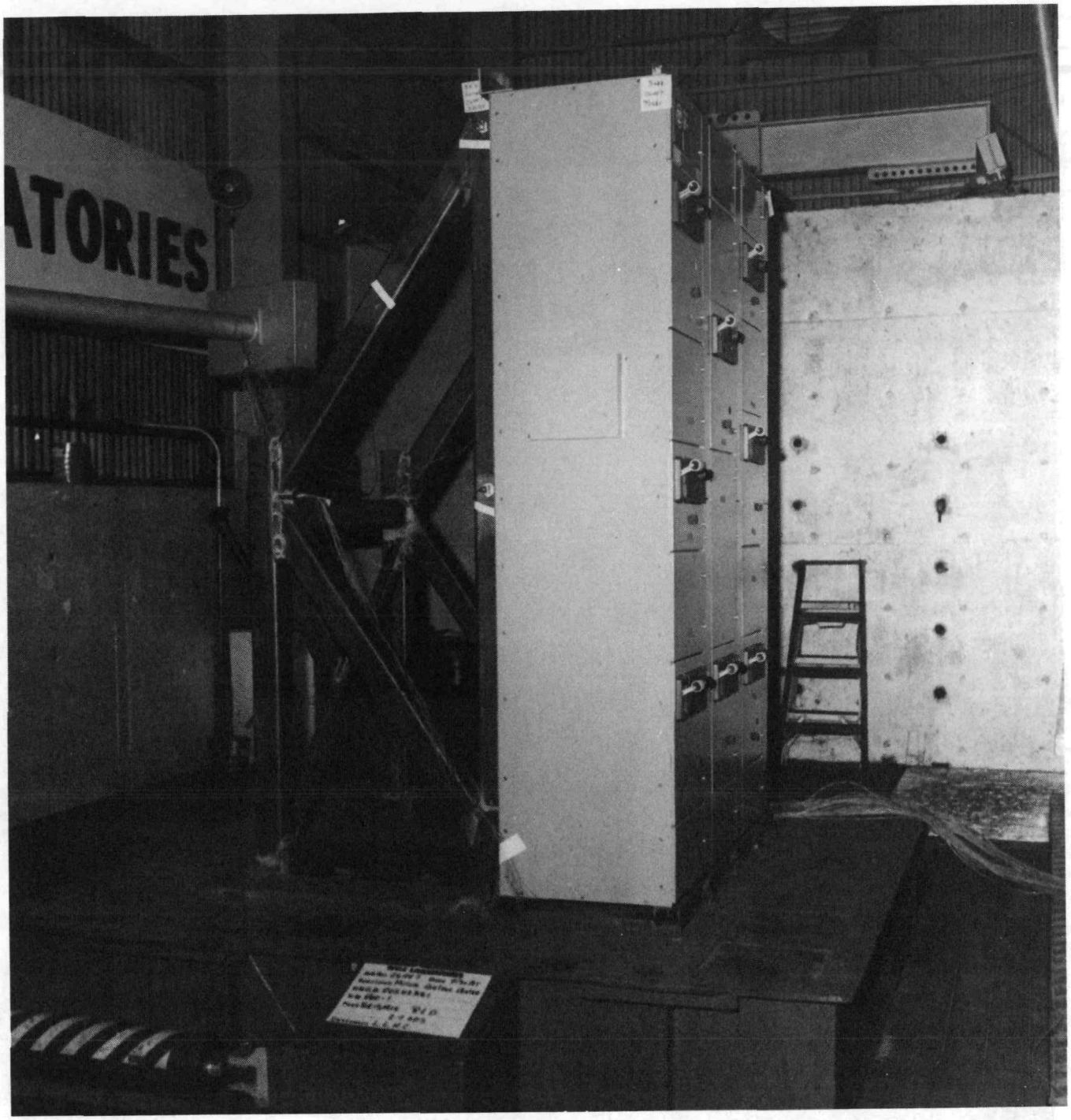

Fig. 2-5. Steel structure used to brace MCC during testing in the "top supported" mounting configuration.

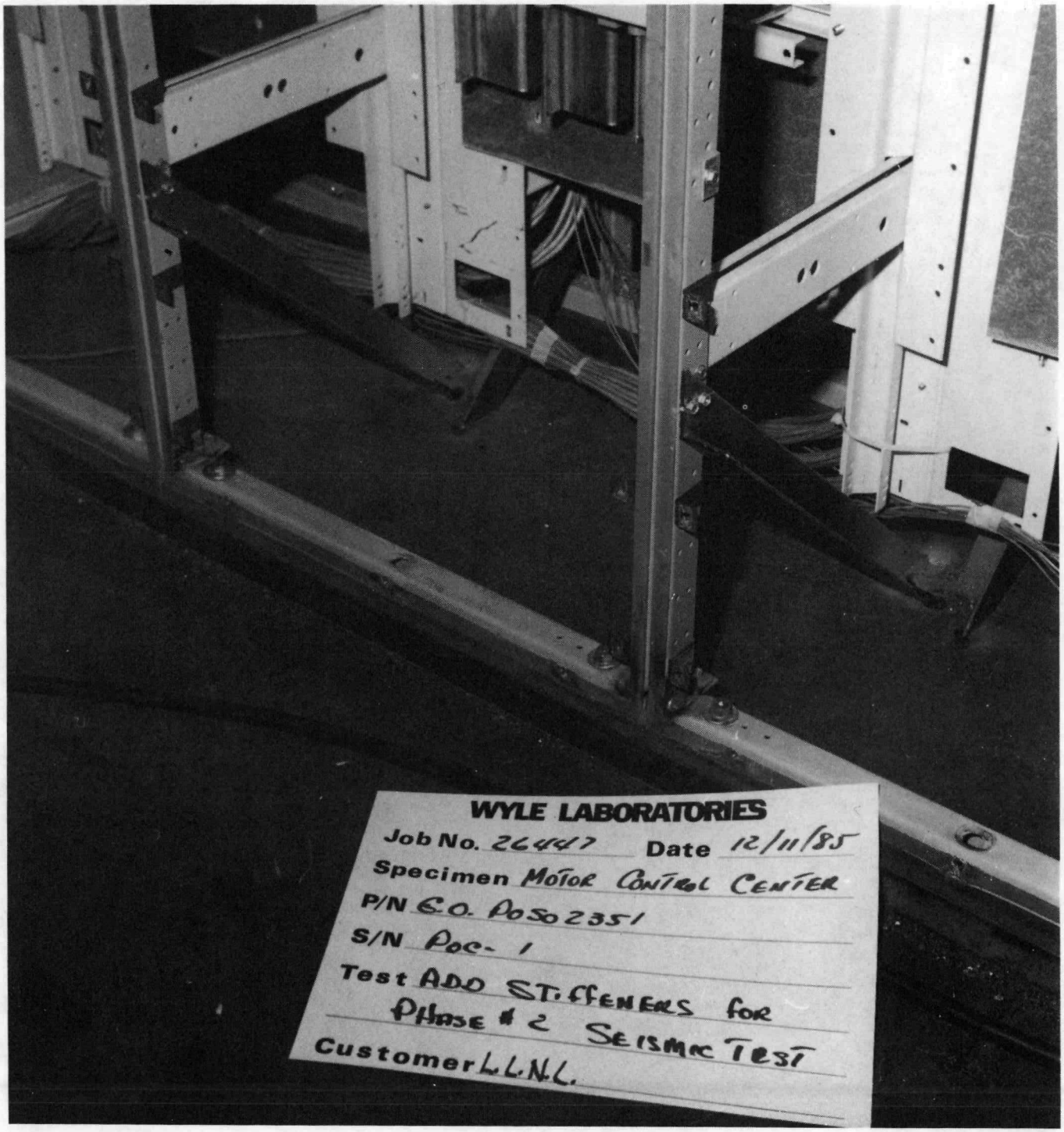

Fig. 2-6. Details of internal diagonal bracing added to MCC during late stages of testing. Note the use of four mounting bolts per column.

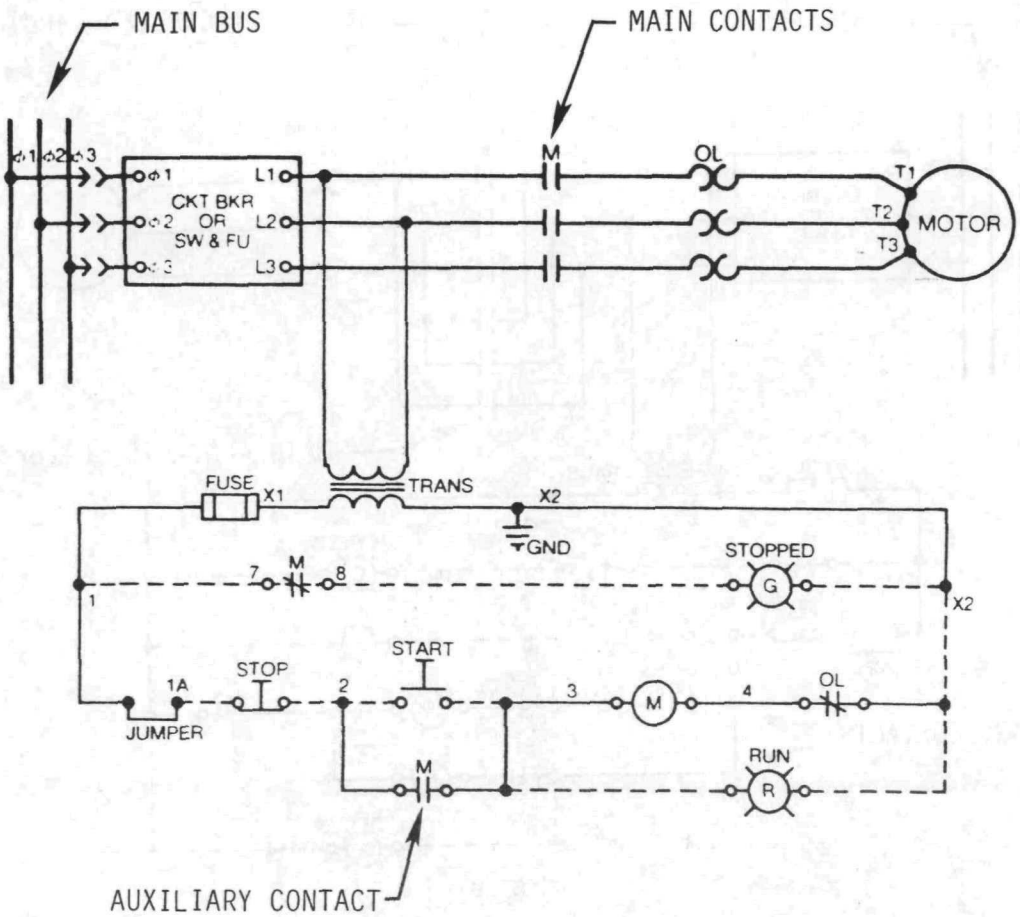

Fig. 2-7. Typical motor control circuit utilizing a full-voltage non-reversing (FVNR) starter.

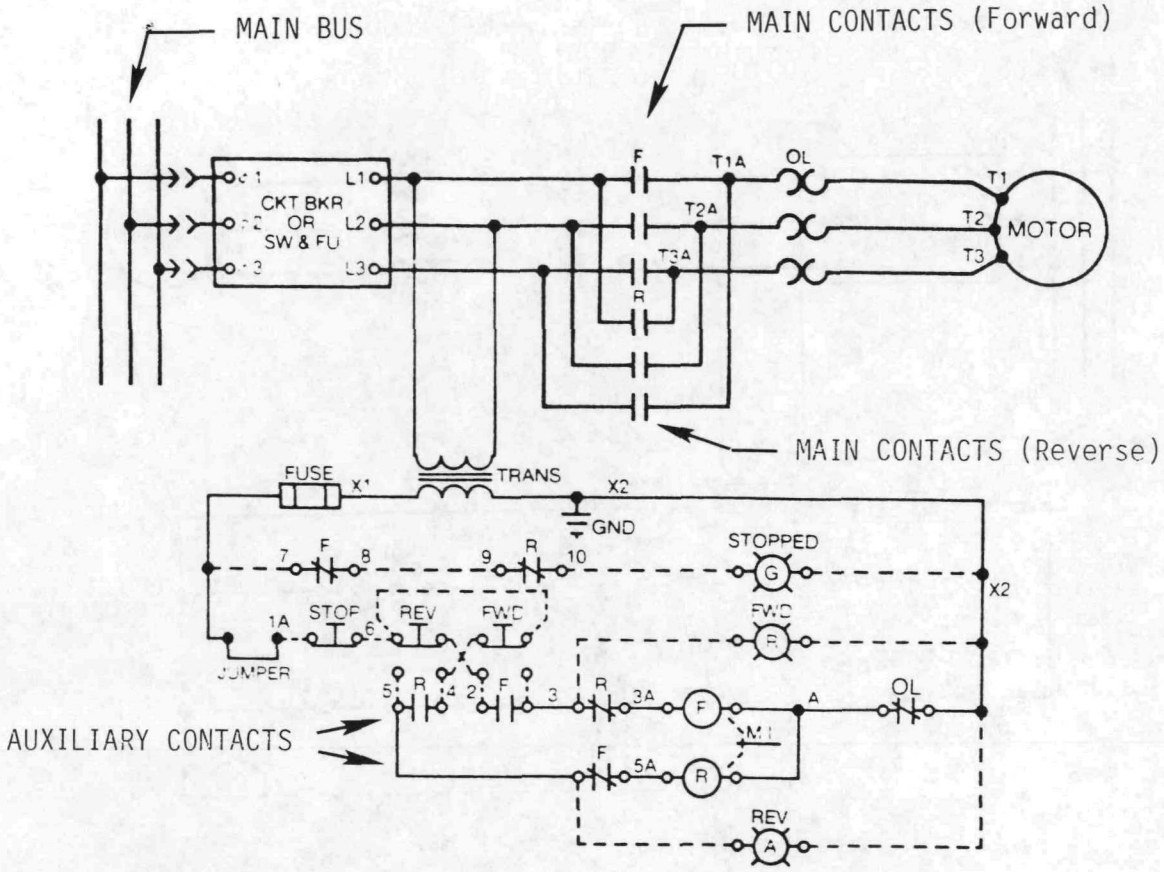

Fig. 2-8. Typical motor control circuit using a full-voltage reversing (FVR) starter.

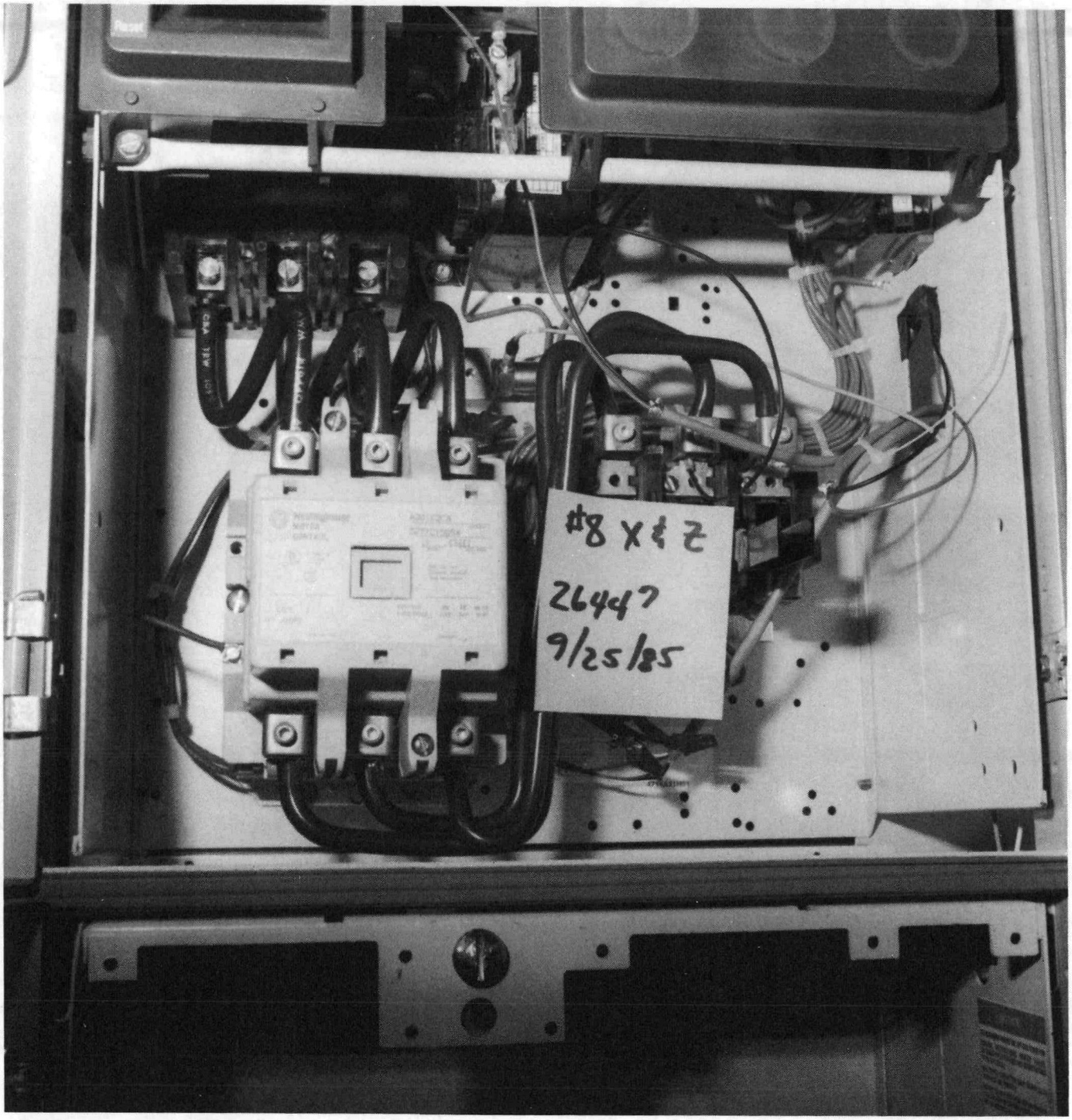

Fig. 2-9. Typical controller installation in the MCC tested. The starter in this case is a Size 3 FVNR unit.

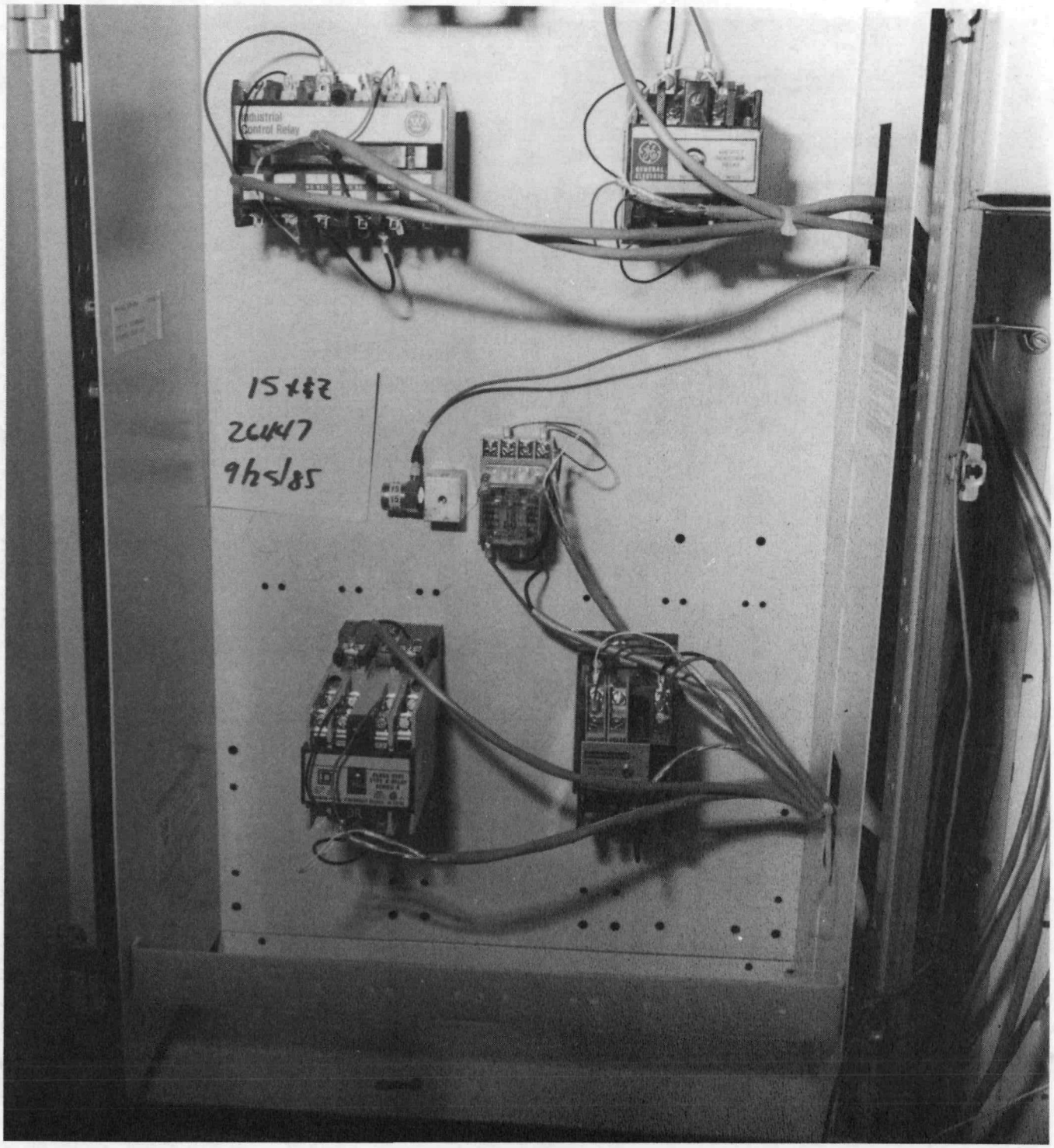

Fig. 2-10. Sample relay installation in the MCC tested.

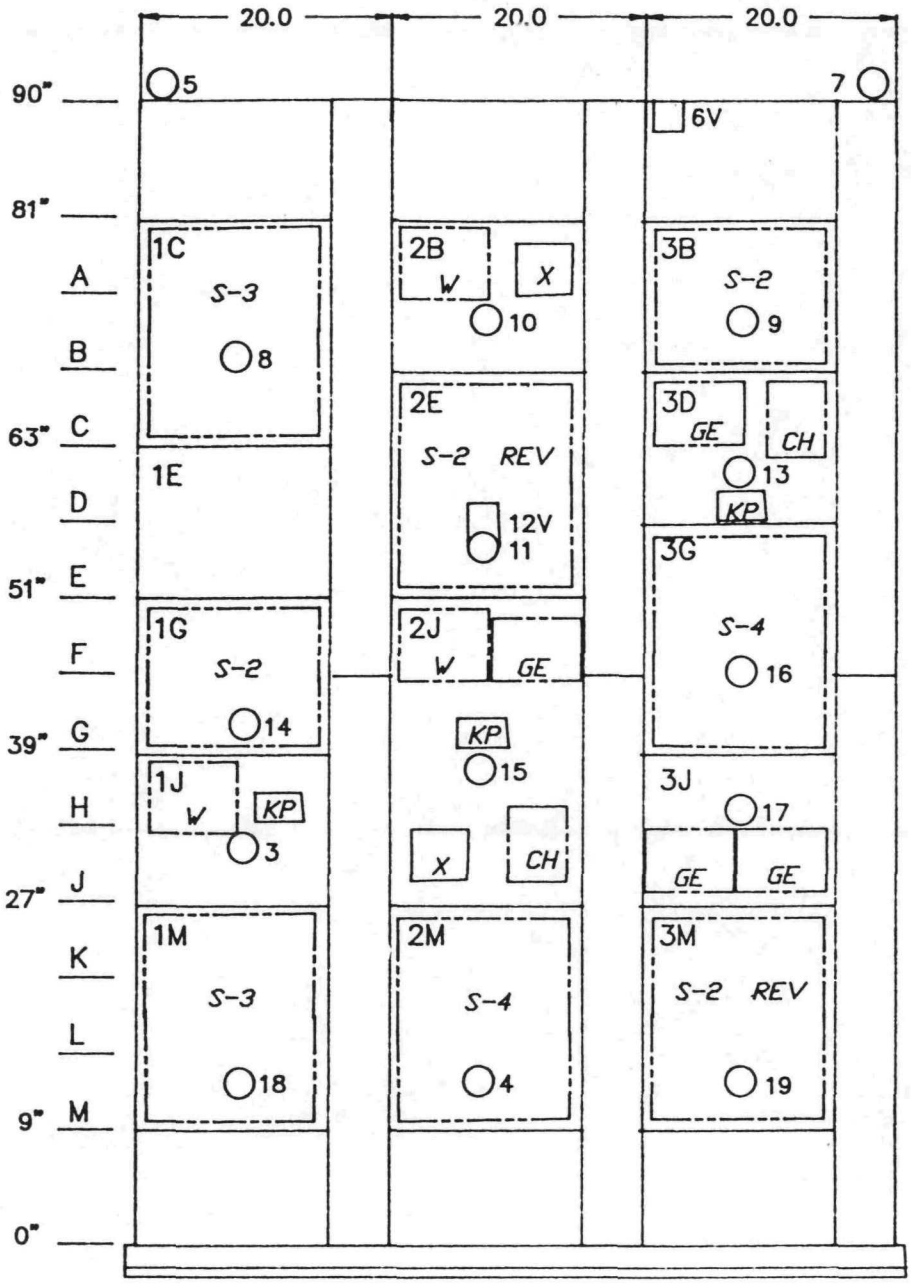

Fig. 2-11. General arrangement of controllers, relays, and accelerometers during MCC testing.

3. TEST PROCEDURES

3.1 Description of Test Facility

All dynamic testing of the MCC was performed on the "G-machine" shaker table operated by Wyle Laboratories at its Norco, California site. A general description of the test table, including pertinent operating data, is presented in Fig. 3-1. Figures 2-2 and 2-4 in the previous section show the motor control center mounted on the test table.

3.2 Dynamic Excitation

Table 3-1 summarizes the input conditions for the Phase I demonstration tests. We completed a total of 56 test runs on the MCC, of which 43 were biaxial random motion tests. Table input motions in the random motion tests ranged up to 2.5g ZPA, which yielded in-cabinet spectral accelerations up to 10g and higher at device locations. We also performed resonance search tests using low-level sinusoidal input to identify resonant frequencies for the cabinet frame and for each draw-out unit.

For each mounting configuration, we also performed pull tests to statically estimate the corresponding cabinet stiffness. The results of these tests were then compared to the results of the resonance search tests.

Following completion of the MCC tests, two devices (one starter and one relay) were removed from the cabinet and subjected to sinusoidal tests to investigate their functional behavior as a function of input motion frequency content.

The following discussion describes in detail the various test conditions that were applied in our Phase I test program.

Resonance Search Tests

In order to characterize cabinet stiffness for the different mounting configurations and horizontal orientations (i.e., front-to-back and side-to-side), each test series included a resonance search prior to the start of random motion testing. The search was performed over the frequency range 5 to 40 Hz at a rate of one octave per minute at a level of 0.2g at the MCC base.

The dynamic resonance search tests were supplemented in certain instances by static pull tests on the MCC structure. In these tests a 580 lb weight was attached to the top of the MCC by a rope and pulley in either the F-B or S-S direction. The corresponding deflection at the top of the cabinet was measured with a linear variable displacement transducer (LVDT). Each pull test was repeated three times to insure an accurate data sample.

Biaxial Random Excitation

The MCC was subjected to biaxial random excitation which was amplitude controlled from 1.25 to 30 Hz. For each mounting configuration, two series of tests were performed, beginning with the side-to-side (S-S) and vertical axes, followed by testing in the front-to-back (F-B) and vertical directions. The test waveforms for both the horizontal and vertical directions were synthesized to match the desired response spectrum (DRS) shape. The independent waveforms included a 2-3 second ramp up, a 15-second strong motion portion, and a 3-4 second ramp down. The primary parameter for test input level was the zero period amplitude (ZPA). Accordingly, the input waveform was low-pass filtered at 30 Hz to permit a clearer indication of the peak acceleration of the waveform in the amplified portion of the DRS (i.e., below 30 Hz). The first test in each series was run at approximately 0.7g ZPA.

The shape of the DRS selected is typical of spectra used in qualification testing. During development of our test program, we gave serious consideration to using "realistic" spectra derived from actual earthquake records; however, the wide disparity among such spectra makes it difficult to select one that would be "most appropriate" for our test purposes. Given our

general interest in actual seismic capacities compared to those inferred by qualification testing (i.e., seismic "margin"), we concluded that the selected DRS shape would offer a more consistent basis for comparison.

The ZPA levels in successive tests were increased stepwise by about 1.5 times the preceding level, up to an approximate maximum of 2.5g. Fig. 3-2 illustrates the DRS shape as well as the starting and maximum input spectra for the test program. These spectra apply both for vertical input motion and for the respective horizontal direction (i.e., F-B or S-S) for each test run.

Sinusoidal Tests

Following completion of the MCC tests, we determined that spectral accelerations had a more significant effect on device behavior than had been originally anticipated. To investigate this effect more closely, a Size 2 starter and a Square-D Type X general purpose relay were removed from the MCC and subjected to single degree of freedom (SDOF) sinusoidal tests. The two devices were rigidly mounted on a uniaxial hydraulic test table in the same orientation as in the biaxial random motion tests. The devices were then subjected to F-B horizontal (i.e., in the direction of contact motion) sine sweeps from 2.5 to 80 Hz at acceleration levels up to 6g. At selected discrete frequencies the devices were then subjected to increasing acceleration levels to determine the chatter threshold at each frequency. Fig. 3-3 shows the test arrangement.

3.3 Instrumentation and Recording Equipment

Input Motion

Two accelerometers were mounted on the test table to control and monitor the horizontal and vertical input motion. Analyses of the input motions were performed with a response spectrum analyzer. Test response spectra were plotted at one-sixth octave frequency intervals from 1.1 to 100 Hz for damping values of one-, three-, and five percent.

Structural Response

Accelerometer data recorded on analog FM tape and by computer was used to monitor MCC structural response. Three accelerometers on top of the cabinet monitored overall response; the photographs in Fig. 3-4 show the mounting of these three accelerometers. Fourteen additional accelerometers mounted throughout the MCC monitored local cabinet responses at the various device locations (see Fig. 2-11); these accelerometers defined the input motions seen by the individual relays and starters. The photographs in Appendix A show the accelerometer mounting locations in each compartment. Note from these photographs that accelerometers were not mounted directly on any electrical device, but rather on the MCC draw-out unit housing the device(s).

All accelerometers were positioned to fully define response of the cabinet structure in the front-to-back (F-B), side-to-side (S-S), and vertical directions. Analyses of the response motions were performed with a response spectrum analyzer. Test response spectra were plotted at one-sixth octave frequency intervals from 1.1 to 100 Hz for damping values of one-, three-, and five percent.

Electrical Monitoring and Control

All starter coils were connected to a common 120VAC control circuit. One phase of the power circuit through each breaker and starter was connected to a 120VAC, 3A power source. Two pairs of auxiliary contacts, one normally-open (NO) and one normally-closed (NC), from each starter were connected to a low-voltage power source for monitoring contact chatter and change of state. Figures 3-5 and 3-6, respectively, diagram typical monitoring circuits for the FVNR and FVR controllers. Note from Fig. 3-6 that for reversing starters, the center phase was selected so that monitoring could be performed with a single measurement channel regardless of whether the controller was placed in forward or in reverse.

Note also that the main contact coils were <u>not</u> energized through the auxiliary contacts, but by a separate circuit. Although contrary to actual

seal-in circuit design, this was done intentionally so that auxiliary contact chatter and main contact chatter induced by inertial loads could be monitored independently. Consequently, the amount of auxiliary contact chatter necessary to cause the main contacts to inadvertently change state could not be determined.

All relay coils were connected to a common 120VAC control circuit. As shown schematically in Fig. 3-7, two poles of each relay, one NO and one NC, were connected to a low-voltage power source for monitoring contact chatter or change of state.

All relays and starters were commanded to change state at least once during the strong-motion random excitation. State changes were executed simultaneously for all relays and all starters by respective master switches located off of the test table. In addition, each device could be controlled individually by remote switches. The initial state of the electrical devices (energized or deenergized) was alternated from run-to-run; every device, however, experienced strong motion in both its deenergized and energized state during every test run. Circuit breakers were left closed at all times.

The photograph in Fig. 3-8 shows the electrical control setup.

Off-Table Relays

The original test plan had anticipated connecting the main (i.e., power) contacts of selected starters to off-table inductive loads to investigate whether or not contact chatter would be sufficient to actuate a connected device. Early testing showed, however, that when energized the main contacts showed no signs of chatter. The off-table loads were therefore deleted in most tests.

During one test run, an off-table relay was energized through the normally-closed contacts of one Square-D Type X relay. A schematic diagram of the monitoring circuit is shown in Fig. 3-9.

Table 3-1. Summary of Phase I demonstration tests.

Run No.	Orientation	Input ZPA (g) Horizontal	Bolts per Column	Top Support	Internal Bracking	Remarks
1	S-S	n/a	4	Yes	No	Resonance search (invalidated)
2	V	n/a	4	Yes	No	Resonance search
3	S-S	n/a	4	Yes	No	Resonance search
4	S-S	1.5	4	Yes	No	
5	S-S	1.3	4	Yes	No	
6	S-S	1.4	4	Yes	No	
7	S-S	1.5	4	Yes	No	
8	S-S	1.4	4	Yes	No	
9	S-S	1.9	4	Yes	No	
10	S-S	2.5	4	Yes	No	
11	F-B	n/a	4	Yes	No	Resonance search
12	F-B	0.9	4	Yes	No	Invalidated
13	F-B	1.0	4	Yes	No	
14	F-B	1.3	4	Yes	No	
15	F-B	1.4	4	Yes	No	
16	F-B	1.8	4	Yes	No	
17	F-B	2.1	4	Yes	No	
18	S-S	n/a	4	No	No	Resonance search
19	V	n/a	4	No	No	Resonance search
20	S-S	0.9	4	No	No	
21	S-S	1.1	4	No	No	
22	S-S	1.2	4	No	No	
23	S-S	1.5	4	No	No	
24	S-S	1.8	4	No	No	
25	S-S	2.1	4	No	No	
26	F-B		4	No	No	Resonance search
27	F-B	1.6	4	No	No	
28	F-B	1.6	4	No	No	
29	F-B	1.9	4	No	No	Cracked welds (repaired)

Table 3-1 (cont.). Summary of Phase I demonstration tests.

Run No.	Orientation	Input ZPA (g) Horizontal	Bolts per Column	Top Support	Internal Bracking	Remarks
30	F-B	1.9	4	No	No	
31	F-B	2.2	4	No	No	Cracked welds (repaired)
32	F-B	1.7	4	No	No	Device interchange
33	S-S	n/a	2	No	No	Resonance search
34	V	n/a	2	No	No	Resonance search
35	S-S	1.2	2	No	No	No device data (power lost)
36	S-S	1.2	2	No	No	Repeat Run 35; add off-table relay
37	S-S	1.3	2	No	No	
38	S-S	1.7	2	No	No	
39	S-S	2.0	2	No	No	
40	S-S	2.1	2	No	No	
41	F-B	n/a	2	No	No	Resonance search
42	F-B	1.1	2	No	No	
43	F-B	1.5	2	No	No	
44	F-B	1.5	2	No	No	
45	F-B	1.5	2	No	No	
46	F-B	2.5	2	No	No	
47	F-B		4	No	Yes	Resonance search; add strain gauges
48	F-B	2.1	4	No	Yes	Cracked welds (repaired)
49	F-B	2.3	4	No	Yes	Extra bolts buckets 2B, 2E, 2J
50	F-B	n/a	4	No	Yes	Resonance search
51	V	n/a	4	No	Yes	Resonance search
52	F-B	1.7	4	No	Yes	
53	F-B	2.4	4	No	Yes	
54	F-B	1.4	4	No	Yes	
55	F-B	2.1	4	No	Yes	
56	F-B	2.2	4	No	Yes	Cracked welds

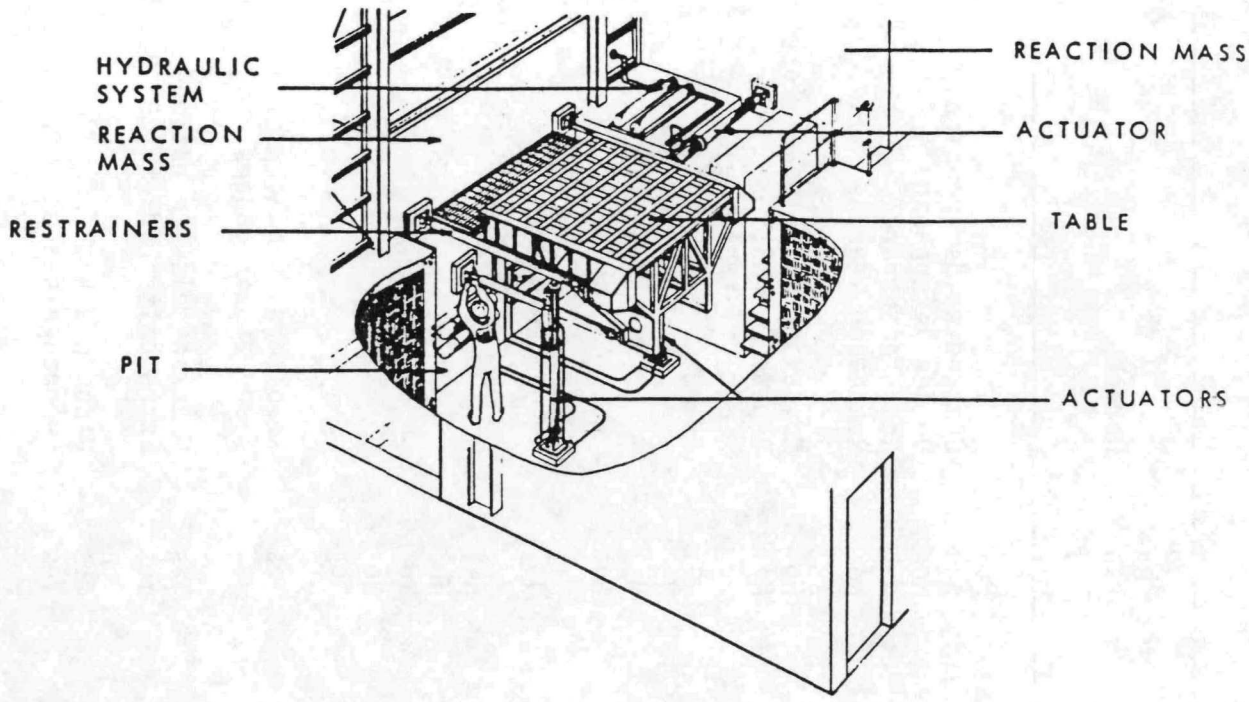

LOCATION:	NORCO, CA, FACILITY
MODE OF OPERATION:	TWO AXES SIMULTANEOUSLY
FORCE RATING:	36,000 FORCE POUNDS VERT. 29,000 FORCE POUNDS HORIZ.
TABLE DIMENSIONS:	8' X 8'
MAX. SPECIMEN SIZE:	8' X 8' X 12' HIGH
MAX. SPECIMEN WT.:	6,000 POUNDS @ 2 G'S
MAX. DISPLACEMENT:	9 INCHES VERTICAL 12 INCHES HORIZONTAL
MAX. VELOCITY BIAXIALLY:	
VERTICAL:	33 IPS TRANSIENT 22 IPS CONTINUOUS
HORIZONTAL:	46 IPS TRANSIENT 31 IPS CONTINUOUS
MAX. ACCELERATION:	8 G'S VERT., 7 G'S HORIZ.
MAX. FREQUENCY:	70 HERTZ

Fig. 3-1. General data on Wyle Laboratories "G-machine" seismic shaker table.

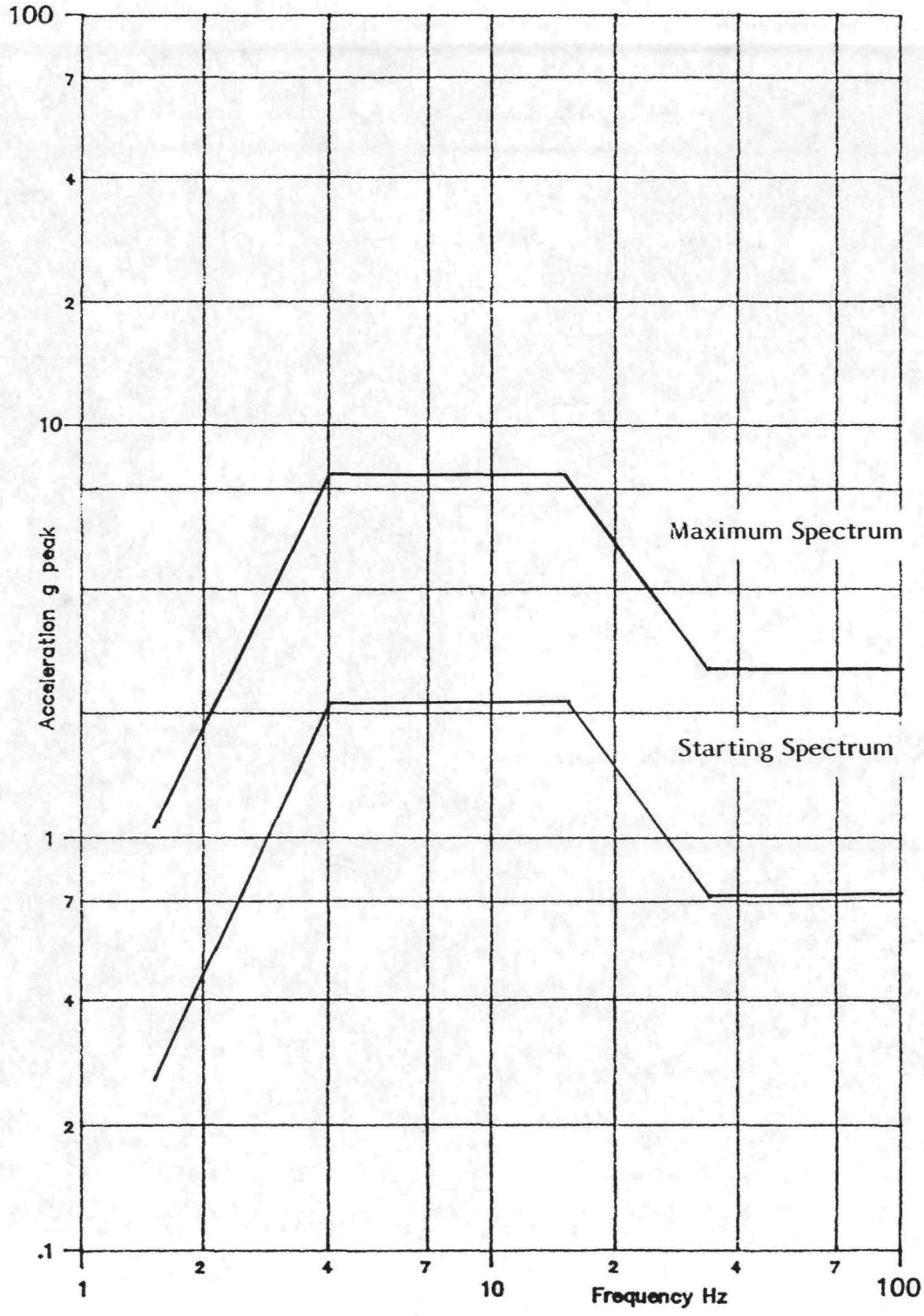

Fig. 3-2. Desired response spectra for table input motion, showing approximate starting and maximum test levels (5% damping). These spectra apply both for horizontal and vertical input motion.

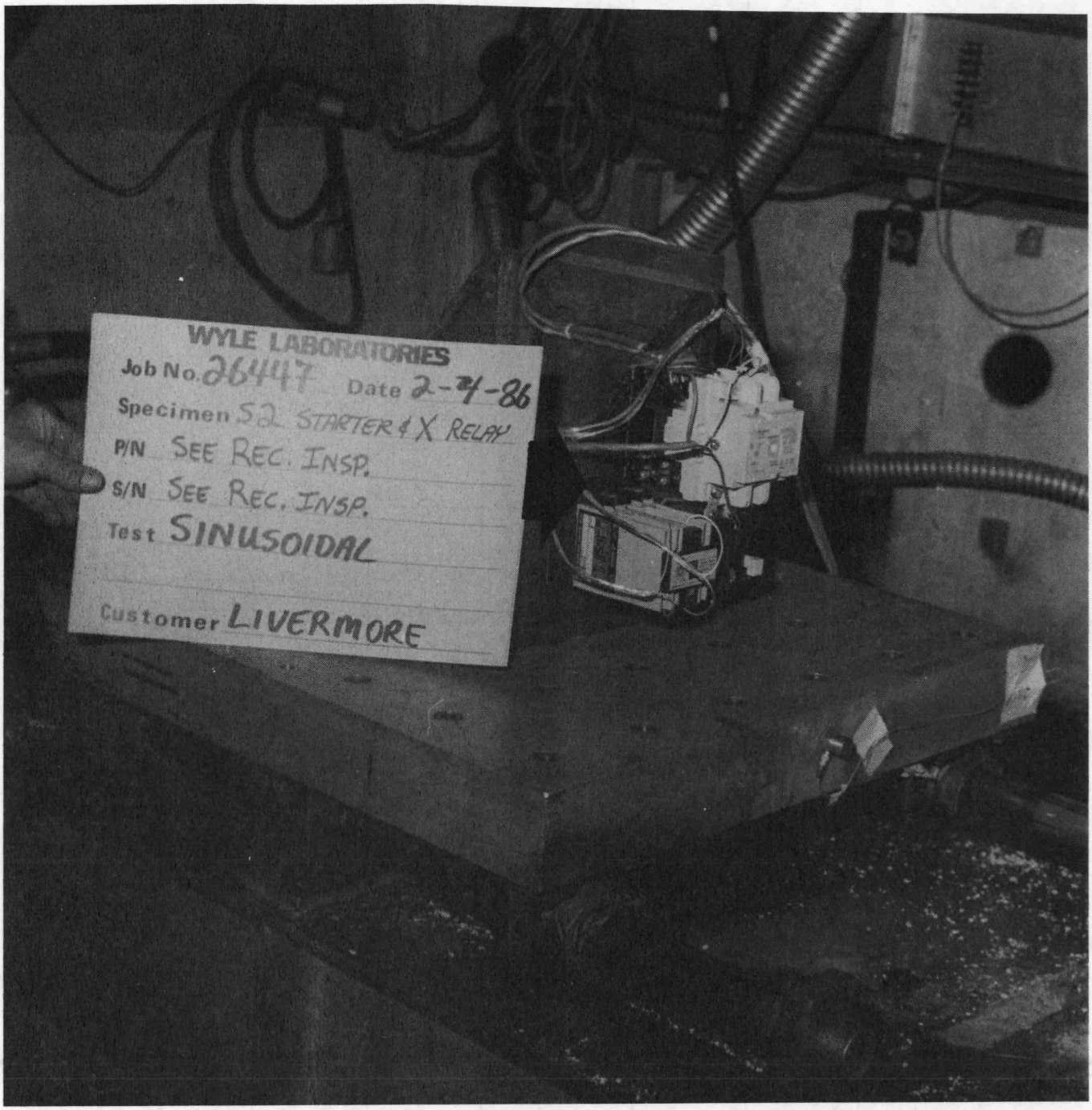

Fig. 3-3. Test arrangement for sinusoidal testing of Size 2 starter and Square-D Type X general purpose relay.

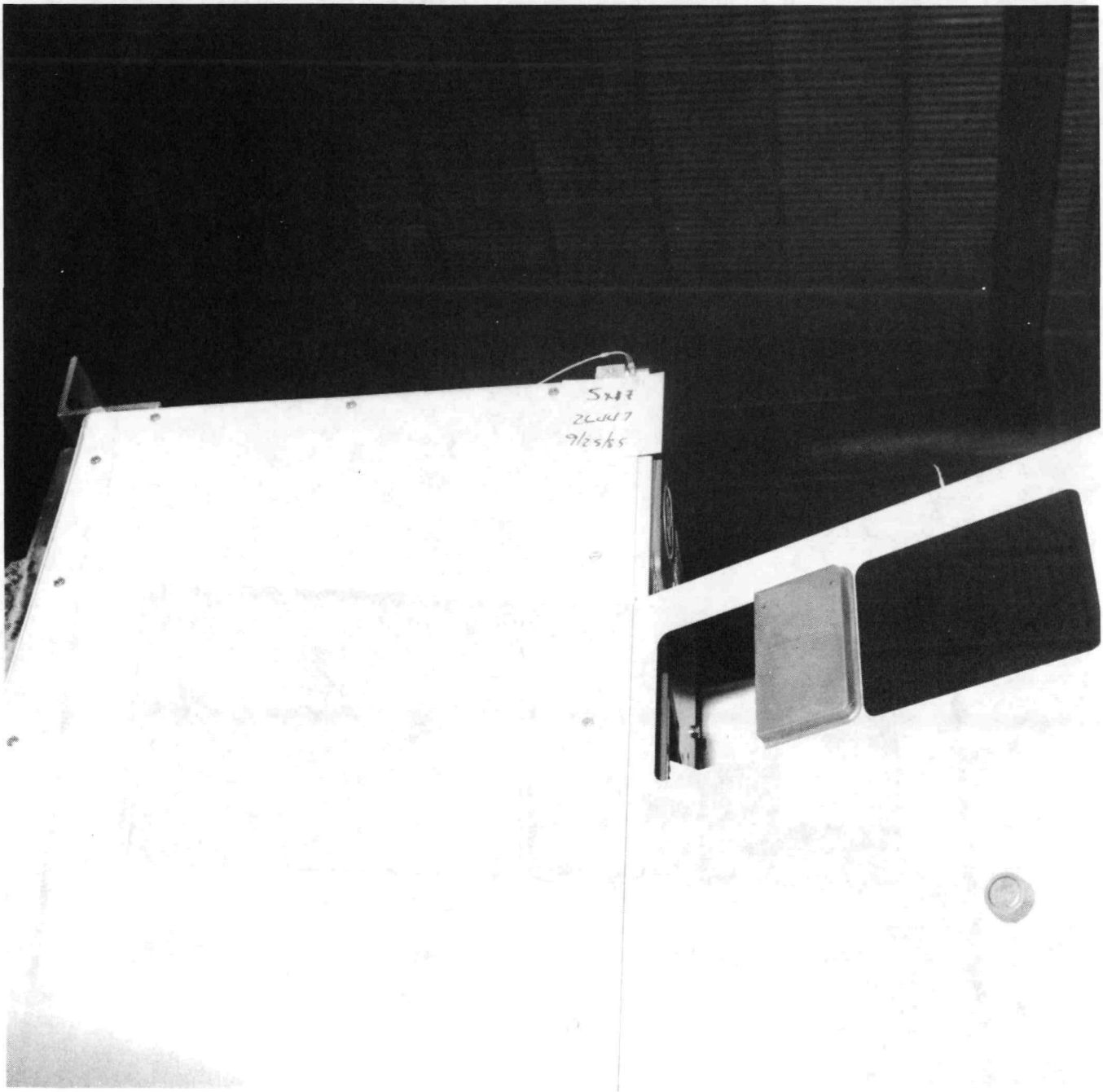

Fig. 3-4. Accelerometer locations along top of MCC cabinet (accelerometer 5).

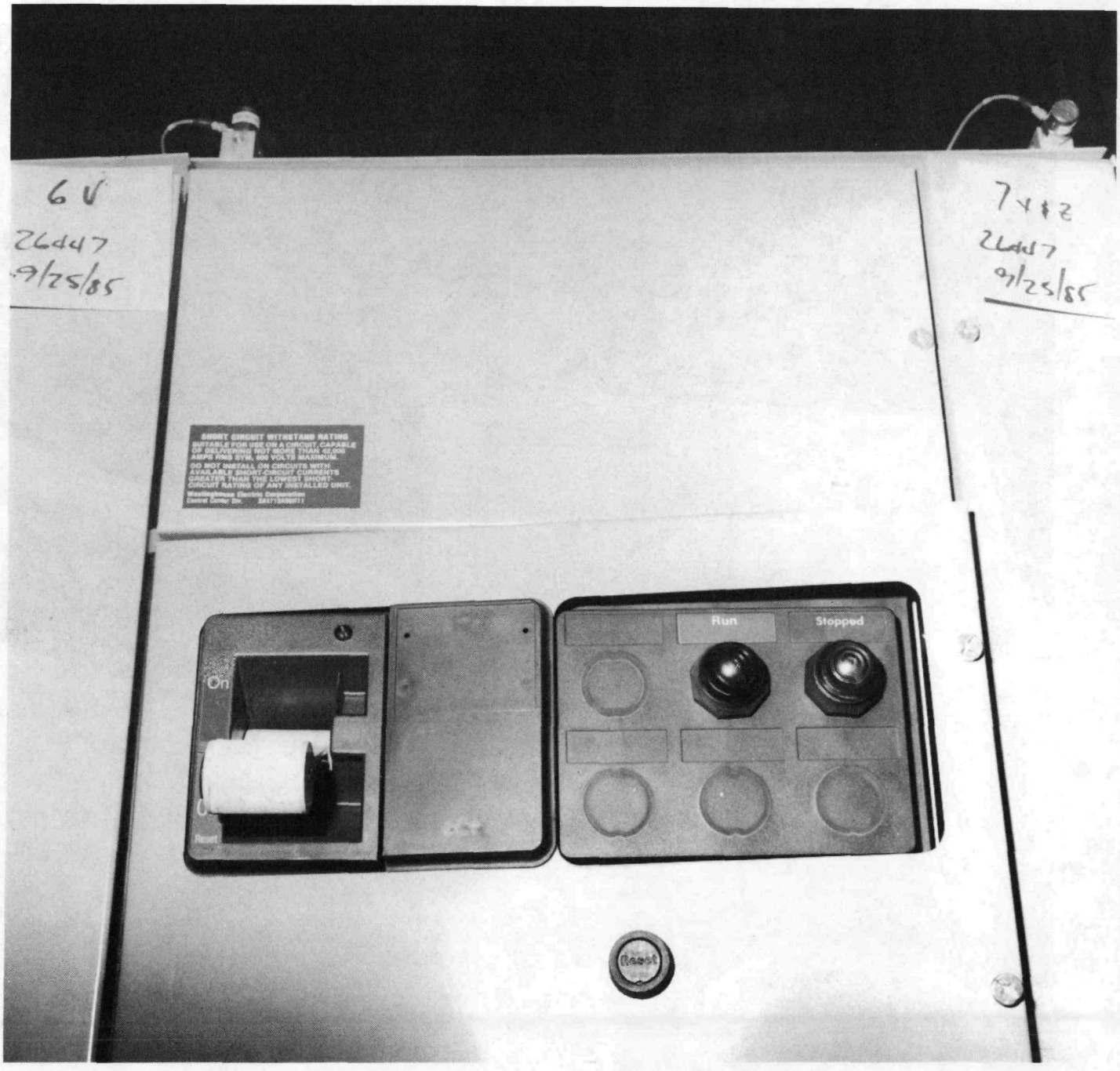

Fig. 3-4 (cont.). Accelerometer locations along top of MCC cabinet (accelerometers 6 and 7 mounted on top of cabinet).

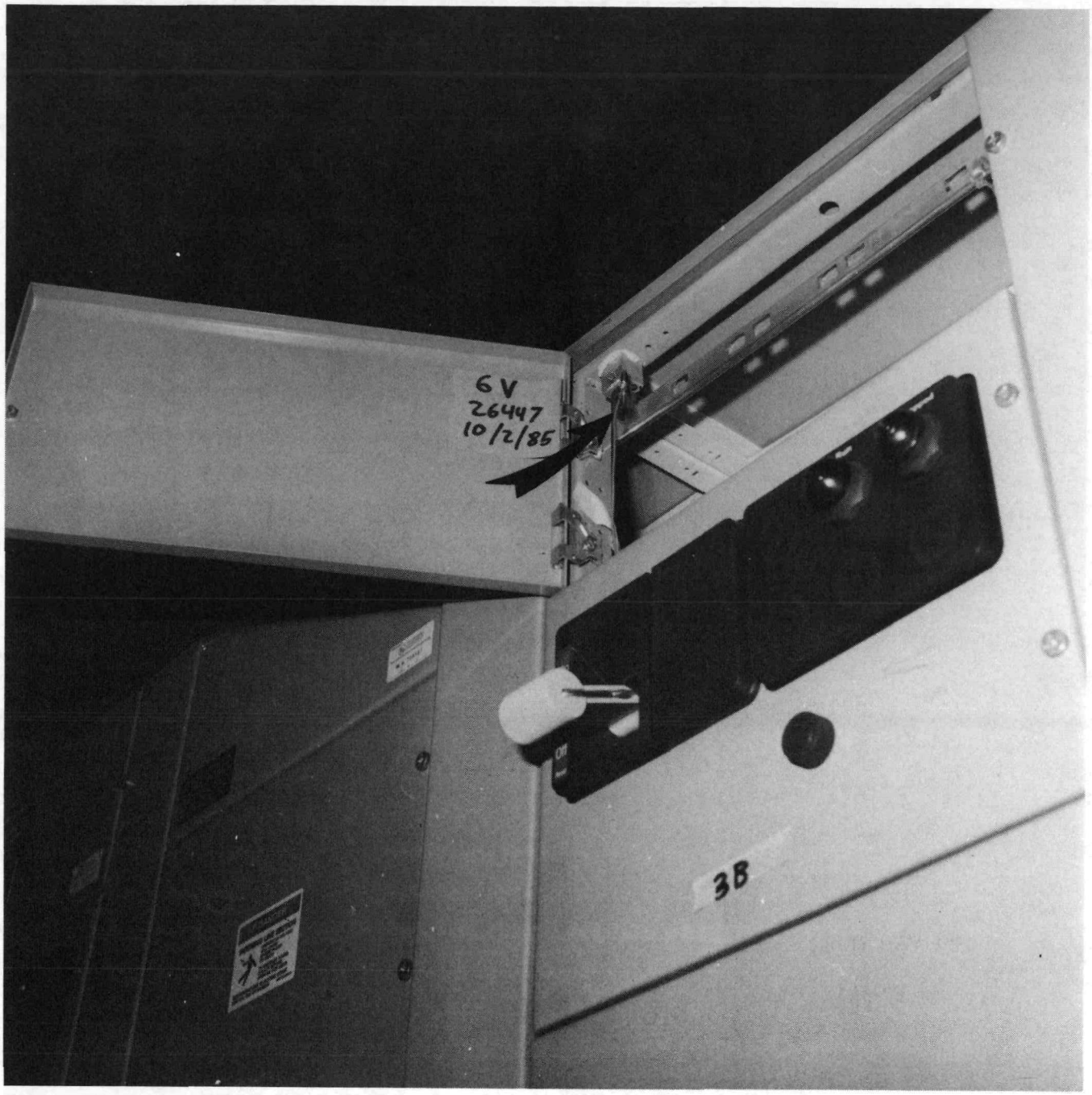

Fig. 3-4 (cont.). Accelerometer locations along top of MCC cabinet (accelerometer 6 remounted inside cabinet after Run 4).

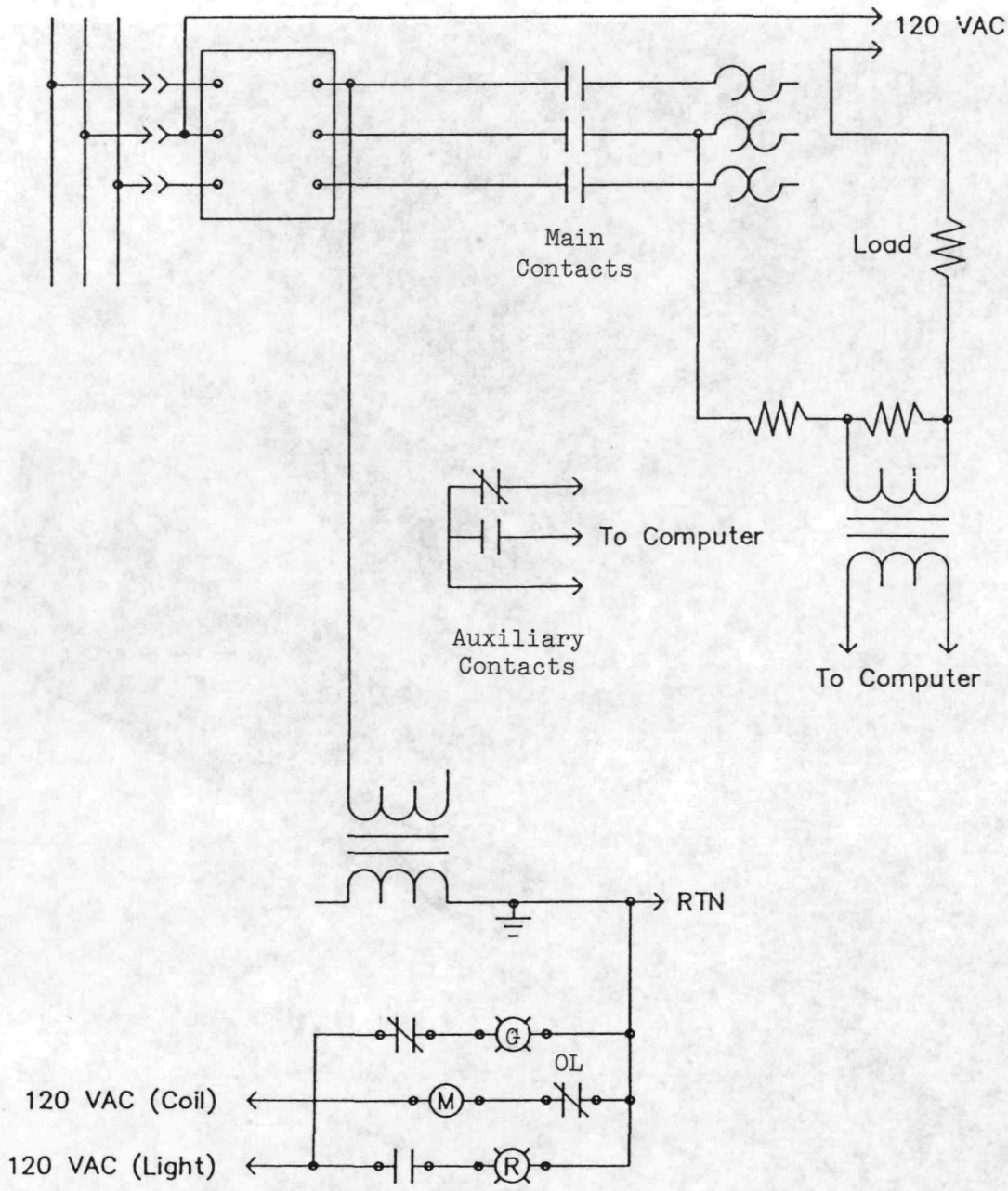

Fig. 3-5. Typical circuit for monitoring function of full-voltage non-reversing starters.

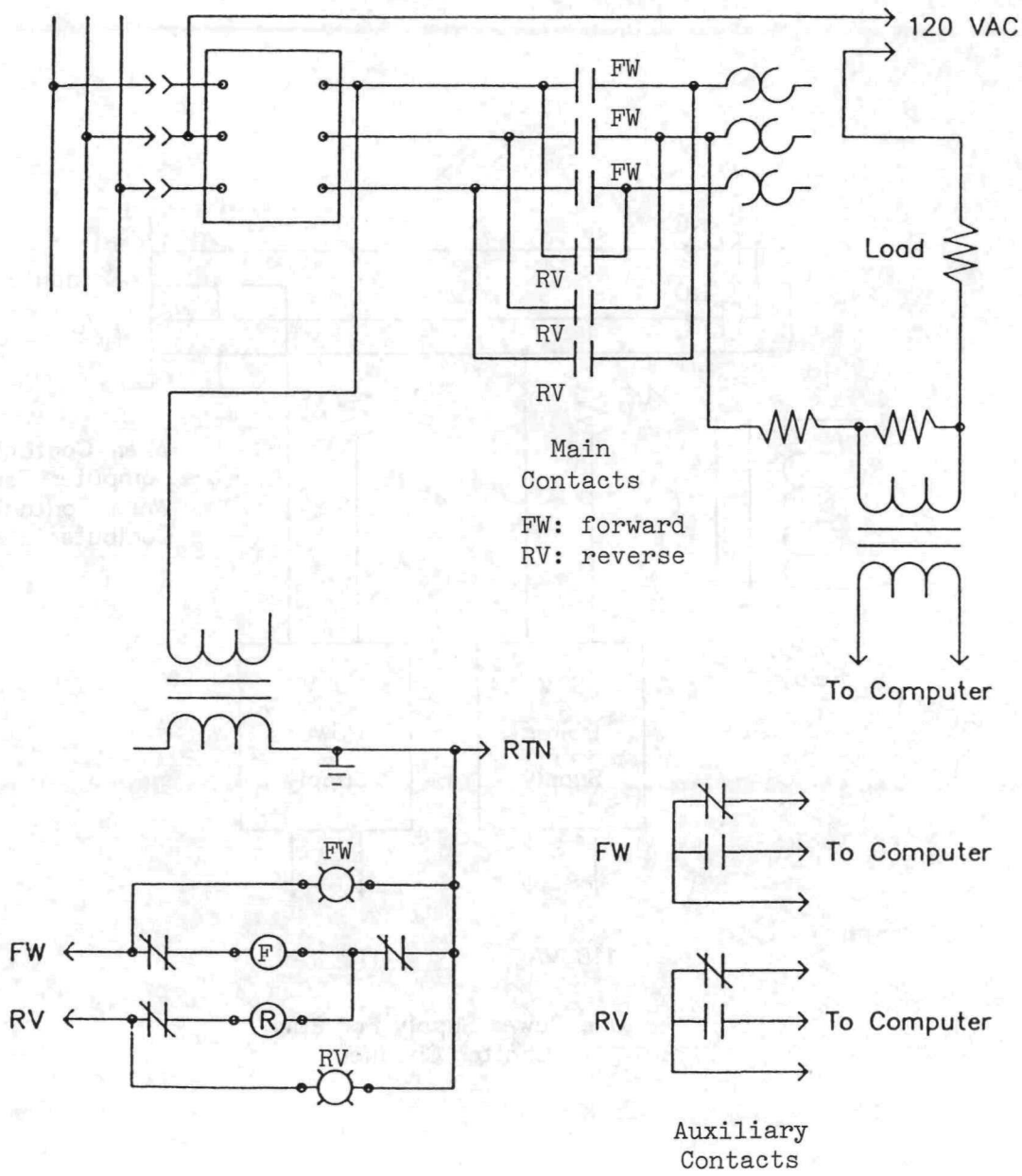

Fig. 3-6. Typical circuit for monitoring function of full-voltage reversing starters.

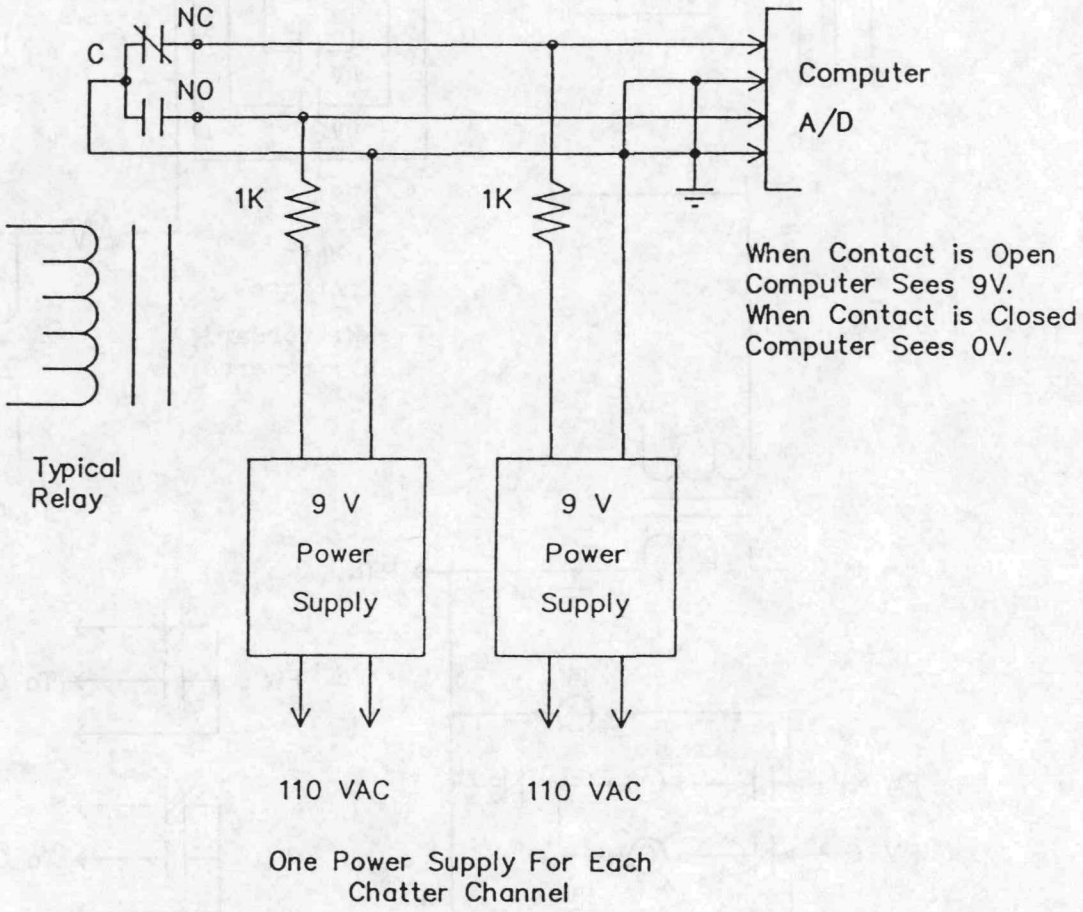

Fig. 3-7. Typical circuit for monitoring relay function.

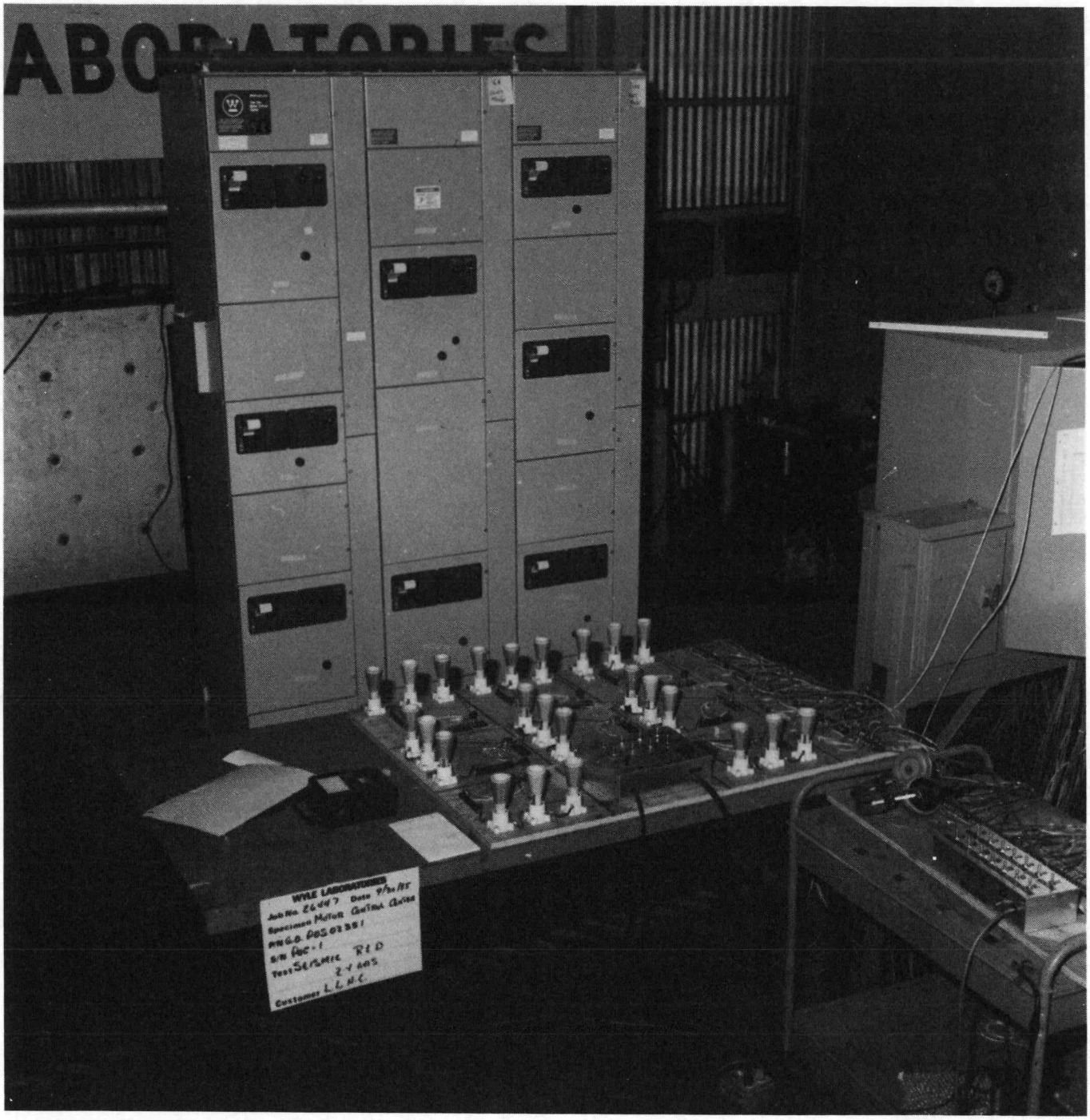

Fig. 3-8. Off-table controls for MCC starters and relays. The conical devices provide resistive loads for the starter main contacts.

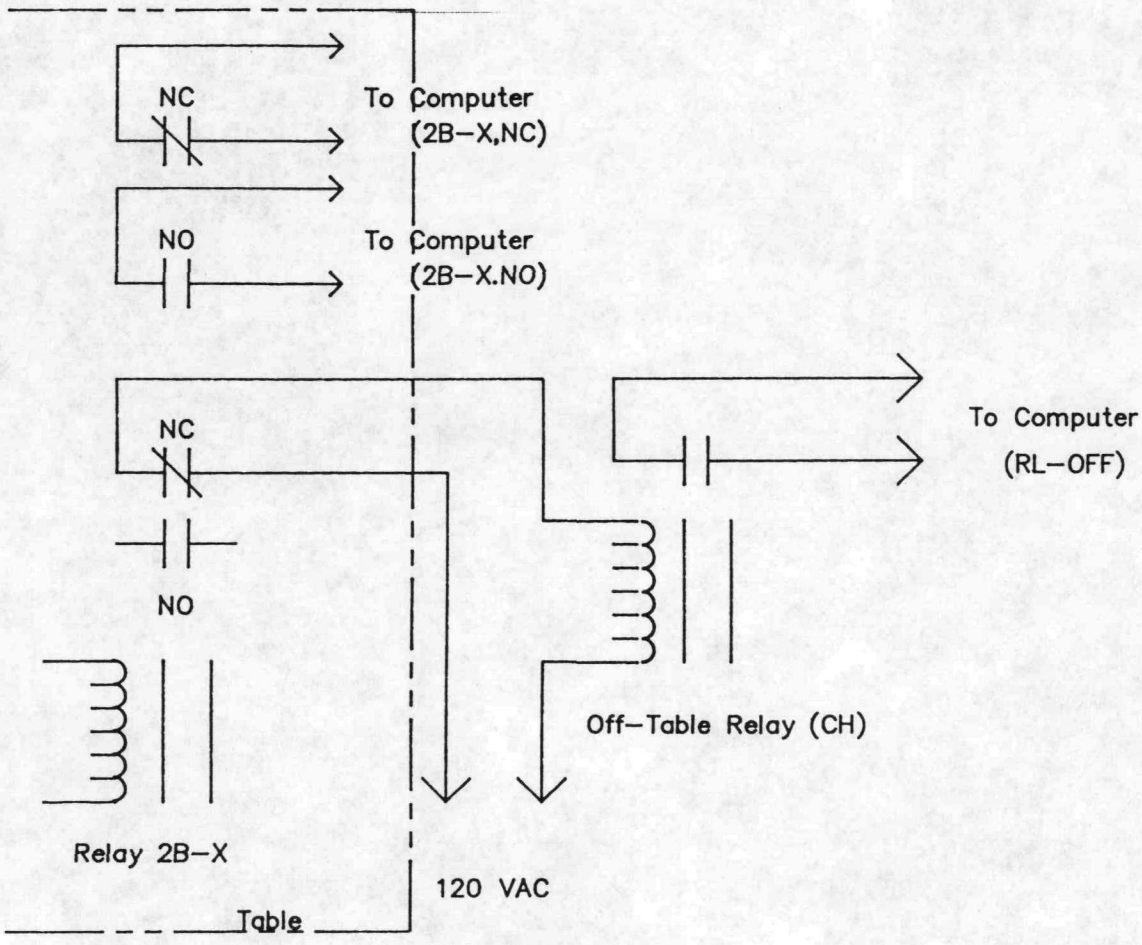

Fig. 3-9. Relay monitoring circuit incorporating off-table relay.

4. TEST RESULTS

4.1 Cabinet Stiffness

Resonance Search

Plots of transmissibility in the front-to-back, side-to-side and vertical directions (the "x", "z" and "y" test axes, respectively) are presented for all accelerometers in Appendix B. The significant resonance frequencies of the overall cabinet as a function of mounting configuration are presented in Table 4-1. For the two bolt per column configuration, the main frame natural frequency was below the 5 Hz limit of the transmissibility instrumentation; therefore, the 3.5 Hz resonant frequency was estimated by reviewing the response spectra plots. The local resonance frequency estimated for each draw-out unit (the "bucket" resonances) is also included in Table 4-1. Recall that these results are based on low-level (0.2g) sine-sweep input motion. A study of transmissibility under high-level random motion input, based on the Phase I test results, is currently in progress.

Static Pull Tests

Three sets of static pull tests were performed: one each in the F-B and S-S directions for the free standing two-bolt per column mounting configuration (i.e., no top support), and one in the F-B direction for the four-bolt per column configuration. The results of these tests are summarized in Table 4-2 in terms of force (580 lb in each case), measured displacement at the cabinet top, and calculated stiffness. The results of these tests indicate that, as expected, the stiffness of the MCC is significantly higher in the S-S direction than in the weaker F-B direction. They also indicate that increasing the number of bolts per column from two to four increases the calculated stiffness by more than a factor of three.

No detailed comparison was made between the results of the static pull tests and those of the dynamic resonance search tests; such a comparison would require development of at least a simple model of the cabinet, which was outside the scope of our original test program. An approximate comparison can

be made, however, by considering that the resonant frequency of the cabinet frame is proportional to the square root of the static stiffness. On this basis, the results of the pull tests imply that the natural frequency of the cabinet should increase by a factor of about 1.8 when the number of mounting bolts is increased from two to four per column. The actual increase in natural frequency determined by the resonance search tests, from 3.5 to about 5 Hz, is somewhat less -- about 1.4 times.

4.2 In-Cabinet Dynamic Response

Effect of Signal Filtering

Test response spectra were routinely generated at assumed cabinet damping values of one-, three-, and five percent. Except where noted otherwise, we elected to discuss our results on the basis of the response spectra generated for three-percent damping. In reality, "real" damping can be expected to vary with the severity of input motion and (conceivably) with cabinet mounting configuration. A study of this effect, based on structural response data recorded in our Phase I tests, is currently in progress.

A comparison of the filtered (at 30 Hz) and unfiltered TRS plots for accelerometers 1, 10, and 15 from Runs 17 and 31 is presented in Figs. 4-1 and 4-2, respectively. As these spectra show, a significant amount of high frequency excitation was generated locally by vibration in the MCC structure. Clearly, the use of frequencies below 30 Hz to define ZPA neglects the potential effect of higher frequencies on device fragility. However, the results of later sinusoidal tests on one starter and one general purpose relay showed, at least for the particular devices tested, that chatter was most sensitive to frequencies well below the 30 Hz limit. Consequently, neglecting frequencies above 30 Hz (which reflects one of the basic assumptions made in our fragilities testing) should not have a significant effect on our results.

Effect of Mounting Configuration

As described above, the mounting configuration influences the overall cabinet response. The mounting also influences the local in-cabinet response. Comparison plots were made for accelerometers 1, 5, and 11 (located, respectively, on the table, at the top of the MCC, and at the MCC mid-elevation) for Runs 17, 31, 46, and 53. These four runs represent the the highest table ZPA applied to each mounting configuration. Figure 4-3 (accelerometer 1) shows that the table TRS is nominally the same for each of the four runs, implying that variations in local in-cabinet responses reflect the cabinet mounting configuration and not the input motion at the base of the MCC. Figure 4-4 (accelerometer 5) shows only minor amplification at the top of the cabinet for Run 17, which is expected because of the top brace. It shows considerable amplification at the overall 5 Hz resonance for Run 31 (four bolts per column, no top brace) and corresponding amplifications at the overall cabinet resonances for runs 46 and 53. The local bucket response at about 14 Hz shows clearly on runs 31 and 53. Figure 4-5 (accelerometer 11) shows the influence of the overall resonances on the center of the cabinet for each mounting configuration; note in particular the response of the top-supported cabinet compared with the three free-standing configurations. Note also the influence of the local bucket response at about 17 Hz.

Extra Bolts (Draw-Out Units)

The standard mounting of the draw-out buckets leaves considerable room for rattling during dynamic excitation. To obtain some data on the influence of this mounting, the side panels of the buckets in compartments 2B, 2E, and 2J were attached to the main frame with two extra screws per bucket after Run 48 (see Figs. 4-6 and 4-7). Unfiltered TRS plots for runs 48 and 49 for accelerometers 10, 11, and 15 show the difference on Figs. 4-8, 4-9, and 4-10. The plots show that the additional screws had little influence on reducing the rattling. The extra screws were left in for the remainder of the test runs.

Although the results of our tests indicated that little was to be gained by stiffening the cabinet-bucket connection in the MCC, other test programs -- in particular testing of vital motor control centers by PG&E as part of its Hosgri requalification program for the Diablo Canyon nuclear power plant -- indicated substantial reductions in high-frequency response can be gained by tying down the draw-out units. The discrepancy between these results and our own can probably be traced to the particular techniques used to reduce rattling and to the degree of additional stiffness accordingly provided.

4.3 Contact Chatter

During each run contact chatter was computer analyzed to determine the number of chatter events, the duration of each chatter, and the times at which the first and last chatter occurred. Table 4-3 shows sample chatter detector output from Run 46 (two bolts per column mounting, 2.5g table ZPA).

Time-history plots were also generated to show contact chatter, time of occurrence, and the local excitation waveform for each device. Figure 4-11 shows a typical set of plots for a starter, in this case the Size 2 non-reversing starter mounted in draw-out unit 3B. These plots, from top to bottom, present the following information (note that the horizontal axis labels in capital letters refer to the plot above the label):

- the voltage signal at the starter state channel ("ST-ST-CH"), which indicates when the master state change switch for starter contacts was actuated. Note that this run began with all device coils deenergized, as denoted by the "high" signal. Compare the first and last state changes with the times in Table 4-3.

- voltage at the instrumented NO auxiliary contact ("3B-NO") indicating when state change occurred, in this case from its energized state ("high", indicating open contacts) to its deenergized state ("low", indicating closed contacts). Note that the single chatter at approximately 8.8 sec is recorded in Table 4-3, and that it was between 5 and 10 msec in duration.

- voltage at the instrumented NC auxiliary contact ("3B-NC") indicating when state change occurred, in this case from its deenergized state ("high", indicating closed contacts) to its energized state ("low", indicating open contacts). Note that the two large spikes between 8 and 11 sec are recorded as chatters in Table 4-3, and that each chatter is between 20 and 40 msec in duration.

- current measured through the starter main contacts ("3B-AMPS). Note the blacked-out areas in this plot indicating 4 amperes of current was flowing between 7.2 and 8.0 seconds, and between 14.4 seconds and test end at 27 seconds. Compare with the state change and voltage time-history data in the preceding plots.

- the local acceleration time-history for the device draw-out unit, in this case measured at accelerometer 9. Note the spikes at approximately 7.2 and 14.4 seconds; these are apparently the result of the accelerometer detecting main contact closure. Note also how these spikes correlate with the data presented in the other plots.

Figure 4-12 shows similar time-history information recorded for relays, in this case the General Electric and Cutler Hammer relays mounted in draw-out unit 3D. These plots, from top to bottom, present:

- the voltage signal at the relay state channel ("RL-ST-CH"), which indicates when the master state change switch for starter contacts was actuated.

- voltage at the instrumented NO and NC contacts of the General Electric general purpose relay ("3D-GE, NO" and "3D-GE, NC" respectively). Note that no chatter was detected.

- voltage at the instrumented NO and NC contacts of the Cutler Hammer reed-type relay ("3D-CH, NO" and "3D-CH, NC" respectively). Note that no chatter was detected.

- the local acceleration time-history for the device draw-out unit, in this case measured at accelerometer 13. Note the large spike at approximately 7.2 seconds; this may result from the accelerometer detecting commanded main contact closure force in the Size 4 starter mounted in the draw-out unit (3G) located immediately below.

Appendix C includes a complete set of time-history plots from Runs 17, 31, 46, and 56 (i.e., for the most severe input motion applied to each mounting configuration) showing contact chatter, times of occurrence, and the corresponding in-cabinet excitation waveform for each device.*

All devices in every run responded normally to commanded state changes, although time-history data indicates that contact "bounce" frequently occurred immediately after a commanded change of state (see Fig. 4-13). Although we do not regard this as a functional anomaly, the computer program for detecting chatter cannot distinguish contact bounce from "real" chatter. Consequently, in some cases the number of chatters implied by the time-history plots may not correspond exactly with the number recorded in the chatter detector output.

We generally observed for starters that as test levels increased, the NC auxiliary contacts chattered first, the NO auxiliary contacts second, and the main contacts last. For the relays, NC contacts chattered before NO contacts. This suggests that for these types of devices, contact chatter is caused by armature movement rather than local response of the contact element; consider that NO contacts must traverse a significantly longer distance than NC contacts in order to change state (i.e., make or break contact).

4.4 Correlation of Chatter with Local Response

For each test run, Tables 4-4 through 4-9 correlate for each device table

*Although Run 53 experienced the highest input ZPA (2.4g) for its mounting configuration, in-cabinet accelerations during Run 56 (2.2g input ZPA) were generally higher and chatter more frequent. Consequently, Run 56 was selected as the "most severe" of this group of runs for inclusion in Appendix C and Appendix D of this report.

ZPA, local ZPA and peak acceleration at the lowest predominant cabinet resonance (based on 3% damping), and the number of chatters recorded. Note that all chatters occurred when the devices were in their deenergized state; no chattering of energized contacts was detected in any test.

Table 4-10 summarizes the number of chatters recorded for each device during each test, and correlates these results according to mounting configuration, direction of horizontal input motion, and horizontal table ZPA in the direction of excitation (i.e., F-B or S-S). Note that this table includes only the random motion tests; the gaps in test numbering account primarily for resonance search tests (see Table 3-1 for the complete summary of test conditions). Note also that this table was constructed after both chatter detector output and device signal time histories had been examined. As a result, the number of chatters indicated may differ from the chatter detector output because the computer software does not distinguish between chatter and contact "bounce" during a commanded change of state.

The three vertical columns on the extreme left side of Table 4-10 provide, respectively, the following information:

- the MCC draw-out units containing electrical devices, each listed with the associated accelerometer measuring local response (see Fig. 2-10). Note that the draw-out units are listed in their top-to-bottom order in the MCC, and that all accelerometers listed measure horizontal response in the respective direction of horizontal input motion (i.e., side-to-side or front-to-back) except for accelerometer 12v which measures vertical response.

- for each draw-out unit, the associated electrical devices listed by device code (see Table 2-1 and 2-2).

- for each device, the instrumented contacts. For relays, these comprise two contact pairs, one normally-open (NO) and one normally-closed (NC). For all starters, one pair of main contacts ("MAIN") is indicated in addition to the NO and NC auxiliary contacts; for reversing starters, the

auxiliary contacts are further identified by whether they are intended for forward ("F") or reverse ("R") operation. Recall that "forward" and "reverse" contacts differ only in circuit function, the contacts themselves being physically identical.

By following any row across the table, the behavior of a particular pair of instrumented contacts can be followed over all tests. Similarly, each column compares the behavior of all instrumented contacts for a given test run.

Close examination of Table 4-10 reveals the following general observations made during the biaxial tests:

- with only one exception (Run 24, Location 2J, Contacts X-NC), no chatter occurred when the MCC was horizontally excited in the side-to-side direction, in other words, when the direction of the input motion was perpendicular to the direction of contact action for all horizontally-oriented devices.

- virtually all chatter in starters occurs in auxiliary rather than main contacts. Single chatters in main contacts most likely reflect "bouncing" during commanded state changes and therefore would not represent functional "failure" according to our definition.

- in the series of tests run on the top-braced MCC, chatter occurs earlier (i.e., at lower levels of table ZPA) and more often in devices located near the mid-plane elevation. In the top-braced configurations, chatter is predominant in devices located near the top of the cabinet. This behavior is consistent with the overall global response of the cabinet, which in turn depends upon the particular mounting configuration (see Figs. 4-4 and 4-5).

- chatter occurs earlier (i.e., at lower levels of table ZPA) and more often in normally-closed contacts than in normally-open contacts. This holds true for starter (auxiliary) contacts as well as for relay

contacts, and implies that chatter is related to the relative distance two contacts must traverse in order to make (or break) contact.

- the two General Electric Type CR relays mounted at location 3J as a replication test exhibited essentially identical behavior with regard to the particular runs during which chatter did or did not occur as well as to the number of chatters recorded, if any.

- for any given device, the number of chatters does not seem to correlate strongly with input ZPA level.

- no chatter is observed in the reed-type relay contacts (CH-NO, CH-NC) regardless of input level, location in the cabinet, or cabinet mounting configuration. This observation is no surprise considering the very low mass (and accordingly low inertial forces resulting from a given input motion) of the reed contacts compared to that typical of armature-type contacts.

For each device, a comparison plot also constructed showing the lowest local test response spectra for which chatter was observed. A second plot was then constructed showing the highest local TRS for which chatter was not indicated for each mounting configuration. These comparison plots are presented in pairs as Figs. 4-14 and 4-15 through 4-19 and 4-21 for starters (auxiliary contacts only) and as Figs. 4-22 and 4-23 through 4-28 and 4-29 for relays. Note that these spectra are all for horizontal motion in the F-B direction and are generated at three percent damping. Our selection of this value is not to imply that we necessarily regard this as the "real" damping for the cabinet, but rather reflects a somewhat arbitrary choice from the one-, three-, and five percent test response spectra routinely generated for each accelerometer location. Note also that the "chatter" spectra simply represent local motion recorded in those instances where chatter was detected, and are not to be interpreted as the frequency-dependent chatter threshold ("fragility level") for the indicated device.

Comparing each pair of comparison plots (i.e., by overlaying one plot on the other) shows that while the "chatter" spectra as a whole tend to exceed the "no-chatter" spectra, considerable overlap exists. This result implies that a clear fragility threshold cannot be uniquely determined on the basis of random input motion characterized by ZPA alone. Instead, it appears that when the local response is near the "threshold" level, relatively minor perturbations in local response (caused by variations in input motion or by other local influences) will dictate whether or not chatter occurs. On the other hand, a response spectrum drawn just below the lowest "no-chatter" TRS could represent a reasonable "lower bound" fragility level.

Figure 4-30 presents the "no-chatter" spectra for the Cutler-Hammer Powerreed relay. At no time during testing, regardless of input motion, was any chatter of this reed-type relay observed.

Our review of this data implies that a unique correlation between chatter and local ZPA cannot be drawn, although it is generally apparent that higher ZPA levels do aggravate chatter.

4.5 Sinusoidal Tests

The results of the random-motion tests, in particular the lack of a strong correlation between chatter threshold and local ZPA, raised questions about the effect of waveform frequency content on device fragility. To gain insight into this effect, two devices -- a Size 2 starter and a Square-D Type X general purpose relay -- were removed from the MCC and subjected to low-level single-frequency sinusoidal input motion. Appendix C contains detailed information on input frequencies and acceleration levels, as well as plots showing the resultant device chatter. The results of these tests, summarized in Fig. 4-31, that each of these devices showed a significant sensitivity to input motion in the 2.5 to 8 Hz range. This result suggests for these two devices that when mounted in the MCC, their chatter threshold may be most affected by that portion of the local in-cabinet TRS between 2.5 and 8 Hz. This could not, however, be firmly established from the response spectra available from the MCC tests.

Note that because the input motions are different (i.e., side-sweep as opposed to random excitation), the acceleration levels in Fig. 4-31 are not to be directly compared with the in-cabinet spectra from the MCC tests. Note conversely that the in-cabinet "chatter" spectra are not to be interpreted in same manner as Fig. 4-31, i.e., chatter threshold as a function of frequency. The in-cabinet "chatter" spectra present local response measured at a given location during a given run when chatter was observed to occur in a given device at that location, and do not themselves indicate which spectral frequencies most affect the behavior of a given electrical device.

4.6. Structural Damage

We observed no indication of structural damage during testing of the MCC in the top-supported configuration in either the S-S or in the F-B directions. Testing of the free-standing MCC in the S-S direction similarly caused no indication of structural damage until late in the testing program. However, testing of the free-standing cabinet in the F-B direction caused significant damage to welds at the bottom of the MCC frame as table ZPA increased (see Figs. 4-32 and 4-33). The first sign of damage -- peeled paint -- was observed after a F-B ZPA of 1.2 to 1.4g. After run 29 (1.9g table ZPA), welds between the base frame and the vertical frame members were cracked in each corner of the cabinet (Figs. 4-34 through 4-37). All cracks were rewelded before testing continued. After run 31 (2.2g table ZPA), the weld at the left front corner of the cabinet base was cracked; again, it was rewelded. The rewelded corners then withstood tests in the S-S and F-B directions up to 2.3g table ZPA. One of the original cabinet welds at the rear of the base was broken during Run 35 (1.2g table ZPA) and rewelded.

Prior to Run 48, two sets of strain gauges, SG-1 through SG-4 and SG-5 through SG-8, were added to the MCC base at the left and right front corners, respectively (see Figs. 4-38 and 4-39). Substantial damage to the cabinet base was noted after Run 48 (2.1g horizontal ZPA, F-B direction). The left front corner experienced significant distortion, plastic deformation, and broken welds (see Figs. 4-40 and 4-41). Local deformation of the base frame was observed at mounting bolt locations (see Fig. 4-42). During Run 48 up to

3000 microstrain was measured, indicating local stresses well above the elastic limit. The frame of the cabinet was again repaired, after which testing continued up to the last run (Run 56), when substantial damage to the left and right front base corners was observed (see Figs. 4-43 and 4-44).

Video recordings made during testing clearly showed that F-B input motion induces a torsional mode of cabinet response; this response mode apparently contributed to the repeated failure of the front left corner of the MCC base. The torsional mode most likely results from structural asymmetry due to the vertical wireway down the right side of each column, which adds a fifth vertical frame member.

It is important to point out that despite the observed damage, at no time was the ability of the cabinet to adequately support the internal devices impaired. In other words, the safety function of the cabinet was not compromised during any test.

4.7 Repeatability

Two General Electric Type CR relays mounted side-by-side in draw-out unit 3J indicated essentially identical response during each and every test.

Following Run 31, two pairs of identical relays and two pairs of identical controllers were interchanged in location and the run repeated (Run 32). Figure 4-45 diagrams the interchange. During these runs the global cabinet response was generally in a cantilever mode, there being no top brace. Consequently, in-cabinet horizontal accelerations associated with the cabinet "frame" response would be expected to be more severe at higher elevations in the cabinet. From these interchanges we made the following observations (refer to Table 4-10):

- at location 1C (i.e., high in the cabinet), the NC auxiliary contacts of the Size 3 starter chattered five times during each of the two runs while the NO contacts chattered three times during each run. At location 1M (near the cabinet base), no chatter was recorded during either run.

- at location 2B (high in the cabinet), the NC contacts of the Westinghouse Type AR relay chatter six and eight times during Runs 31 and 32, respectively. The corresponding NO contacts chattered four times during each run. By contrast, no chatter was recorded in either the NC or NO contacts in the relay mounted lower in the cabinet (location 1J).

- no contact chatter was recorded during either run in the Square-D Type KP relays interchanged between locations 3D and 2J (higher and lower in the cabinet, respectively).

These results clearly suggest that the chatter behavior of nominally identical devices is dependent more on location (particularly elevation) in the cabinet and less on any random "unit variations" among individual devices.

The correlation between chatter and elevation also suggests that the lower frequency "frame" response of the MCC (around 5 Hz for this particular mounting configuration) has a greater influence on device behavior than the higher frequency "bucket" responses of the individual draw-out units. The results of the low-level transmissibility tests performed on the MCC in each mounting configuration (see Table 4-1) indicate that the local resonant frequencies within each pair of interchange locations are similar (and between locations 1C and 1M, identical). Given this observation, if chatter were highly dependent on local response we would then expect to see nominally identical devices behaving similarly regardless of elevation in the cabinet. Similarly, if the specific devices tested were not truly "identical" due to unit variations, then the occurrence of chatter would tend to be device- rather than location-specific. In other words, the device that chatters high in the cabinet during one run might be expected to chatter during the next when interchanged with its counterpart lower in the cabinet. Neither situation, however, is inferred by the test results. Instead, whether or not the Size 3 auxiliary contacts and the Type AR relay contacts chatter depends on location and not on the individual device being tested. The results for the Type KP relays are less conclusive in this regard, although the consistent "no chatter" behavior of this relay pair does not contradict conclusions drawn from the behavior of the other two device pairs.

4.8 Discussion of Results

We completed a total of 56 test runs on the motor control center, 43 of which were biaxial random motion tests. Table input motions in the random motion tests ranged up to 2.5g ZPA, resulting in spectral accelerations up to 20g and higher at device locations.

From the results of these tests we have made the following observations.

Functional Behavior

- all 14 relays and all 8 starters responded normally to commanded changes of state for all input levels and MCC support configurations. This held true for each device regardless of whether it was initially energized or deenergized.

  Only one case was observed when a device (a Size 2 FVR starter) did not respond to a commanded state change. This was attributed to a control switch being inadvertently left open, which disconnected the starter from the common power source. As a result, the contacts remained deenergized over several runs before the error was corrected.

- for all devices, chatter occurred only when the device contacts were in their deenergized state. Without exception, no chatter of energized contacts was recorded.

- for all devices, virtually all chatter occurred when the MCC was tested in its front-to-back orientation. Only isolated instances of contact chatter were recorded when the MCC was tested in its side-to-side orientation; these were attributed to possible variations in local in-cabinet waveforms.

  Given the mounting orientation of most devices in the cabinet (i.e., direction of contact action oriented with the F-B axis of the cabinet),

these results imply that chatter is most likely to occur when the input motion is aligned with the direction of contact action. Virtually no chatter was observed when the input motion was oriented perpendicular to the direction of contact action.

- for starters, virtually all chatter occurred in auxiliary contacts. Only isolated occurrences of spurious main contact action were recorded, most of which could be attributed to contact "bounce" during a commanded state change.

- for all devices, normally-closed contacts consistently chattered at lower input levels and more often than normally-open contacts. This suggests for these devices that contact chatter is caused by armature movement rather than local response of the contact element.

- neither reed-type relay was observed to chatter, regardless of input level or MCC mounting configuration. This observation was not surprising considering the extremely low contact mass of the reed-type relays compared that of the armature-type relays tested.

- the occurrence of chatter appears to correlate only weakly with local in-cabinet ZPA. The significant overlap in "chatter" and "no chatter" in-cabinet response spectra implies that spectral acceleration may be a more appropriate parameter to define the "threshold" above which chatter occurs.

- the results of single-axis, single-frequency tests performed on one Size 2 starter and one relay removed from the MCC indicate that chatter is most likely to occur for input motions in the 2.5 to 8 Hz range. This result further supports the conclusion that spectral acceleration, rather than ZPA, is a more appropriate basis for characterizing device fragility.

Structural Behavior

- with the brace at the top of the MCC and a four bolt-per-column connection at the cabinet base, the resonant frequency of the cabinet frame was about 12 Hz. Removing the top brace caused the resonant frequency to drop to about 5 Hz. Reducing from four to two the number of mounting bolts per column (the standard mounting recommended by the MCC manufacturer) further reduced the cabinet frequency to about 3.5 Hz.

  The effect of mounting configuration on cabinet response takes on added significance when the results of the single-axis single-frequency device tests are considered. The one relay and one starter tested both indicated highest sensitivity to input motions in the 2.5 to 8 Hz range. Removing the top brace from the MCC lowered the F-B cabinet frequency from well outside this range to a point where it could conceivably have a significant effect on device behavior.

- the predominant "bucket" resonances ranged from about 14 to 26 Hz, well outside the "sensitive" range indicated by the sinusoidal tests. An attempt to raise the resonant frequencies of three compartments (2B, 2E, and 2J) by adding mounting screws was not successful, although testing by others of similar cabinets has indicated that sufficient bracing can reduce or eliminate high-frequency response caused by compartment rattling. In any case, high-frequency input motion (i.e., greater than about 10 Hz) does not appear to significantly affect the functional behavior of the devices tested.

- although no detailed modal analyses were performed to generate in-cabinet transfer functions, an initial comparison of test response spectra in the F-B direction suggests that the free-standing cabinet amplifies floor motions by a factor of three to four.

- we observed no cabinet damage when the MCC was braced at the top. Testing of the free-standing MCC in the side-to-side direction similarly caused no indication of structural damage until after the MCC had been subjected to a large number of prior strong motion tests. Substantial physical damage was first noted after Run 29 (1.9g table ZPA) in the form of cracked welds between the base frame and the vertical frame members; by this run the MCC had been subjected to 20 prior strong motion tests. After rewelding, the corner welds withstood tests in the S-S and F-B directions up to 2.3g table ZPA.

  From Run 48 onwards, the base welds in the cabinet broke with relative regularity. We believe this to be due to fatigue rather than to any inherent weakness in the cabinet; note that by Run 48 the MCC had already experienced 35 prior strong motion tests.

Although substantial damage occurred in later tests, the cabinet nevertheless withstood some 20 strong motion tests at ZPA levels up to 1.9g before any significant damage was observed; by comparison, the highest horizontal floor response predicted for any vital motor control center at Diablo Canyon is 1.2g ZPA. Furthermore, the damage that was observed in no way affected the ability of the internal devices to perform their intended functions. Based on the guidelines discussed in Section 1.6, the test results imply that the MCC cabinet very nearly fits our definition of a "high capacity" component.

Table 4-1. Resonance frequency tabulation.

Bolts per Column	Top Support	Internal Bracing	Axis	Main Frame	Compartment												
					1C	1G	1J	1M	2B	2E	2J	2M	3B	3D	3G	3J	3M
4	Yes	No	F-B	12	No predominant bucket resonance												
			S-S		No predominant bucket resonance												
4	No	No	F-B	5	15	20	23	15	19	17	22	15	20	20	18	18	16
			S-S	9	16	20							20		15		
4	No	Yes	F-B	5.2	15	22	19	20	22	19	22	16	22	26	16	18	15
			S-S		No test performed												
2	No	No	F-B	3.5	18	22	22	14	19	17	22	15	21	25	17	19	16
			S-S	6.3	No predominant bucket resonance												

Note: No significant vertical responses were detected in the test range.

Table 4-2. Results of static pull tests.

Bolts per Column	Top Support	Internal Bracing	Direction	Force (lb)	Deflection (in)	Stiffness (kips/in)
2	No	No	Side-Side	580	0.06	9.7
2	No	No	Back-Frnt	580	0.39	1.5
4	No	No	Back-Frnt	580	0.12	4.8

Table 4-3. Sample chatter detector output.

WYLE LABORATORIES,NORCO,CA. FACILITY CHATTER AND PULSE ANALYSIS PROGRAM 12/05/85 16:15:56 HOURS PAGE 1

START TIME= 0.0000 STOP TIME= 26.980

TEST NAME=LLNL 26447, RUN 46, X-Y AXIS, 5TH LEVEL/6 BOLTS, OFF-ON FW
TEST DATE=12/05/85 16: 9:46 HOURS

CHANNEL ID	CHANNEL NUMBER	FIRST CHATTER	LAST CHATTER	STATE CHANGE	NUMBER OF CHATTER FAILURES PER TIME LENGTH 2.00-5.00	5.00-10.0	10.0-20.0	20.0-40.0	40.0-80.0	>80.0	TOTAL
1C-NO	2	7.194	14.387	3	1	0	0	0	0	0	1
1C-NC	3	7.991	10.557	3	0	0	1	1	0	0	2
1C-AMPS	4			3	NO CHATTER						
2B-W.NO	6	8.807	14.381	3	1	1	0	0	0	0	2
2B-W.NC	7	8.032	12.018	3	0	2	1	2	0	0	5
2B-X.NO	8	8.804	8.818	3	0	0	1	0	0	0	1
2B-X.NC	10	8.144	12.022	3	0	0	2	4	0	0	6
1G-NO	11			2	NO CHATTER						
1G-NC	12			3	NO CHATTER						
1G-AMPS	13			3	NO CHATTER						
1J-W.NO	14			3	NO CHATTER						
1J-W.NC	15			3	NO CHATTER						
1J-KP.NO	16			3	NO CHATTER						
1J-KP.NC	17			3	NO CHATTER						
1M-NO	18			3	NO CHATTER						
1M-NC	19			3	NO CHATTER						
1M-AMPS	20			3	NO CHATTER						
2E-FW.NO	21			3	NO CHATTER						
2E-FW.NC	22	8.533	12.016	3	0	2	7	0	0	0	9
2E-RV.NO	23			0	NO CHATTER						
2E-RV.NC	24	8.813	12.007	1	0	0	0	0	2	5	7
2E-AMPS	25			3	NO CHATTER						
2J-W.NO	26	14.380	14.382	3	1	0	0	0	0	0	1
2J-W.NC	27			3	NO CHATTER						
2J-GE.NO	28			3	NO CHATTER						
2J-GE.NC	29	8.697	8.707	3	0	1	0	0	0	0	1
2J-KP.NO	30			3	NO CHATTER						
2J-KP.NC	31			3	NO CHATTER						
2J-X.NO	32			3	NO CHATTER						
2J-X.NC	33			3	NO CHATTER						
2J-CH.NO	34			3	NO CHATTER						
2J-CH.NC	35			3	NO CHATTER						
2M-NO	36			2	NO CHATTER						
2M-NC	38	7.982	7.992	2	1	0	0	0	0	0	1
2M-AMPS	39	7.980	14.389	1	0	0	0	0	0	1	1
3B-NO	40	8.810	8.816	3	0	1	0	0	0	0	1
3B-NC	42	8.802	10.551	3	0	0	0	2	0	0	2
3B-AMPS	43			3	NO CHATTER						
3D-GE.NO	44			3	NO CHATTER						

Table 4-3 (cont.). Sample chatter detector output.

WYLE LABORATORIES,NORCO,CA FACILITY CHATTER AND PULSE ANALYSIS PROGRAM 12/05/85 16:15:56 HOURS PAGE 2

TEST NAME=LLNL 26447 RUN 46, X-Y AXIS, 5TH LEVEL/6 BOLTS, OFF-ON FW
TEST DATE=12/05/85 16: 9:46 HOURS

CHANNEL ID	CHANNEL NUMBER	FIRST CHATTER	LAST CHATTER	STATE CHANGE	NUMBER OF CHATTER FAILURES PER TIME LENGTH	TOTAL
3D-GE NC	45			3	NO CHATTER	
3D-CH NO	46			3	NO CHATTER	
3D-CH NC	47			3	NO CHATTER	
3D-KP NO	48			3	NO CHATTER	
3D-KP NC	49			3	NO CHATTER	
3G-NO	50			2	NO CHATTER	
3G-NC	51			3	NO CHATTER	
3G-AMPS	52	7 980	14 389	1	0 0 0 0 0 1	1
3J-GE1NO	53			3	NO CHATTER	
3J-GE1NC	54			3	NO CHATTER	
3J-GE2NO	55			3	NO CHATTER	
3J-GE2NC	56			3	NO CHATTER	
3M-FW NO	57			3	NO CHATTER	
3M-FW NC	58	6 417	14 272	3	4 5 5 0 0 0	14
3M-RV NO	59			0	NO CHATTER	
3M-RV NC	60	11 208	13 772	1	0 0 0 0 0 2	2
3M-AMPS	61			3	NO CHATTER	
ST-ST-CH	62			3	STATE SW # 2 FIRST CHANGE AT 7 1700 LAST CHANGE AT 14 359	
RL-ST-CH	63			3	STATE SW # 1 FIRST CHANGE AT 7 1570 LAST CHANGE AT 14 366	
RL-OFF	92			3	NO CHATTER	
ST-OFF	94			3	NO CHATTER	
					TOTAL=	57

Table 4-4. Chatter vs ZPA Tabulation for Size 2 Reversing Starters

Location /Accel. No.	Run No.	Table ZPA (g)	Local ZPA (g)	Local Peak (g/Hz)	Number of Chatters NO		NC	
2E/11	13	1.0	3.1	16/12	0	0	0	0
	14	1.3	4.2	22/12	0	0	9	1
	15	1.4	5.0	34/12	1	0	27	10
	16	1.8	5.2	38/12	3	0	49	19
	17	2.1	6.0	40/12	12	0	102	57
	27	1.6	3.2	14/5	0	0	2	1
	28	1.6	3.9	17/5	0	0	2	2
	29	1.9	5.4	21/5	0	1	12	11
	30	1.9	5.0	27/5	0	1	15	14
	31	2.2	6.4	25/5	0	0	11	6
	32	1.7	4.8	22/5	0	0	9	12
	43	1.5	4.1	11/3	0	0	0	0
	44	1.5	4.2	13/3	0	0	1	3
	45	1.5	4.6	16/3	0	0	2	5
	46	2.5	5.2	16/3	0	0	9	7
	48	2.1	5.4	28/5	0	0	18	19
	49	2.3	7.0	30/5	0	1	14	30
	52	1.7	2.9	11/5	0	0	0	1
	53	2.4	8.1	20/5	0	0	3	11
	54	1.4	2.8	14/5	0	0	0	1
	55	2.1	7.8	23/5	0	3	10	22
	56	2.2	8.3	21/5	0	0	3	10
3M/19	13	1.0	4.2	10/11	0	0	0	0
	14	1.3	2.8	13/11	0	0	0	0
	15	1.4	5.3	19/11	0	0	1	3
	16	1.8	4.4	22/11	0	0	6	10
	17	2.1	5.5	26/11	0	0	18	14
	27	1.6	2.7	5/5	0	0	0	0
	28	1.6	3.7	16/5	0	0	0	0
	29	1.9	4.5	6.5/5	0	0	4	0
	30	1.9	4.9	8.8/5	0	0	5	2
	31	2.2	6.2	9.4/5	0	0	6	2
	32	1.7	3.6	7.3/5	0	0	1	1
	43	1.5	3.2	4.5/3	0	0	0	0
	44	1.5	5.2	5.4/3	0	0	1	0
	45	1.5	4.8	6.5/3	0	0	8	2
	46	2.5	5.7	6.5/3	0	0	14	2
	48	2.1	4.4	6.5/3	1	0	14	5
	49	2.3	5.0	10/3	1	0	18	8
	52	1.7	3.0	4.1/5	0	0	0	0
	53	2.4	4.5	10/5	0	0	3	1
	54	1.4	3.2	6/5	0	0	0	0
	55	2.1	4.4	8.5/5	0	0	14	5
	56	2.2	4.4	7/5	0	0	18	4

Table 4-5. Chatter vs ZPA Tabulation for Size 2 FVNR Starters

Location /Accel. No.	Run No.	Table ZPA (g)	Local ZPA (g)	Local Peak (g/Hz)	Number of Chatters NO	NC
3B/ 9	13	1.0	1.8	6.3/5	0	0
	14	1.3	2.9	11/5	0	0
	15	1.4	4.0	15/5	0	0
	16	1.8	4.0	16/5	0	2
	17	2.1	5.5	20/5	0	1
	27	1.6	3.0	13/5	0	2
	28	1.6	3.8	16/5	0	5
	29	1.9	5.3	20/5	6	11
	30	1.9	3.7	18/5	0	3
	31	2.2	4.8	17/5	1	3
	32	1.7	3.8	15/5	0	3
	43	1.5	2.9	11/3	0	0
	44	1.5	4.3	13/3	0	1
	45	1.5	4.2	16/3	0	1
	46	2.5	4.5	19/3	2	8
	48	2.1	4.9	9/3	2	8
	49	2.3	5.2	15/3	5	16
	52	1.7	2.5	10/5	0	0
	53	2.4	6.0	18/3	0	5
	54	1.4	3.0	14/5	0	0
	55	2.1	4.8	24/5	5	13
	56	2.2	6.2	19/5	2	8
1G/14	13	1.0	1.5	3.6/5	0	0
	14	1.3	1.7	4.7/5	0	0
	15	1.4	2.6	6/5	0	0
	16	1.8	3.2	7.8/5	0	0
	17	2.1	4.0	10/5	0	3
	27	1.6	1.6	8/5	0	0
	28	1.6	2.3	9.5/5	0	0
	29	1.9	2.8	11/5	0	1
	30	1.9	4.3	17/5	0	5
	31	2.2	5.7	16/5	0	2
	32	1.7	3.8	13/5	0	7
	43	1.5	2.4	6.5/3	0	0
	44	1.5	2.5	9/3	0	0
	45	1.5	2.8	11/3	0	0
	46	2.5	3.6	11/3	0	0
	48	2.1	4.6	14/5	0	2
	49	2.3	5.4	20/5	7	17
	52	1.7	2.3	8/5	0	0
	53	2.4	4.8	16/5	0	2
	54	1.4	3.3	12/5	0	0
	55	2.1	5.3	17/5	0	7
	56	2.2	5.4	17/5	0	2

Table 4-6. Chatter vs ZPA Tabulation for Size 3 FVNR Starters

Location /Accel. No.	Run No.	Table ZPA (g)	Local ZPA (g)	Local Peak (g/Hz)	Number of Chatters NO	NC
1C/8	13	1.0	1.9	4/5	0	0
	14	1.3	2.7	5.1/5	0	0
	15	1.4	4.2	6.6/5	0	0
	16	1.8	4.0	8.2/5	0	0
	17	2.1	4.3	11/5	0	0
	27	1.6	2.4	13/5	0	0
	28	1.6			0	0
	29	1.9	5.2	20/5	0	2
	30	1.9	6.6	29/5	2	5
	31	2.2	8.8	28/5	3	5
	32	1.7	7.0	24/5	3	5
	43	1.5	3.9	9.5/5	0	0
	44	1.5	4.7	14/3	0	0
	45	1.5	5.0	10/5	0	0
	46	2.5	5.2	10/5	0	2
	48	2.1	8.2	28/5	7	8
	49	2.3	8.0	33/5	4	10
	52	1.7	3.3	13/5	0	0
	53	2.4	9.6	30/5	0	1
	54	1.4	4.8	20/5	0	0
	55	2.1	6.8	30/5	5	7
	56	2.2	7.5	28/5	2	4
1M/18	13	1.0			0	0
	14	1.3			0	0
	15	1.4			0	0
	16	1.8			0	0
	17	2.1			0	0
	27	1.6			0	0
	28	1.6			0	0
	29	1.9			0	0
	30	1.9			0	0
	31	2.2			0	0
	32	1.7			0	0
	43	1.5			0	0
	44	1.5			0	0
	45	1.5			0	0
	46	2.5			0	0
	48	2.1			0	0
	49	2.3			0	0
	52	1.7			0	0
	53	2.4			0	0
	54	1.4			0	0
	55	2.1			0	0
	56	2.2			0	0

Table 4-7. Chatter vs ZPA Tabulation for GE Type CR Relays

Location /Accel. No.	Run No.	Table ZPA (g)	Local ZPA (g)	Local Peak (g/Hz)	Number of Chatters NO	NC
3D/13	13	1.0			0	0
	14	1.3			0	0
	15	1.4	6.5	7/5	0	0
	16	1.8			0	1
	17	2.1	7.5	11.5	0	3
	27	1.6			0	0
	28	1.6			0	0
	29	1.9			0	0
	30	1.9			0	0
	31	2.2	7.0	18/5	0	0
	32	1.7			0	0
	43	1.5			0	0
	44	1.5			0	0
	45	1.5			0	0
	46	2.5	4.5	16/3	0	0
	48	2.1			0	0
	49	2.3	5.5	27/5	0	3
	52	1.7			0	0
	53	2.4	6.7	20/5	0	0
	54	1.4			0	0
	55	2.1			0	0
	56	2.2			0	0
2J/15	13	1.0	3.6	14/11	0	0
	14	1.3	5.0	21/11	0	1
	15	1.4	6.5	32/11	0	1
	16	1.8	6.0	36/11	0	7
	17	2.1	7.5	38/11	1	10
	27	1.6	3.0	11/5	0	0
	28	1.6	4.3	13/5	0	0
	29	1.9	5.3	14/5	0	1
	30	1.9	5.2	20/5	0	0
	31	2.2	6.2	17/5	0	0
	32	1.7	5.0	16/5	0	0
	43	1.5	2.8	8/3	0	0
	44	1.5	3.3	10/3	0	0
	45	1.5	3.6	11/3	0	0
	46	2.5	4.2	12/3	0	1
	48	2.1	6.8	16/5	0	0
	49	2.3	5.5	23/5	0	5
	52	1.7	2.1	8/5	0	0
	53	2.4	5.2	15/5	0	0
	54	1.4	2.8	11/5	0	0
	55	2.1	4.1	15/5	0	3
	56	2.2	6.2	15/5	0	1

Table 4-7 (cont.). Chatter vs ZPA Tabulation for GE Type CR Relays

Location /Accel. No.	Run No.	Table ZPA (g)	Local ZPA (g)	Local Peak (g/Hz)	Number of Chatters NO	NC
3J/17	13	1.0	2.7	4.4/5	0	0
	14	1.3	3.9	5.6/5	0	0
Relay 1	15	1.4	5.8	7/5	0	0
	16	1.8	6.5	10/5	0	1
	17	2.1	6.7	12/5	0	3
	27	1.6	2.5	7.5/5	0	0
	28	1.6	3.1	8.7/5	0	0
	29	1.9	5.2	10/5	0	0
	30	1.9	5.1	13/5	0	0
	31	2.2	6.6	13/5	0	0
	32	1.7	5.0	10/5	0	0
	43	1.5	3.4	5.6/3	0	0
	44	1.5	4.0	7.5/3	0	0
	45	1.5	5.4	9/3	0	0
	46	2.5	7.0	9.5/3	0	0
	48	2.1	6.1	13/5	0	0
	49	2.3	6.0	16/5	0	0
	52	1.7	2.8	5.8/5	0	0
	53	2.4	5.2	13/5	0	0
	54	1.4	3.8	8/5	0	0
	55	2.1	6.0	12/5	0	0
	56	2.2	5.9	11/5	0	0
3J/17	13	1.0	2.7	4.4/5	0	0
	14	1.3	3.9	5.6/5	0	0
Relay 2	15	1.4	5.8	7/5	0	1
	16	1.8	6.5	10/5	0	1
	17	2.1	6.7	12/5	0	3
	27	1.6	2.5	7.5/5	0	0
	28	1.6	3.1	8.7/5	0	0
	29	1.9	5.2	10/5	0	0
	30	1.9	5.1	13/5	0	0
	31	2.2	6.6	13/5	0	0
	32	1.7	5.0	10/5	0	0
	43	1.5	3.4	5.6/3	0	0
	44	1.5	4.0	7.5/3	0	0
	45	1.5	5.4	9/3	0	0
	46	2.5	7.0	9.5/3	0	0
	48	2.1	6.1	13/5	0	0
	49	2.3	6.0	16/5	0	0
	52	1.7	2.8	5.8/5	0	0
	53	2.4	5.2	13/5	0	0
	54	1.4	3.8	8/5	0	0
	55	2.1	6.0	12/5	0	0
	56	2.2	5.9	11/5	0	0

Table 4-8. Chatter vs ZPA Tabulation for Westinghouse Type AR Relays

Location /Accel. No.	Run No.	Table ZPA (g)	Local ZPA (g)	Local Peak (g/Hz)	Number of Chatters NO	NC
2B/10	13	1.0	2.5	3.9/5	0	0
	14	1.3	3.4	5.1/5	0	0
	15	1.4	3.8	7/5	0	0
	16	1.8	4.3	8.4/5	0	0
	17	2.1	6.0	11/5	0	1
	27	1.6	4.2	15/5	0	0
	28	1.6	5.5	17/5	0	0
	29	1.9	7.0	24/5	7	8
	30	1.9	7.5	28/5	4	7
	31	2.2	9.0	27/5	4	6
	32	1.7	6.0	23/5	4	8
	43	1.5	4.8	13/3	0	0
	44	1.5	5.0	15/3	0	1
	45	1.5	5.7	17/3	0	0
	46	2.5	7.0	20/3	2	5
	48	2.1	8.5	30/5	10	12
	49	2.3	8.0	24/5	10	18
	52	1.7	3.4	13/5	0	0
	53	2.4	9.5	30/5	0	2
	54	1.4	4.5	18/5	0	0
	55	2.1	7.5	27/5	10	10
	56	2.2	7.5	25/5	1	3
2J/15	13	1.0	3.6	14/11	0	0
	14	1.3	5.0	21/11	0	0
	15	1.4	6.5	32/11	0	0
	16	1.8	6.0	36/11	1	1
	17	2.1	7.5	38/11	6	4
	27	1.6	3.0	11/5	0	0
	28	1.6	4.3	13/5	0	0
	29	1.9	5.3	14/5	0	0
	30	1.9	5.2	20/5	0	0
	31	2.2	6.2	17/5	0	0
	32	1.7	5.0	16/5	0	0
	43	1.5	2.8	8/3	0	0
	44	1.5	3.3	10/13	0	0
	45	1.5	3.6	11/3	0	0
	46	2.5	4.2	12/3	0	0
	48	2.1	6.8	16/5	0	0
	49	2.3	5.5	23/5	2	1
	52	1.7	2.1	8/5	0	0
	53	2.4	5.2	15/5	0	0
	54	1.4	2.8	11/5	0	0
	55	2.1	4.1	15/5	0	0
	56	2.2	6.2	15/5	0	0

Table 4-9. Chatter vs ZPA Tabulation for Square-D Type X Relays

Location /Accel. No.	Run No.	Table ZPA (g)	Local ZPA (g)	Local Peak (g/Hz)	Number of Chatters NO	NC
2B/10	13	1.0	2.5	3.9/5	0	0
	14	1.3	3.4	5.1/5	0	0
	15	1.4	3.8	7/5	0	0
	16	1.8	4.3	8.4/5	0	1
	17	2.1	6.0	11/5	0	5
	27	1.6	4.2	15/5	0	0
	28	1.6	5.5	17/5	0	2
	29	1.9	7.0	24/5	7	11
	30	1.9	7.5	28/5	1	12
	31	2.2	9.0	27/5	2	10
	32	1.7	6.0	23/5	4	10
	43	1.5	4.8	13/3	0	0
	44	1.5	5.0	15/3	0	2
	45	1.5	5.7	17/3	0	1
	46	2.5	7.0	20/3	1	6
	48	2.1	8.5	30/5	7	14
	49	2.3	8.0	34/5	12	21
	52	1.7	3.4	13/5	0	0
	53	2.4	9.5	30/5	0	4
	54	1.4	4.5	18/5	0	0
	55	2.1	7.5	27/5	8	12
	56	2.2	7.5	25/5	2	6
2J/15	13	1.0	3.6	14/11	0	0
	14	1.3	5.0	21/11	1	5
	15	1.4	6.5	32/11	7	26
	16	1.8	6.0	36/11	20	37
	17	2.1	7.5	38/11	23	38
	27	1.6	3.0	11/5	0	0
	28	1.6	4.3	13/5	0	0
	29	1.9	5.3	14/5	0	2
	30	1.9	5.2	20/5	0	3
	31	2.2	6.2	17/5	0	5
	32	1.7	5.0	16/5	0	1
	43	1.5	2.8	8/3	0	0
	44	1.5	3.3	10/3	0	0
	45	1.5	3.6	11/3	0	0
	46	2.5	4.2	12/3	0	0
	48	2.1	6.8	16/5	1	8
	49	2.3	5.5	23/5	0	9
	52	1.7	2.1	8/5	0	0
	53	2.4	5.2	15/5	0	0
	54	1.4	2.8	11/5	0	0
	55	2.1	4.1	15/5	0	2
	56	2.2	6.2	15/5	0	1

Table 4-10. Correlation of contact chatter with mounting configuration, input motion, and in-cabinet device location.

LOC. ACC#	DEV. CODE	CONFIG. / RUN# / H.ZPA	S–S: TOP SUPT. 4 BOLTS 4 5 6 7 8 9 10 1.5 1.3 1.4 1.5 1.4 1.9 2.5	F–B: TOP SUPT. 4 BOLTS 13 14 15 16 17 1.0 1.3 1.4 1.8 2.1	SIDE–SIDE 4 BOLTS 20 21 22 23 24 25 .9 1.1 1.2 1.5 1.8 2.1	FRT–BCK 4 BOLTS 27 28 29 30 31 32 1.6 1.6 1.9 1.9 2.2 1.7	SIDE–SIDE 2 BOLTS 36 37 38 39 40 1.2 1.3 1.7 2.0 2.1	FRT–BCK 2 BOLTS 42 43 44 45 46 1.1 1.5 1.5 1.5 2.5	F–B 4 BLTS 48 49 2.1 2.3	FRT–BCK 4 BOLTS 52 54 55 56 53 1.7 1.4 2.1 2.2 2.4
2B 10	W	NO				7 4 4 4		2	10 12	10 1
		NC		1		8 7 6 8		1 5	10 18	10 3 2
	X	NO				7 1 2 4		1	7 12	8 2
		NC		1 5		2 11 12 10 10		2 1 6	14 21	12 6 4
3B 9	S–2	NO				6 1		1	2 5	5 2
		NC		2 1		2 5 11 3 3 3		2 1 2	8 16	13 8 5
		MAIN		1		4				3
1C 8	S–3	NO				2 3 3			7 4	5 2
		NC				2 5 5 5		2	8 10	7 4 1
		MAIN				1 1 3			8 7	7
3D 13	GE	NO								
		NC		1 3					3	
	CH	NO								
		NC								
	KP	NO								
		NC		1						
2E 11 12v	S–2 REV	F–NO		1 3 6						
		F–NC		9 27 49 51		2 2 12 15 11 9		1 2 9	18 14	10 3 3
		R–NO				11 1			1	3
		R–NC		1 10 19 25		1 2 11 14 6 12		3 5 7	19 30	1 1 22 10 11
		MAIN								
1G 14	S–2	NO							2	
		NC		3		1 5 2 7			7 17	7 2 2
		MAIN								
3G 16	S–4	NO		4						
		NC		6 11						
		MAIN		2						
1J 3e	W	NO								
		NC								
	KP	NO								
		NC								
2J 15	W	NO		1 6					2	
		NC		1 4					1	
	GE	NO		1						
		NC		1 1 7 10		1		1	5	3 1
	KP	NO								
		NC		5 2						
	X	NO		1 7 20 23					1	
		NC		5 26 37 38	1	2 3 5 1			8 9	2 1
	CH	NO								
		NC								
3J 17	GE1	NO								
		NC		1 3						
	GE2	NO								
		NC		1 1 3						
1M 18	S–3	NO								
		NC								
		MAIN								
2M 4e	S–4	NO								
		NC		2 6				1		
		MAIN								
3M 19	S–2 REV	F–NO							1 1	
		F–NC		1 6 18		4 5 6 1		1 8 14	14 18	14 18 3
		R–NO								
		R–NC		3 10 14		2 2 1		2 2	5 8	5 4 1
		MAIN								

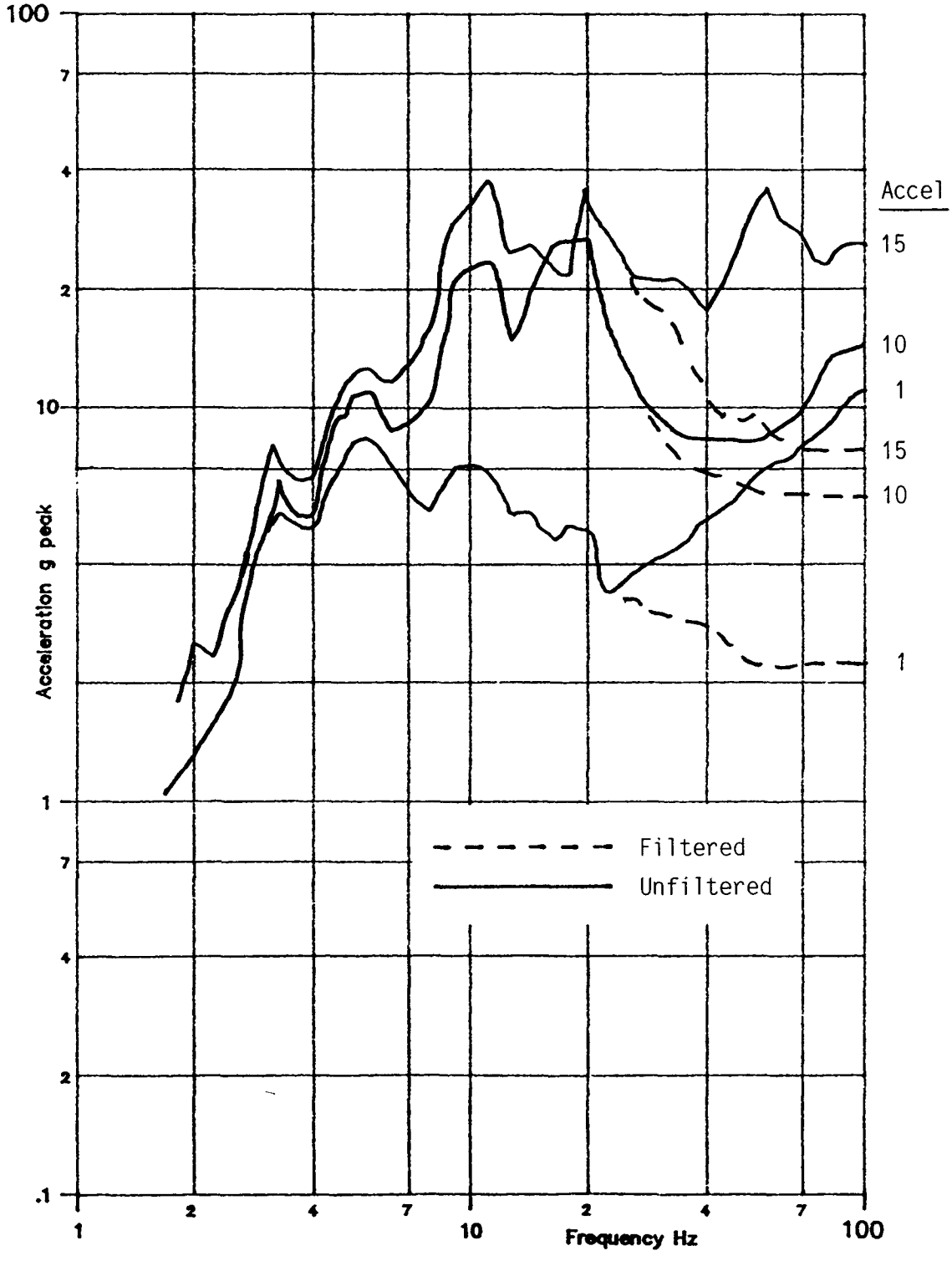

Fig. 4-1. Comparison of filtered and unfiltered TRS plots for Run 17.

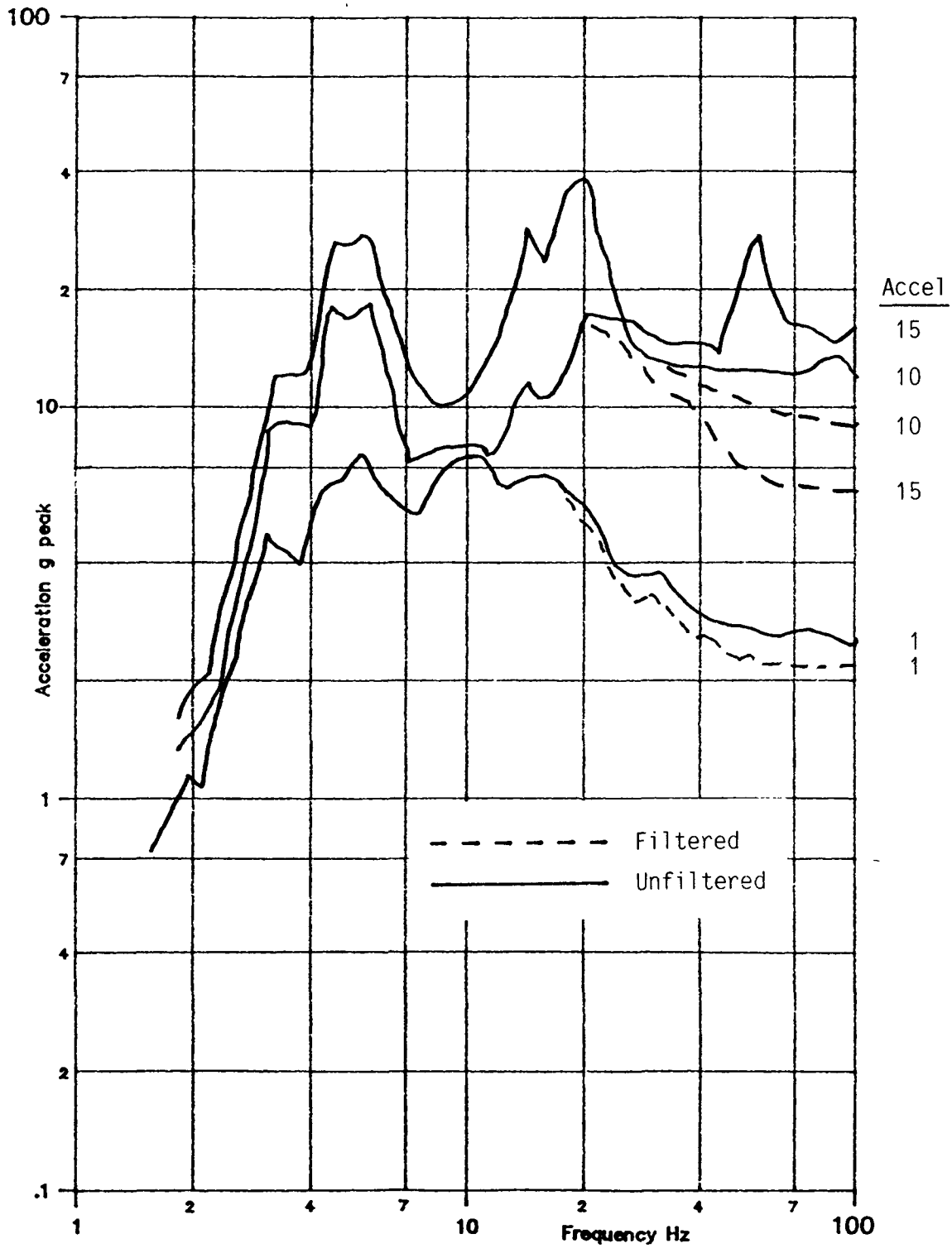

Fig. 4-2. Comparison of filtered and unfiltered TRS plots for Run 31.

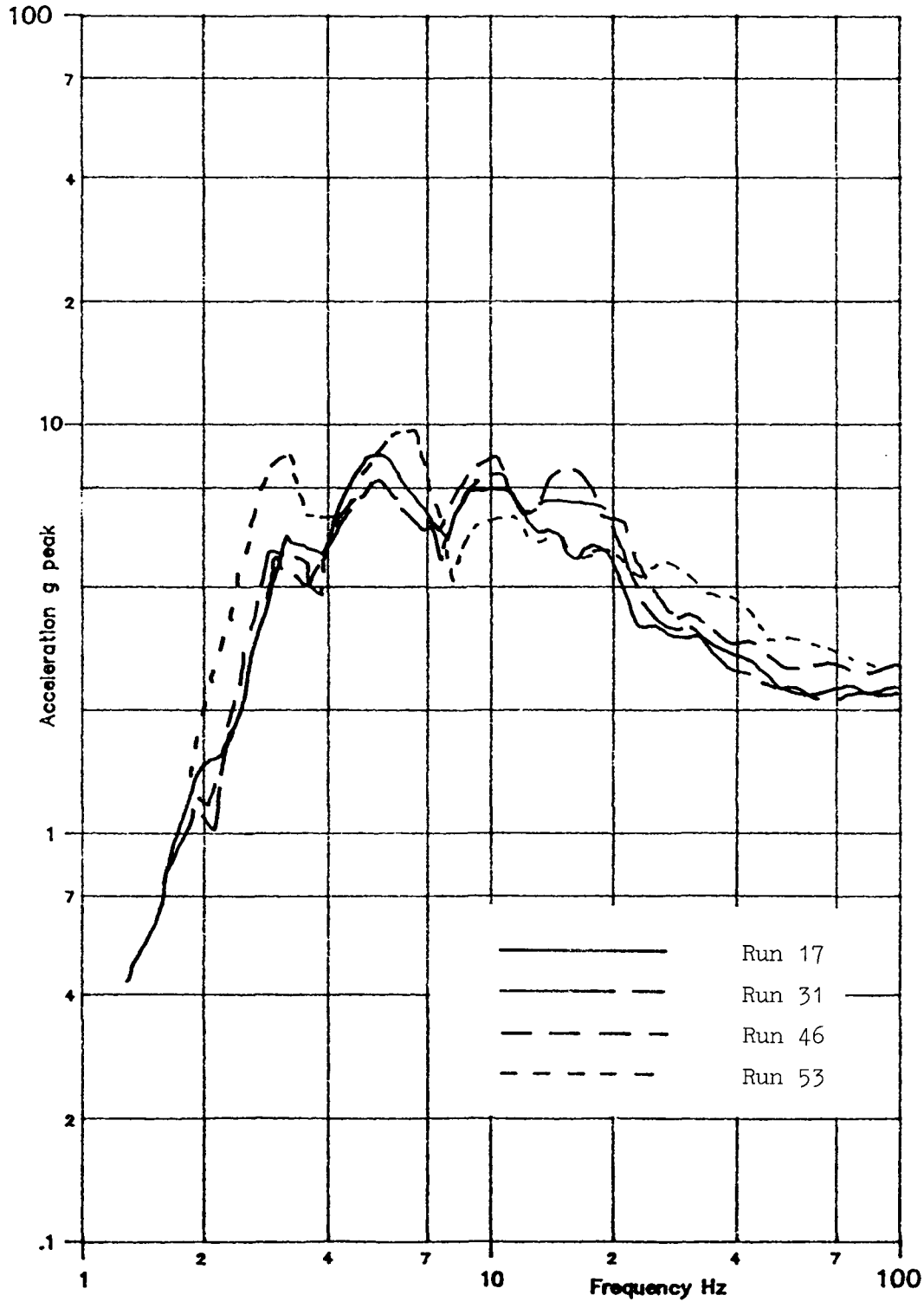

Fig. 4-3. Influence of cabinet mounting configuration on table TRS.

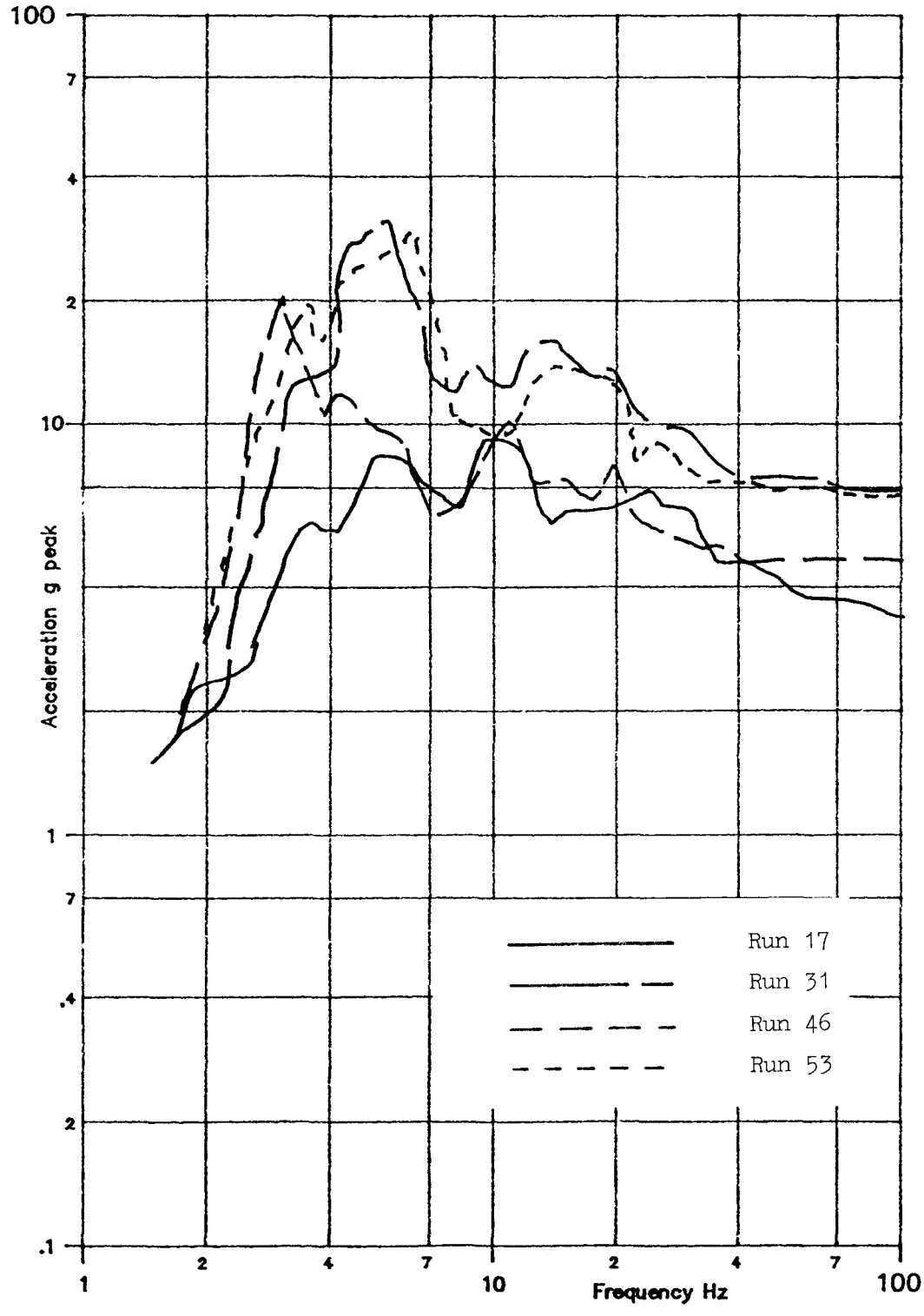

Fig. 4-4. Influence of cabinet mounting configuration on local TRS at top of MCC cabinet.

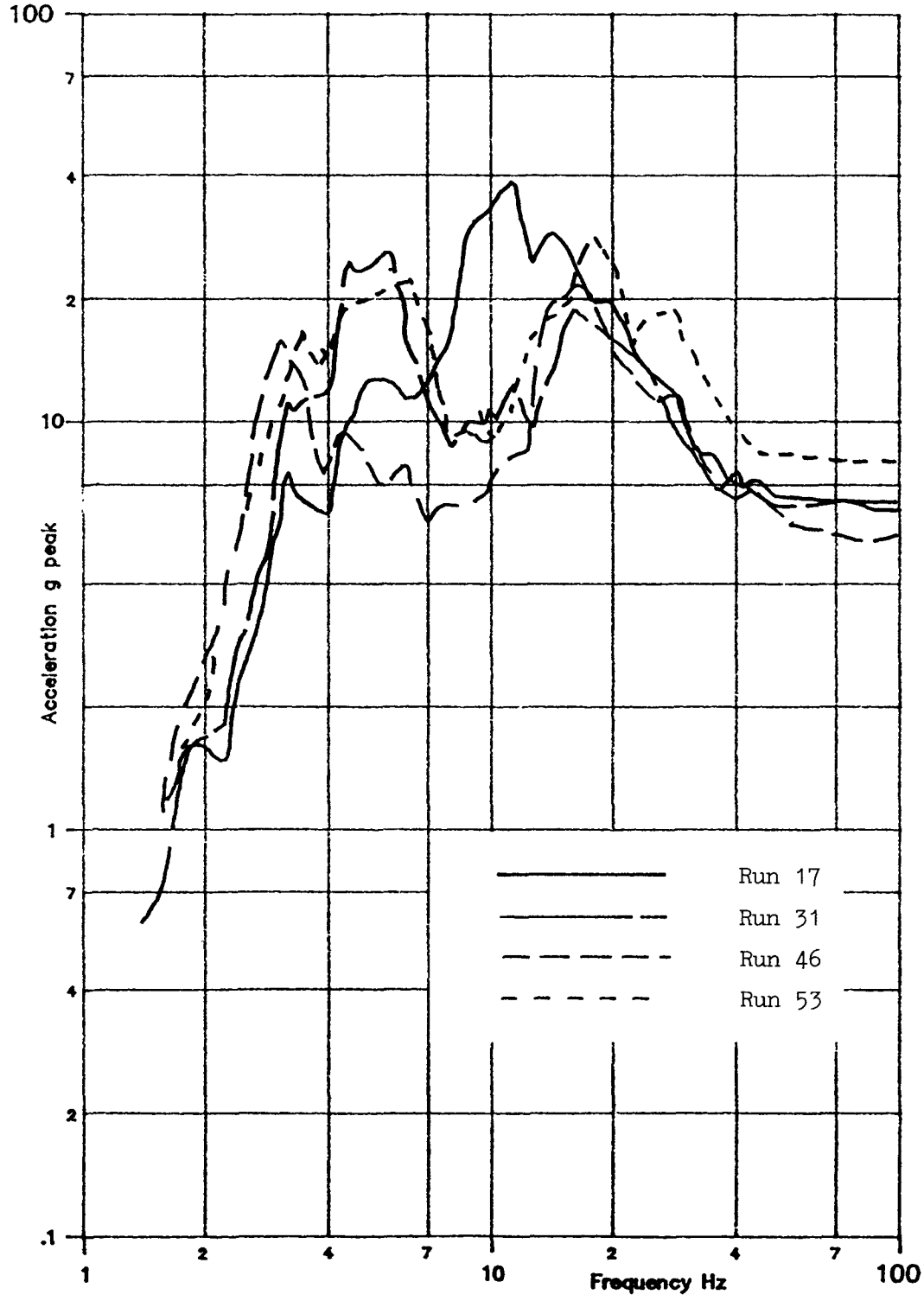

Fig. 4-5. Influence of cabinet mounting configuration on local TRS at mid-plane of MCC cabinet.

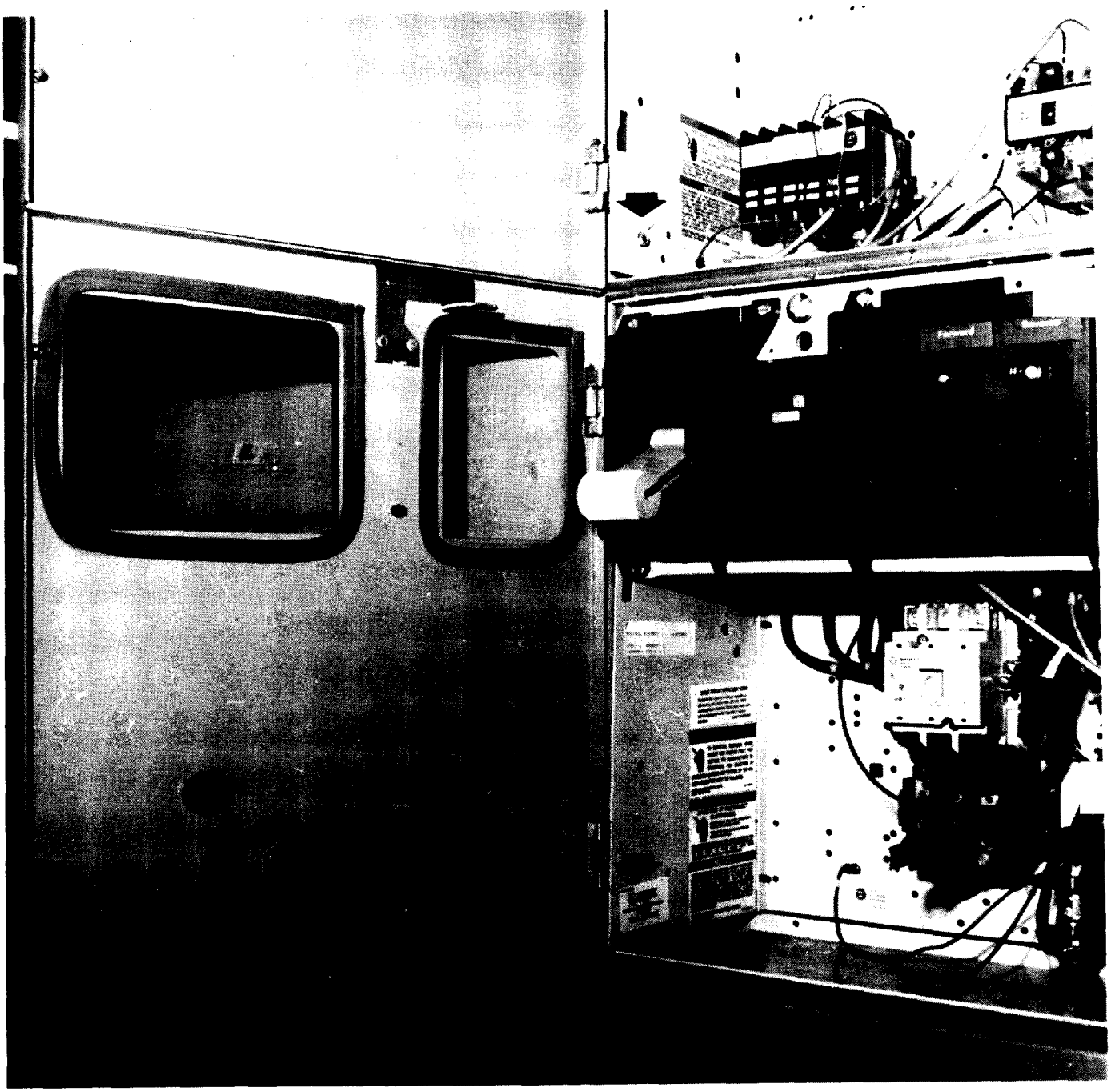

Fig. 4-6. Detail of MCC draw-out units 2B and 2E, showing location of additional mounting screws.

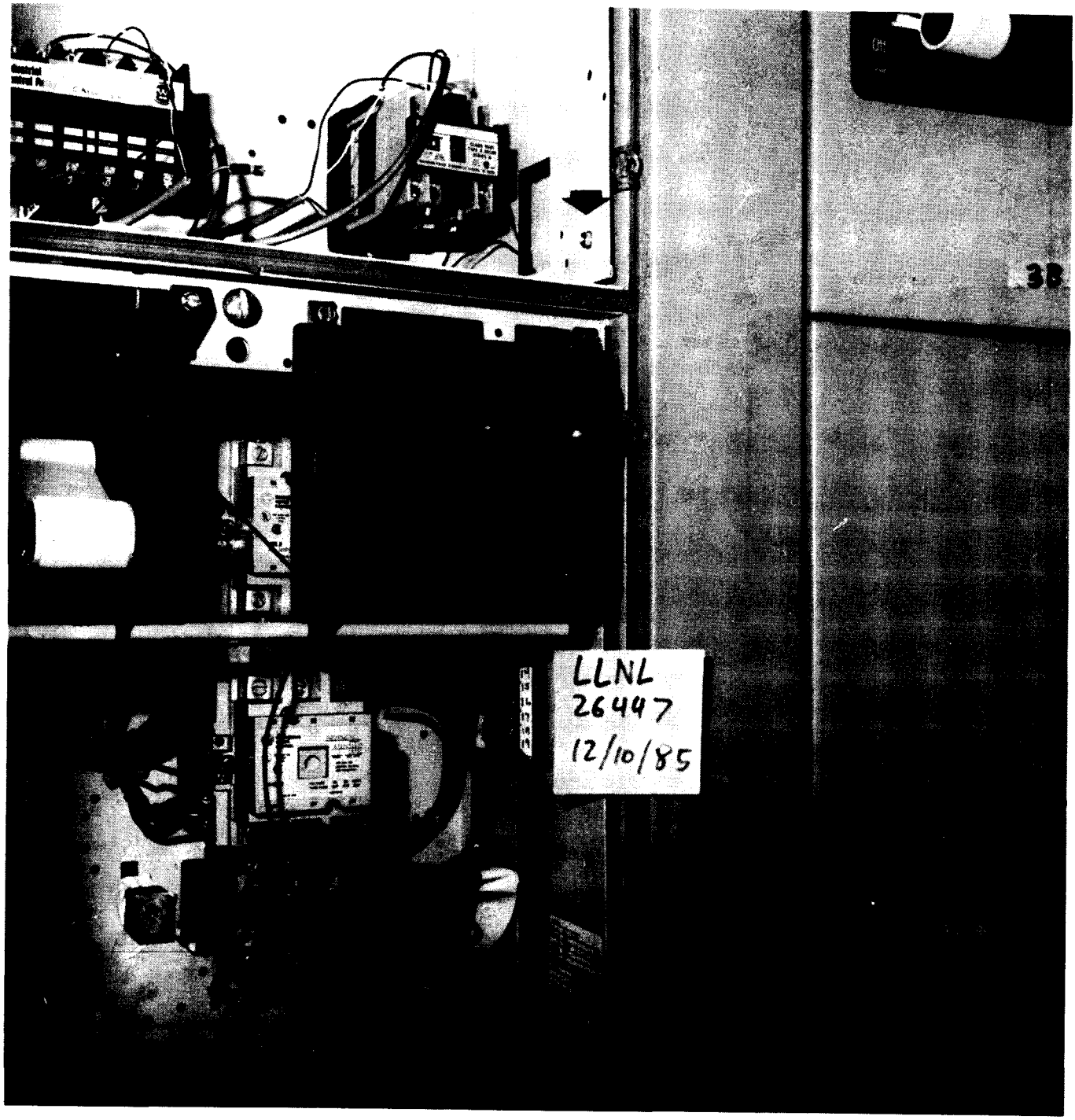

Fig. 4-7. Detail of MCC draw-out units 2B and 2E, showing location of additional mounting screws.

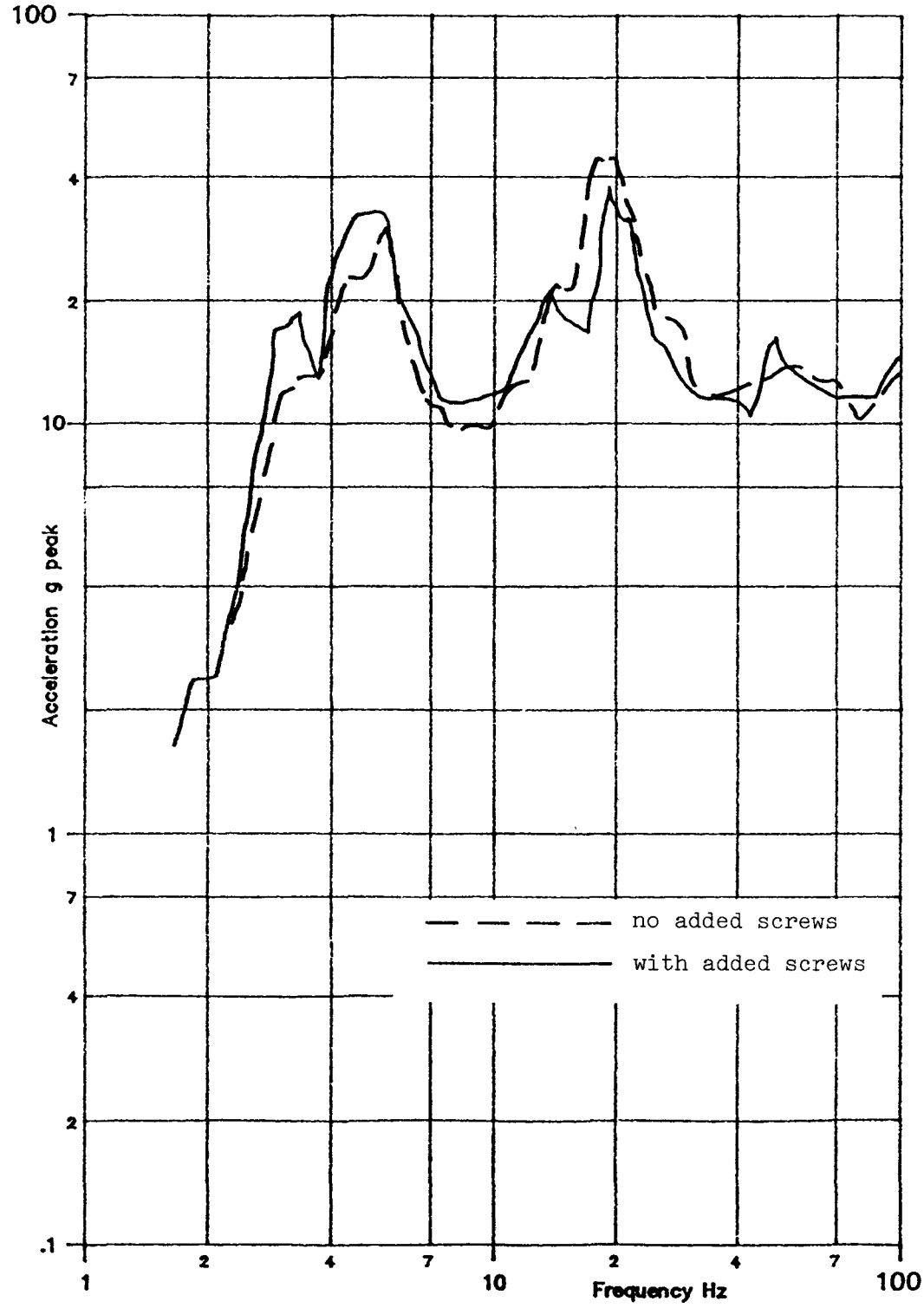

Fig. 4-8. Effect of extra mounting screws on local TRS for draw-out unit 2B.

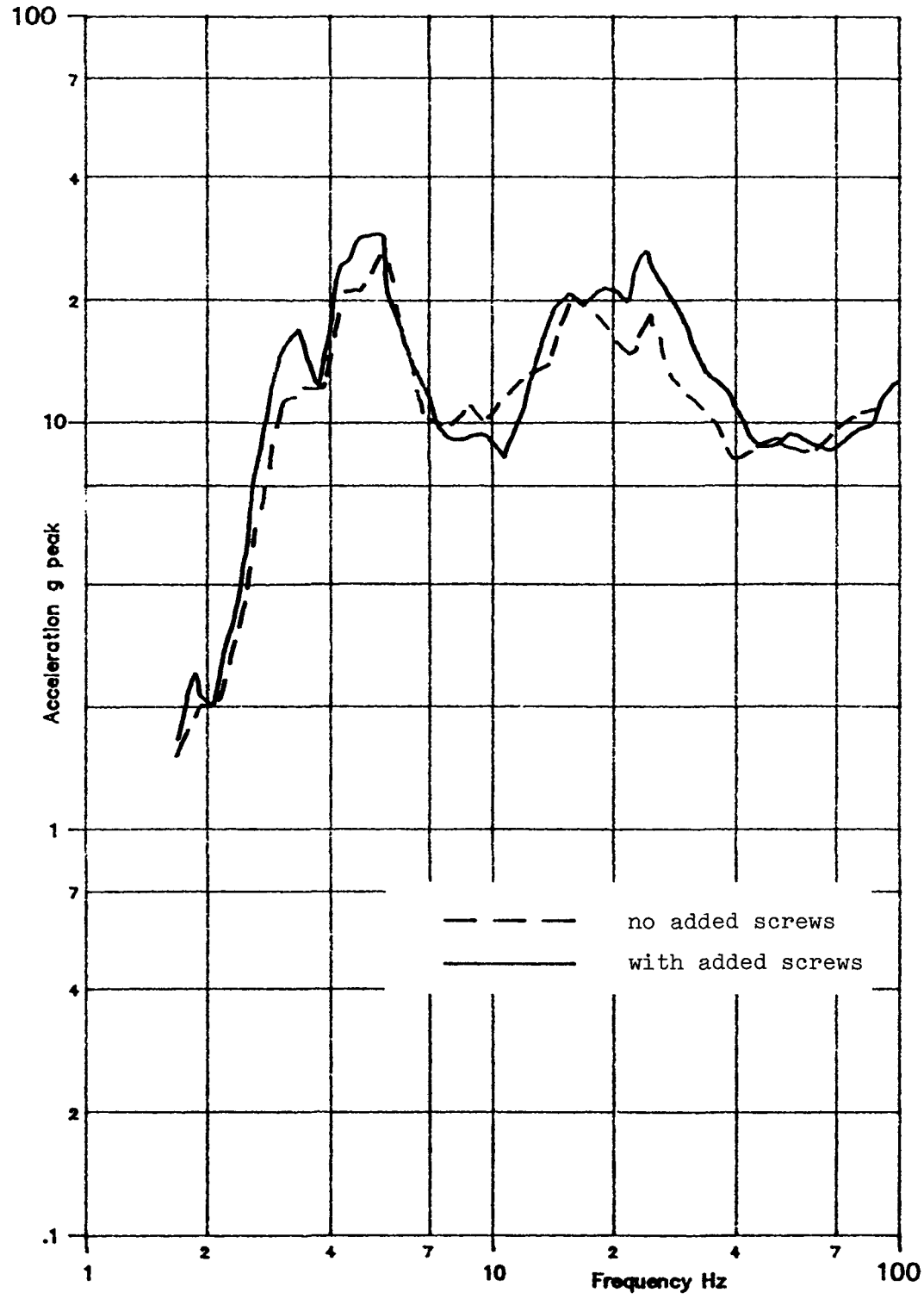

Fig. 4-9. Effect of extra mounting screws on local TRS for draw-out unit 2E.

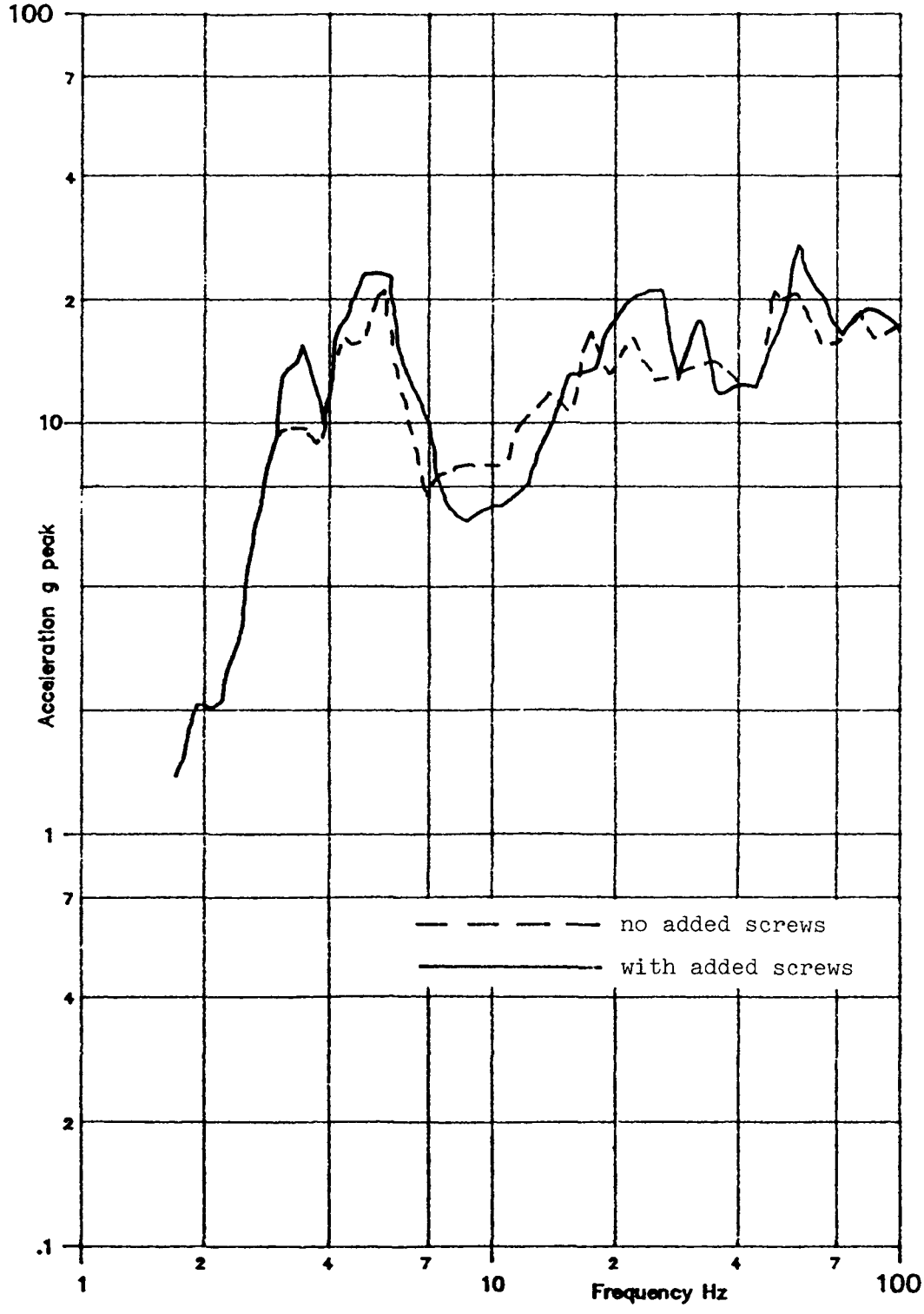

Fig. 4-10. Effect of extra mounting screws on local TRS for draw-out unit 2J.

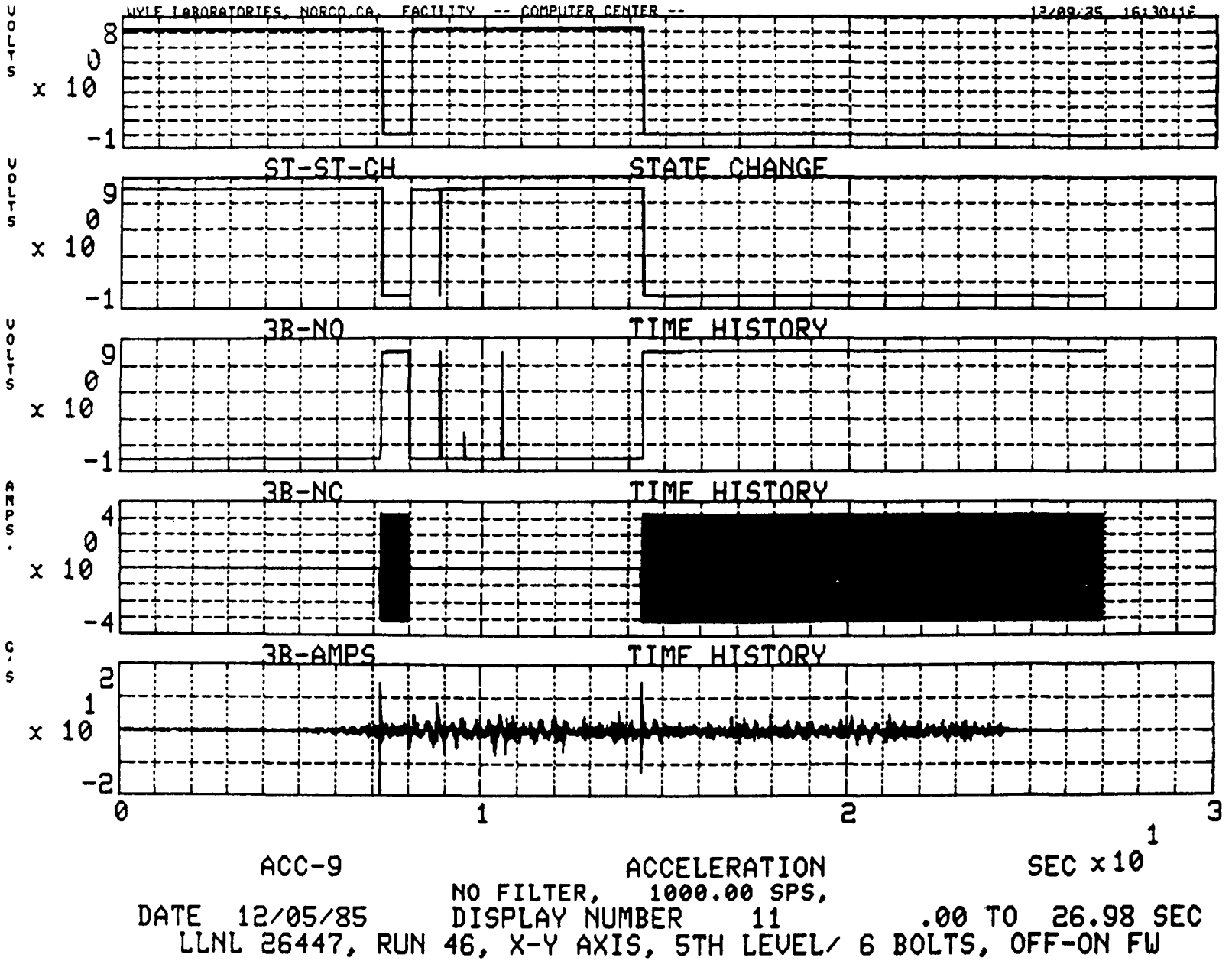

Fig. 4-11. Typical time-history data recording state change and chatter of starter contacts.

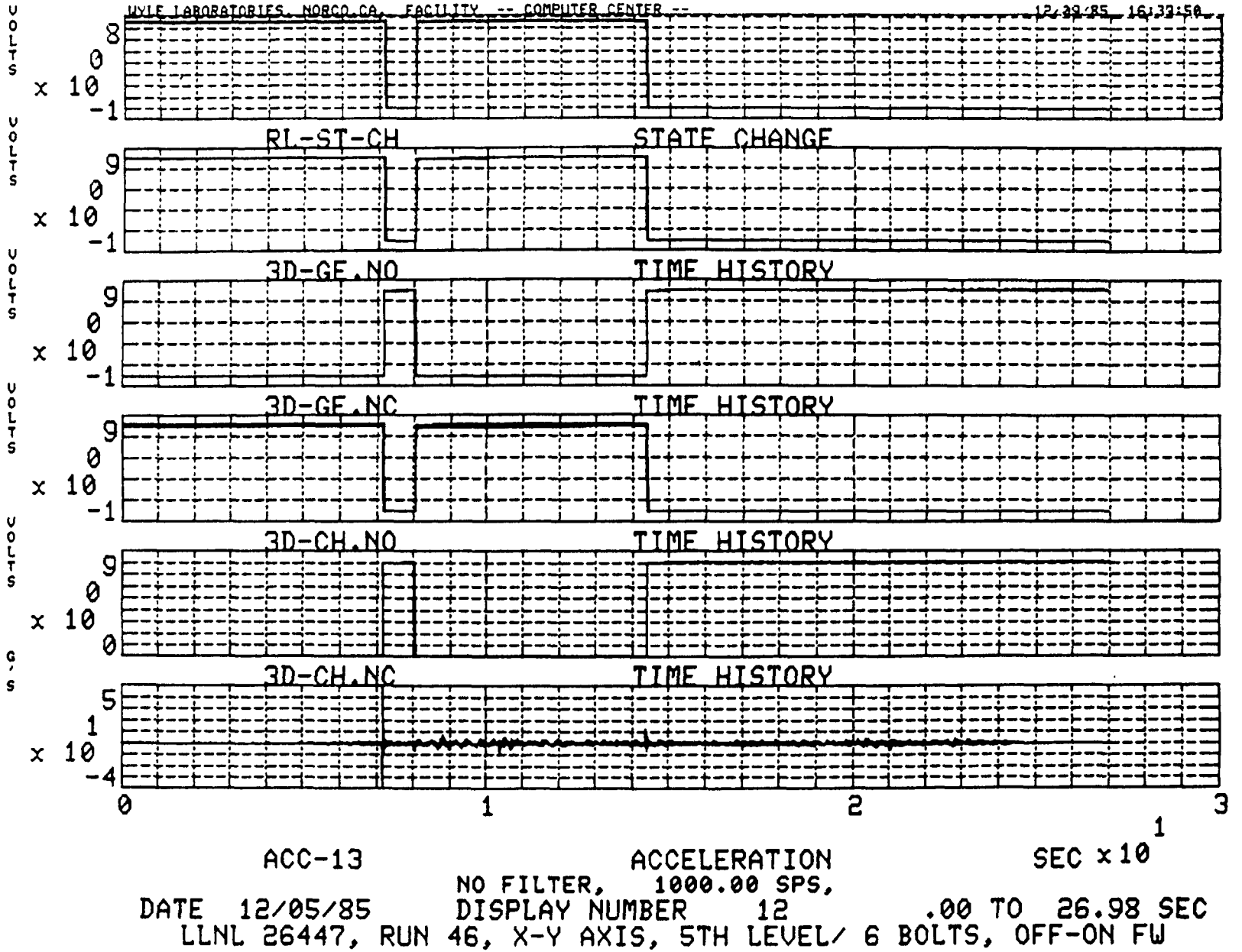

Fig. 4-12. Typical time-history data recording state change and chatter of relay contacts.

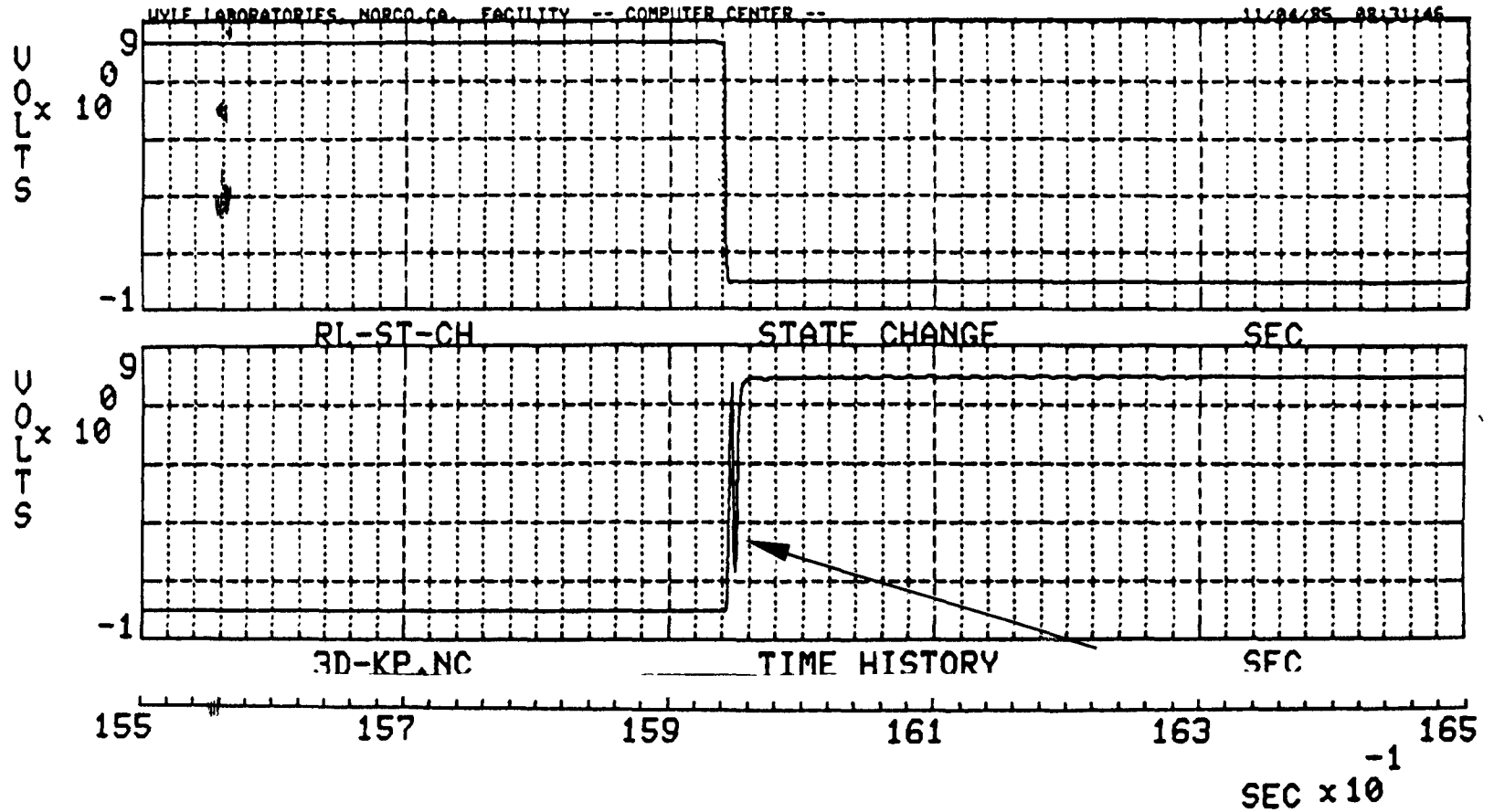

Fig. 4-13. Typical voltage signal evidencing contact "bounce" during state change.

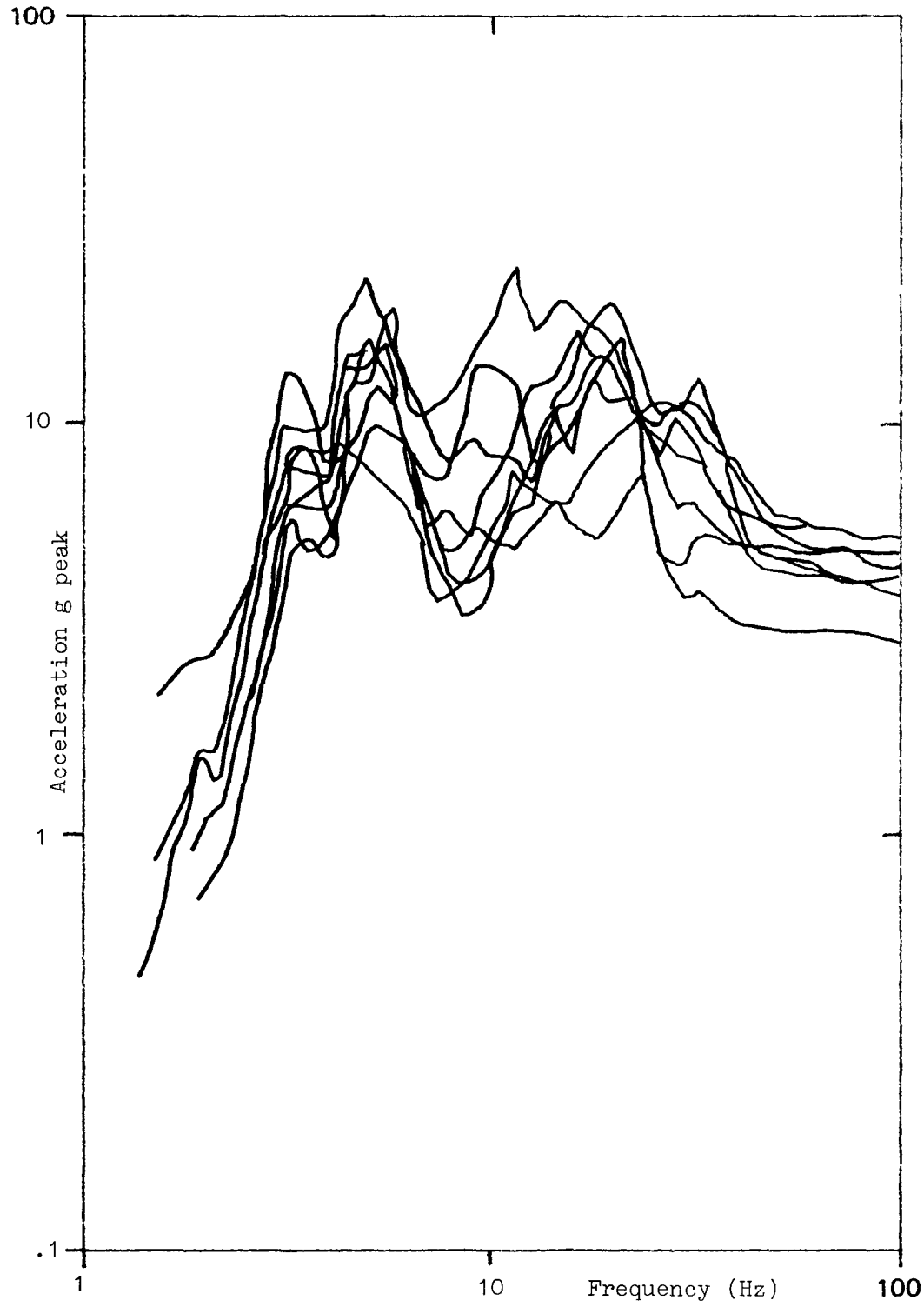

Fig. 4-14. Local test response spectra for Size 2 FVNR starters - chatter. Overlay on "no chatter" spectra in Fig. 4-15 for comparison.

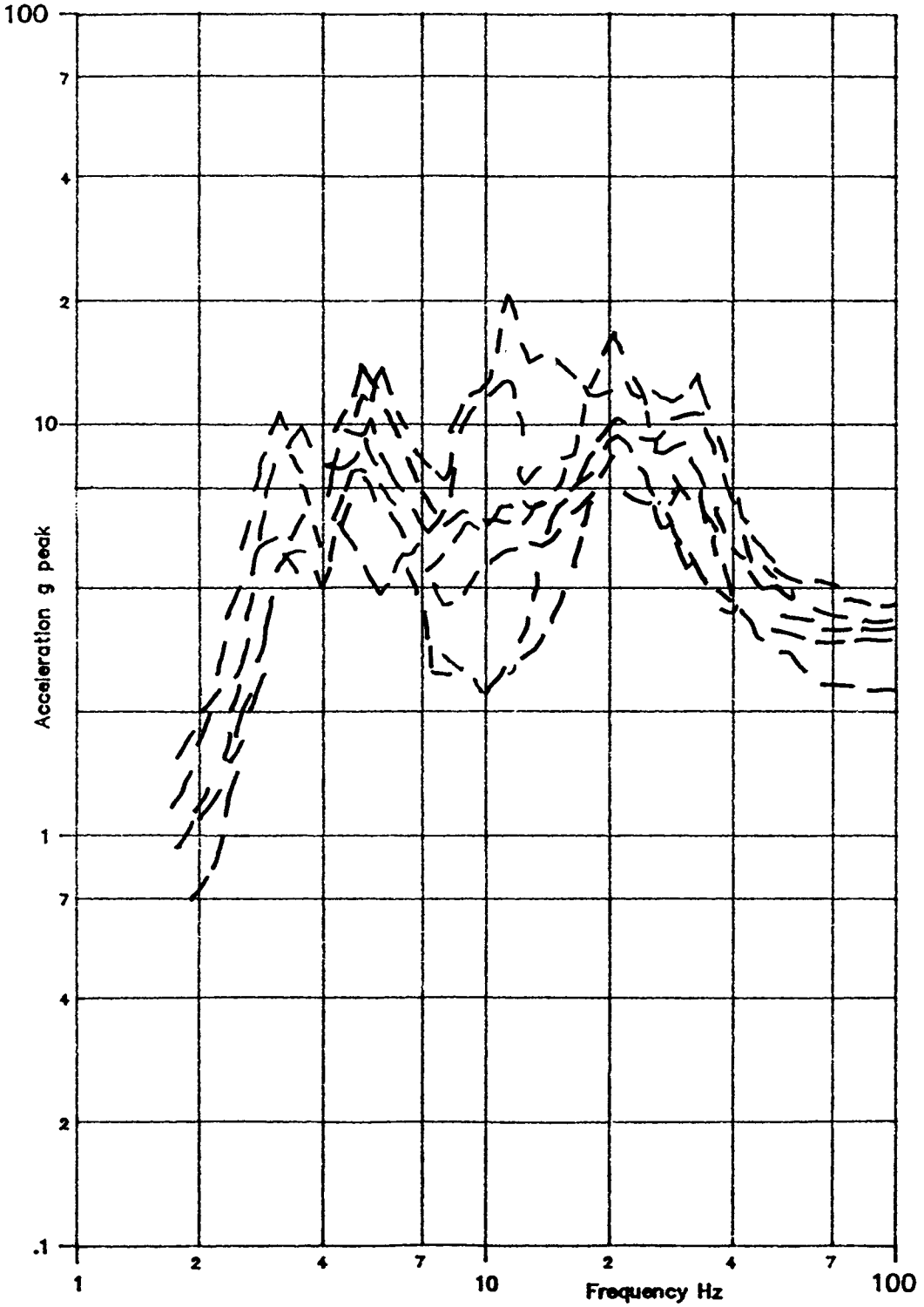

Fig. 4-15. Local test response spectra Size 2 FVNR starters - no chatter.

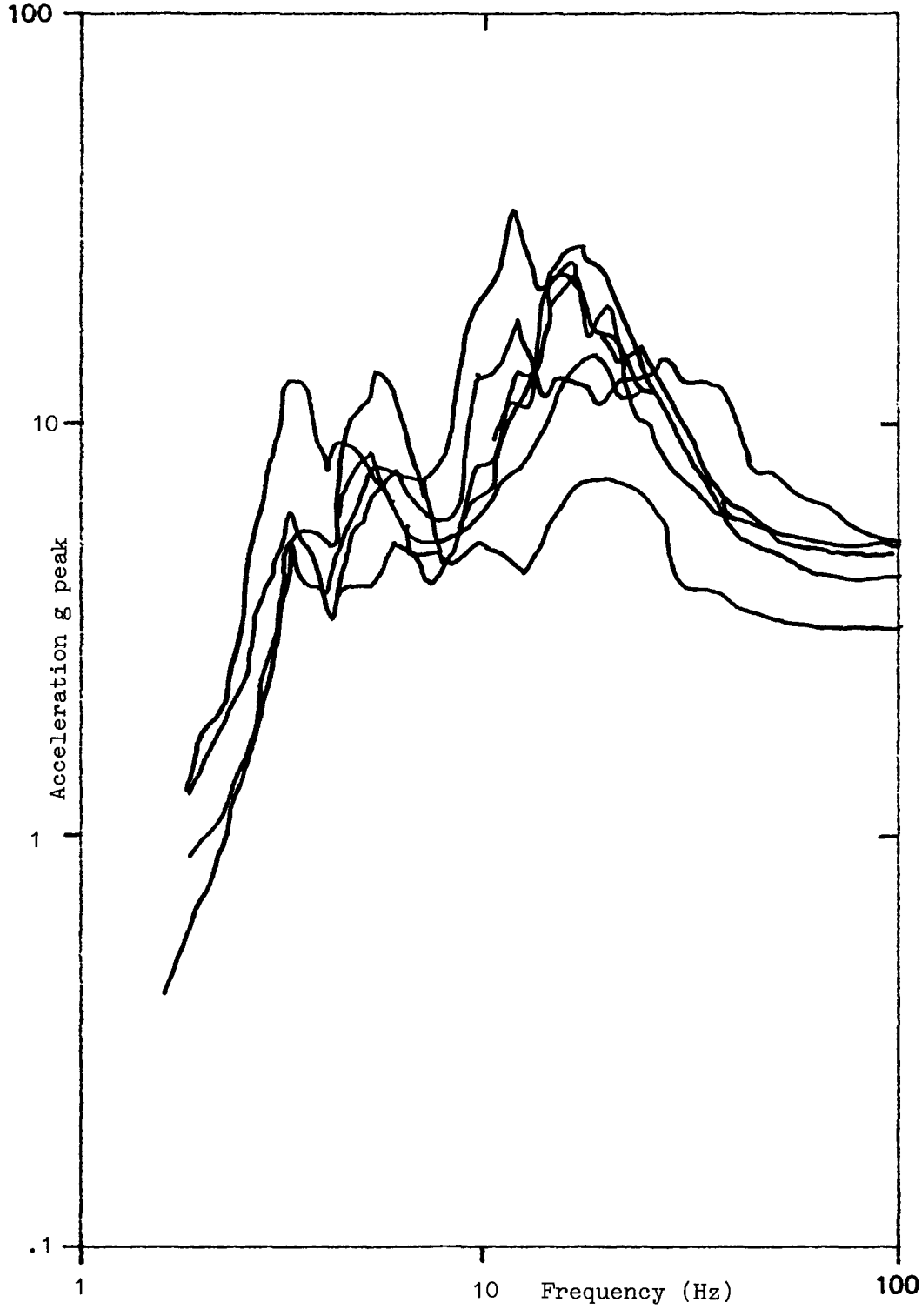

Fig. 4-16. Local test response spectra for Size 2 FVR starters - chatter. Overlay on "no chatter" spectra in Fig. 4-17 for comparison.

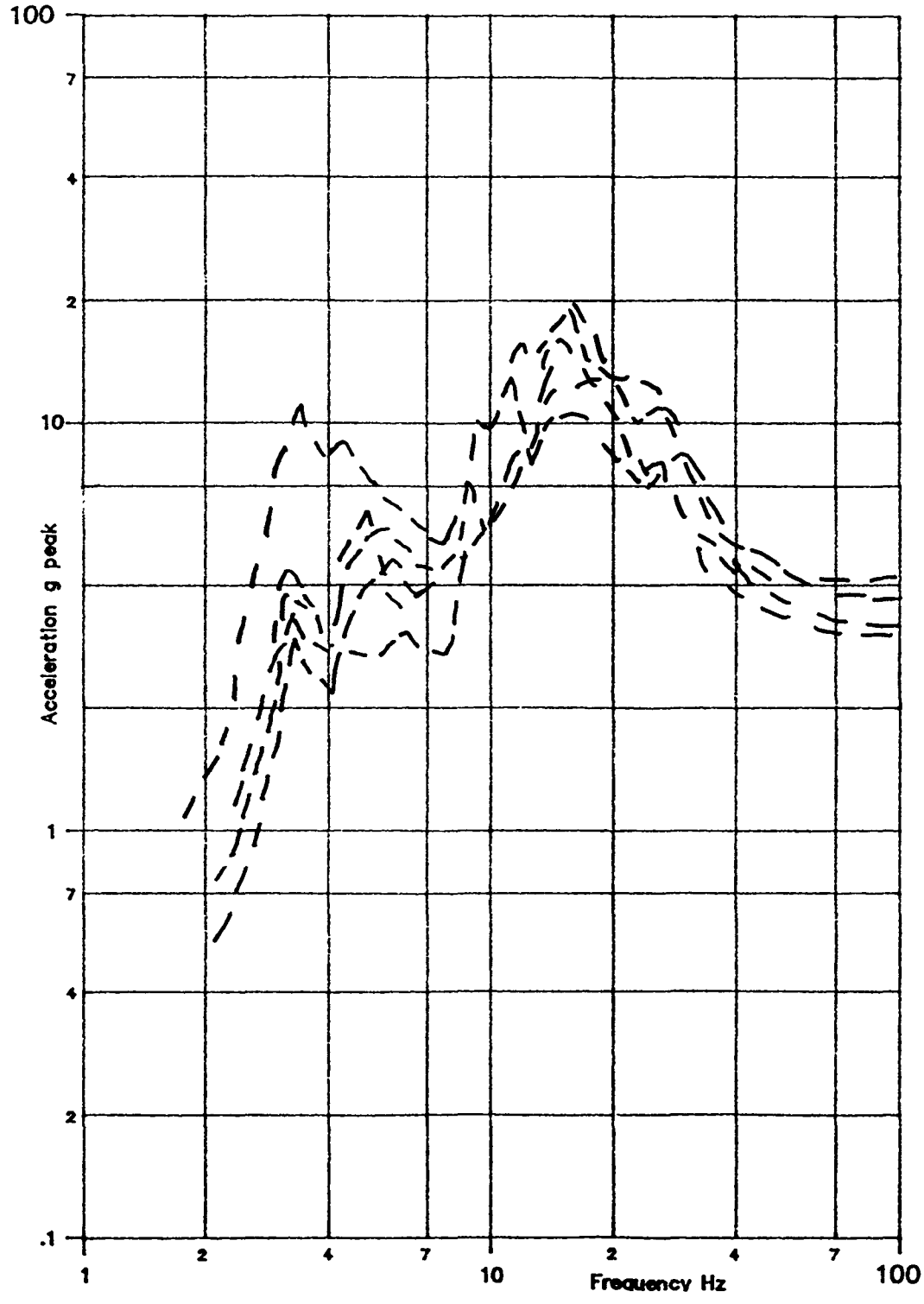

Fig. 4-17. Local test response spectra Size 2 FVR starters - no chatter.

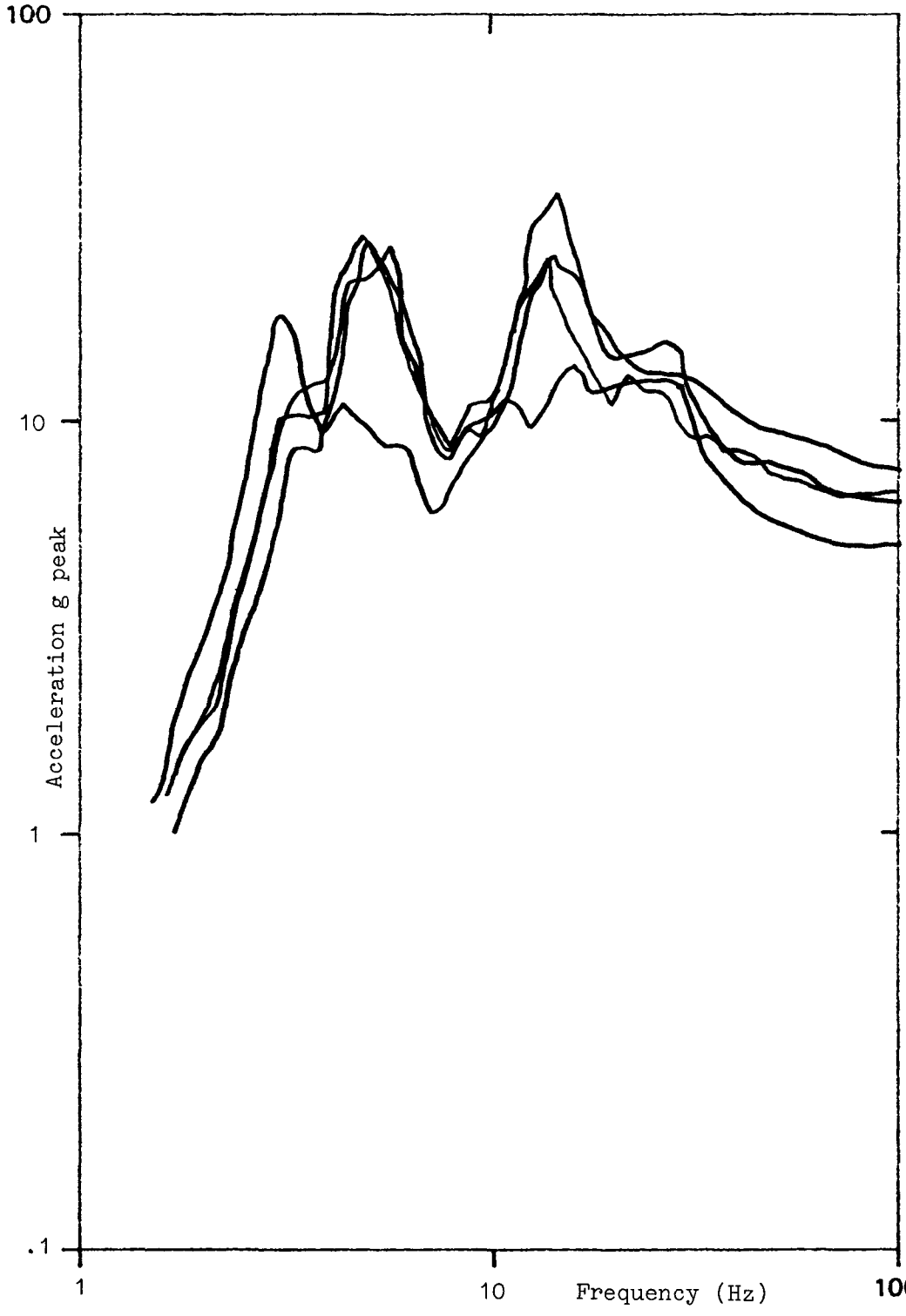

Fig. 4-18. Local test response spectra for Size 3 FVNR starters - chatter. Overlay on "no chatter" spectra in Fig. 4-19 for comparison.

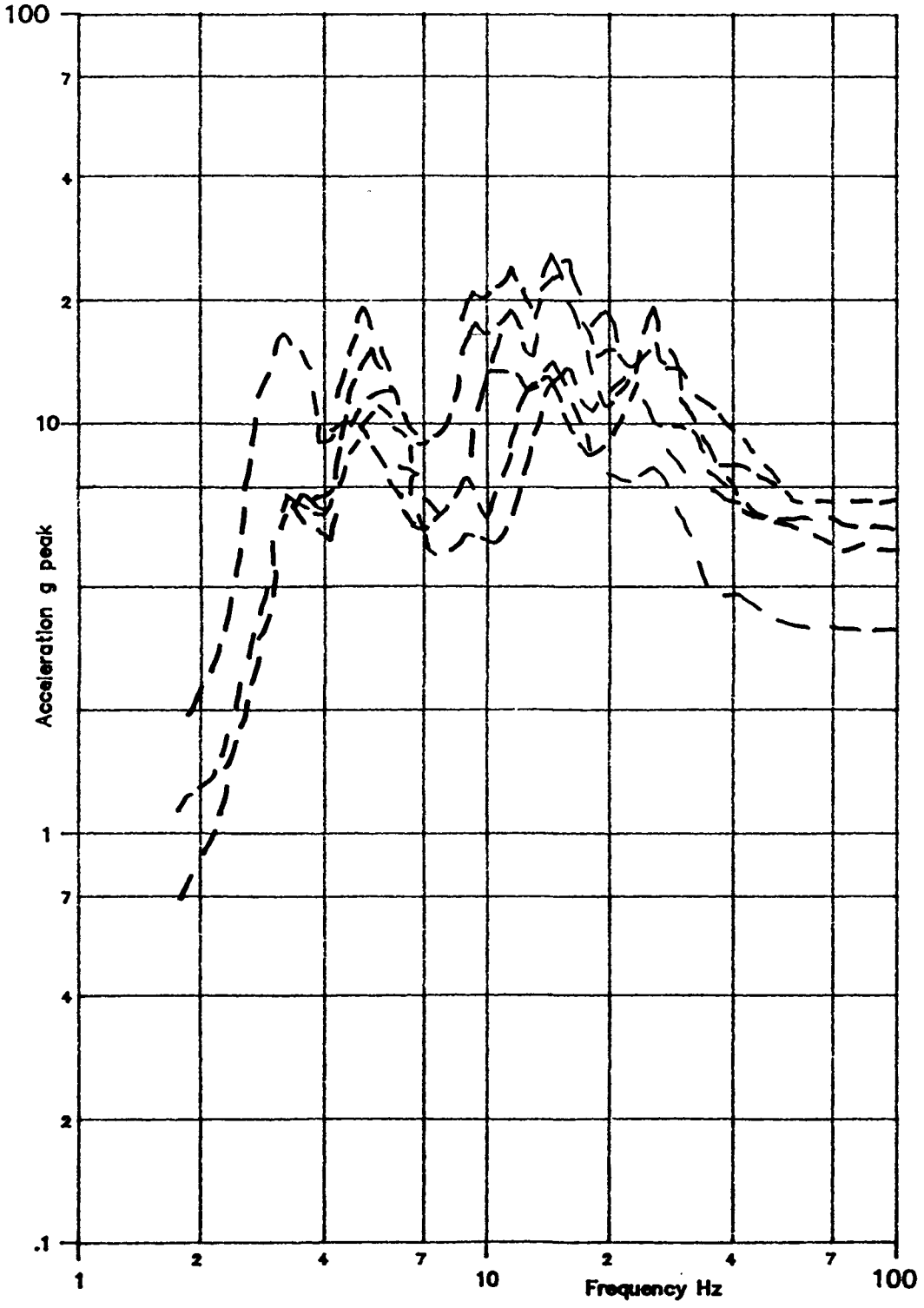

Fig. 4-19. Local test response spectra for Size 3 FVNR starters - no chatter.

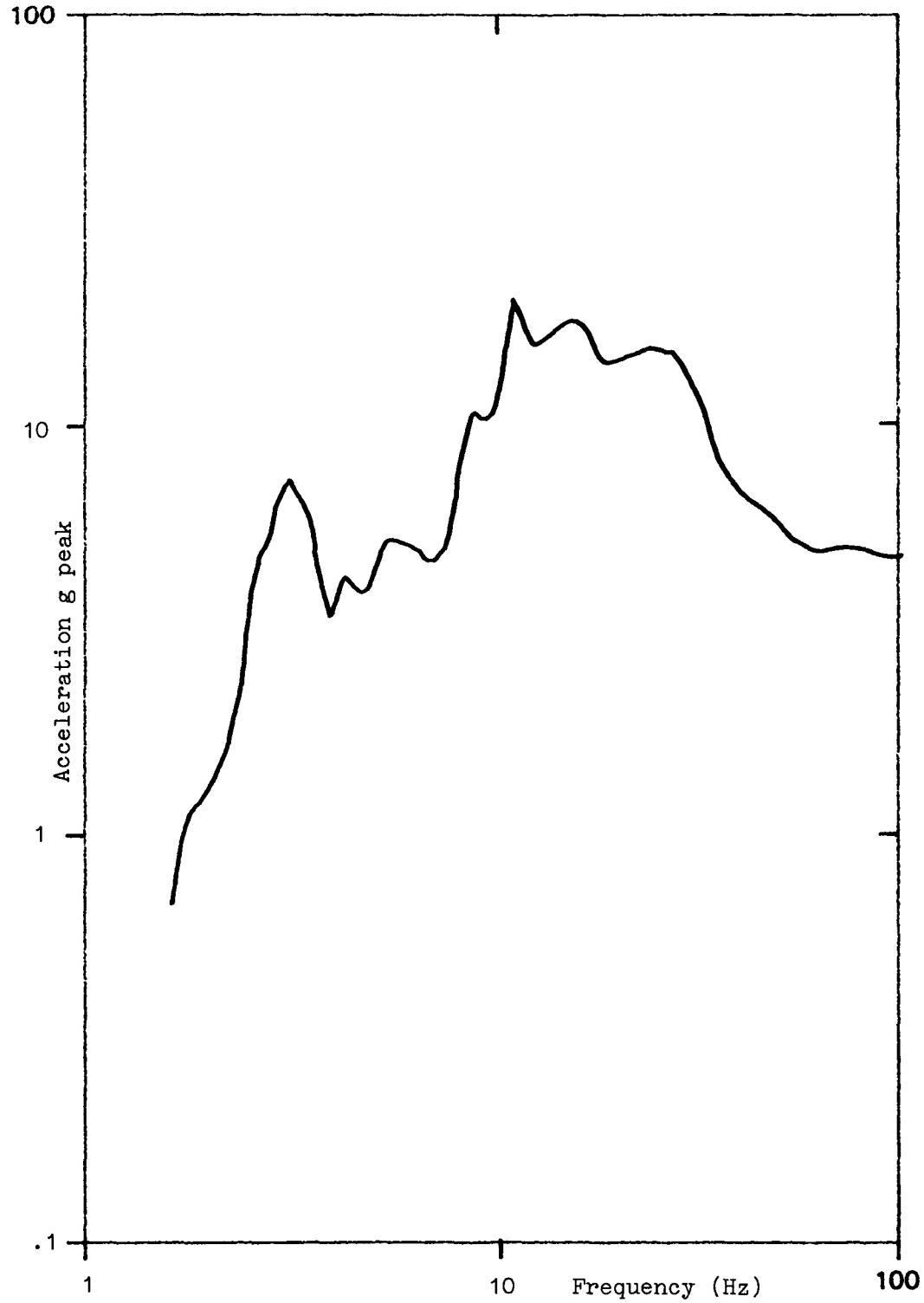

Fig. 4-20. Local test response spectra for Size 4 FVNR starters - chatter. Overlay on "no chatter" spectra in Fig. 4-21 for comparison.

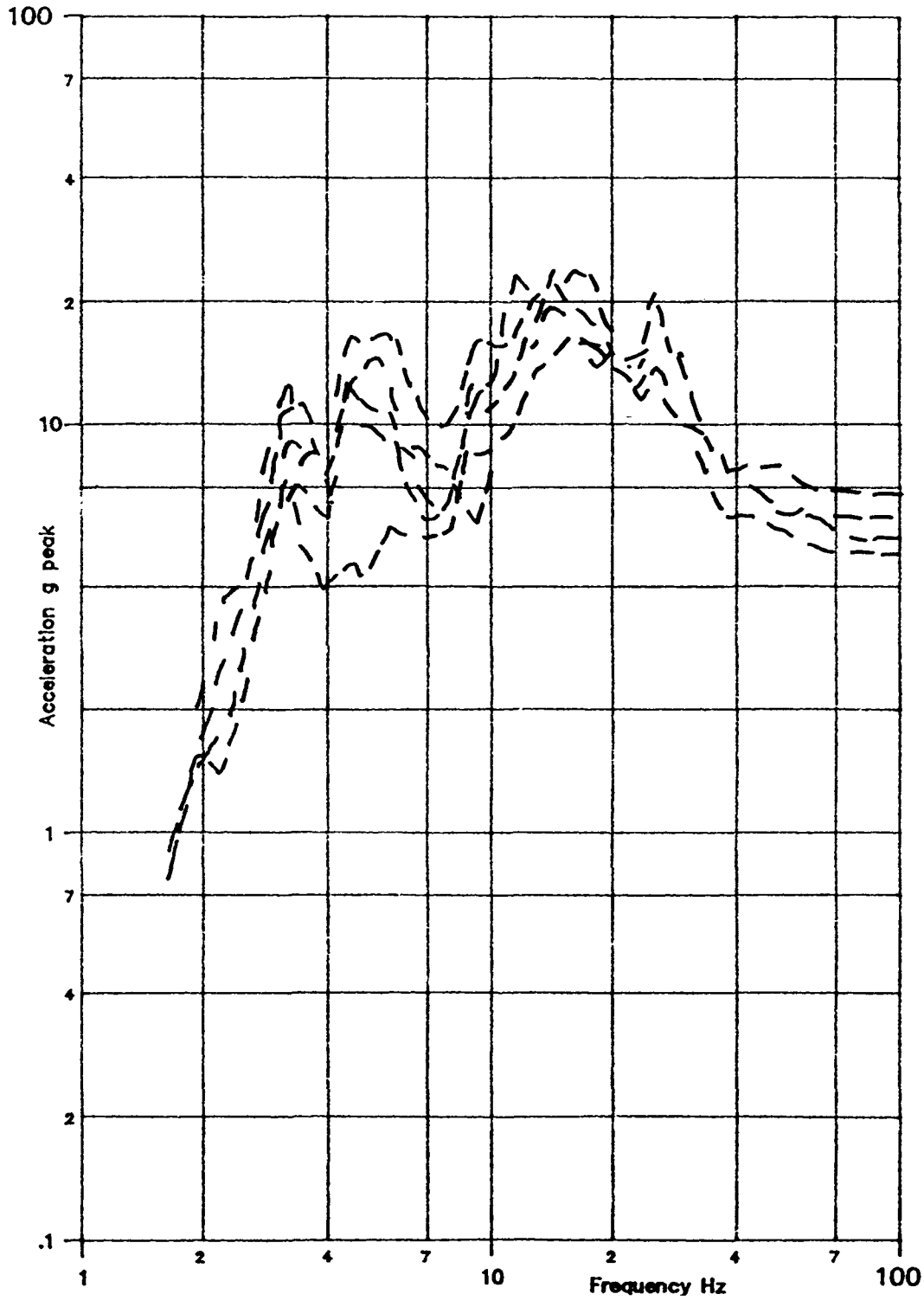

Fig. 4-21. Local test response spectra for Size 4 FVNR starters - no chatter.

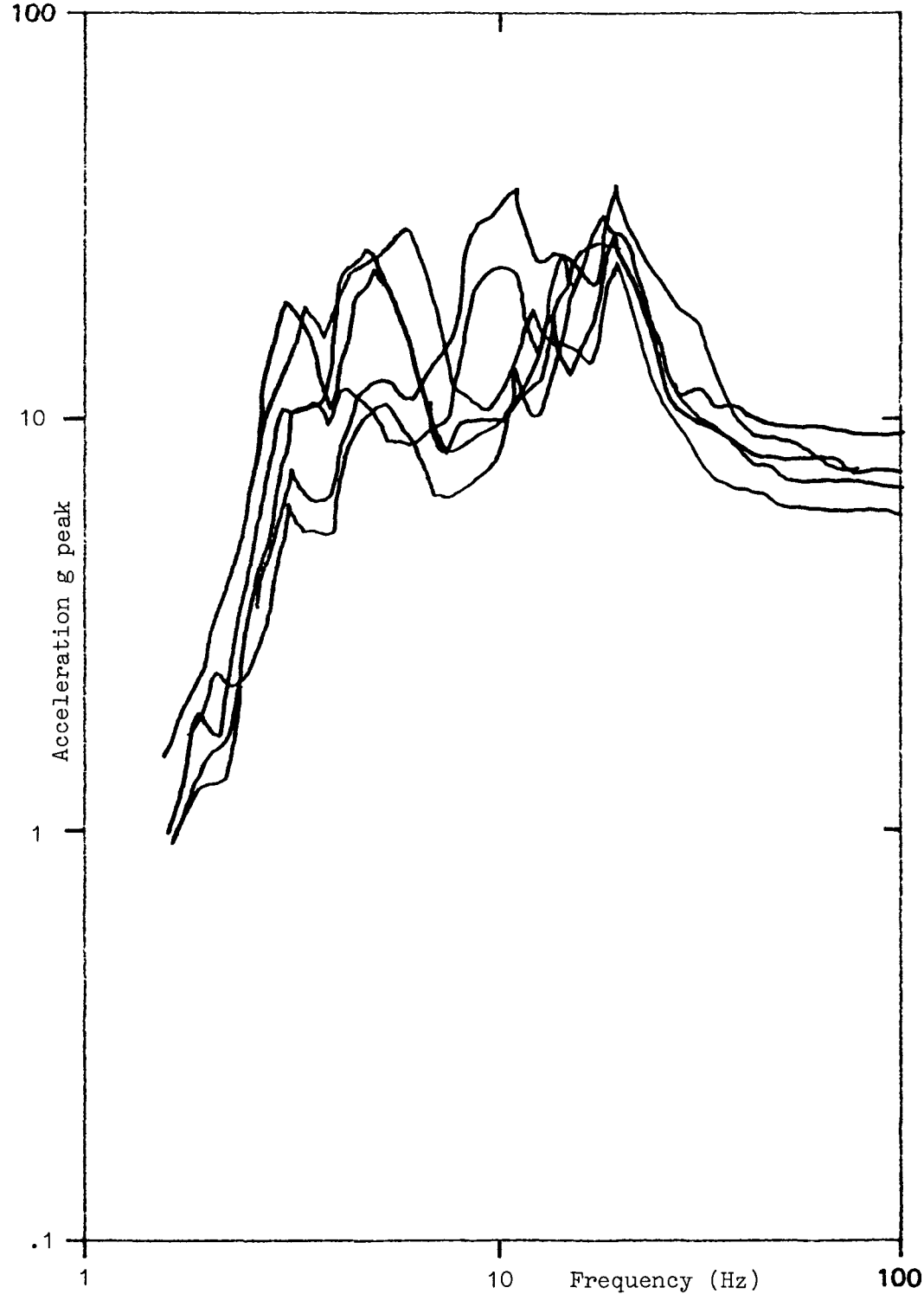

Fig. 4-22. Local test response spectra for Westinghouse Type AR relays - chatter. Overlay on "no chatter" spectra in Fig. 4-23 for comparison.

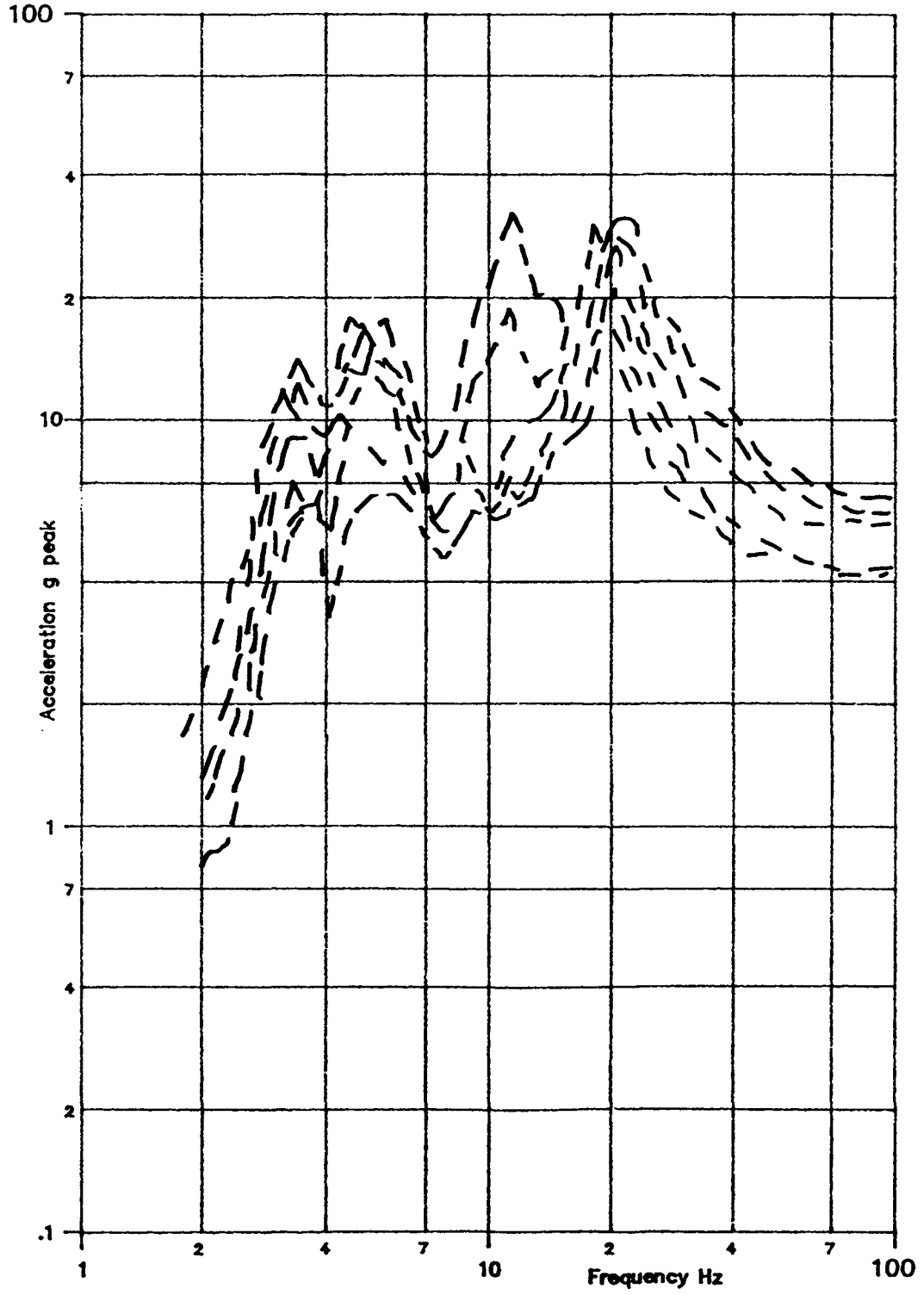

Fig. 4-23. Local test response spectra for Westinghouse Type AR relays - no chatter.

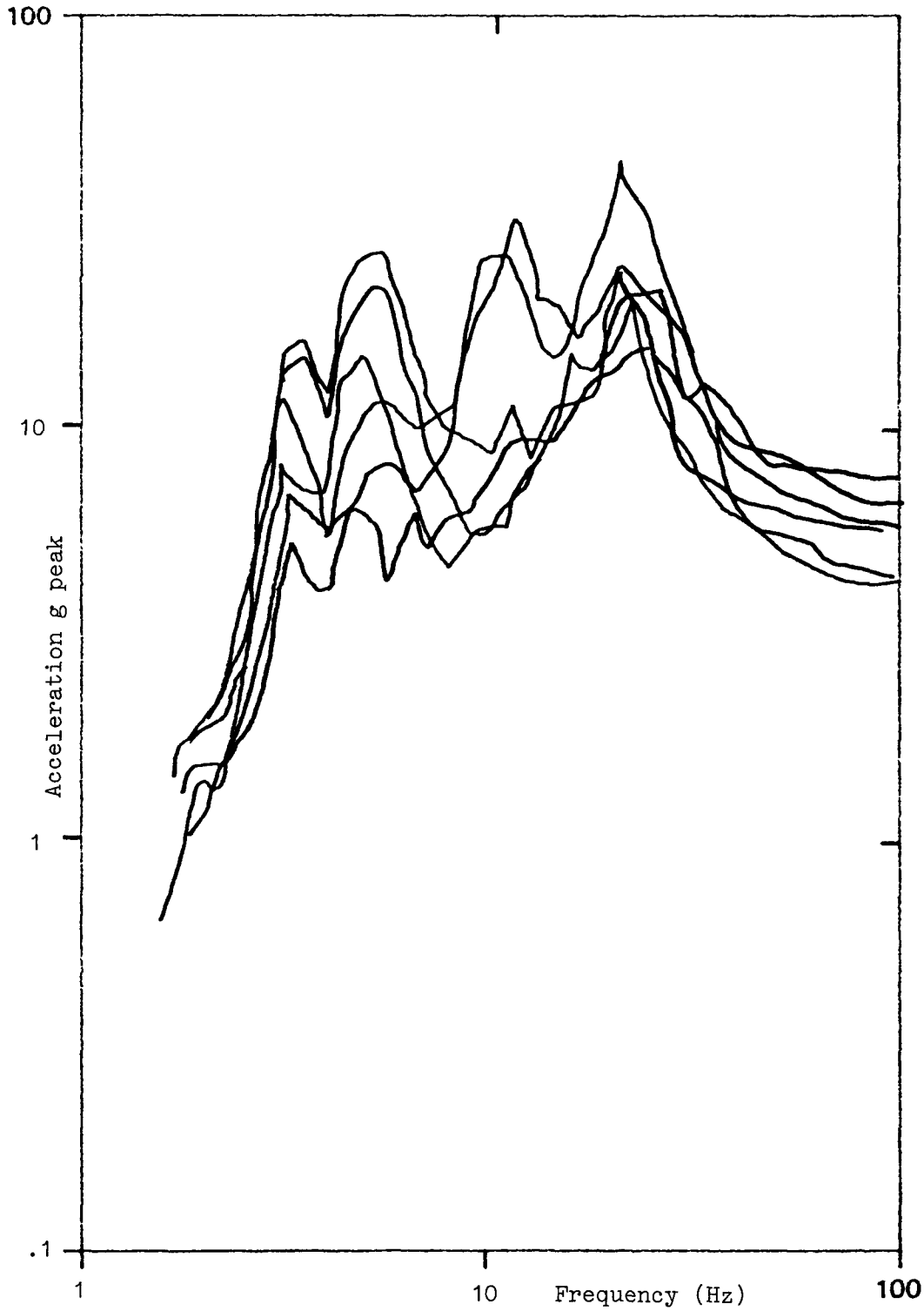

Fig. 4-24. Local test response spectra for General Electric Type CR relays - chatter. Overlay on "no chatter" spectra in Fig. 4-25 for comparison.

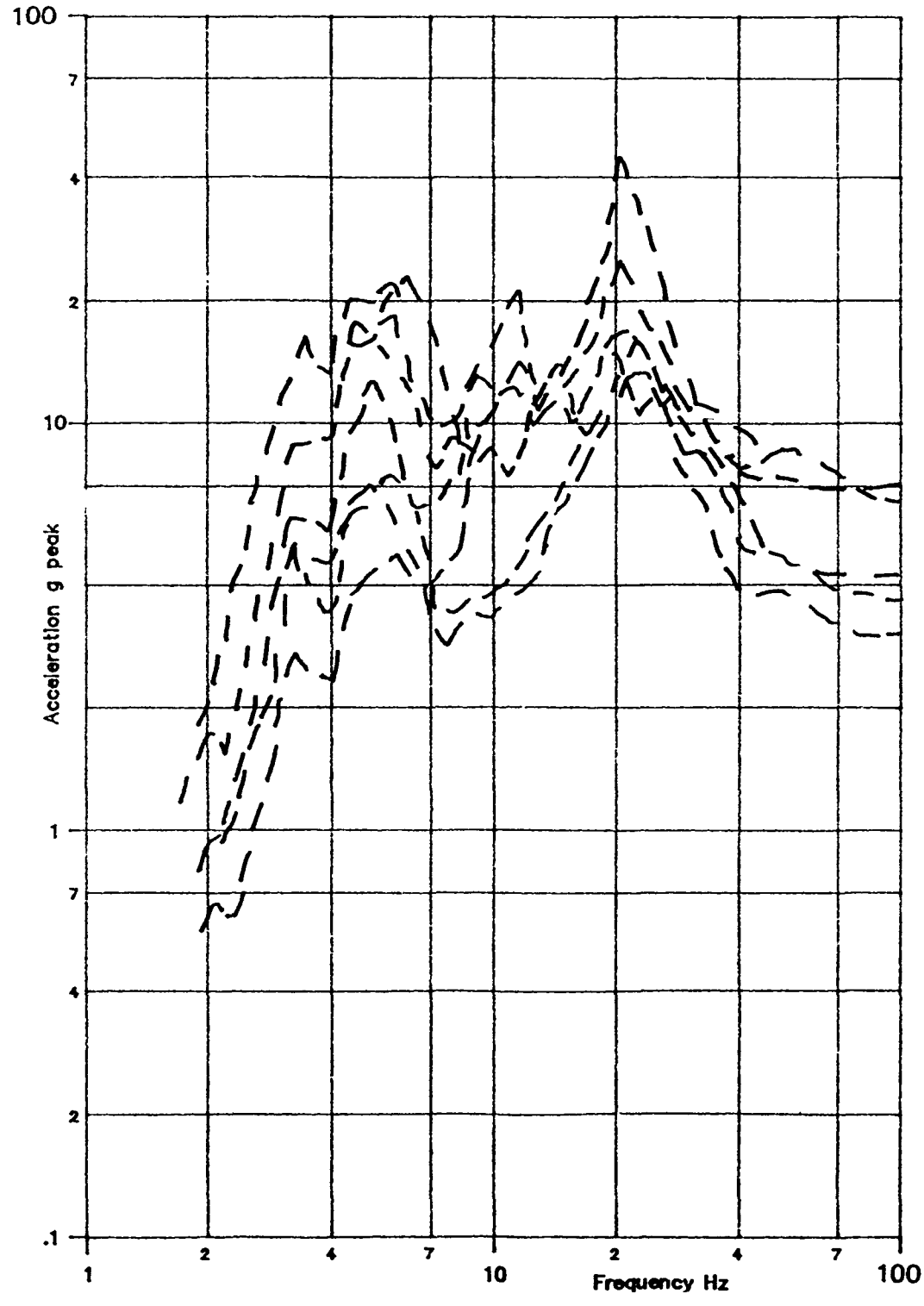

Fig. 4-25. Local test response spectra for General Electric Type CR relays - no chatter.

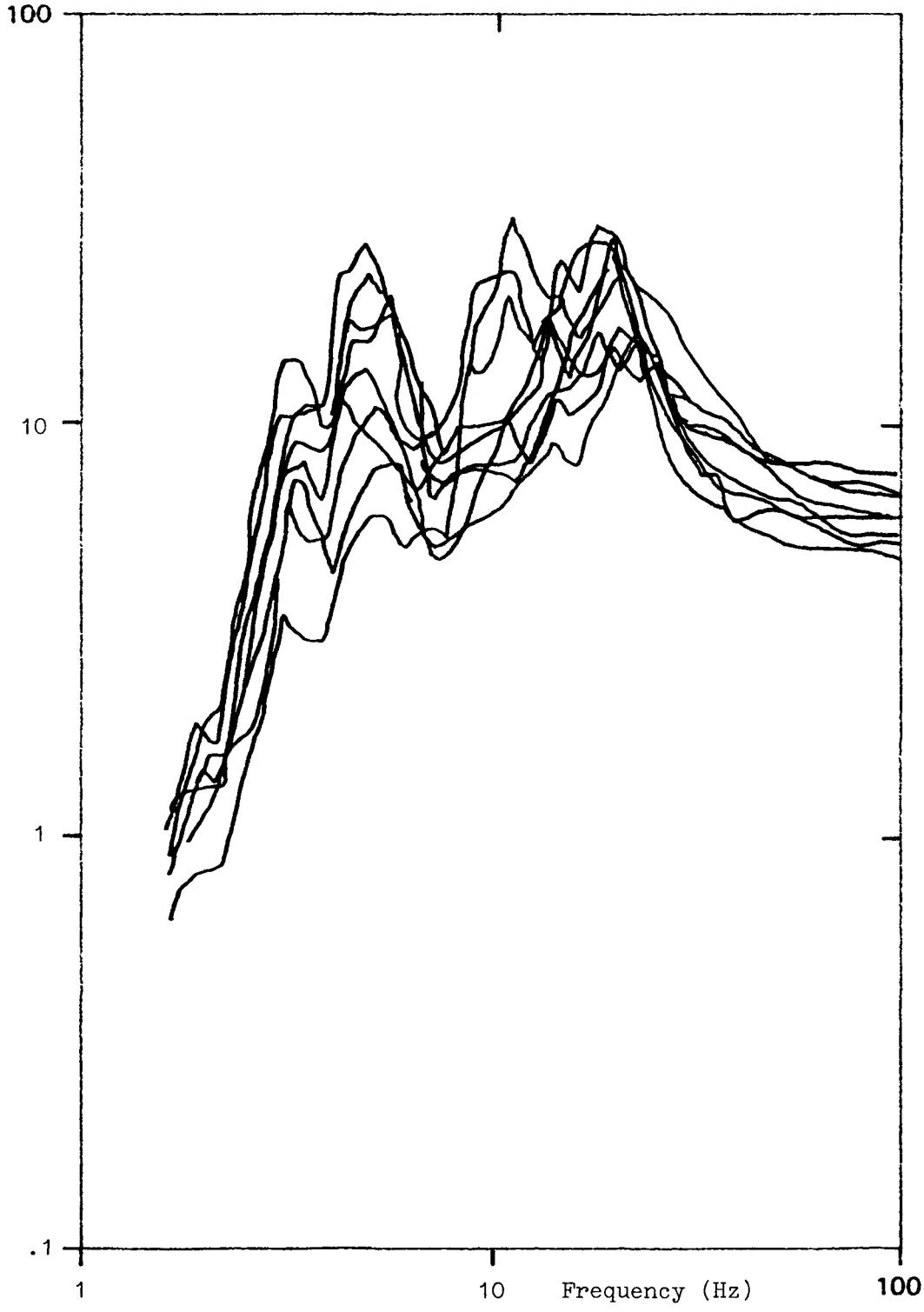

Fig. 4-26. Local test response spectra for Square-D Type X relays - chatter. Overlay on "no chatter" spectra in Fig. 4-27 for comparison.

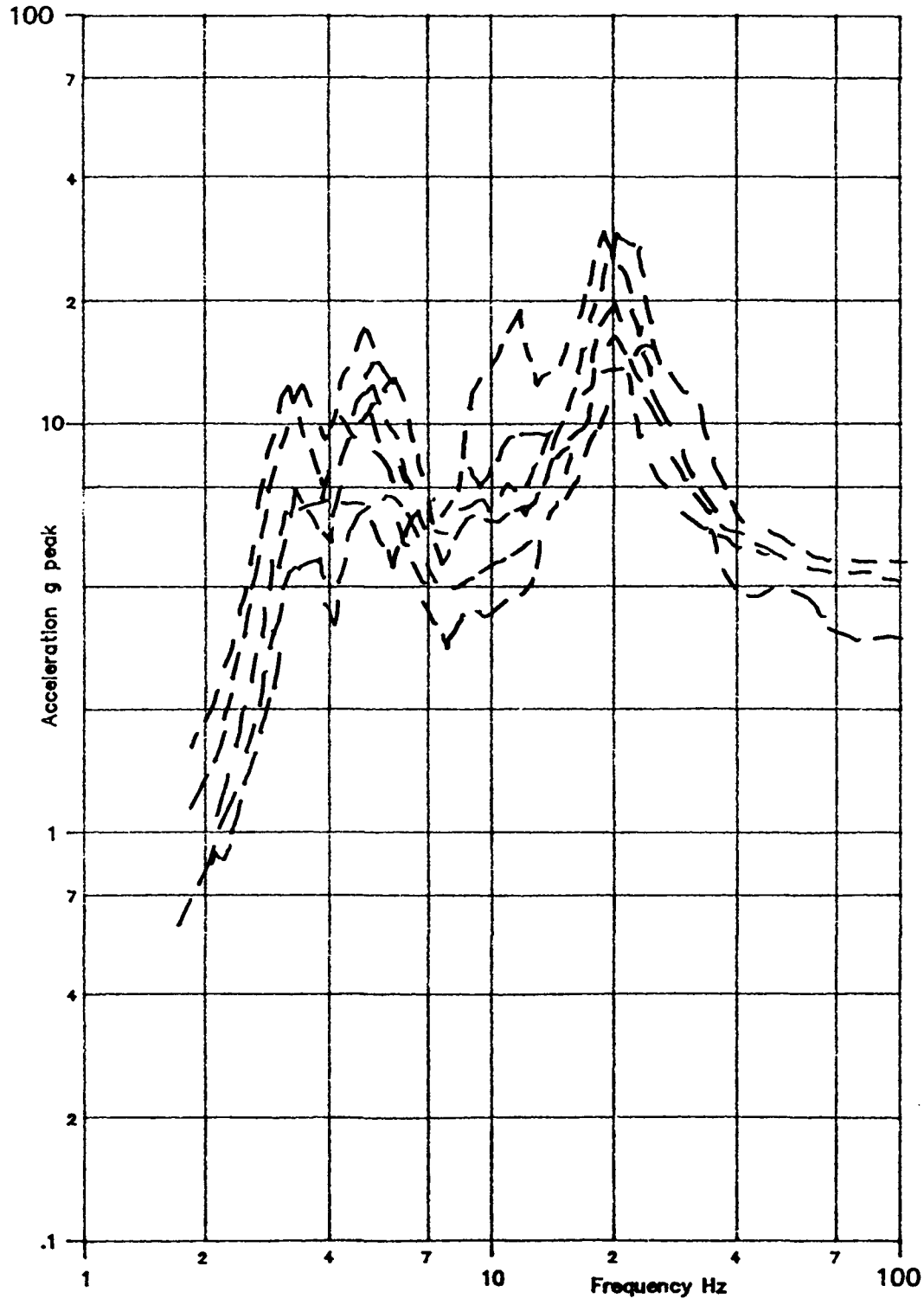

Fig. 4-27. Local test response spectra for Square-D Type X relays - no chatter.

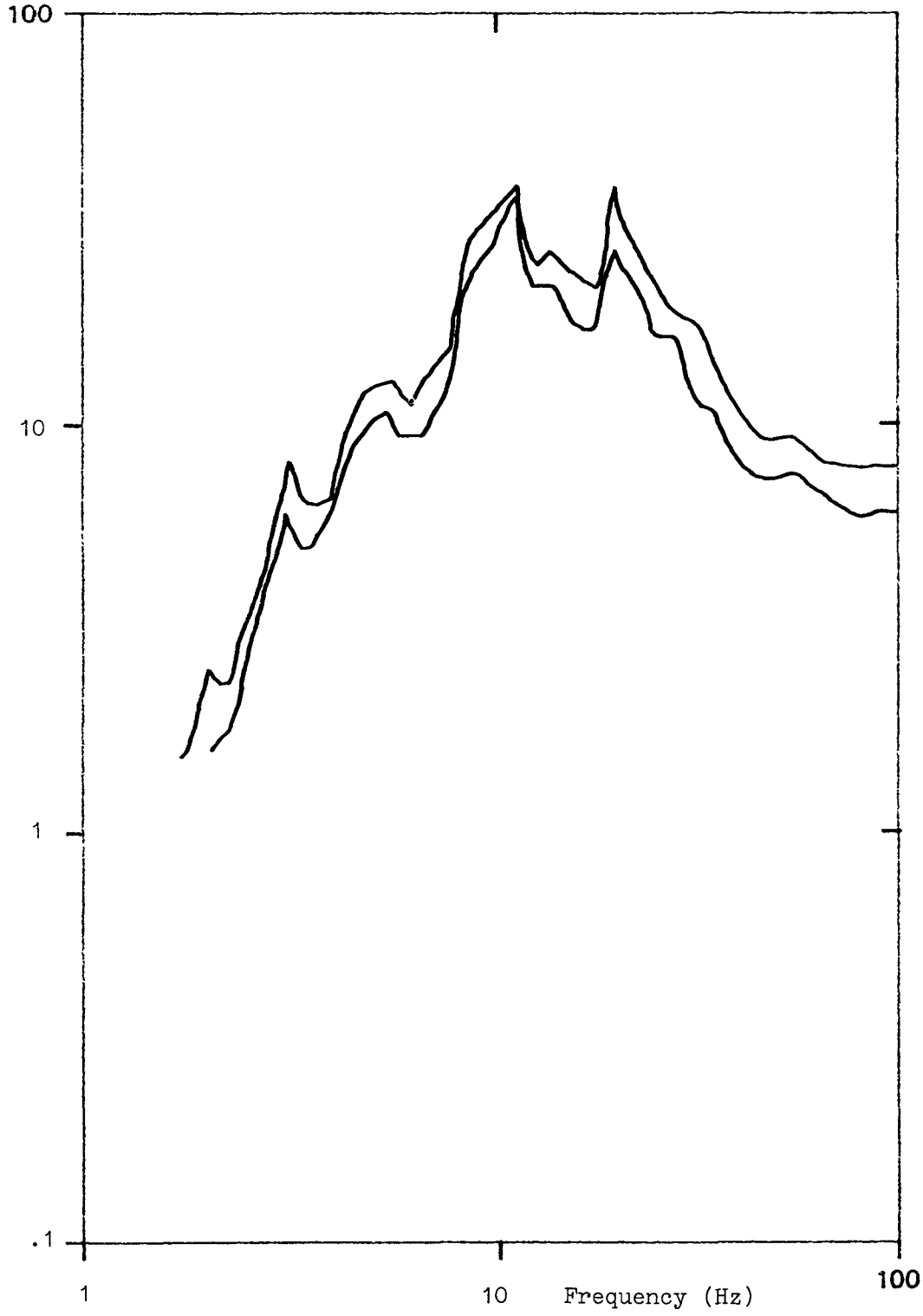

Fig. 4-28. Local test response spectra for Square-D Type KP relays - chatter. Overlay on "no chatter" spectra in Fig. 4-29 for comparison. Note that motion is in the vertical direction.

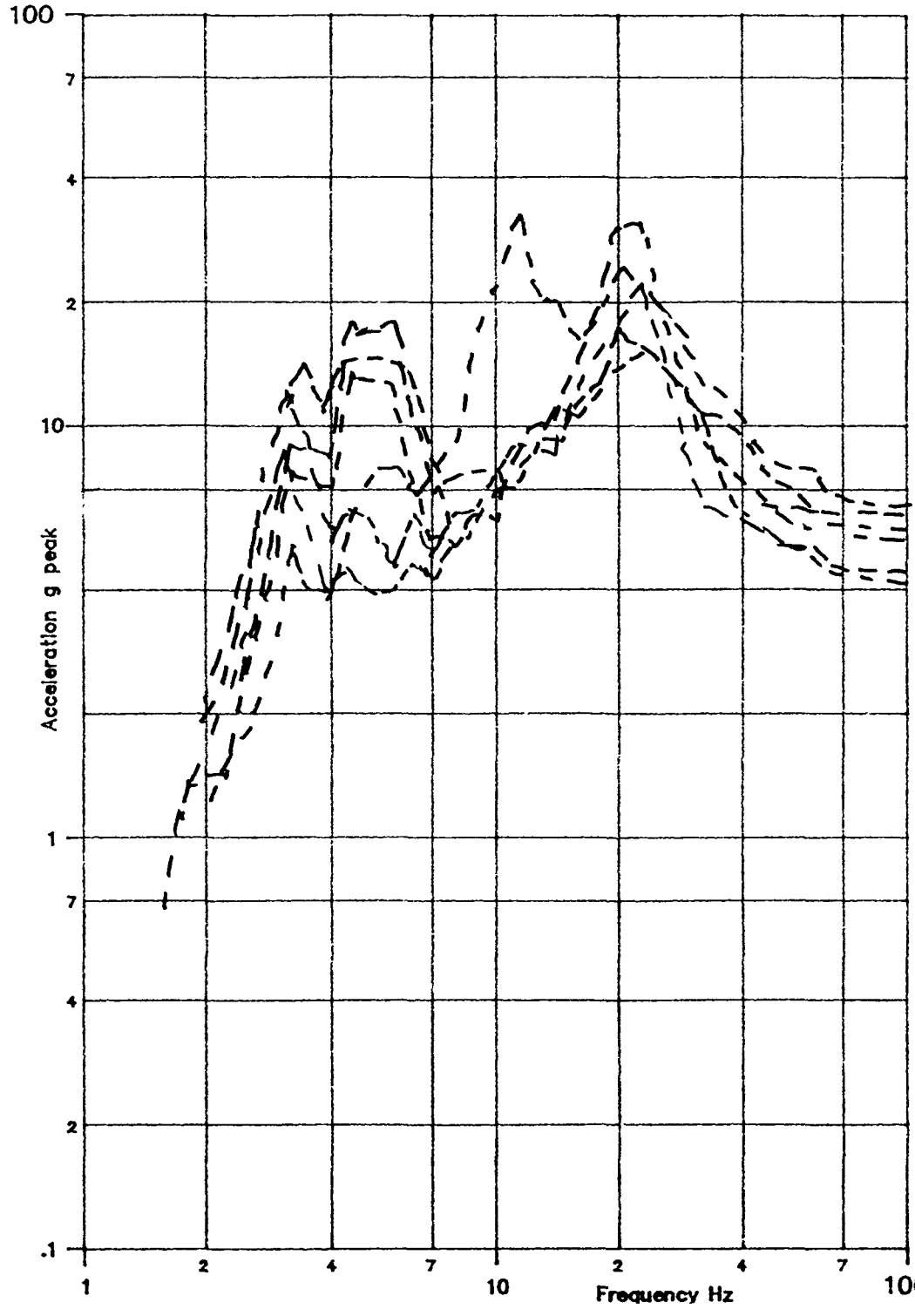

Fig. 4-29. Local test response spectra for Square-D Type KP relays - no chatter. Note that motion is in the vertical direction.

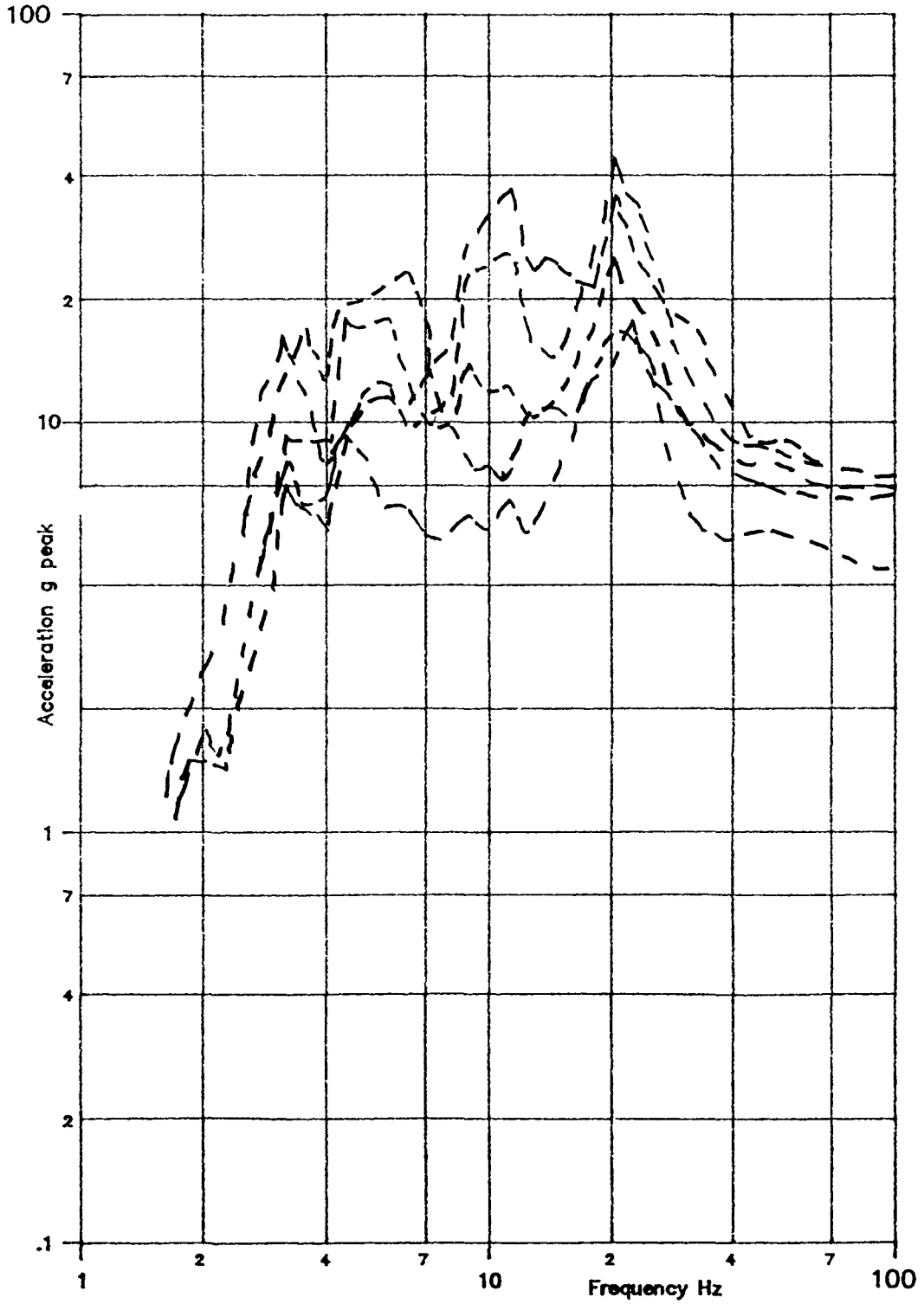

Fig. 4-30. Local test response spectra for Cutler-Hammer Powerreed relays - no chatter.

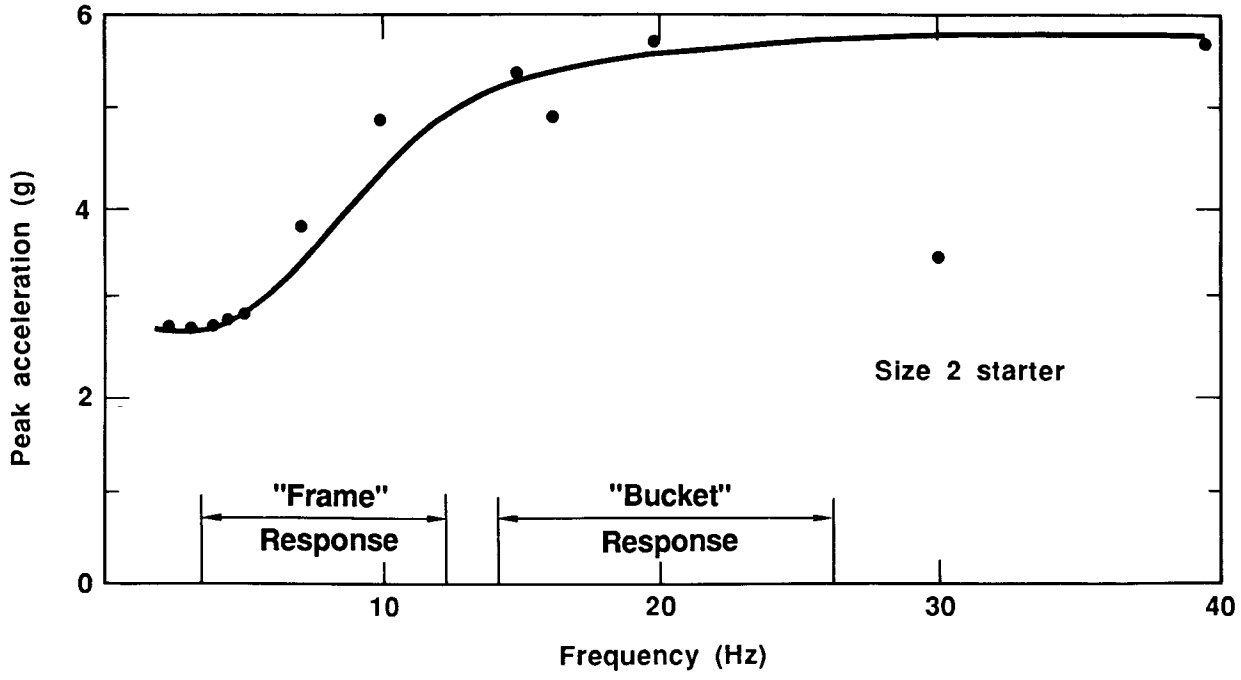

(a)

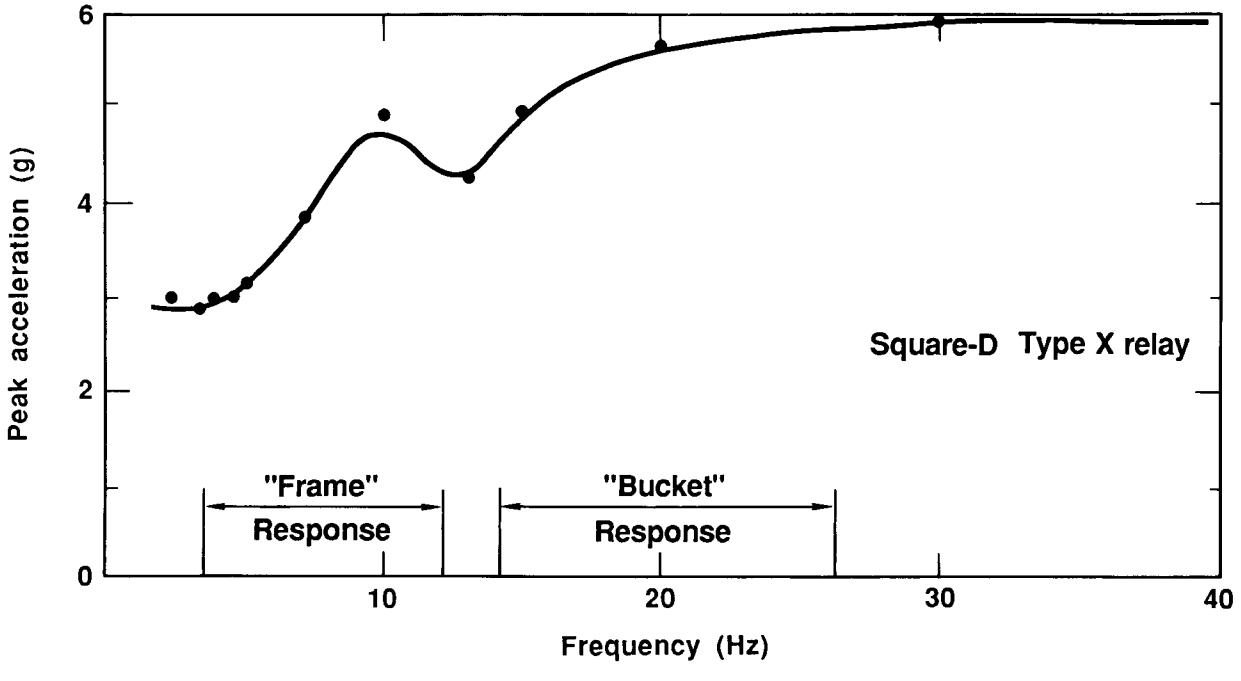

(b)

Fig. 4-31. Frequency-dependent chatter threshold under sinusoidal excitation for (a) Size 2 starter and (b) Square-D Type X relay.

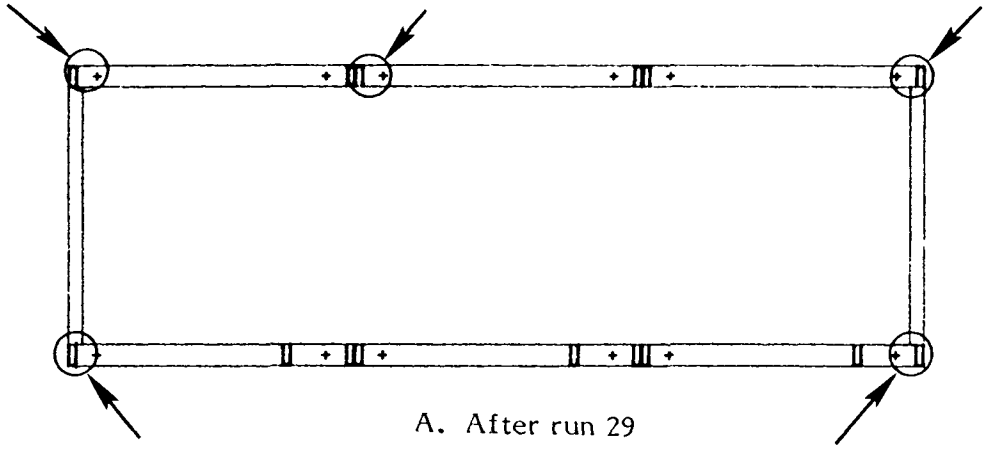

A. After run 29

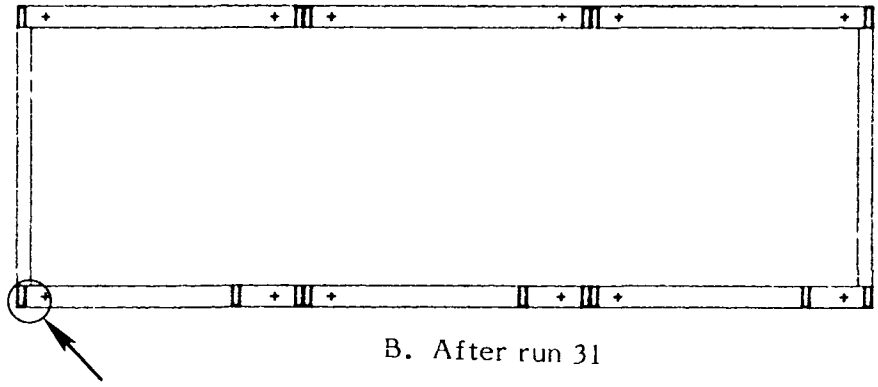

B. After run 31

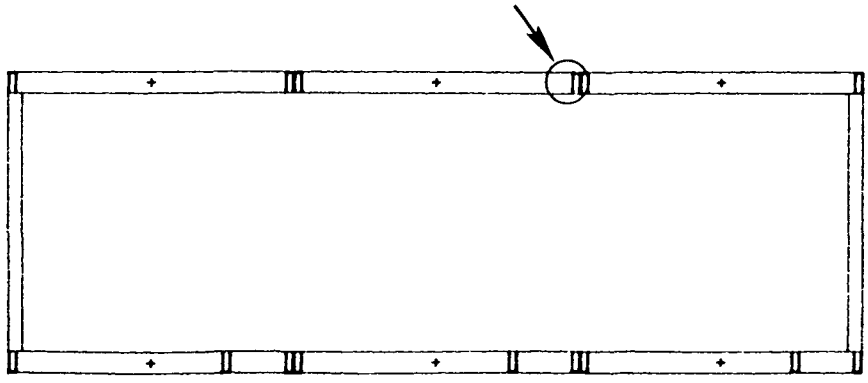

C. After run 35

Fig. 4-32. Locations of broken welds after indicated runs.

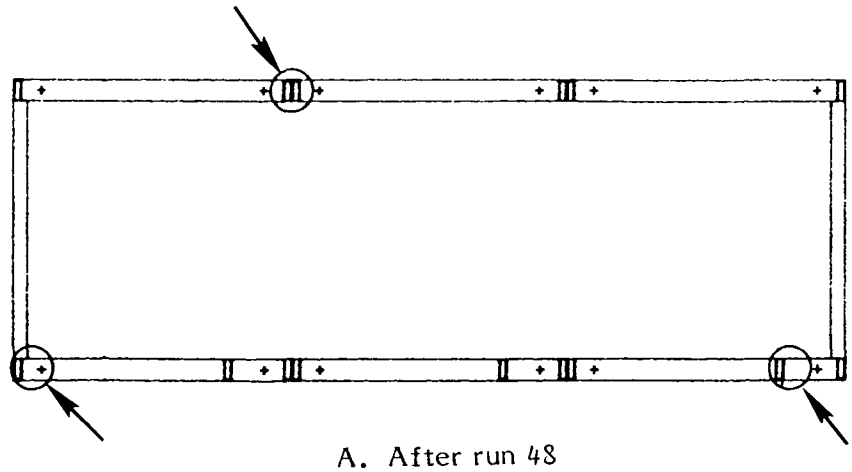

A. After run 48

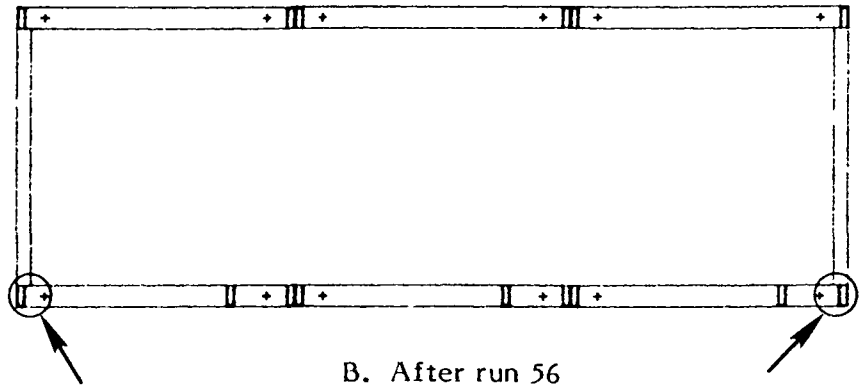

B. After run 56

Fig. 4-33. Location of broken welds following Runs 48 and 56.

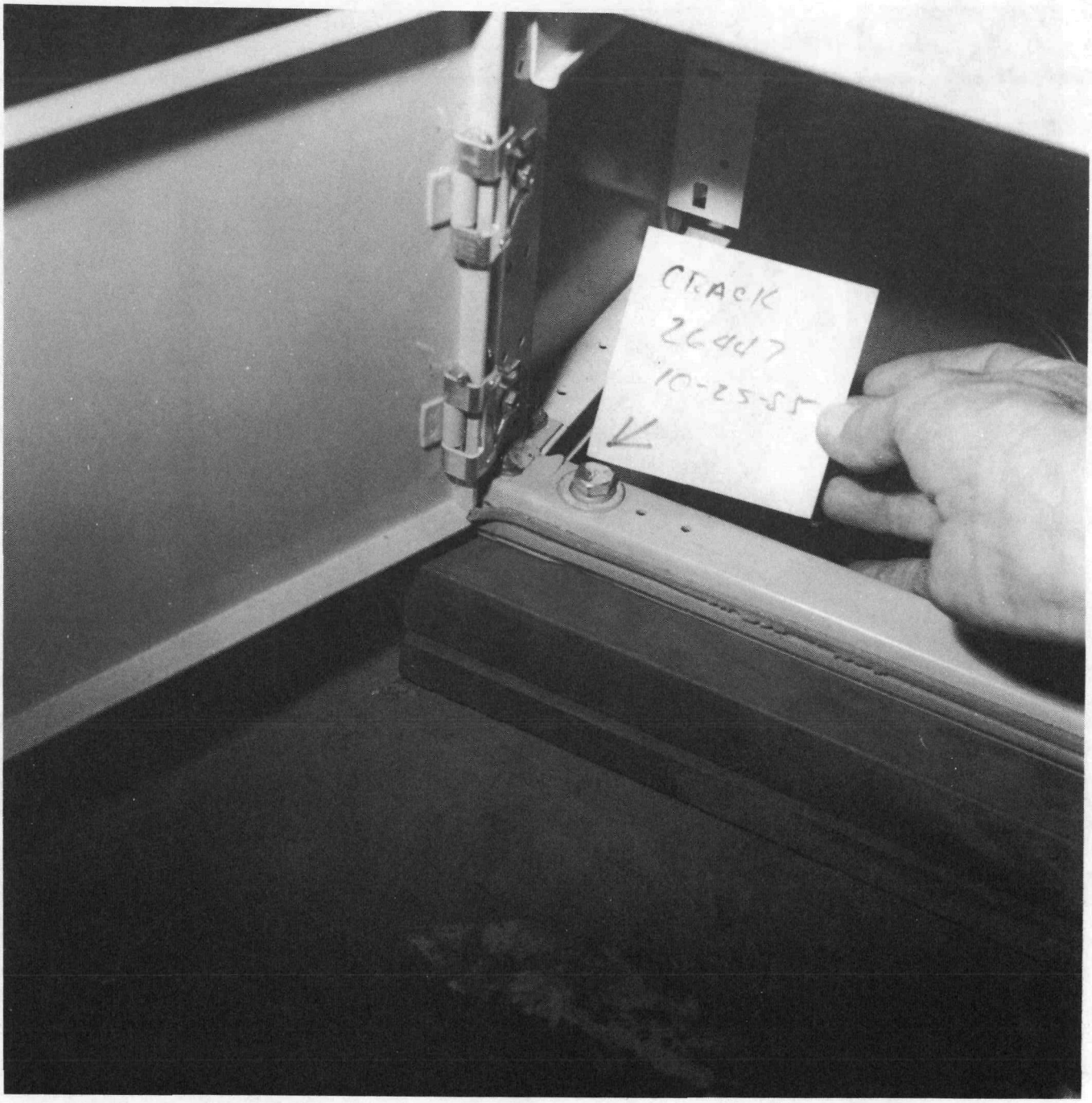

Fig. 4-34. Details of cracked welds following Run 29 (1.6g table ZPA).

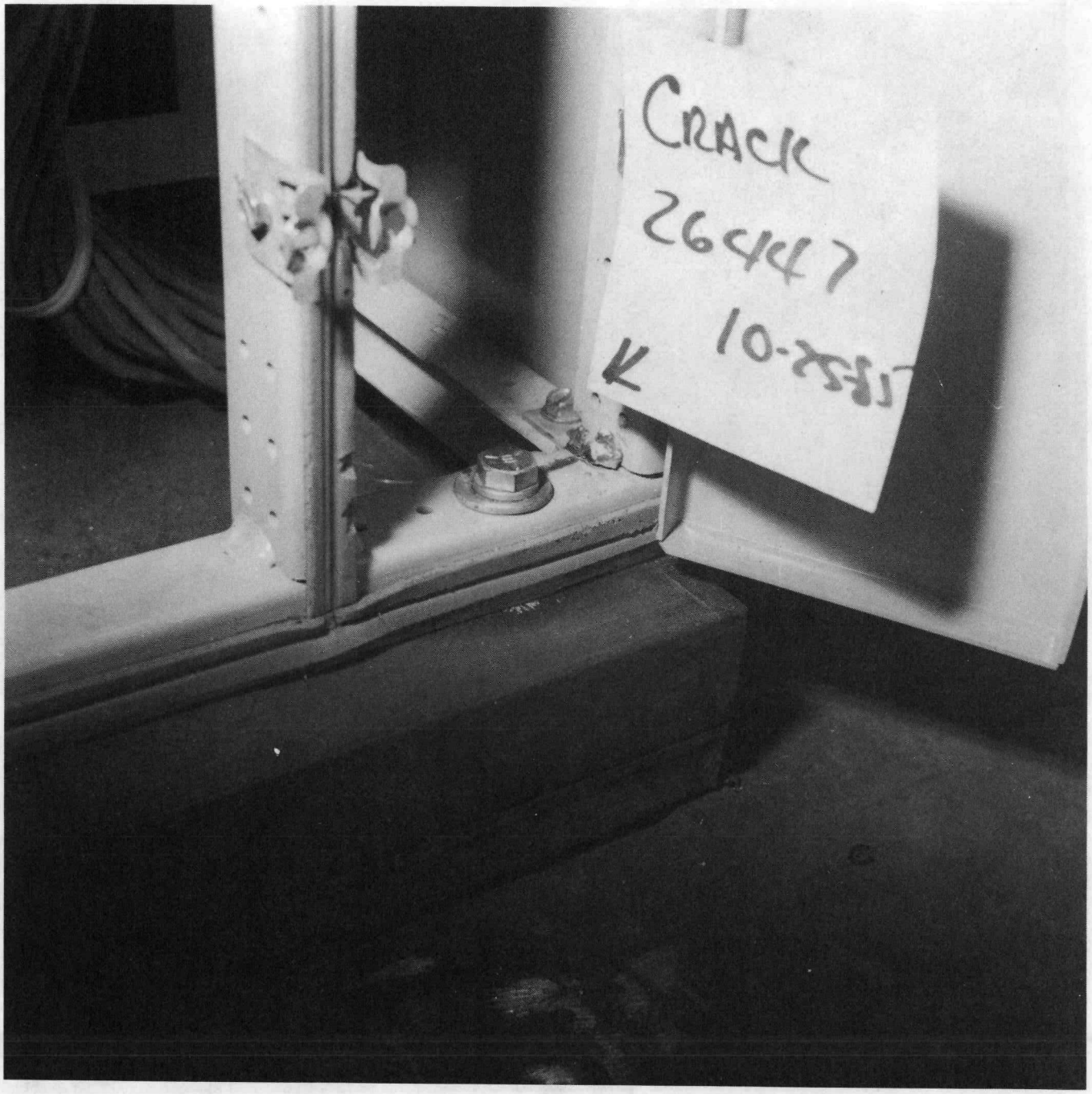

Fig. 4-35. Details of cracked welds following Run 29 (1.6g table ZPA)

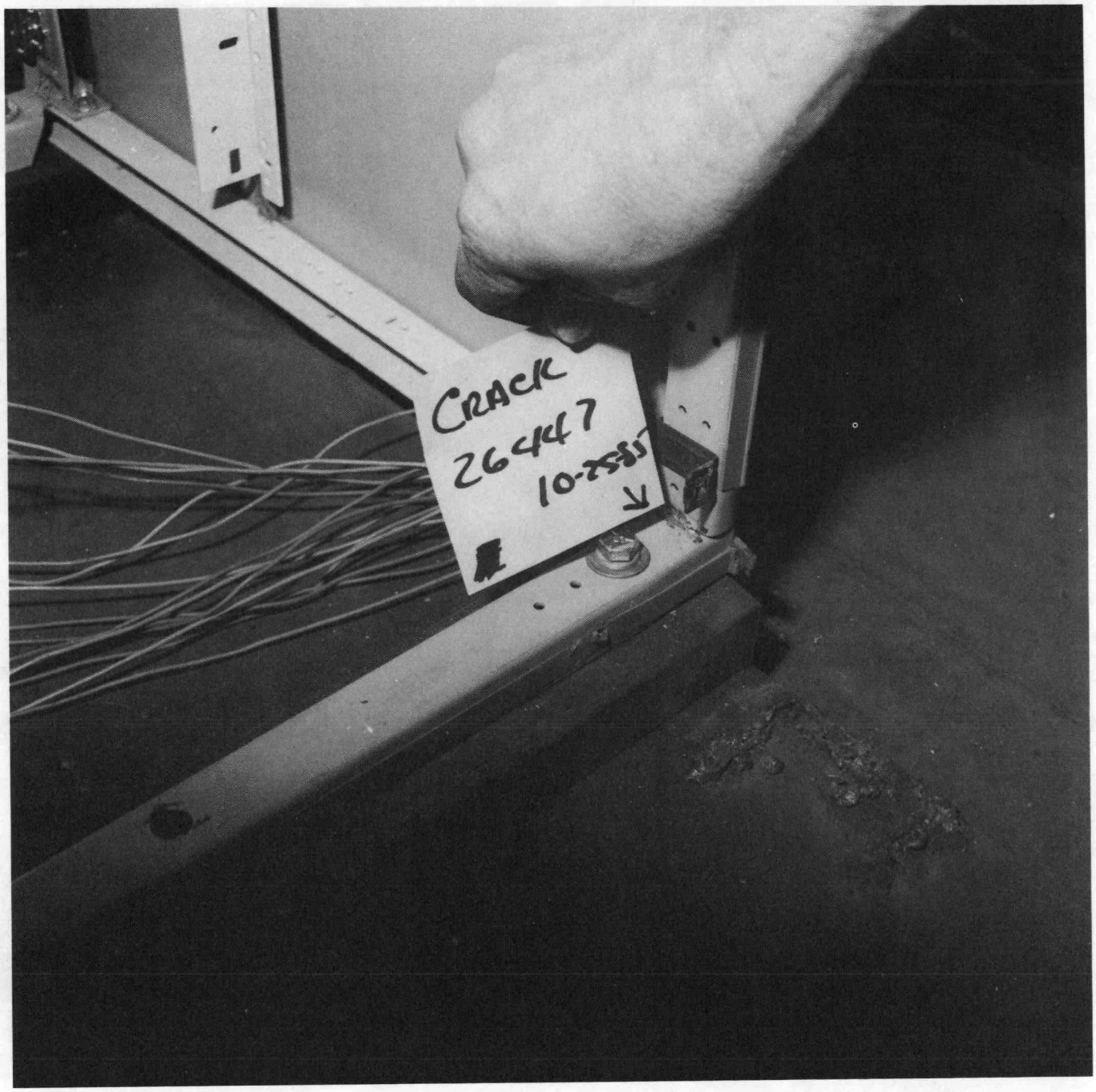

Fig. 4-36. Details of cracked welds following Run 29 (1.6g table ZPA).

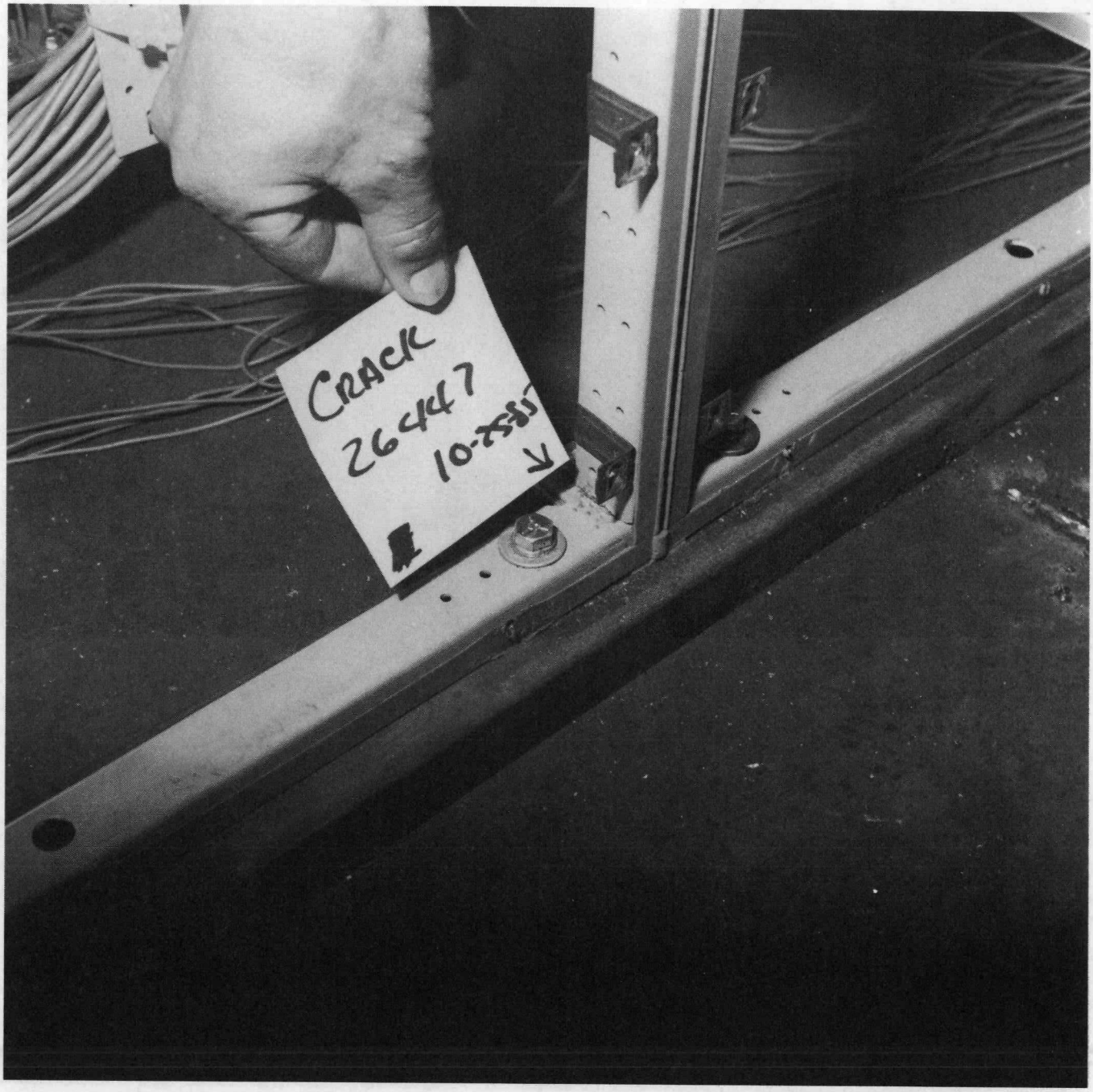

Fig. 4-37. Details of cracked welds following Run 29 (1.6g table ZPA).

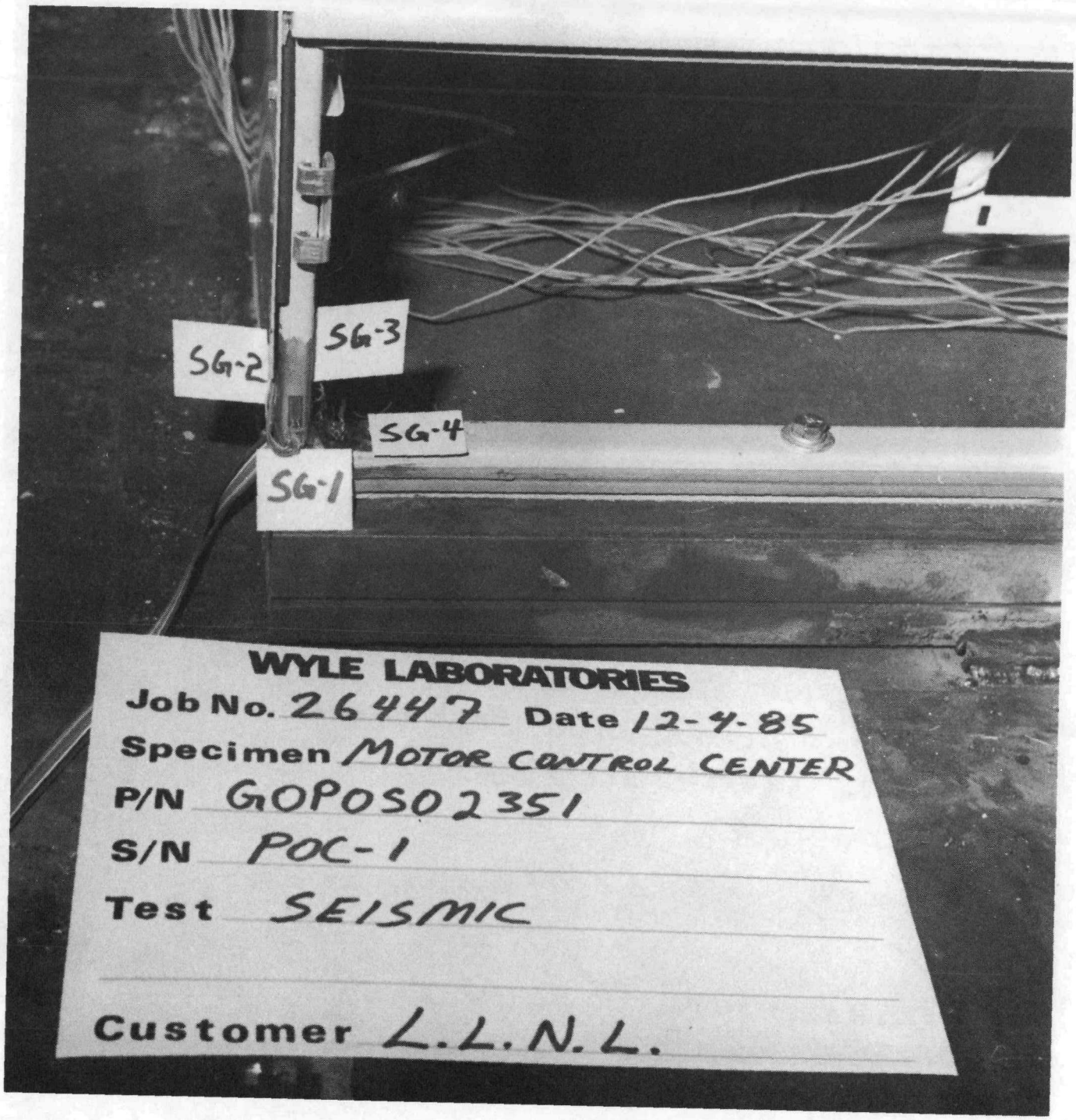

Fig. 4-38. Strain gauges added to cabinet base prior to Run 48 (SG-1 through SG-4).

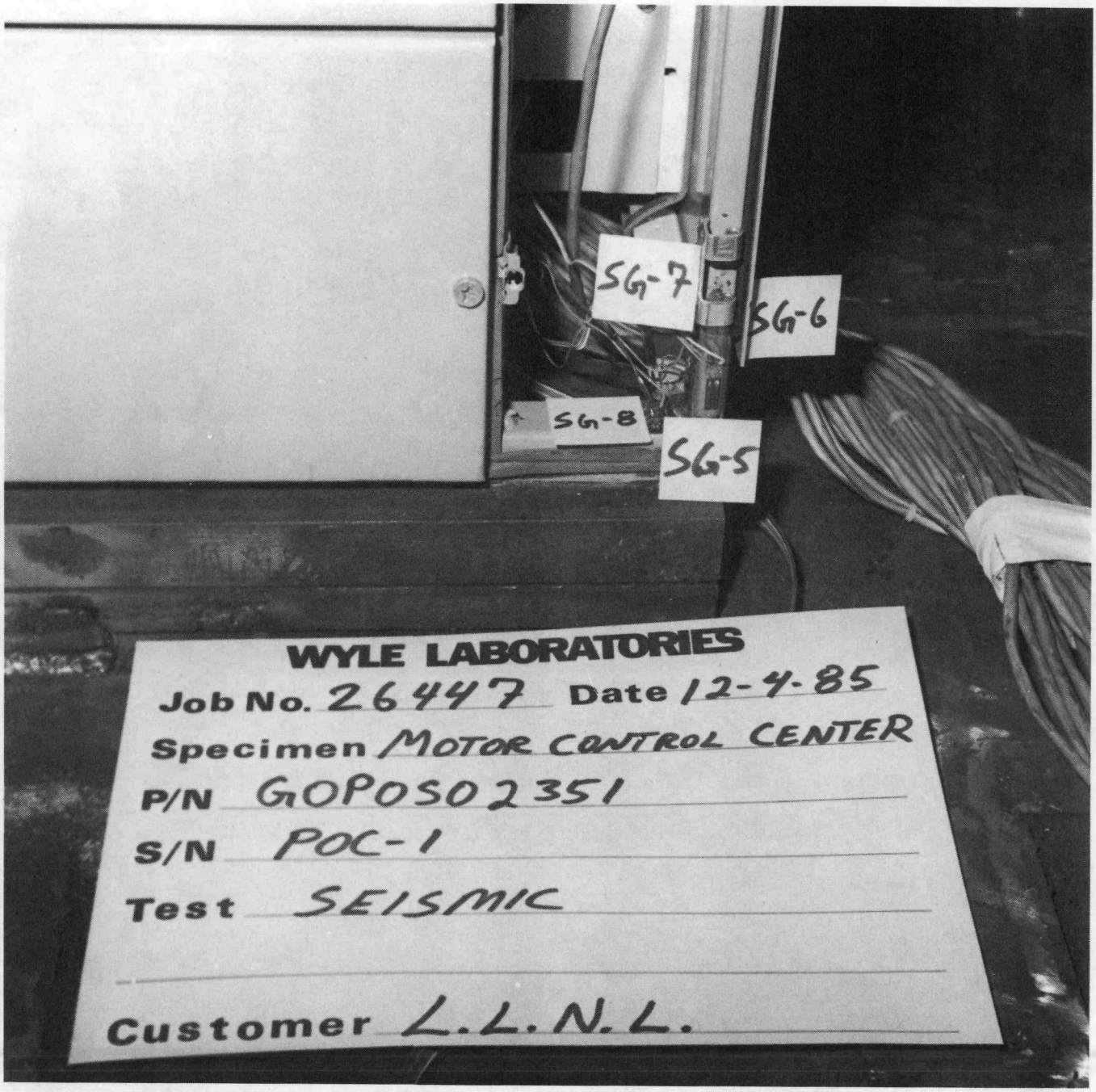

Fig. 4-39. Strain gauges added to cabinet base prior to Run 48 (SG-5 through SG-8).

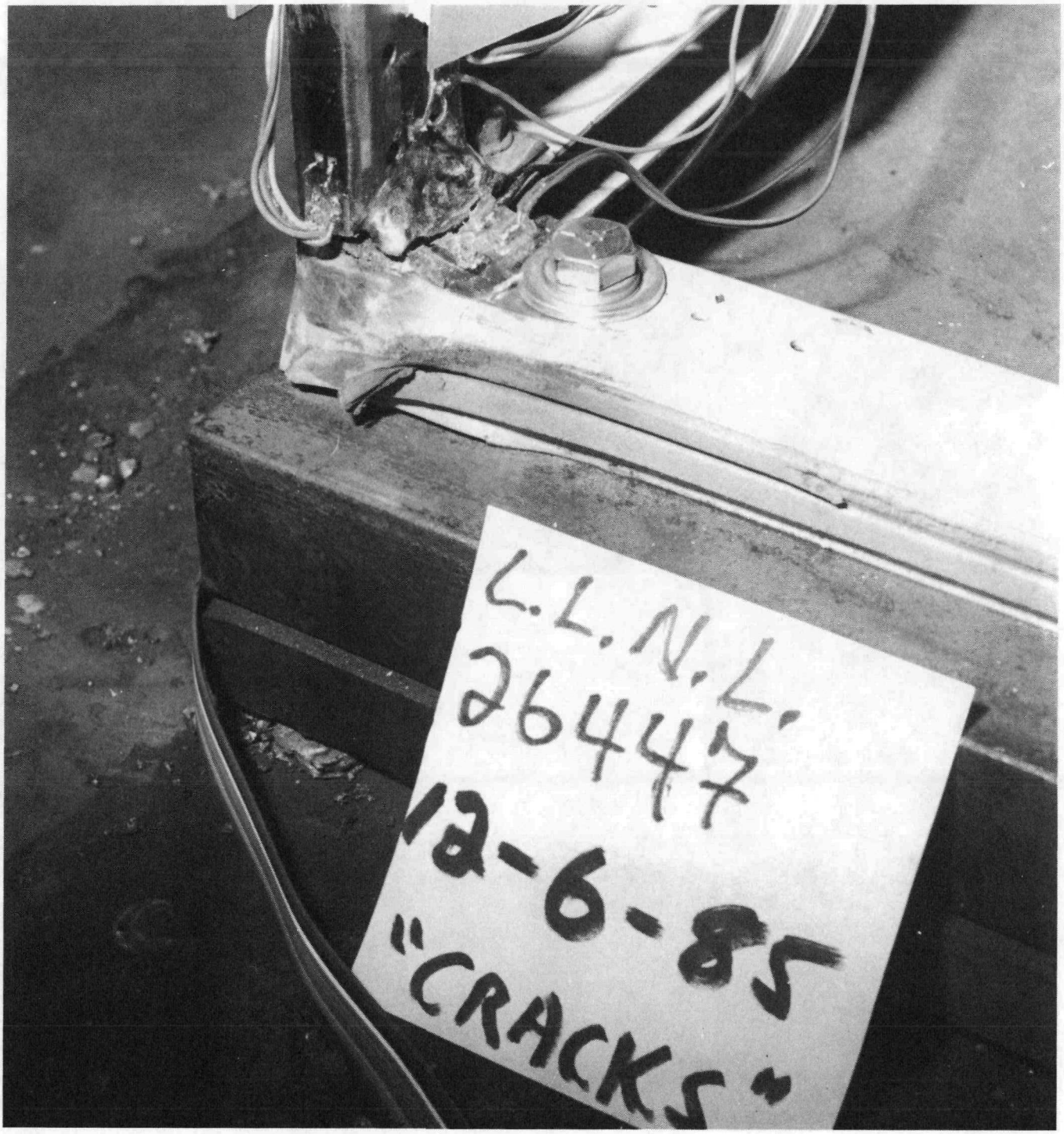

Fig. 4-40. Damage to left front corner of cabinet base sustained during Run 48 (2.1g ZPA).

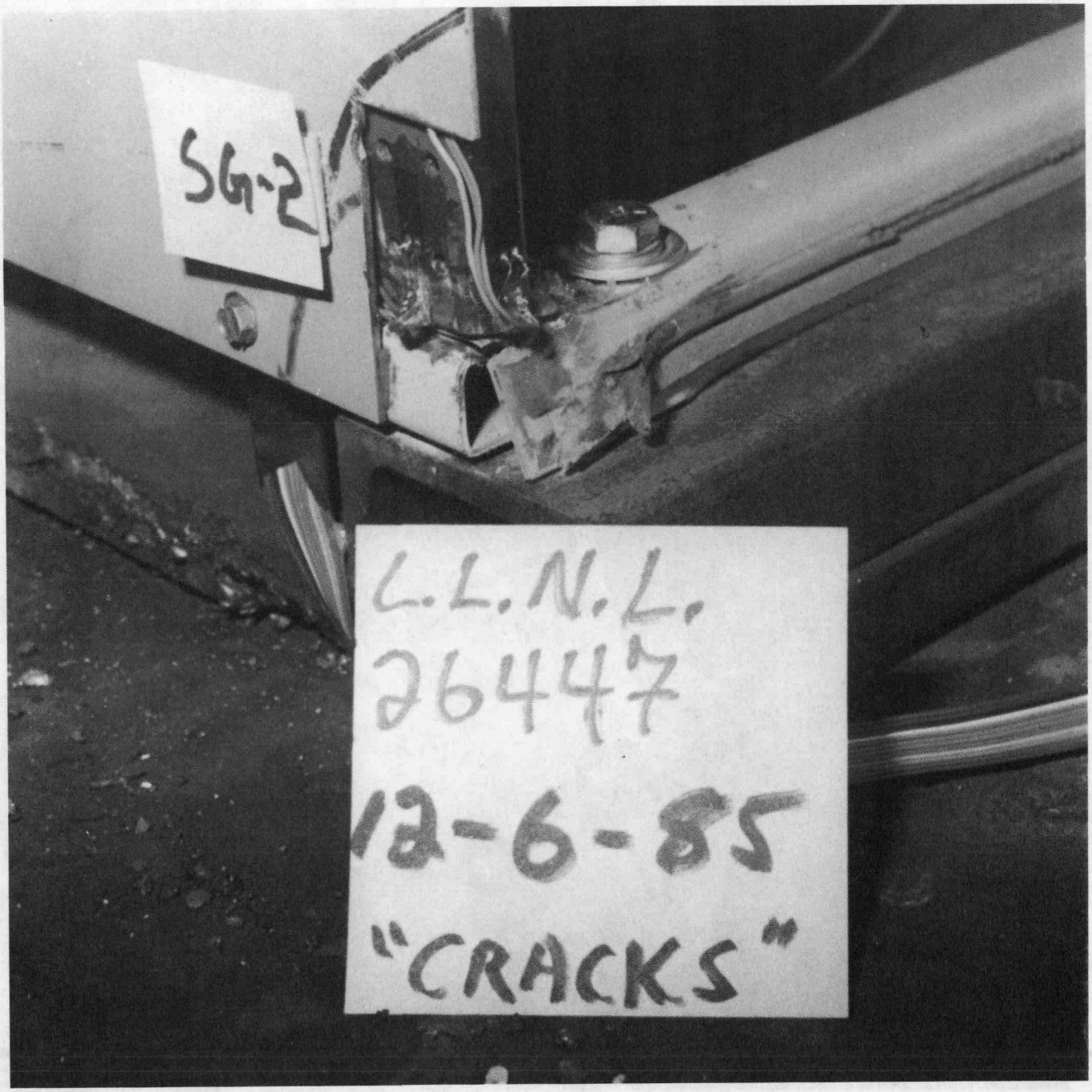

Fig. 4-41. Damage to left front corner of cabinet base sustained during Run 48 (2.1g ZPA).

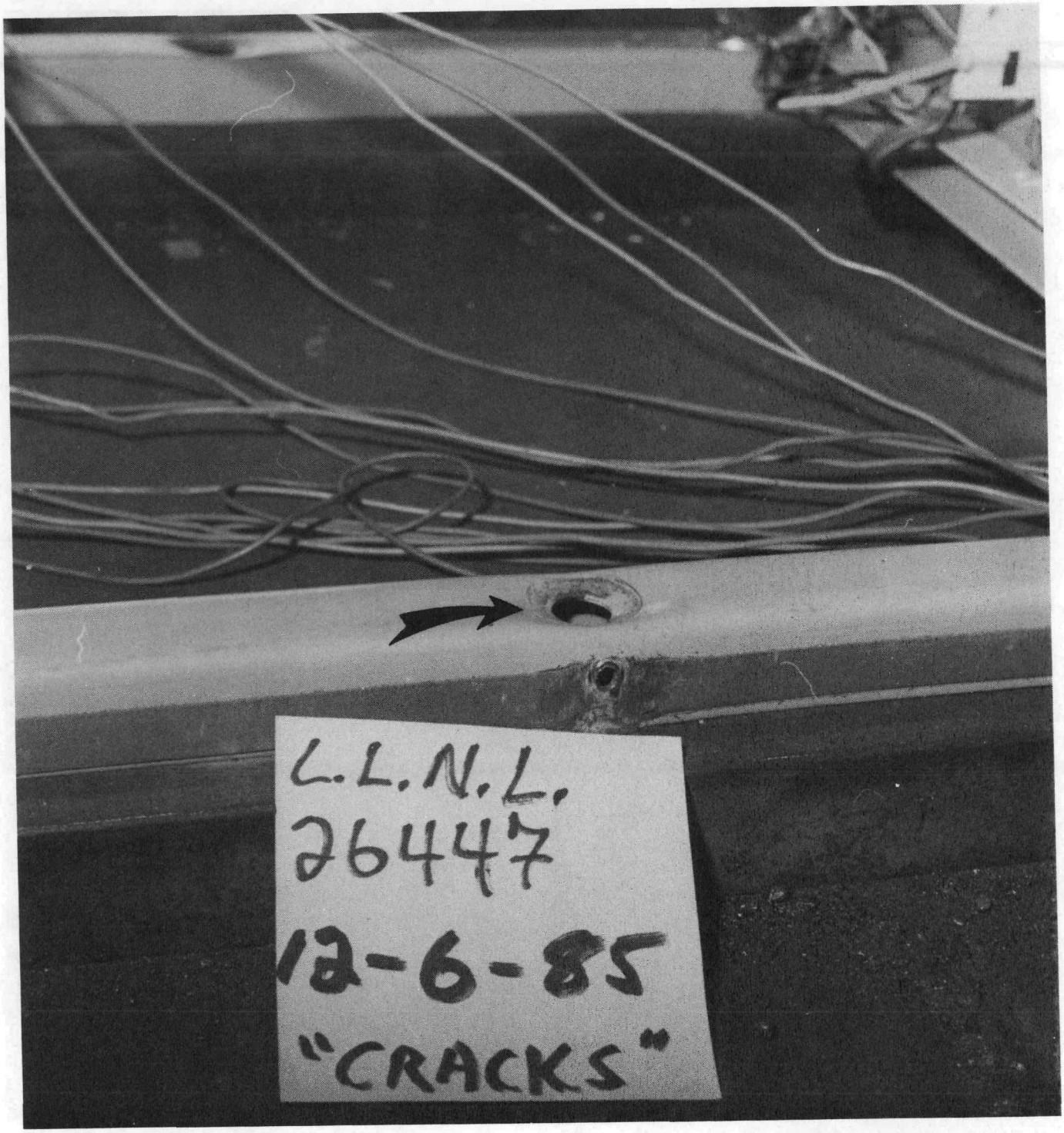

Fig. 4-42. Bolt hole deformation sustained during Run 48 (2.1g ZPA).

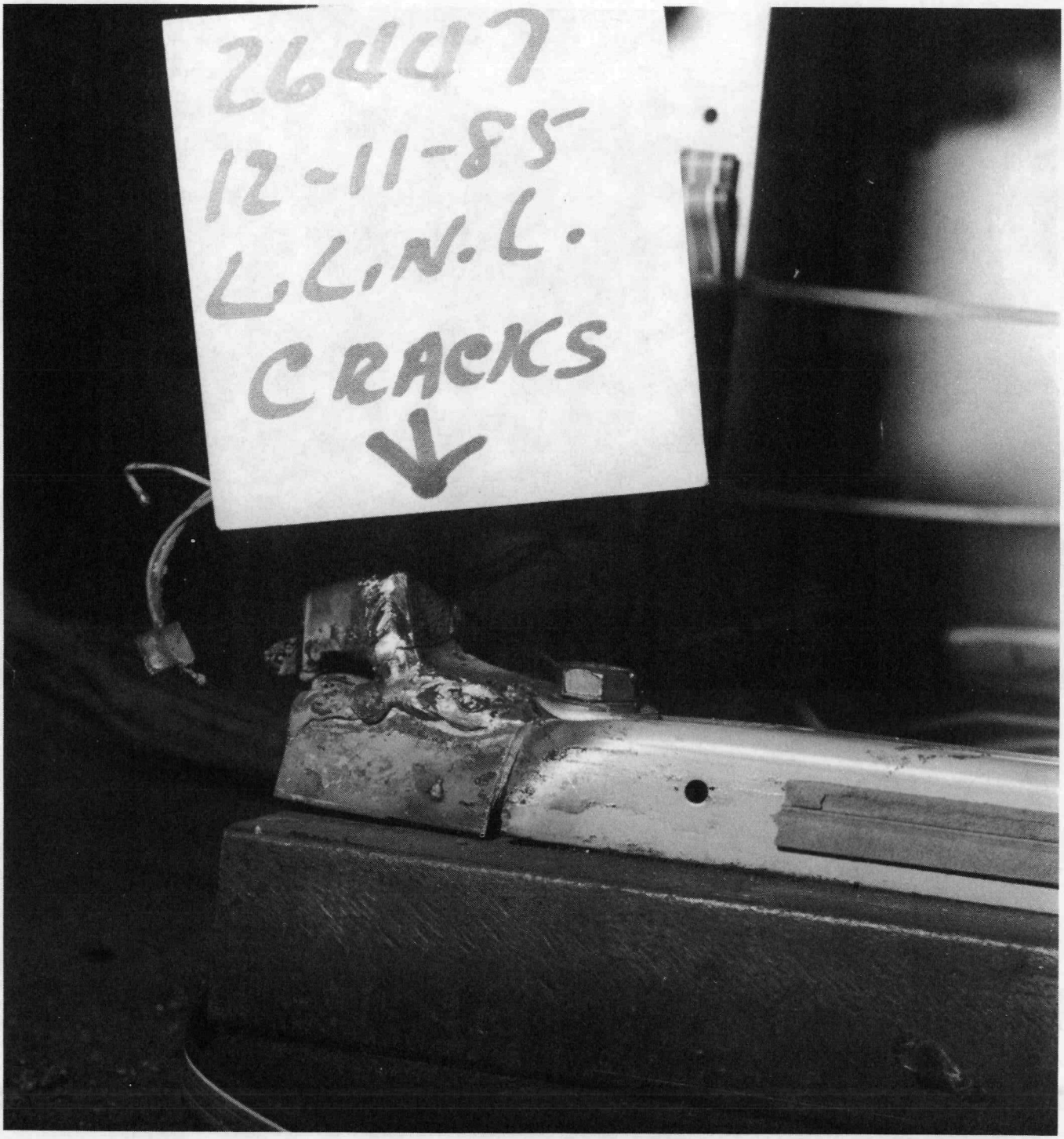

Fig. 4-43. Damage to cabinet base sustained during Run 56 (2.2g ZPA).

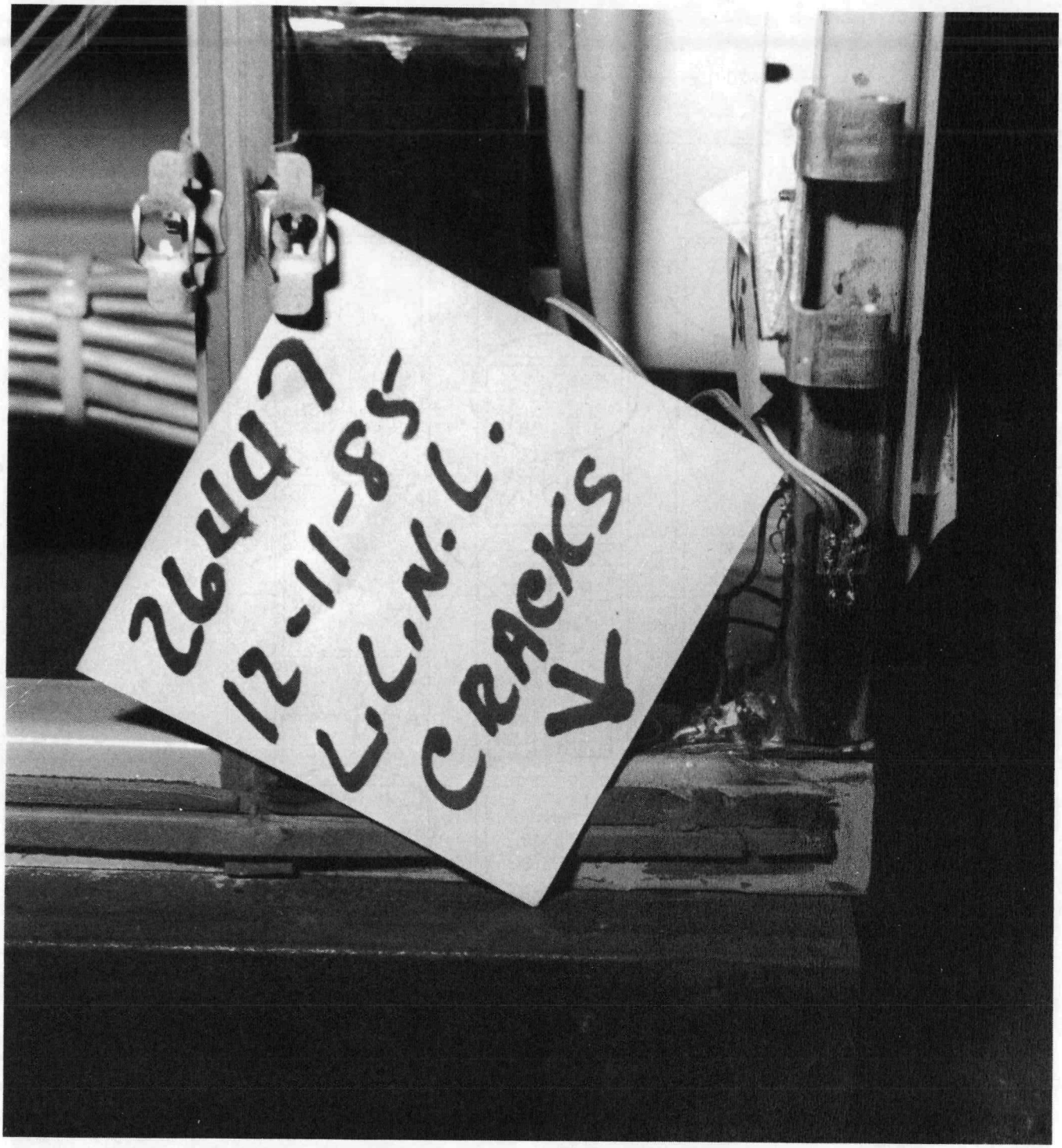

Fig. 4-44. Damage to cabinet base sustained during Run 56 (2.2g ZPA).

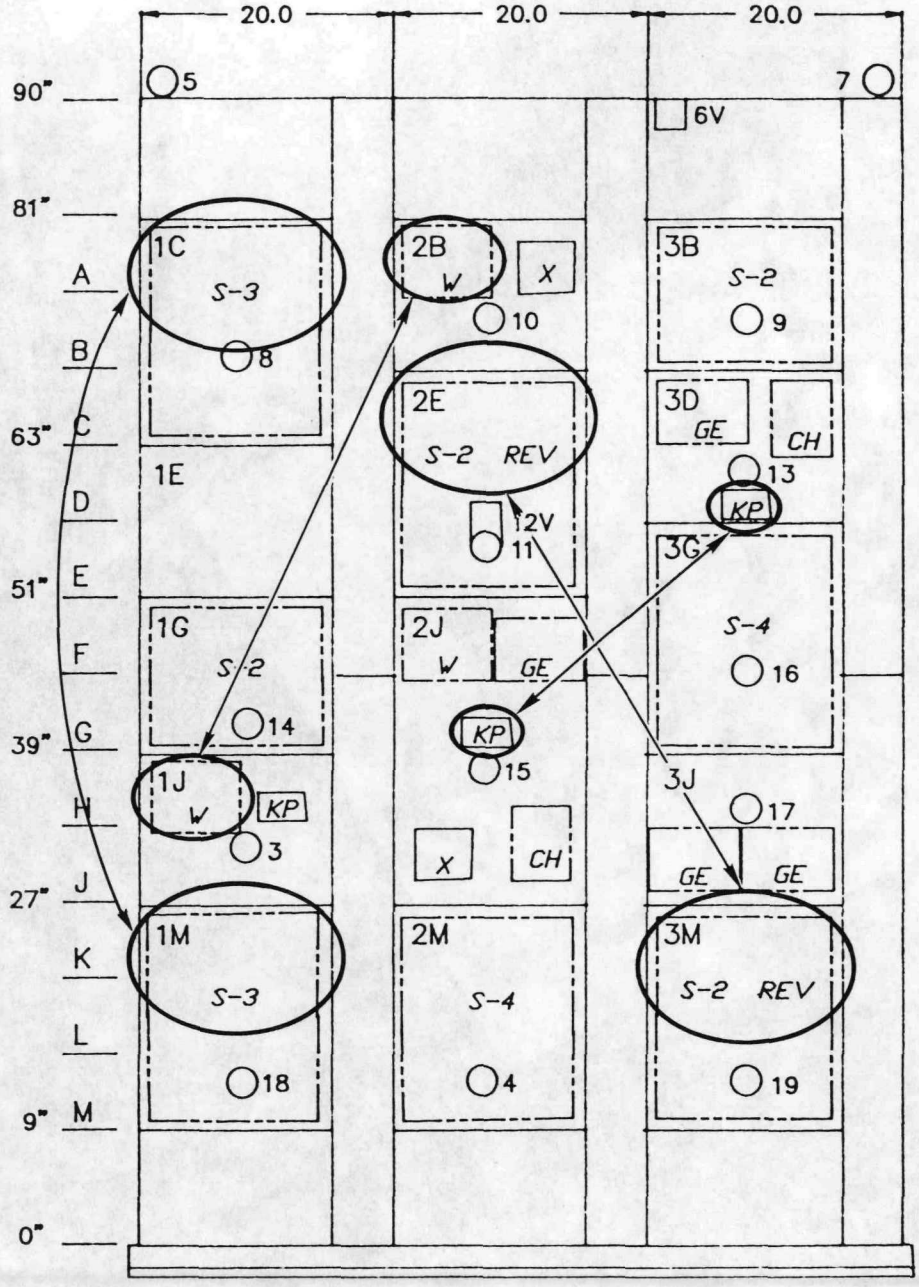

Fig. 4-45. Interchange of devices between Runs 31 and 32.

5. DEVELOPMENT OF DEVICE FRAGILITIES

5.1 General Discussion

This section presents a method by which test results can be used to derive practical fragility curves for application in probabilistic risk assessment. It is important to understand that the fragilities developed in this manner still rely heavily on expert judgment; in other words, the fragility curves are not themselves empirical fits to experimental data. However, testing to "failure" (in this case, defined as electrical device chatter) improves the basis on which these judgments are made.

The results of our MCC tests allow us to make general conclusions regarding parameters to which fragility descriptions may be anchored. As discussed earlier, these results indicated that a fragility threshold anchored to a random input cannot be defined with a high degree of precision. This is not surprising considering the complex transmissibility of the table (i.e., floor) motion imparted by the MCC cabinet. Even with an identical time-history input to the same basic cabinet configuration, changes in damping with input motion level, non-linear response due to rattling of cabinet internals, non-linear response of yielding materials, and differences in response due to variations in base flexibility introduce uncertainties in the responses at device locations. Nevertheless, such tests can provide information useful both in the deterministic evaluation of equipment capacity ("seismic margin") and in probabilistic risk assessment.

5.2 Selection of Fragility Parameters

In our demonstration tests, the MCC and its electrical devices were subjected to random biaxial input motion of varying amplitude applied at the cabinet base. The desired response spectrum (DRS) of the table input motion was broad-banded with a constant spectral acceleration between 4 and 15 Hz (see Fig. 3-2). Figure 4-3 shows actual input motion spectra for the control accelerometer on the shake table, measured during the highest-level test

performed for each mounting configuration. The input motion typically had energy peaks between 5 and 20 Hz. As discussed earlier, tests were performed in either the front-to-back (F-B) or side-to-side (S-S) horizontal direction, either of which was coupled with a vertical component. With two exceptions (the Square-D Type KP relays), each device was oriented such that its "weak" direction -- the direction of contact motion -- was aligned with the F-B cabinet direction.

In addition to the biaxial random input motion tests, one relay and one motor starter were removed from the MCC and individually subjected to sinusoidal input motion along their weak axes to determine for each its frequency-dependent chatter threshold, in other words, its frequency-dependent fragility level. Figure 4-31 shows the input level chatter thresholds versus frequency derived from these two tests; recall that the starter results are for the auxiliary contacts only. The results of these tests indicate for these two devices that contact chatter is most sensitive to low frequency input, typical of that produced by earthquakes and transmitted by structures. This observation is consistent with data on relay and switch fragility from Refs. 3 and 4.

The data from the the biaxial random input motion tests are presented in terms of several parameters including the following:

- table zero period acceleration (ZPA).
- table motion response spectra from control accelerometers.
- device ZPA, equal to local response of the cabinet at the device location. Recall that accelerometers were not mounted directly on any of the devices, but on the respective MCC draw-out units.
- device location response spectra.

These parameters are not all completely described for all of the tests; consequently, the selection of a parameter for describing fragility is biased by the amount of data reduced as well as by purely technical considerations.

Depending on how fragilities are to be used, one might choose a different parameter for reference. If a deterministic minimum threshold of successful performance (i.e., no chatter) is desired, the response spectrum at the device or at the cabinet base might be compared with the required response spectrum (RRS) at the appropriate location. Minimum chatter thresholds are represented by the "chatter" and "no chatter" spectra in Figs. 4-14 through 4-21 for starters (auxiliary contacts only) and Figs. 4-22 through 4-30 for relays.

A minimum envelope drawn below the "no chatter" spectra could be compared directly to an RRS for a deterministic assessment of whether the device would function as desired. This is the approach being taken in an Electric Power Research Institute (EPRI) program to develop so-called generic equipment response spectra (GERS) for various types of nuclear power plant equipment [5].

If a probabilistic fragility description is desired, then one is faced with selecting the best parameter to define the fragility as well as with quantifying the uncertainty in the chosen parameter. Based upon available data, it appears that the devices tested are most sensitive to spectral accelerations in the 2.5 to 8 Hz range (see Fig. 4-31). However, fragilities are most often expressed in terms of ZPA, as in the Fragility Handbook developed as part of the Seismic Safety Margins Research Program [6] and in commercial PRAs. Zero period acceleration is also a parameter commonly computed by equipment qualification engineers. For this reason, the initial focus in our MCC tests was on ZPA and less on frequency-dependent effects; we have therefore selected local ZPA as the parameter on which to base "single-parameter" device fragilities derived from our demonstration tests.

Incorporating effects of spectral acceleration in a refined definition of device fragility would clearly require more comprehensive data than we now have on the frequency-dependency of device fragility. It would also require more complex application of the data. In a similar fragility test program, for example, devices such as relays, pressure switches and breakers were subjected initially to single-axis, single-frequency sine-beat tests to define frequency-dependent fragility levels such as those in Fig. 4-31 [7]. In that

program, however, the fragility was based on response to the sine beat input instead of on the input itself, thus defining a fragility spectrum. Consequently, an in-cabinet response spectrum could be compared to the device fragility spectrum. To further define the fragility in terms of a spectrum, the devices were then tested to biaxial random motion input whose spectra matched the device fragility spectra. Due to the multi-mode, multi-axis input the devices were found to chatter at input motion levels as low as 40 percent of those required to achieve the single-axis, single-frequency response spectra. Given such precise fragility information, one could conceivably refine the probabilistic approach to incorporate the data. This would require significantly more effort to achieve such precision and would be more difficult to apply in practice (such as in a PRA). For purposes of demonstrating how data from fragility tests can be reduced for application we have selected ZPA as our reference parameter, recognizing at the same time that other parameters may be better suited.

The local ZPA values contained in this report are pseudo-ZPAs with spectral accelerations above 30 Hz filtered out. Referencing fragility to filtered ZPA in this case is valid as long as the devices are most sensitive to frequencies below 30 Hz; the sinusoidal tests showed this to be true, at least for the two devices tested. As indicated earlier, this low-frequency sensitivity is consistent with the numerous tests conducted in the Safeguards Program.

When considering cabinet-mounted electrical devices in a probabilistic approach, the fragility analyst typically has limited knowledge of the cabinet fundamental frequency and of device location, manufacturer and model. We will assume that one of the following two states of knowledge exists:

(1) the analyst knows cabinet response at the device in terms of peak acceleration (i.e., from a cabinet response spectrum analysis). He also knows the manufacturer and model of the device.

(2) the analyst knows or can estimate the natural frequency of the cabinet. He does not know the exact location of the device, and may or may not

know the manufacturer and the type. He can only estimate the response of the device using the cabinet fundamental frequency and the approximate location of the device in a simple cabinet model.

In either case, having the fragility anchored to device ZPA will result in a workable and practical fragility description. In the first case, the analyst will want a fragility description by individual manufacturer and type. For Case 2, he may want a generic device fragility description (e.g., for all relays) and an estimate of transmissibility from the floor motion to the device. This information is available for the devices in our demonstration tests, recognizing that only a few manufacturers and device types are represented, and that only one time-history -- corresponding to a broad-banded floor spectrum -- was used in testing. These results are further limited by the fact that only one cabinet model was tested, although the four different mounting configurations do provide insight into the effects of varying cabinet transmissibility. Additional variability in the derived fragility description will be present when applied to PRA due to the randomness of the earthquake input motion and the uncertainty in the transmissibility from the ground up through the structure to the cabinet mounting location. Ground motion and structural response, however, are separate issues and are not included in this discussion.

5.3 Fragility Derivations

The remainder of this discussion centers on the development of device fragility descriptions based on local ZPA. Of the devices tested, sufficient data was collected to develop fragility descriptions for the following six:

- Westinghouse Size 2 full-voltage non-reversing motor starters (auxiliary contacts only)

- Westinghouse Size 2 full-voltage reversing motor starters (auxiliary contacts only)

- Westinghouse Size 3 full-voltage non-reversing motor starter (auxiliary contacts only)
- General Electric Type CR relay
- Westinghouse Type AR relay
- Square-D Type X relay

Two other relay models tested were not included. Two Square-D Type KP relays were mounted so that contact motion was in the cabinet vertical direction; insufficient data was available from which to characterize the behavior of the relay. Two Cutler-Hammer Powerreed (reed-type) relays exhibited no chatter during any of the nearly 60 test runs conducted. Note also that the Size 3 starters have only three failure threshold data points combined; consequently, the fragility descriptions derived from this data must be regarded as very approximate.

Resistance to chatter showed a clear correlation with contact type and electrical state. In general, chatter was observed only in deenergized contacts. For the starters, normally-closed (NC) auxiliary contacts were the first to chatter, followed by the normally-open (NO) auxiliary contacts. The main contacts were the last to chatter and, in fact, only did so in isolated cases. For relays, NC contacts chattered before NO contacts.

We based device fragilities on the first sign of chatter in normally closed contacts in their deenergized state. As the "chatter" and "no-chatter" spectra in Figs. 4-11 through 4-29 illustrate, in some runs contact chatter was observed at a lower ZPA level that associated with no chatter in other runs. In these cases, the lowest "chatter" level and the highest "no chatter" level were equally weighted and used in a regression analysis of the data.

All fragilities discussed here are described as lognormal distributions, as is done in the Fragilities Handbook. Basically, a median capacity (expressed in terms of local ZPA) and its random variability and modeling

uncertainty (β_R and β_U, respectively), expressed as logarithmic standard deviations, are developed from the raw data.

The threshold of chatter for each device at each location and for each cabinet mounting configuration tested was used as a data point. Most devices were tested at two locations for four cabinet mounting configurations, resulting in eight data points. However, some test conditions produced no chatter; in these cases, no failure data point was defined.

The method chosen to best fit the data to a lognormal distribution was to perform a linear regression analysis on the logarithm of ZPA versus probability. The best fit of the data and the one standard deviation bounds on the best fit are plotted on probability paper in Figs. 5-1 through 5-5 for each type and model of device tested. For each device, the data points were ordered in ascending ZPA from 1 to N data points. The probability of failure for the first data point was taken as 1/N+1, the second as 2/N+1, and so forth. The data points thus represent a cumulative distribution function from 1/N+1 to N/N+1. Figures 5-6 and 5-7 plot the same parameters for, respectively, all relays and for the Size 2 FVR and FVNR starters. Note that the FVR and FVNR starters can be combined as a class because both use identical contactors (the reversing starter using two).

The slope of the data fit on probability paper defines β_U; the median capacity is defined as the intersection of the data fit with the 50% probability line. The random variability, β_R, is defined by the width of the one standard deviation scatter band about the data fit. Table 5-1 summarizes the data fits individually for the six types of devices considered, and for the three relays and the Size 2 FVR and FVNR starters taken as groups. The Size 3 starters were <u>not</u> grouped with the Size 2 starters owing to their markedly different capacity, most likely a result of their substantially different physical size. It should be recognized that a grouping of only three devices of the same generic category is a very small data set for purposes of defining broadly applicable generic fragilities. However, keep in mind that we are not attempting such generic characterizations with the data from these demonstration tests.

The variabilities β_R and β_U represent several unknowns about the actual capacity level and are somewhat subjectively defined. Classically, fragility descriptions have been developed under the pretense that β_u defines the uncertainty associated with lack of exact knowledge on how to analytically model the strength and response of structures and equipment. With increasing effort the uncertainty can be theoretically reduced to zero, i.e., there is only a single value of strength and a single value of response for a given input. The uncertainty, β_u, is a measure of the imprecision in computing these single values. On the other hand, there is random variability associated with the actual earthquake input and other analytically undefinable parameters. Even with increased study, these random uncertainties cannot be reasonably reduced.

With this concept of randomness and uncertainty in mind, the test data are examined to differentiate between randomness and uncertainty. First, the test data show that the ratio of the local ZPA to the table ZPA is not constant for the same input. For example, Table 4-7 indicates that at location 2J/15 (accelerometer 15, draw-out unit 2J) the local ZPA during Run 28 is 43 percent greater than for Run 27 even though the table ZPA is the same. The time-history input is assumed to be the same but may actually be sufficiently different to have a pronounced effect on cabinet response. Also, non-linearities in the cabinet response can affect the response in a random manner; such an effect was suggested as one possible reason for the significant overlap in the "chatter" and "no-chatter" spectra in Figs. 4-11 through 4-29. Similarly, the ratio between peak spectral acceleration and ZPA is not constant for the same input and same ZPA. Table 4-4, for example, shows that at location 3M/19 the peak spectral acceleration for Run 55 is 30 percent greater than for Run 48 and occurs at a different frequency despite having the same table input and the same local ZPA. The same device may chatter at one level of local ZPA and not chatter at a higher level; this anomaly is demonstrated, for example, by location 2J/15 during Runs 53 and 55. Run 53 has a higher table ZPA, has higher local ZPA and the same device peak spectral acceleration as during Run 55, yet chatter is observed in Run 55 and not in Run 53. These types of variability cannot reasonably be reduced by

further study of the available data, and constitute the random variability β_R in the fragility descriptions.

On the other hand, using ZPA instead of local spectral acceleration introduces uncertainty. A great deal of variability in spectral acceleration versus ZPA is present due to the variations in cabinet mounting stiffness and device location. These parameters affect the frequency content at the device and constitute uncertainty, β_U, in the fragility description. This uncertainty can be reduced with further knowledge of the location, cabinet mounting stiffness and resulting frequency response at the device location.

Application of the above logic suggests that β_R should be defined by the scatter band about the best-fit to the test data, and that β_u should be defined by the slopes of the best-fit curves. The best fit curves and the scatter bands about the curves, as shown in Figures 5-1 through 5-7, are cumulative distribution curves of ZPA capacity vs. probability, thus, they are, in fact, fragility curves. These fragility curves are plotted in the more familiar linear scale in Figure 5-8 through 5-14. Note, that traditionally, fragility curves such as shown in Figures 5-8 through 5-14 have had their slope represented by β_R and the uncertainty bound by β_u. This representation has been developed for fragility curves referenced to peak ground acceleration where the randomness, β_R, is predominantly a function of the earthquake time history input and the uncertainty, β_u, is defined by the distribution in strength and response associated with imprecise knowledge of how to accurately model these parameters.

In this case, the randomness of the earthquake input is not present, nor is any uncertainty in the structural response to the earthquake. Consequently, the fragility curves take on a form to best reflect the situation at hand. In this case, the fragility curve slope is best described as uncertainty, β_u, and the scatter band about the most probable fragility curve is best described as randomness, β_R.

5.4 Discussion of Results

The test data collected and analyzed indicate that local spectral acceleration is probably a more appropriate parameter than local ZPA for defining device fragility. However, due to a lack of suitable data on the frequency dependency of device chatter, we selected local ZPA as an alternate basis for describing device fragility and demonstrating how test data can be used to develop practical "single-parameter" fragilities for PRA applications.

Variability in the fragility description results from random parameters that cannot reasonably be defined. These parameters include the randomness of time-history motion input, non-linearities due to rattling of draw-out units, and non-linearities in structural response and damping. Uncertainties in the fragility estimate arise due to use of local ZPA as the fragility parameter due to different cabinet mounting stiffnesses tested and due to the various in-cabinet locations at which the devices were mounted.

Further refinement in the fragility description using local spectral acceleration could be accomplished through extended analysis of the available raw data, particularly through development of more local spectra and more detailed information on how cabinet transmissibility varies with cabinet mounting configuration and shaking level. Single-frequency single-axis tests on the remaining devices would also be valuable.

In addition, it would be very useful to develop simple single-degree-of-freedom (SDOF) models of the MCC and determine the uncertainty in predicted transmissibilities through comparisons with experimental data. Such a study could also determine suitable effective damping for the SDOF models and also how amplification of floor response by the cabinet structure varies with mounting configuration and shaking level.

5.5 Alternate Fragility Analysis

The foregoing discussion described an "engineering" analysis intended to develop workable "single-parameter" fragility descriptions suitable for PRA use. The following discussion describes an alternate derivation of the same fragility descriptions, more rigorous from a statistical point of view.

In estimating a median threshold acceleration ("capacity") of a given device from experimentally measured fragility data, the original analysis used only the applied acceleration values at which chatter was observed. Using the data from all runs, thus combining results over different units, cabinet mounting configurations and input accelerations (runs), the applied accelerations are ordered, i.e., ZPA_1, ZPA_2, ... ZPA_N, assuming chatter is observed.* For the most part, the original analysis ignores information derived from runs in which no chatter was observed (i.e., for applied accelerations less than threshold values), except in those instances where chatter was observed at an acceleration lower than one at which chatter was not observed. In such cases, the average of the two applied accelerations was used as the threshold acceleration. The ZPAs are treated as a random sample from a lognormal distribution. Using the ordered values of ZPA_m and the associated estimated quantiles $m/(N+1)$, the parameters (μ,σ) of the log-normal distribution can be estimated using least-squares based on the model

$$\ln ZPA_m = \mu + \sigma Z_m + E_m \qquad (5\text{-}1)$$

where Z_m is the standard normal "m"th quantile and E_m represents the experimental variation. Note that this is equivalent to the "probability paper" analysis in Figs. 5-1 through 5-7, from which estimates of the following parameters are derived:

$e^{\mu} = \breve{A}$ median threshold acceleration ("median capacity")

$\sigma = \beta_U$ modeling uncertainty

---

* in this discussion, the term "unit" refers to a device of a given type, manufacturer and model (e.g., a Westinghouse Type AR relay)

β_R random uncertainty based on the variation of the data about the modeled straight line in Eqn. (5-1), i.e., the variation in the values of E_m

Although convenient to apply for "engineering" purposes, the original analysis is less than optimum because it:

- only uses a subset of the data, i.e., only those runs during which chatter occurred, except as previously discussed.

- artificially assumes the measured acceleration is itself the threshold acceleration. In reality, the measured acceleration associated with device chatter is an upper bound on the "actual" threshold acceleration.

- artificially defines as the threshold acceleration the average of the measured "chatter" and "no chatter" accelerations in those instances where the latter exceeds the former.

- improperly models the sources of variation. The original estimate of modeling uncertainty β_U includes unit, mounting, and run variability; it can be argued on conceptual grounds, however, that only the former two should be treated as modeling uncertainty. As a result, β_U is artificially high. The estimated random uncertainty β_R derived from the least-squares analysis is based solely on the difference between "chatter" acceleration and "no chatter" acceleration when the latter exceeds the former. By not including run variability, this estimate of random uncertainty is artificially low.

Alternate Analysis Method

The following discussion describes an alternate, more rigorous method of developing probabilistic fragility descriptions from the experimental data.

As the original analysis did, the alternate method assumes that device response is linear so that device failure ("capacity") can be correlated with the threshold acceleration at which chatter occurs.

For any given unit, the fragility reference parameter (i.e., the measured experimental data) is taken as local excitation, characterized by local ZPA at the support points of the device. These acceleration values represent the in-cabinet structural response to the fixed excitations applied to the base of the MCC cabinet. Associated with each applied acceleration level is an observation as to whether device chatter does or does not occur. Given an applied acceleration, the occurrence of chatter implies that the device threshold acceleration ("capacity") is less than or equal to the measured acceleration. Conversely, if chatter does not occur, the implication is that device capacity exceeds the measured acceleration. Thus, if we assume that the acceleration at which a device will fail is a random variable, (due, for example, to "unit" variations among identical devices) there is for each experimental run and applied acceleration a_0 a probability

$$\begin{aligned} &P(A \leq a_0), \text{ if chatter occurs, or} \\ &P(A \geq a_0), \text{ if chatter does not occur} \end{aligned} \tag{5-2}$$

where A denotes the device capacity (threshold acceleration). In this case, random uncertainty is presumed to result from variability in the structure (e.g., local non-linear response), in the applied acceleration (e.g., frequency content), and in the response of the device to that acceleration.

The alternate analysis, like the original analysis, models this probability as a log-normal distribution. However, the alternate analysis uses all the data for a given unit-by-cabinet-mounting combination in which chatter occurs on at least one run, not just the runs in which chatter occurs. The alternate analysis comprises two steps:

Step 1. For each unit-by-cabinet-mounting for which chatter occurs during at least one run (e.g., data for the Westinghouse relay was available for two units and four cabinet mounting configurations; for six of the eight combinations chatter occurred on at least one run) the observed data ($a_{o,k}$, x_k; k = 1,...K), where $a_{o,k}$ is the applied acceleration (i.e., local ZPA) and x_k= 1 if chatter occurs and x_k= 0 if chatter does not occur, are used to estimate the parameters (μ,σ) of the log-normal distribution using the maximum likelihood estimation (MLE) method. However, estimation of τ is restricted to those combinations in which chatter occurs during at least one run at a lower applied acceleration than when it does not occur. Note that this condition is equivalent to the overlap of "chatter" spectra and "no chatter" spectra previously discussed in Section 4 (see Figs. 4-14 through 4-29).

Step 2. The estimated (log) means $\{ \mu_{ij} ; i=1,...n_u, j=1,...n_m\}$ for the "i"th unit and the "j"th cabinet mounting configuration are modeled as

$$\mu_{ij} = \mu + A_i + B_j + E_{ij} \qquad (5\text{-}3)$$

where:

μ = overall (log) mean threshold acceleration

A_i = deviation (from μ) of "i"th unit mean threshold acceleration, $N(0,\sigma_\alpha^2)$

B_j = deviation (from μ) of threshold acceleration for the "j"th cabinet mounting configuration, $N(0,\sigma_\beta^2)$

E_{ij} = uncertainty in estimates μ, ~ $N(0,\sigma_E^2)$

Because the values of μ_{ij} are correlated, MLE is used to estimate μ and the measures of variability σ_α, σ_β, and σ_E. The final outputs are then estimates of the following parameters:

μ = the (log) mean of threshold acceleration (capacity)

σ = the (log) standard deviation due to random variation from run-to-run

τ_α = the (log) unit-to-unit variability in the mean threshold acceleration

σ_β = the (log) variability in the mean threshold acceleration due to differences in cabinet mounting configuration

σ_E = the (log) uncertainty due to estimation

The estimates of uncertainty can be combined as appropriate to estimate the random and modeling uncertainty in estimating fragility. For example, one approach holds that a given unit mounted in a cabinet has a deterministic threshold acceleration. The fact that it is unknown and will vary among units and mounting configurations is modeling uncertainty. Under this interpretation, random variation reflects the variation in unit response over different inputs (e.g., earthquakes) with a given applied acceleration. Thus, using the prior notation,

$$\beta_U = (\sigma_\alpha^2 + \sigma_\beta^2 + \sigma_E^2)^{1/2}$$

$$\beta_R = \tau \qquad (5\text{-}4)$$

Application to Experimental Data

To illustrate this methodology, the data for the Westinghouse Type AR relays was used to reestimate the median threshold acceleration (capacity) and

the parameters β_U and β_R in the fragility description. In the Step 1 analysis, Unit 1 (Location 2B/10) for the third mounting configuration (Runs 43 through 46) and Unit 2 (Location 2J/15) for the first mounting configuration (Runs 13 through 17) were used to estimate σ. The pooled estimate was $\tau = 0.203$. The remaining "Unit x" mounting combinations with usable data resulted in the following estimates of the (log) means:

(i,j)	$\mu_{i,j}$
1,1	1.661
1,2	1.712
1,3	1.704
2,1	1.693
2,2	1.826
2,3	1.913

Using these estimates in the Step 2 analysis, the resultant estimates of variability are:

$$\mu = 1.783$$

$$\sigma_\alpha = 0.091$$

$$\sigma_\beta = 0.023$$

$$\sigma_E = 0.025$$

Using the philosophy stated above, which motivated the original analysis, the final estimates of median threshold acceleration, random variation and modeling uncertainty are (compared with the equivalent estimates):

Parameter	Revised Analysis	Original Analysis
Median = $e^{\mu} = \check{A}$	5.95	6.10
β_R	0.203	0.08
β_U	0.097	0.13
A_{HCLPF}	4.10	4.74

where the high-confidence, low-probability-of-failure ("HCLPF") capacity is given by:

$$A_{HCLPF} = A \exp [-1.65 (\beta_R^2 + \beta_U^2)^{1/2}] \quad (5\text{-}5)$$

rather than by Eqn. 1-1 from Section 1 of this report. Note that the median threshold acceleration ("median capacity") yielded by the alternate analysis is within three percent of that derived in the original analysis. Note also that the increased random uncertainty estimated in the alternate analysis "flattens" the fragility curves, which in turn reduces the HCLPF capacity by about 14 percent.

Discussion of Results

The original estimate of random variability β_R is approximated on the basis of the difference between the acceleration values at which chatter occurred and at which it did not occur, when the former is less than the latter. Since these values are upper and lower bounds, respectively, for the actual threshold acceleration, the original estimate of β_R is too low. On the other hand, the original estimate of β_U includes the variation between units, cabinet mounting configurations, and runs. Since only the first two

sources of variation contribute to modeling uncertainty (based on the original concept of uncertainties), the original estimate of β_U is biased high. The estimates of β_R and β_U yielded by the alternate analysis more appropriately model the different sources of variation in the median threshold acceleration. In other words,

- $\beta_R = \tau$ is estimated by more appropriately modeling the variation in applied accelerations at which chatter is observed.
- $\beta_U = (\sigma_\alpha^2 + \sigma_\beta^2 + \sigma_E^2)^{1/2}$ more appropriately accounts for the sources of variation considered to be modeling uncertainty, i.e., variation in the median threshold acceleration among units and cabinet mounting configurations.

Furthermore, the alternate analysis uses all the data (which contains information about unit failure and non-failure), and properly treats the measured data as upper and lower bounds on the threshold acceleration rather than as itself an artificial threshold acceleration as was done in the original analysis.

One disadvantage of the alternate method is that it requires at least one instance in which a "no chatter" acceleration exceeds a "chatter" acceleration. This condition must exist to estimate β_R for at least one (and preferably more) "Unit x" mounting configurations. As a result, more experimental data may be required as compared to the original method. This condition may not be necessary for the original analysis but its absence may still make it more difficult to estimate β_R even using the simpler method.

From a statistical analysis viewpoint, however, the alternate method of deriving the fragility descriptions is preferable to the original analysis even with these limitations.

Table 5-1. Fragility parameters for relays and motor starters.

Devices	Median Local ZPA	β_R	β_U	HCLPF
Relays				
Westinghouse Type AR	6.1	.08	.13	4.3
Square-D Type X	5.2	.10	.20	3.2
G-E Type CR	5.5	.08	.23	3.3
All Relays*	5.6	.07	.19	3.6
Starters (aux contacts only)				
Size 2 FVNR	3.9	.08	.25	2.3
Size 2 FVR	3.9	.06	.21	2.5
Size 3 FVNR+	6.5	n/a	.32	n/a
All Size 2*	3.9	.06	.21	2.5

Notes:

* all relays for which frequency descriptions were developed.

\+ only three data points available to define fragility parameter. β_R not estimated due to sparse data.

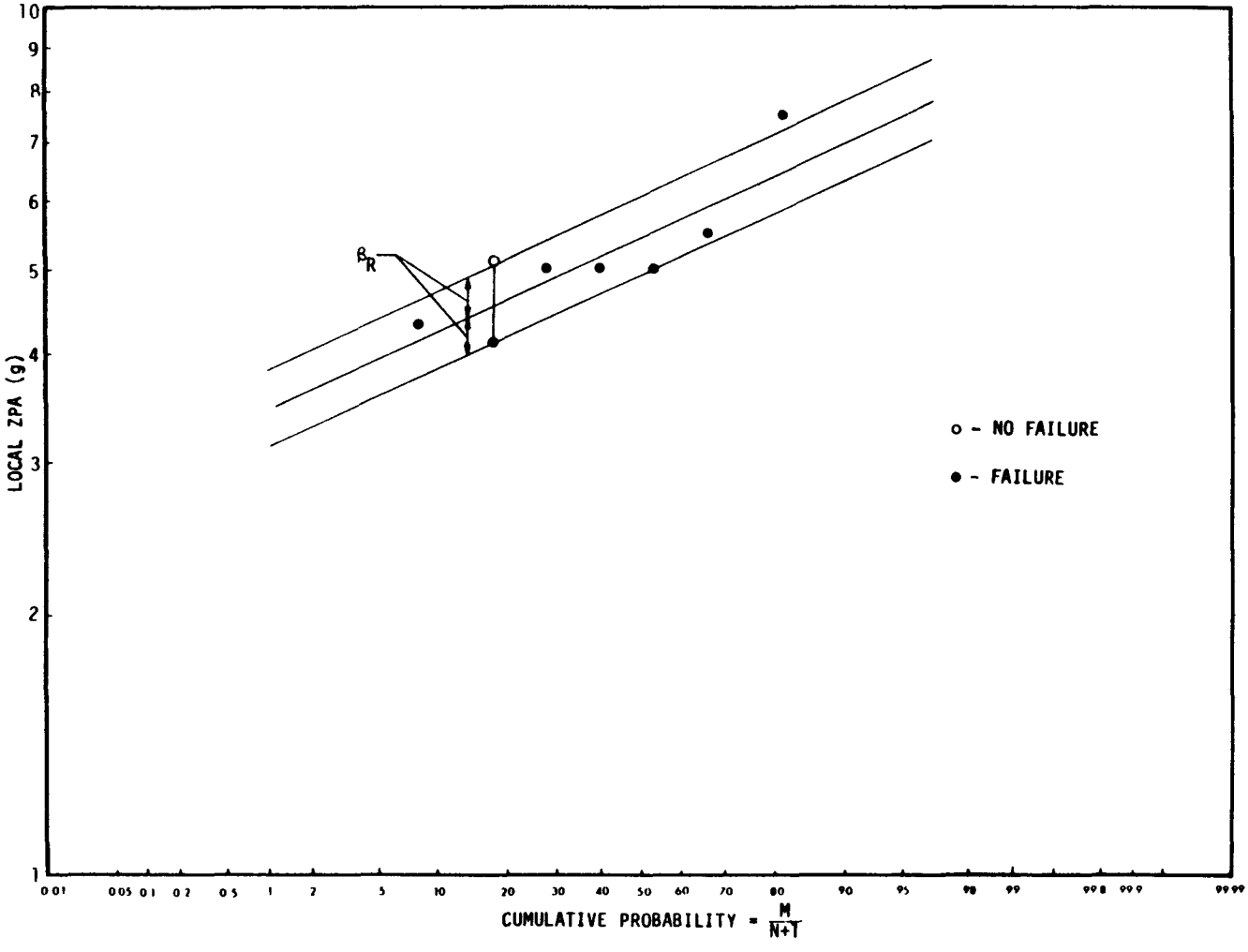

Fig. 5-1. Development of failure probabilities for Square-D Type X relays.

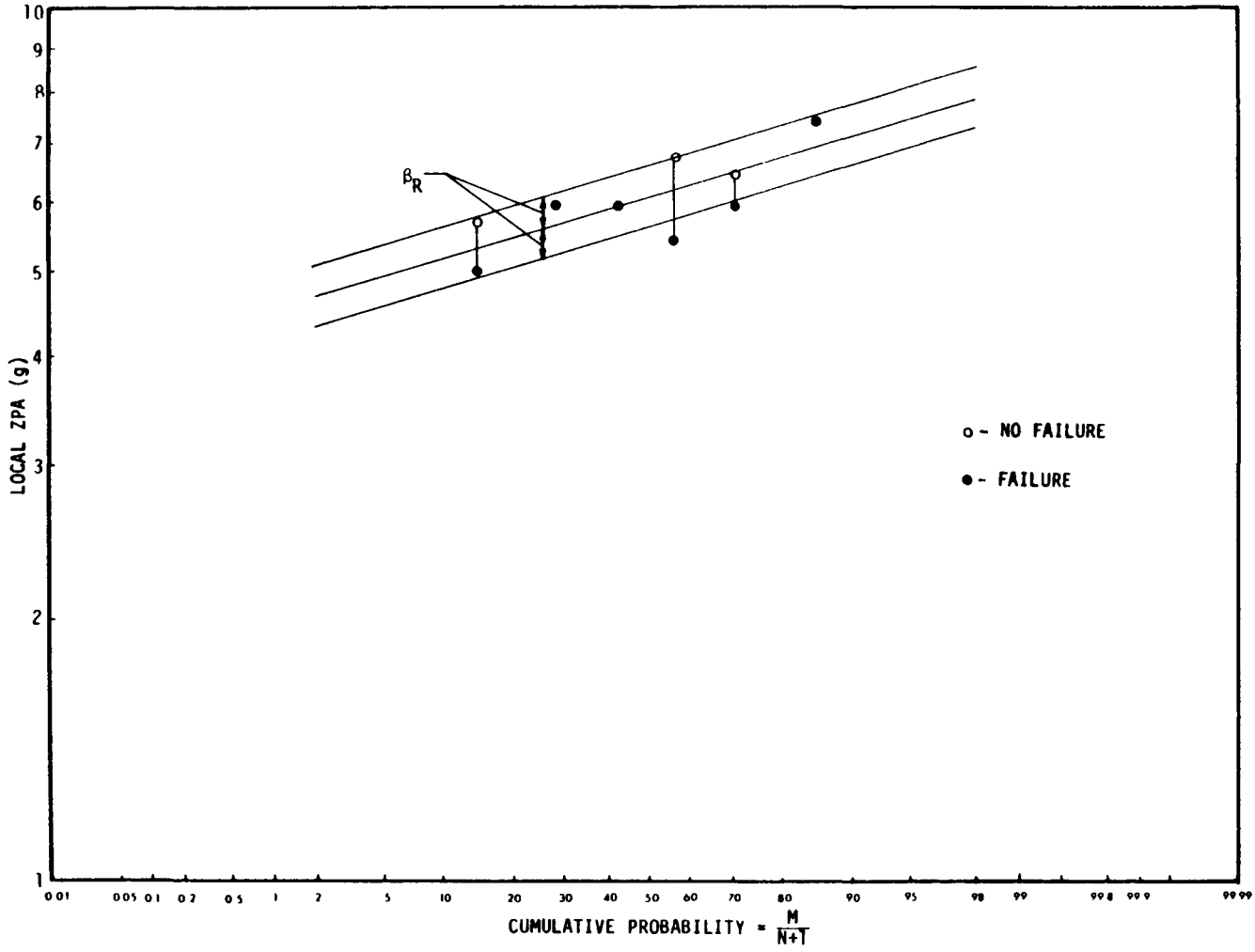

Fig. 5-2. Development of failure probabilities for Westinghouse Type AR relays.

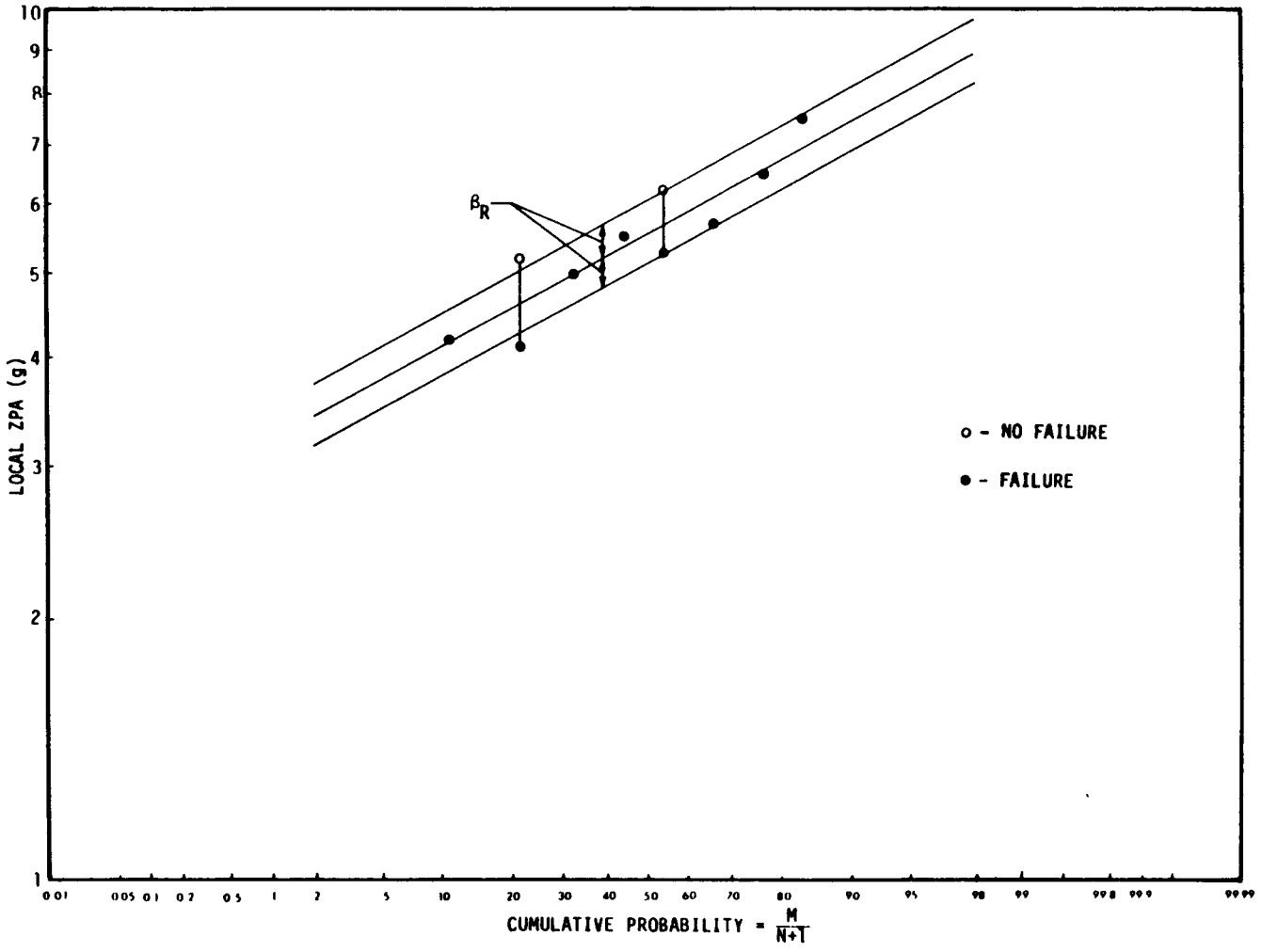

Fig. 5-3. Development of failure probabilities for General Electric Type CR relays.

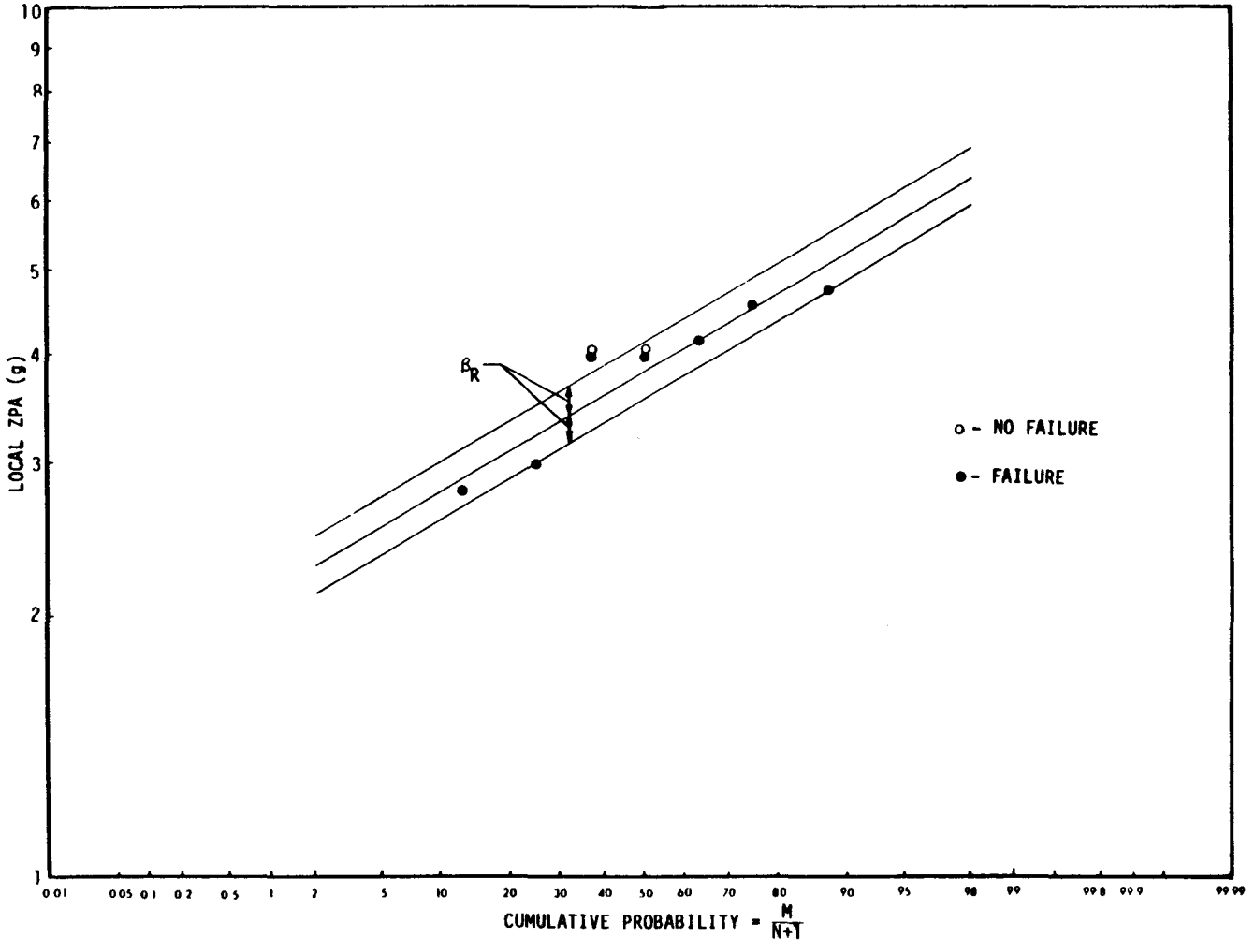

Fig. 5-4. Development of failure probabilities for Size 2 FVNR starters.

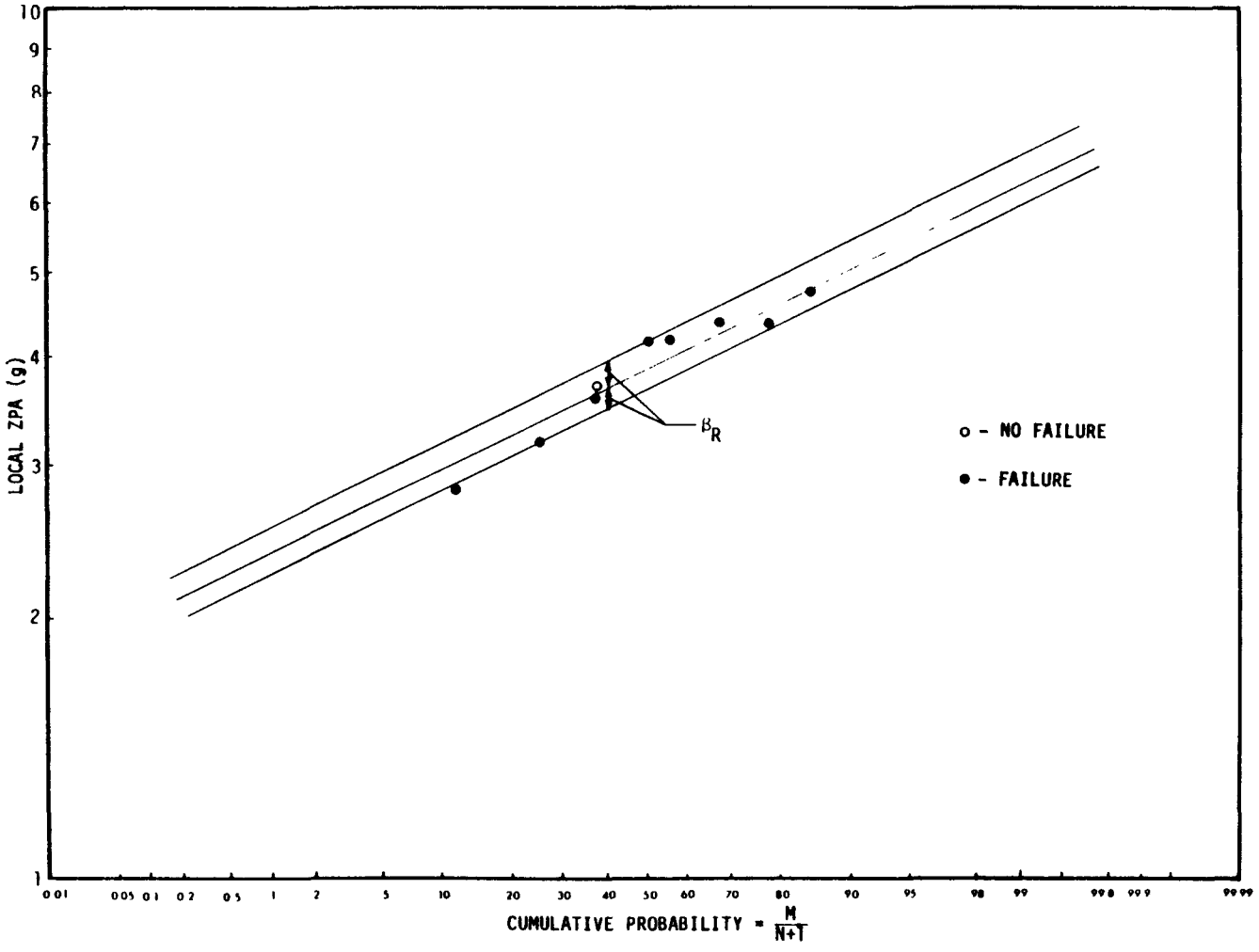

Fig. 5-5. Development of failure probabilities for Size 2 FVR starters.

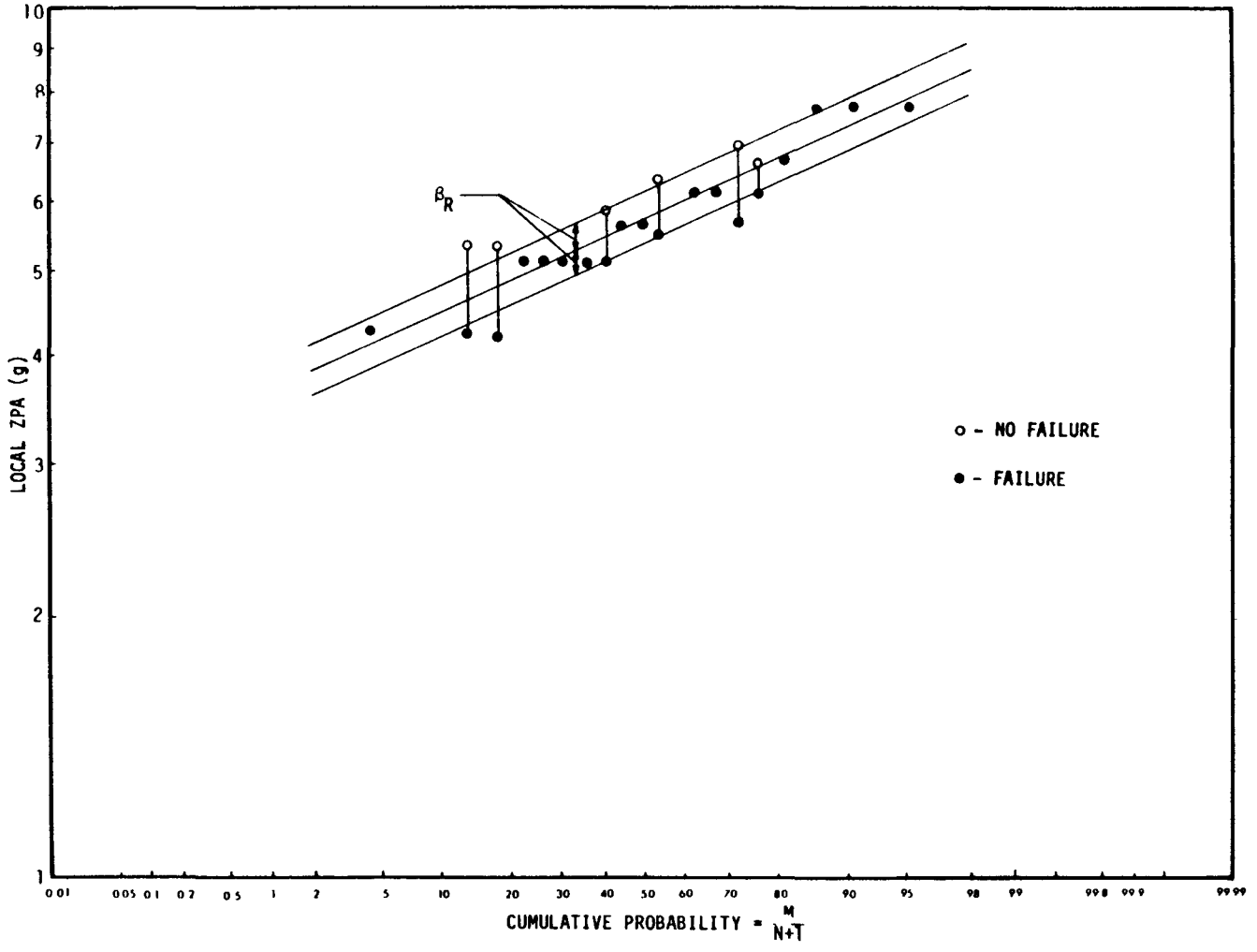

Fig. 5-6. Development of failure probabilities for all relays considered.

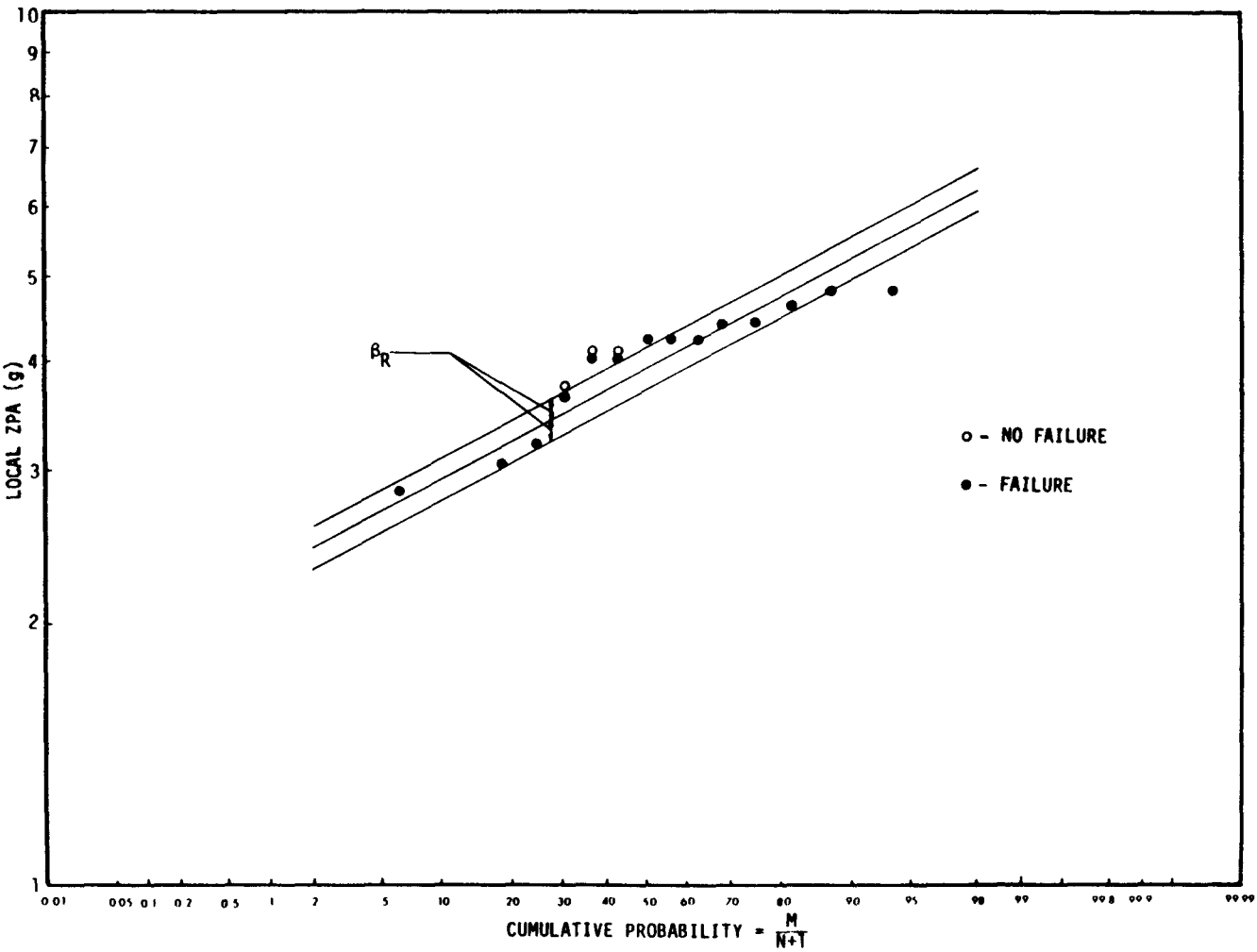

Fig. 5-7. Development of failure probabilities for Size 2 FVR and FVNR starters.

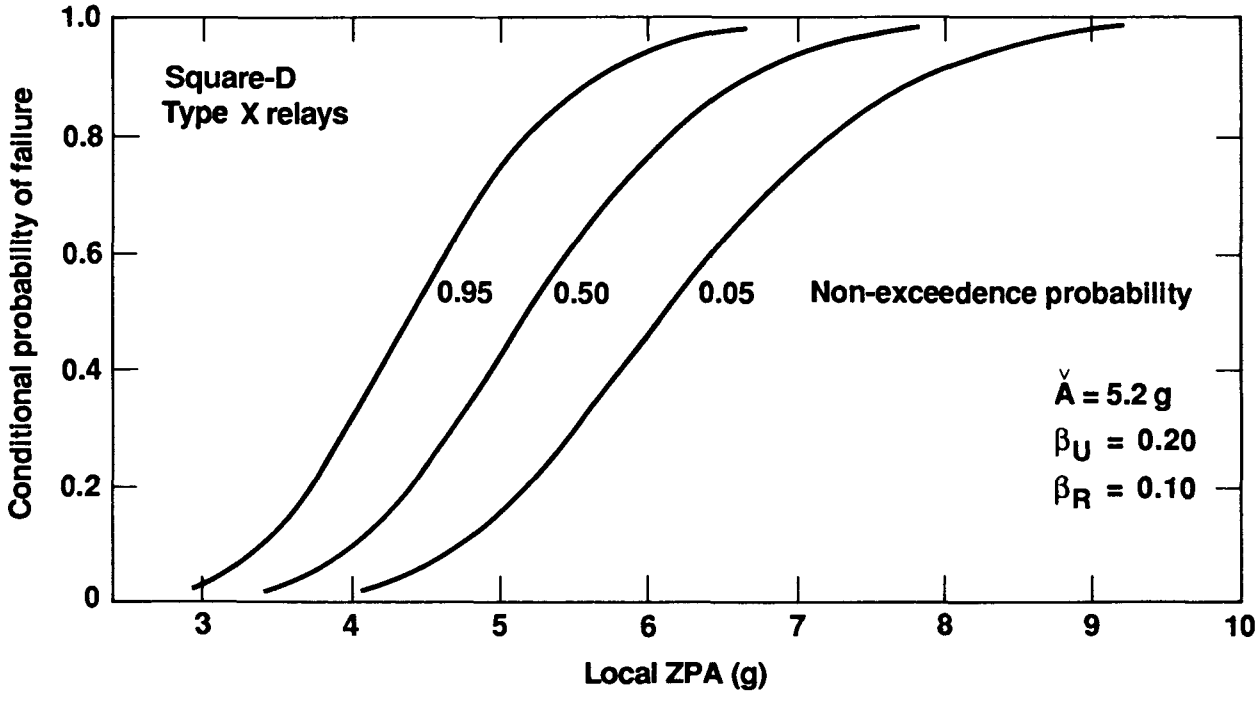

Fig. 5-8. Fragility curves for Square-D Type X relays.

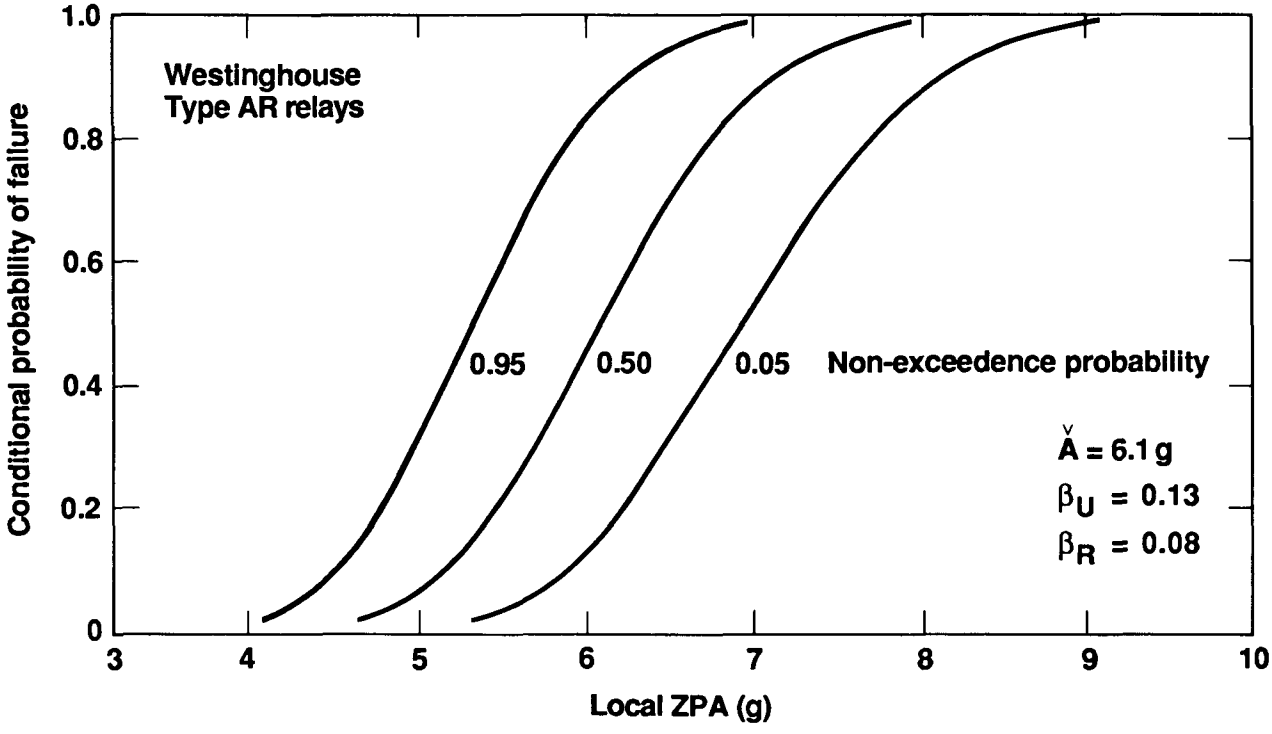

Fig. 5-9. Fragility curves for Westinghouse Type AR relays.

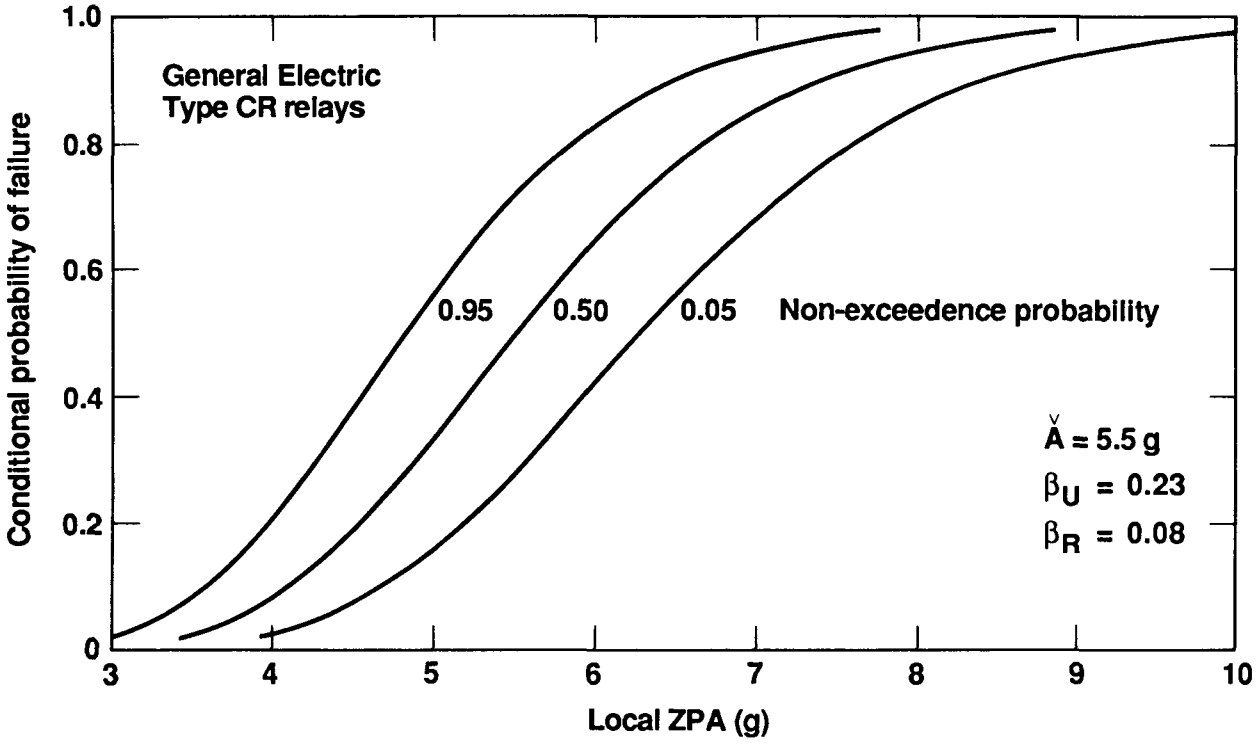

Fig. 5-10. Fragility curves for General Electric Type CR relays.

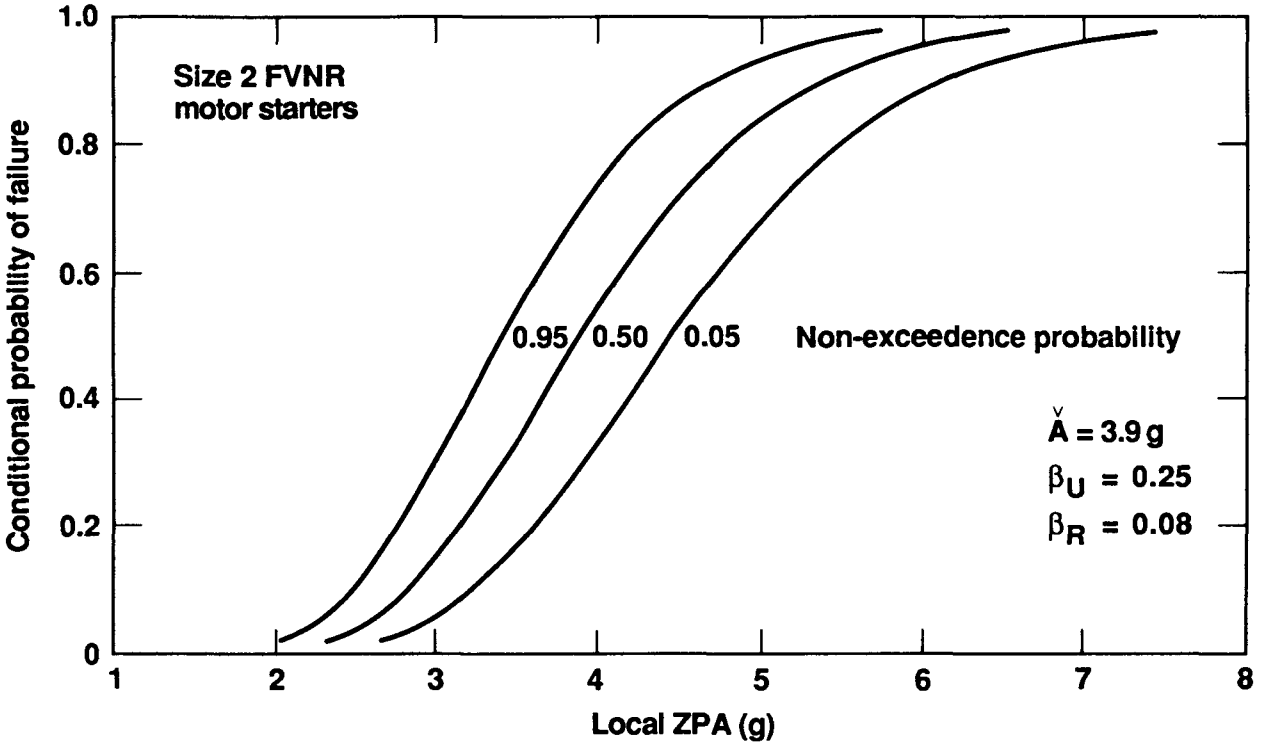

Fig. 5-11. Fragility curves for Size 2 FVNR motor starters.

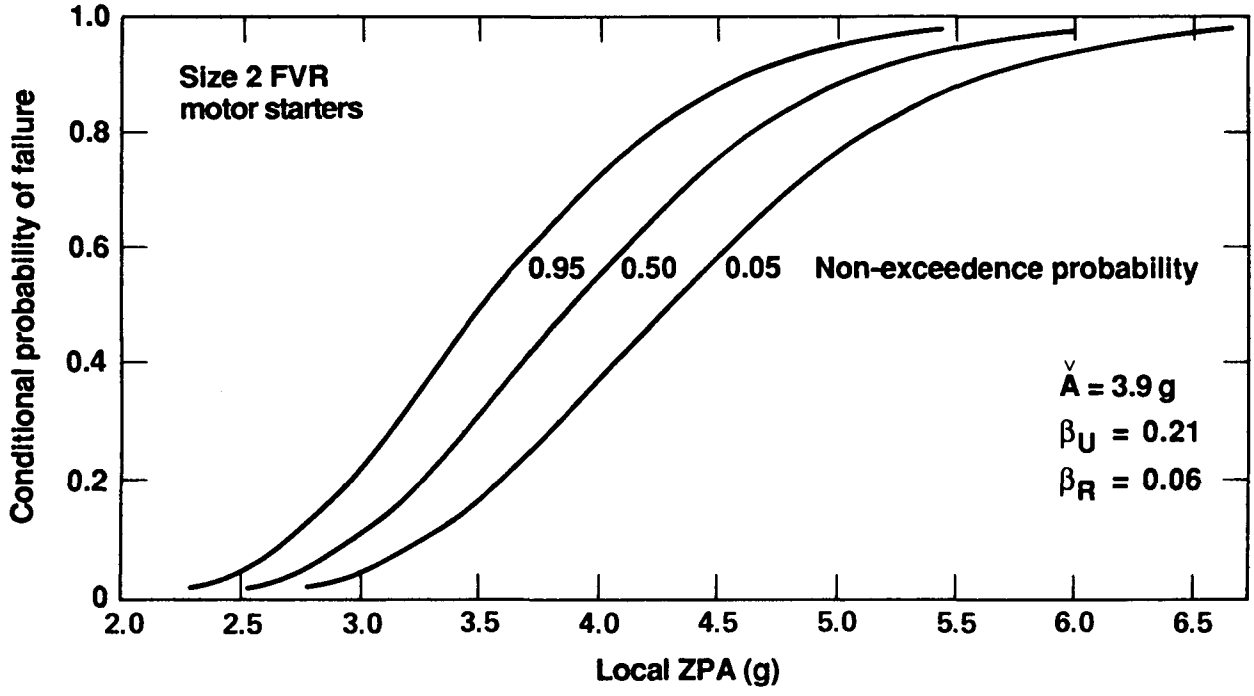

Fig. 5-12. Fragility curves for Size 2 FVR motor starters.

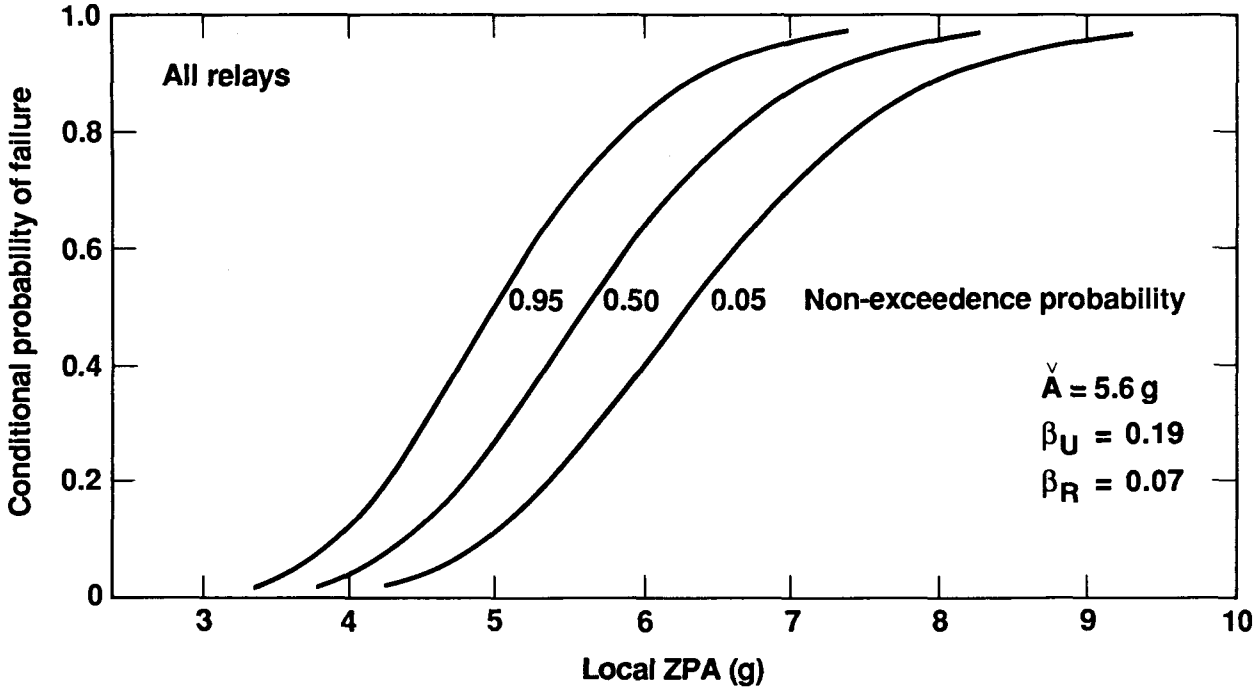

Fig. 5-13. Fragility curves for all relays considered.

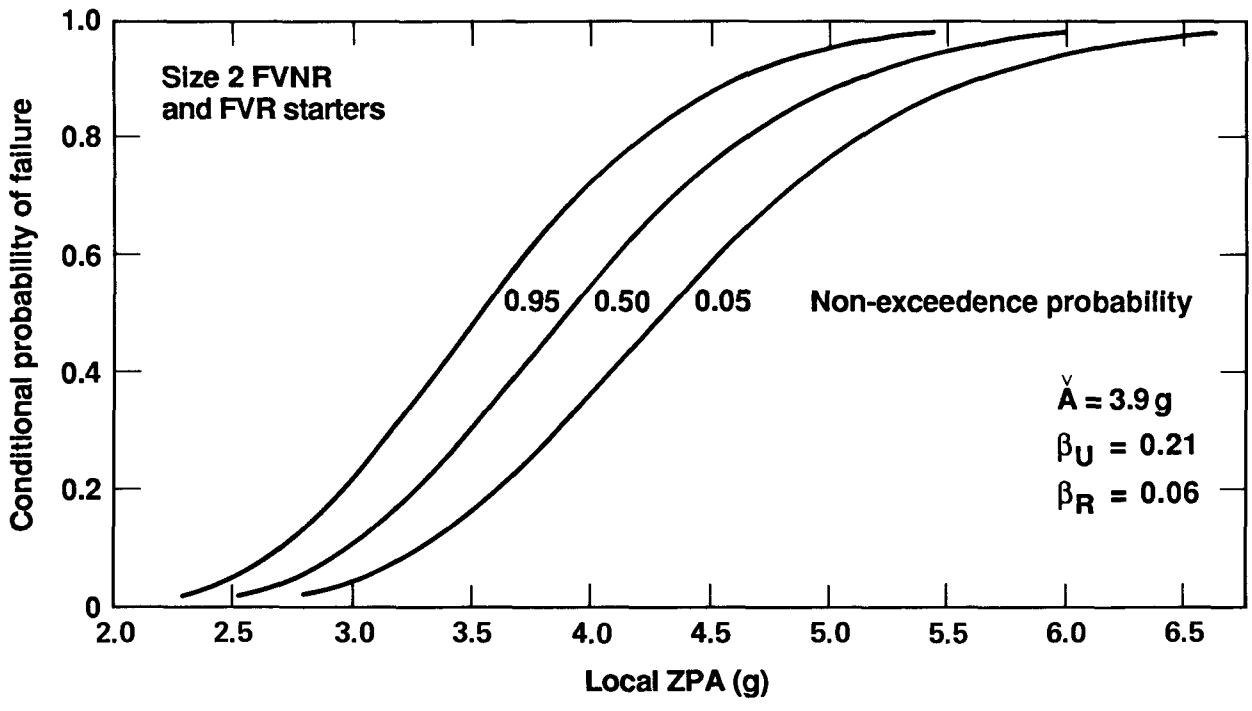

Fig. 5-14. Fragility curves for Size 2 FVNR and FVR motor starters.

6. SUMMARY AND CONCLUSIONS

6.1 Discussion of Results

As part of the Phase I Component Fragility Research Program, we completed demonstration fragility tests on a three-column Westinghouse Five-Star motor control center containing 8 Westinghouse motor controllers of various types and sizes as well as 14 relays of different types and manufacturers. The Five-Star is the current basic model marketed by Westinghouse for industrial and power system applications; it is essentially identical to the Type W motor control center manufactured by Westinghouse from 1965 to 1975, various configurations of which are found in many nuclear power plants of this vintage. The particular electrical devices selected represent a sample of standard MCC devices typical in function of those found in actual plants; however, we do not represent that these are necessarily generic for all similar devices.

To investigate the effect of base flexibility on the structural behavior of the MCC and on the functional behavior of the electrical devices, we conducted multiple tests on each of the following four mounting configurations:

- four bolts per column with top bracing
- four bolts per column with no top bracing
- four bolts per column with internal diagonal bracing
- two bolts per column with no top or internal bracing

We performed a total of 56 test runs, including 43 biaxial tests (vertical plus one horizontal axis) using random motion input. Table input motions in the random motion tests ranged up to 2.5g zero period acceleration (ZPA), which yielded in-cabinet spectral accelerations up to 20g and higher at the device locations.

In these tests we investigated both the functional behavior of the individual electrical devices -- relays and starters -- and the structural

response of the MCC cabinet for various levels of table input motion and for four different cabinet mounting configurations. Device "fragility" was characterized by contact chatter correlated to local in-cabinet response measured at the device location, with functional "failure" being defined as the first sign of chatter. Among the topics investigated were (1) the relative susceptibility of normally-open and normally-closed contacts to chatter, (2) the chatter susceptibility of energized vs deenergized contacts, and (3) the ability of the devices to respond to commanded changes of state during strong seismic excitation. The following discussion summarizes the key results of our Phase I demonstration test program.

Functional Behavior

The more significant observations made regarding device functional behavior include the following:

- all 14 relays and all 8 starters responded normally to commanded changes of state for all input levels and MCC support configurations. This held true for each device regardless of whether it was initially energized or deenergized. Only in one case did a device not respond to a commanded state change; this was attributed to technician error.

- for all devices, chatter occurred only when the device contacts were in their deenergized state. Without exception, no chatter of energized contacts was recorded.

- for all devices, virtually all chatter occurred when the MCC was tested in its front-to-back orientation. Only isolated instances of contact chatter were recorded when the MCC was tested in its side-to-side orientation; these were attributed to possible variations in local in-cabinet waveforms.

Given the mounting orientation of most devices in the cabinet (i.e., direction of contact motion oriented with the F-B axis of the cabinet), these results imply that chatter is most likely to occur when the input motion is oriented with the direction of contact action. Virtually no chatter was observed when the input motion was oriented perpendicular to the direction of contact action.

- for starters, virtually all chatter occurred in auxiliary contacts. Only isolated occurrences of spurious main contact action were recorded, most of which could be attributed to contact "bounce" during a commanded state change.

- for all devices, normally-closed contacts consistently chattered at lower input levels and more often than normally-open contacts. This suggests for these devices that contact chatter is caused by armature movement rather than local response of the contact element. Note also that the greater resistance of NO contacts to chatter has added significance in a safety sense because these (rather than the more sensitive NC contacts) are more commonly used in seal-in circuit design.

- neither reed-type relay was observed to chatter, regardless of input level or MCC mounting configuration. This observation was not surprising considering the extremely low contact mass of the reed-type relays compared to that of the armature-type relays tested.

- the occurrence of chatter appears to correlate only weakly with local in-cabinet ZPA. The significant overlap in "chatter" and "no chatter" in-cabinet response spectra implies that spectral acceleration may be a more appropriate parameter to define the "threshold" above which chatter occurs.

- the results of single-axis, single-frequency tests performed on one Size 2 starter and one relay removed from the MCC indicate that chatter is

most likely to occur for input motions in the 2.5 to 8 Hz range. This result further supports the conclusion that spectral acceleration, rather than ZPA, is a more appropriate basis for characterizing device fragility.

We applied these experimental results to develop "single-parameter" probabilistic fragility descriptions for each type of electrical device in the MCC. We defined as the relevant "failure" mode the first sign of chatter in normally closed contacts in their deenergized state, and based device fragility on local horizontal ZPA at the device location. In addition to developing "best estimate" descriptions of device fragility, we estimated the random variability and modeling uncertainty to arrive at a "high confidence, low probability of failure" (HCLPF) capacity for each type of device. Our fragility estimates can be summarized as follows:

- for those relays for which fragility descriptions were developed (Square-D Type X, Westinghouse Type AR, GE Type CR), the median capacity ("best estimate" curve, 50 percent failure probability) ranged from 5.2g to 6.1g local ZPA with HCLPF values ranging from 3.2g to 4.3g local ZPA. When considered as a single group, these relays have a median estimated capacity of 5.6g and a HCLPF of 3.6g. Keep in mind these are local in-cabinet levels, not the motion at the cabinet base, and that input motion is oriented in the direction of contact action. Assuming an amplification factor of three (typical of industry practice), the HCLPF base motion would be about 1.2g ZPA.

  No fragility description was developed for the Cutler-Hammer Powerreed relay because no chatter was observed. Insufficient data was available from which to develop a fragility description for the two Square-D Type KP relays, the only relays that were mounted with their direction of contact action oriented vertically.

- the Size 2 reversing and non-reversing starters have median capacities of 3.9g and HCLPF capacities of 2.5g and 2.3g, respectively. Note that these results reflect auxiliary contact chatter; for all practical purposes, no chatter of main contacts was observed. When all Size 2 starters are taken as a single group, the median and HCLPF capacities are 3.9g and 2.5g, respectively. This result is not surprising when it is considered that reversing and non-reversing starters differ only in the number of contact sets used (two vs one); the contact sets themselves are identical.

- for the two Size 3 starters tested, the median capacity was 6.5g local ZPA. The markedly different capacity compared to that of the Size 2 starters most likely results from the substantial difference in starter size. Note however that only three data points were available from which to estimate the fragility parameters, and that the data were too sparse to estimate random variability. As a result, a HCLPF capacity could not be defined. It seems reasonable to expect, however, that the HCLPF capacity for the Size 3 starters (and, based on the limited data, for Size 4 starters as well) would be at least as high as that for the Size 2 starters.

Note that these results assume that input motion is oriented with the direction of contact motion. As discussed in Section 4, the results of our tests indicated that virtually no chatter occurs when the direction of input motion is perpendicular to that of contact motion.

As noted earlier, the results of our tests -- the random motion tests on the MCC as well as sinusoidal tests on two devices removed from the cabinet -- imply that local spectral acceleration is a more appropriate parameter for describing device fragility than local ZPA. Fragility descriptions incorporating frequency effects would, however, be less "generic" than those developed in this study, and would be more complex to apply in a PRA due to increased information requirements. Frequency issues notwithstanding, the results of this study do demonstrate how test data can be used to develop practical fragilities for PRA applications.

Structural Behavior

During these tests we also observed the structural behavior of the MCC cabinet for various levels of table input motion and for the different mounting configurations. The more significant observations regarding structural behavior of the MCC cabinet include the following:

- in general, two distinct response modes can be identified for the MCC cabinet. The first of these, which we refer to as the "frame" response, reflects global motion of the MCC structure. Results of low-level (0.2g) transmissibility tests indicated that the cabinet frame resonance lies between about 3.5Hz and 12Hz, depending on cabinet mounting configuration. The second mode, typically lying between about 14 Hz and 26 Hz, reflects the local response of the individual draw-out units (or "buckets") which house the relays and starters. We refer to this as the "bucket" response; the resonant frequency measured for each draw-out unit is referred to as its "bucket" resonance.

- as discussed in Section 1, our demonstration tests focused on low-frequency input motions, i.e., less than 9 Hz. We found that with the brace at the top of the MCC, the resonant frequency of the cabinet frame was about 12 Hz, well above this level. Removing the top brace caused the F-B resonant frequency to drop to about 5 Hz. Reducing from four to two the number of mounting bolts per column further reduced the frame frequency to about 3.5 Hz.

  The effect of mounting configuration on cabinet response takes on added significance when the results of the single-axis single-frequency device tests are considered. The one relay and one starter tested both indicated highest sensitivity to input motions in the 2.5 to 8 Hz range. Consequently, the lower-frequency "frame" resonances will affect device performance more than high-frequency local "rattling" of the cabinet structure. Removing the top brace from the MCC lowered the F-B frame frequency (i.e., in the direction of contact action for most

devices in the MCC) from well outside this range to a point where it could conceivably have a significant effect on device behavior. Note that top bracing also shifts the "frame" response of the cabinet from a cantilever mode to a "bowing" mode, increasing (in a relative sense) cabinet response at the mid-place elevations. At the same time, it tends to increase local responses at the "bucket" frequencies of the individual draw-out units. This implies that top bracing of the cabinet might have a negative effect for MCC internal devices sensitive to high-frequency input motions such as compartment rattling or banging of compartment doors.

- the predominant "bucket" resonances lie well outside the "sensitive" range indicated by the sinusoidal tests. An attempt to raise the resonant frequencies of three compartments (2B, 2E, and 2J) by adding mounting screws was not successful, although testing by others of similar cabinets has indicated that sufficient bracing can reduce or eliminate high-frequency response caused by compartment rattling. In any case, input motion in this frequency range does not appear to significantly affect the functional behavior of the devices tested.

- based on local in-cabinet ZPA levels, the cabinet amplifies base motion by a maximum factor of about 2 to 4 over all input ZPA levels and all mounting configurations considered.

- we observed no cabinet damage when the MCC was braced at the top. Testing of the free-standing MCC in the side-to-side direction similarly caused no indication of structural damage until late in the testing program. Substantial physical damage was first noted after Run 29 (1.9g table ZPA) in the form of cracked welds between the base frame and the vertical frame members; by this run the MCC had been subjected to 20 prior strong motion tests. After being rewelded, the corner welds withstood tests in the S-S and F-B directions up to 2.3g table ZPA.

From Run 48 onwards, the base welds in the cabinet broke with relative regularity. We believe this reflects test-induced fatigue rather than any inherent weakness in the cabinet; note that prior to Run 48 the MCC had already experienced 35 strong motion tests.

Although substantial damage was observed in later tests, the cabinet nevertheless withstood some 20 strong motion tests at ZPA levels up to 1.9g before any significant damage was observed; by comparison, the highest horizontal floor response predicted for any MCC at Diablo Canyon (0.75g PGA safe shutdown earthquake) is 1.2g ZPA. Furthermore, at no time did the physical damage sustained by the cabinet impair its safety function, i.e., providing adequate support for the MCC internals. Based on the guidelines discussed in Section 1.4, our test results imply that even the free-standing MCC cabinet very nearly fits our definition of a "high capacity" component. The results further imply that significant gains in seismic capacity (measured in terms of input motion at the cabinet base) can be gained -- both structurally for the cabinet and functionally for the electrical devices -- through top bracing of the MCC cabinet.

Strictly speaking, the preceding observations -- and by inference, and conclusions drawn from them -- apply only to the specific motor control center tested and may therefore be limited in their broader applicability; we do not represent that the results discussed here are necessarily "generic" for all motor control centers, or for all relays and starters. Developing generic fragility descriptions for broad classes of components was outside the scope of our Phase I test program. However, it is reasonable to expect that the general trends indicated might apply to other components (particularly motor control centers and their internals) sharing "commonality" of form and function (as opposed to strict statistical "similarity" in a Buckingham-Pi sense) with the equipment tested.

With these caveats noted, the following general conclusions are suggested by the results of this study:

- contact "chatter" appears to be influenced more by spectral acceleration than by ZPA, although the likelihood of chatter will, on the whole, increase with ZPA. Device fragilities based on spectral accelerations should in principle be "more appropriate" but at the same time would be more difficult to use in PRA applications.

- chatter appears to be influenced by low-frequency input motion (i.e., less than 9 Hz) than by high-frequency motion. Consequently, frame response will affect device performance more than local effects such as "rattling" of the cabinet structure or banging of compartment doors.

- reed-type relays appear to be more resistant to seismic motion than armature-type relays.

- top bracing of the motor control center can increase the seismic capacity of both the MCC structure (by limiting cabinet motion) and the internal electrical devices (by increasing the resonant frequency of the cabinet frame).

6.2 Recommendations for Further Research

Given the apparent importance of in-cabinet spectral accelerations on device behavior, the structural behavior of the cabinet takes on added significance. In particular, it would be useful -- and in fact necessary, if fragilities were based on spectral acceleration -- to know how cabinet transmissibility varies with mounting configuration and with level of input motion at the cabinet base. Our Phase I test program included low-level resonance search tests for each cabinet mounting configuration, the results of which were used to generate transmissibility at various locations in the cabinet. Further insight into cabinet behavior could be gained through extended analysis of the available raw data, particularly development of more local spectra as well as cabinet transmissibility (e.g., transfer functions, local power spectral densities) for strong random motion input.

Fragility descriptions anchored to spectral acceleration would also require additional single-frequency single-axis ("sinusoidal") tests on individual devices to characterize their frequency-dependent functional behavior. These tests would be equivalent to those already performed in the Phase I program for two devices -- a Size 2 starter and a Square-D Type X relay -- removed from the motor control center.

Based on these considerations, the following discussion describes additional testing and data analysis that would allow us to develop frequency-dependent fragility descriptions for the devices in our Phase I tests.

Functional Behavior

In order to fully characterize the dependence of device fragility on input motion frequency content, we recommend that all starters and relays be removed from the MCC and subjected individually or in groups to the following additional tests:

- single-axis, single-frequency tests to develop frequency-dependent chatter spectra ("fragility levels") for all starters and relays as was done for the one Size 2 FVNR starter and the one Square-D Type X relay. Group starters according to size, relays according to type and manufacturer.

- for each group of devices above, use random motion input to synthesize the shape of the frequency-dependent fragility level derived from the results of the sinusoidal tests. Increase input level until chatter is observed. Compare the resultant test response spectrum against the fragility level derived from the results of the single-axis, single-frequency tests.

The latter series of tests would compare device fragilities developed from sinusoidal vs random motion input. As discussed in Section 5, a fragility test program similar to ours found that when devices such as relays were

subjected to multi-mode, multi-axis input, chatter occurred at input motion levels as low as 40 percent of those required to achieve the single-axis, single-frequency response spectra.

It would also be useful during such tests to wire the starter circuits such that the main contact coils are energized through the auxiliary contacts, i.e., as is done in actual seal-in circuit design. This would allow us to determine the amount of auxiliary contact chatter (i.e., number and duration of chatter events) necessary to cause the main contacts to inadvertently change state. Recall that this was not done in the Phase I tests so that chatter in auxiliary contacts and in main contacts could be monitored independently. This would provide useful information on the safety implications of chatter vs the occurrence of chatter per se.

Structural Behavior

In order to fully characterize cabinet response during the Phase I tests (and therefore the input motions seen by the individual devices), we recommend that the following be performed:

- using the Phase I test data, estimate transmissibility at various in-cabinet locations as a function of cabinet mounting configuration and shaking level.

- using the Phase I test data, estimate "real" cabinet damping as a function of cabinet mounting configuration and shaking level.

- using the above results, estimate a general amplification factor for the cabinet as a function of cabinet mounting configuration and shaking level.

- develop simple single-degree-of-freedom models of the MCC and estimate the uncertainty in predicted transmissibilities through comparisons with experimental data. Estimate suitable effective damping for the SDOF models.

- perform detailed analyses to resolve differences in natural frequencies indicated by the static pull tests and by the dynamic resonance search tests.

This analysis of existing data would provide valuable information on how mounting and severity of input motion affect structural response, and thereby help to resolve the current issue of what "real" damping values should be used for cabinets of this general type.

We also recommend further tests to investigate whether the structural damage observed during Phase I reflects test-induced fatigue or the real capacity of the MCC cabinet. This would be done by obtaining a new Five-Star cabinet identical to that previously tested, installing the electrical devices from the Phase I tests, and then repeating only the one or two highest-level runs for each mounting configuration. The tests would also provide additional information on the repeatability of fragility data for the various electrical devices.

6.3 Implications for Future Fragilities Testing

As the introduction to this report discussed, resource and time constraints make it impractical to explicitly develop meaningful fragility descriptions by empirical means alone. Meaningful yet cost-effective fragilities testing can, however, be conducted within these constraints if it seeks not to explicitly develop "generic fragilities" broadly applicable to wide ranges of components, but rather to enhance understanding of how certain components fail ("failure modes"), what the important factors are that affect component performance, and what the relative influence of these factors is.

Testing in the form of "sensitivity studies" provides one method of gaining this understanding. In our Phase I demonstration tests, for example, we investigated the effect of "base flexibility" on MCC behavior (primarily for electrical devices but also for the cabinet itself) through a carefully structured series of sensitivity tests. The test results provided actual

seismic capacities of the specific components tested, as well as a basis for estimating "single-parameter" fragility descriptions (i.e., referenced to local ZPA) including confidence limits and practical "lower bound" (i.e., HCLPF) seismic capacities. The tests also suggested possible hardware modifications to increase seismic capacity, such as top bracing of the cabinet or use of reed-rather than armature-type relays. More importantly perhaps, the test results suggest that other descriptions of fragility -- incorporating frequency effects, for example -- might be "more appropriate" for characterizing component behavior.

The "sensitivity study" concept applies to the interpretation of existing (e.g., qualification) data as well. For example, as part of its Phase I component prioritization activities, LLNL developed fragility descriptions for five components based on high-level seismic qualification data [1]. Although not true "fragility" data, these test results provided useful information on component behavior under conditions exceeding any anticipated change in peak ground acceleration for eastern plant sites. Following the approach described in Section 1 of this report, it was assumed that the qualification test results represented the "high-confidence, low probability of failure" (HCLPF) value for each. Besides providing a basis for developing probabilistic fragility descriptions, these tests yielded insight into the influence of such parameters as support arrangement, cabinet rigidity and mass distribution on seismic capacity. In some cases the results of these tests identified practical -- and often relatively minor -- hardware modifications which substantially improved the seismic performance of the equipment tested.

It is important to recognize, however, that "sensitivity studies" in qualification testing often arise out of necessity as equipment is modified to meet requirements. The fragility analyst must therefore pay careful attention to the specific modifications made, particularly when seeking to apply data to similar components.

Clearly, even for functionally identical components, variations among manufacturers and models, in size and type, and in mounting and loading conditions imply that any fragility estimate -- or, for that matter, other

methods of assessing component performance -- will be based to a certain extent on engineering judgment. It is important that this judgment be supported by as firm a technical basis as possible within practical constraints. Testing for "understanding" rather than for explicit fragilities would provide the following:

- guidance to the fragility analyst as to what should be considered in developing a specific fragility description for a specific component.

- an improved basis for interpreting and applying test data obtained from other sources. This is particularly valuable, for example, using qualification data to assess actual component capacity.

- an improved basis for defining test conditions if more rigorous testing of a specific component is required.

- guidance for developing screening techniques for reviewing actual plant equipment ("walkdown" techniques) and suggesting modifications for enhancing the seismic capacity of critical components.

We demonstrated through our Phase I tests how these objectives can be achieved for a motor control center and its internal devices. Testing of other components will be addressed in a Phase II program plan consolidating our Phase I test experience with the results of the Phase I prioritization activities.

REFERENCES

1. G. Holman, et al., **Component Fragility Research Program: Phase I Component Prioritization,** Lawrence Livermore National Laboratory, report in preparation (May 1986).

2. R.J. Budnitz, et al., **An Approach to the Quantification of Seismic Margins in Nuclear Power Plants,** Lawrence Livermore National Laboratory, Report UCID-20444, NUREG/CR-4334 (August 1985).

3. Westinghouse Electric Corporation, "Motor Control Centers Five-Star", Descriptive Bulletin 12-155 (January 1985).

4. U.S. Army Corps of Engineers, **Subsystem Hardness Assurance Program,** Report HNDDSP-71-57-ED-R.

5. U.S. Army Corps of Engineers, **Subsystem Hardness Assurance Program,** Report HNDDSP-349-57-ED-R.

6. Electric Power Research Institute, "Seismic Equipment Qualification using Existing Test Data," Report NP-4297 (October 1985).

7. L. Cover, M. Bohn, R. Campbell and D. Wesley, **Handbook of Nuclear Power Plant Seismic Fragilities,** Lawrence Livermore National Laboratory, Report UCRL-53455, NUREG/CR-3558 (June 1985).